

Self-assembling functionalised peptides into decellularised materials for application in small diameter vascular grafts

Robert Stephen Guilliat

Submitted in accordance with the requirements for the degree of Doctor of Philosophy

Faculty of Engineering

University of Leeds

July 2013

The candidate confirms that the work submitted is his own and that appropriate credit has been given within the thesis where reference has been made to the work of others.

This copy has been supplied on the understanding that it is copyright material and that no quotation from the thesis may be published without proper acknowledgement.

The right of Robert Stephen Guilliat to be identified as Author of this work has been asserted by him in accordance with the Copyright, Designs and Patents Act 1988.

©2013 The University of Leeds and Robert Stephen Guilliat

Acknowledgements

It would not have been possible to conduct the research and write this thesis without the help and support of many kind and helpful people around me, to only some of whom it is possible to give particular thanks.

First and foremost, I am especially grateful to my supervisors Dr Amalia Aggeli and Professor Eileen Ingham, who have patiently supervised my research, providing excellent support, encouragement and advice whilst allowing me to direct my own project. I would particularly like to thank Dr Stacy-Paul Wilshaw for the training, knowledge, skills and wisdom he has imparted that have aided in my growth as a researcher and a person throughout my time at Leeds.

I would like to thank everyone in the Aggeli and Ingham labs that have made my time in and out of the lab enjoyable and have taken the time to show me what I needed to know in the early stages of this work. It is not possible to mention everyone but particular note should be given to Dr Phil Davies, Dr Steven Maude and Dr Danielle Miles, who have acted as sounding board, critic, supporter and friend as and when needed.

Special thanks go to my family who have always been there to support me even if they do not fully understand what it is I do. My mum Sue has been a rock to me, offering help, advice and support; even when it was not wanted but was sorely needed. I would like to thank the rest of my family for always believing in me, especially my nana who is no longer with us. I would finally like to thank my friends; Becky who has constantly reminded me to have a life outside work and in particular Sylvia without whose support I am not sure I would have survived the dark times.

“Nothing has such power to broaden the mind as the ability to investigate systematically and truly all that comes under thy observation in life.” Marcus Aurelius

Abstract

There is a clear clinical need for small diameter blood vessel grafts. Previous studies have shown that decellularised porcine arteries have potential for future development and clinical translation. However, in order to overcome the problems of thrombogenesis and encourage endothelialisation in small diameter applications, it will be necessary to devise innovative approaches. In this study it was hypothesised that a bioactive peptide could be self-assembled within the decellularised tissue to overcome the problems of thrombogenesis and to aid and enhance re-endothelialisation. A method for self-assembling the tape forming peptide, P₁₁₋₄ within decellularised tissues was developed. The study then went on to explore the P₁₁ series of peptides as materials for tissue engineering by examining biocompatibility and haemocompatibility and demonstrated the use of self-assembled peptide coatings to prevent thrombus formation and enhance re-endothelialisation. The self-assembly of peptide P₁₁₋₄ within decellularised porcine internal carotid artery was assessed using a range of microscopic and spectroscopic techniques. Fluorescent microscopy was used to show the penetration of the peptide throughout the decellularised conduit. Self-assembly of the peptide was assessed by FTIR spectroscopy. Using CLSM and MPLSM it was shown that the peptide self-assembled around the extracellular matrix of the acellular tissue. Fluorescent microscopy was used in conjunction with a specially designed flow cell to show that the peptide coating remained in the decellularised vessel for over 14 days under model flow conditions. The biocompatibility and haemocompatibility of a library of 43 peptides was assessed to identify ideal candidate peptides for use and to develop design characteristics for the application of self-assembling peptides in biomedical settings. Testing was carried out using cytotoxicity testing, the Chandler loop thrombosis model, a haemolysis assay and a complement inhibition assay. The results showed that large poly-cationic peptides were non-bio or haemo compatible, large neutral peptides enhanced thrombosis formation and that poly-anionic peptides with hydrophobic cores inhibited the complement system. Peptide coatings of P₁₁₋₄, P₁₁₋₈ and P₁₁₋₁₂ were shown to decrease, and in the case of P₁₁₋₁₂ prevent, thrombus formation; showing potential for application in small diameter acellular blood vessels. Peptide P₁₁₋₄, functionalised with cyclic RGD, was shown to enhance the attachment and retention of ovine endothelial cells on the decellularised vessel, demonstrating the potential of functionalised peptide to enhance re-endothelialisation. In conclusion, this study has demonstrated the potential of self assembling peptide technology for improving the function of acellular porcine arteries *in vitro*.

Table of contents

Acknowledgements.....	i
Abstract.....	ii
Table of contents	iii
List of Figures	xi
List of Tables	xvi
List of Abbreviations	xvii
1 Introduction	1
1.1 Clinical need.....	1
1.2 Blood vessels.....	1
1.2.1 Structure	1
1.2.2 Extracellular matrix.....	3
1.2.3 Cells.....	5
1.2.4 Mechanical properties	7
1.3 Arterial disease	10
1.4 Approaches to developing small diameter blood vessel replacements	14
1.4.1 Autografts	14
1.4.2 Allografts.....	16
1.4.3 Xenografts.....	17
1.4.4 Synthetic biomaterials	18
1.4.4.1 Prostheses.....	18
1.4.4.2 Regenerative.....	20
1.4.4.3 Composite materials.....	22
1.4.5 Natural biomaterials	22
1.4.6 Cell derived replacements	25
1.4.7 Decellularised scaffolds.....	29
1.4.8 Advantages and limitations to current approaches to vascular tissue engineering	34
1.5 Development of decellularised small diameter blood vessel grafts.....	35
1.5.1 Decellularisation methods	35
1.5.2 Sterilisation & Disease transmission.....	37
1.6 Thrombus formation.....	38
1.6.1 Thrombus prevention	44

1.6.2	Non-fouling surfaces	45
1.6.3	Anti-clotting agents.....	45
1.6.4	Endothelium formation.....	48
1.6.4.1	Growth factors	48
1.6.4.2	Attachment ligands	50
1.6.5	Advantages and limitations of current methods associated with thrombus prevention.....	52
1.7	Self-assembled peptides as biomaterials for tissue engineering.....	53
1.7.1	Self-assembly	53
1.7.2	Nucleated and non-nucleated 1D self-assembly	54
1.7.3	Complementary self-assembly.....	54
1.7.4	Peptide self-assembly	55
1.7.4.1	β -Sheet.....	55
1.7.4.2	β -Hairpin	56
1.7.4.3	π - π Stabilised β -sheet	57
1.7.4.4	α -Helix coiled coils	58
1.7.5	Peptide biocompatibility.....	58
1.7.5.1	RAD-based peptides.....	58
1.7.5.2	P ₁₁ series of peptides	59
1.7.5.3	β -Hairpin	60
1.7.5.4	Fmoc-dipeptides	61
1.7.5.5	α -Helix.....	62
1.7.5.6	Peptide amyloidogenicity.....	62
1.7.6	Rational design and modification of peptides	63
1.7.7	Advantages and limitations of peptides as biomaterials for tissue engineering	65
1.8	Hypothesis.....	66
1.9	Aims and objectives	66
2	Materials and methods.....	67
2.1	Materials	67
2.1.1	Equipment.....	67
2.1.2	Glassware	67
2.1.3	Plastic ware	67
2.1.4	Chemicals	67
2.1.5	Cell biology reagents and solutions	68

2.1.5.1	Dulbecco's phosphate buffered saline (DPBSa).....	68
2.1.5.2	Ringer's solution.....	68
2.1.5.3	Tris buffered saline (TBS).....	68
2.1.5.4	Tryptone phosphate broth 50 % stock solution (TPB).....	68
2.1.5.5	3T3 culture medium.....	68
2.1.5.6	2X 3T3 culture medium.....	69
2.1.5.7	BHK culture medium.....	69
2.1.5.8	2X BHK culture medium.....	69
2.1.5.9	Endothelial cell culture medium.....	69
2.1.6	Cells and biological tissues.....	70
2.1.6.1	Cells.....	70
2.1.6.2	Biological tissue.....	70
2.1.7	Antibodies.....	71
2.1.8	Peptides.....	72
2.2	General Methods.....	73
2.2.1	Sterilisation.....	73
2.2.1.1	Dry heat sterilisation.....	73
2.2.1.2	Moist heat/ autoclave sterilisation.....	73
2.2.1.3	Gamma irradiation sterilisation.....	73
2.2.2	Measurement of pH.....	73
2.2.3	Decellularisation of porcine arterial conduits.....	74
2.2.4	Analysis of decellularisation.....	76
2.2.4.1	Paraffin wax embedding of tissue samples.....	76
2.2.4.2	Sectioning of paraffin wax embedded samples.....	76
2.2.4.3	De-waxing and rehydration of sectioned paraffin wax embedded samples..	77
2.2.4.4	Haematoxylin and Eosin staining.....	77
2.2.4.5	DAPI staining.....	77
2.2.4.6	Mounting of sections.....	78
2.2.4.6.1	Mounting of stained sections using DPX mountant.....	78
2.2.5	Mounting of sections using DABCO:glycerol.....	78
2.2.6	Triggering peptide self-assembly.....	79
2.2.6.1	Peptide monomer solution.....	79
2.2.6.2	Self-assembly triggers.....	80
2.2.6.2.1	pH trigger.....	80

2.2.6.2.2	Ionic trigger	80
2.2.7	Peptide self-assembly in decellularised porcine internal carotid artery	80
2.2.8	Inclusion of fluorescently labelled peptide for fluorescent microscopy	81
2.2.9	Fourier transform infrared (FTIR) spectroscopy	81
2.2.10	Field emission gun scanning electron microscope (FEGSEM) imaging	83
2.2.11	Fluorescent microscopy imaging	84
2.2.11.1	Sectioning of fluorescent samples	84
2.2.11.2	Fluorescent imaging	84
2.2.12	Confocal laser scanning microscopy (CLSM) and multi-photon laser scanning microscopy (MPLSM)	84
2.2.12.1	Confocal laser scanning microscopy (CLSM) imaging	85
2.2.12.2	Multi-photon laser scanning microscopy (MPLSM) imaging	85
2.2.13	Cell culture	86
2.2.13.1	Resurrection and culture of primary cells and cell lines	86
2.2.13.2	Sub-culture of primary cells and cell lines	86
2.2.13.3	Trypan blue estimation of cell viability and number	87
2.2.13.4	Cryopreservation of primary cells and cell lines	88
2.2.14	Biocompatibility testing	88
2.2.14.1	ATPLite-M® assay	89
2.2.15	Chandler loop thrombosis model	90
2.2.15.1	Chandler loop model for testing addition of material to blood	91
2.2.15.2	Modified Chandler loop model for testing the thrombogenicity of the decellularised artery	93
2.2.16	Haemolysis assay	94
2.2.16.1	Washed erythrocytes	94
2.2.16.2	Haemolysis assay	95
2.2.17	Complement inhibition assay	95
2.2.17.1	CH50 assay	96
2.2.17.2	Modified CH50 complement inhibition assay	97
2.2.18	Isolation and growth of ovine endothelial cells	99
2.2.18.1	Isolation of ovine arterial endothelial cells	99
2.2.18.2	Subculture of ovine arterial endothelial cells	100
2.2.18.3	Cryopreservation of ovine endothelial cells	101
2.2.18.4	Characterisation of ovine arterial endothelial cells	101

2.2.18.4.1	Indirect immunofluorescent antibody method	102
2.2.18.4.2	Direct immunofluorescent antibody method.....	103
2.2.19	Endothelial cell attachment and proliferation.....	104
2.2.20	Flow cell model of flow over luminal surface in small diameter blood vessels used to test peptide stability under flow.....	105
2.2.21	Statistical analysis	106
2.2.21.1	Confidence limits.....	106
2.2.21.2	Statistical analysis	107
3	Development of methodologies and testing of peptide self-assembly in decellularised arterial conduits.....	108
3.1	Introduction	108
3.1.1	Peptide self-assembly	108
3.1.2	Peptide P ₁₁₋₄	109
3.1.3	Decellularisation	111
3.1.4	Aims and objectives	111
3.2	Methods.....	112
3.2.1	Histological evaluation of decellularised porcine internal carotid artery.....	112
3.2.2	Evaluation of peptide self-assembly triggers.....	112
3.2.3	Cross sectioning and imaging of fluorescent peptide penetration into decellularised vessel	113
3.2.4	FTIR spectroscopy and analysis of peptide presence in decellularised vessel .	113
3.2.5	Field emission gun scanning electron microscopy (FEGSEM) imaging of peptide in decellularised vessel	114
3.2.6	Confocal laser scanning microscopy (CLSM) imaging of peptide in decellularised vessel	114
3.2.7	Multi-photon laser scanning microscopy (MPLSM) imaging of peptide in decellularised vessel	115
3.2.8	The effect of concentration on peptide distribution throughout decellularised vessel	115
3.2.9	The effect of self-assembled state on peptide penetration into decellularised vessel	115
3.2.10	Evaluation of peptide stability in decellularised vessel under flow.....	116
3.3	Results.....	116
3.3.1	Histological evaluation of decellularised porcine internal carotid artery.....	116
3.3.2	Evaluation of peptide self-assembly triggers.....	118

3.3.3	Cross sectioning and imaging of fluorescent peptide penetration into decellularised vessel	120
3.3.4	FTIR spectroscopy and analysis of peptide in decellularised vessel	121
3.3.5	FEGSEM imaging of peptide on the surface of decellularised vessel	122
3.3.6	CLSM imaging of peptide in decellularised vessel	124
3.3.7	MPLSM imaging of peptide in decellularised vessel	126
3.3.8	Effect of concentration on peptide distribution throughout decellularised vessel	129
3.3.9	Effect of self-assembled state on peptide penetration into decellularised vessel	131
3.3.10	Peptide stability in decellularised vessel under flow	133
3.4	Discussion.....	137
3.4.1	Histological analysis of decellularised porcine internal carotid artery.....	137
3.4.2	Evaluation of self-assembly triggers	138
3.4.3	Peptide penetration into decellularised vessel.....	139
3.4.4	FTIR analysis of peptide self-assembly.....	139
3.4.5	FEGSEM imaging of peptide on decellularised vessel surface	139
3.4.6	CLSM and MPLSM imaging of peptide within decellularised vessel.....	140
3.4.7	Effect of concentration on peptide distribution in decellularised vessel	141
3.4.8	Effect of the self-assembled state of peptide on distribution in the decellularised vessel	142
3.4.9	Peptide stability in decellularised vessel under flow	142
3.4.10	Summary	143
4	Systematic study of peptide biocompatibility and haemocompatibility.....	144
4.1	Introduction	144
4.1.1	Biocompatibility	145
4.1.2	Haemocompatibility.....	145
4.1.3	Thrombus formation/blood clotting	145
4.1.4	Complement system	149
4.1.5	Animal models	152
4.1.6	Peptides	152
4.1.7	Peptides from the literature	152
4.1.8	Aims and objectives	153
4.2	Methods.....	154
4.2.1	Peptides	154

4.2.2	Biocompatibility testing	156
4.2.3	Chandler loop thrombosis model	156
4.2.4	Haemolysis assay	157
4.2.5	Complement inhibition assay.....	157
4.3	Results.....	157
4.3.1	Effects of peptides on cell growth	157
4.3.2	Effects of peptides on thrombus formation	163
4.3.3	Effects of peptides on the haemolysis of ovine erythrocytes.....	167
4.3.4	Peptide complement inhibition	173
4.4	Discussion.....	177
4.4.1	Effects of peptides on cell growth	178
4.4.2	Effects of peptides on thrombus formation	181
4.4.3	Effects of peptides on haemolysis of ovine erythrocytes	184
4.4.4	Complement inhibition	186
4.4.5	Design characteristics	188
5	Effects of peptide coatings on decellularised arterial conduits.....	190
5.1	Introduction	190
5.1.1	Anti-thrombogenic coatings	190
5.1.2	Endothelial cells	191
5.1.3	Cell attachment motifs.....	192
5.1.4	Aims and objectives	193
5.2	Methods.....	193
5.2.1	Chandler loop thrombosis model	193
5.2.2	Endothelial cell isolation and characterisation	194
5.2.3	Endothelial cell attachment and proliferation.....	194
5.3	Results.....	195
5.3.1	Thrombus formation in uncoated and peptide coated decellularised vessels.	195
5.3.2	Endothelial cell isolation and characterisation	196
5.3.2.1	Observations from cell culture.....	196
5.3.2.2	Phenotype of isolated ovine vascular cells	197
5.3.3	Effect of peptide and functionalised peptide on the attachment of ovine arterial endothelial cells	199
5.4	Discussion.....	205
5.4.1	Thrombus formation in uncoated and peptide coated decellularised vessels.	205

5.4.2	Endothelial cell isolation and characterisation	205
5.4.3	Endothelial cell attachment to peptide and functionalised peptide coated decellularised vessels.....	206
6	Conclusions	209
6.1	Summary	209
6.2	Future work.....	210
6.3	Outlook	212
A.	Appendix	214
A.1	Equipment.....	214
A.2	Chemicals	216
A.3	Images of peptide P ₁₁₋₄ self-assembly under different conditions	218
A.4	Fluorescent image of fluorescein tagged P ₁₁₋₄	219
A.5	CH50 assay	220
A.6	Test of normal clotting behaviour of sheep blood	221
A.7	Presentations and applications.....	222

List of Figures

FIGURE 1.1; SCHEMATIC OF BLOOD VESSEL STRUCTURE	2
FIGURE 1.2; SCHEMATIC OF CLASSICAL MODEL OF ELASTOGENESIS, A. TROPOELASTIN RELEASED FROM CELLS AND CROSS-LINKED INTO ELASTIN. B. ELASTIN MOLECULES “CHAPERONED” TO MICROFIBRILS ASSEMBLY. C. ELASTIN AND MICROFIBRILS ASSEMBLE TO FORM ELASTIC FIBRES. TAKEN FROM (MOORE AND THIBEAULT, 2012).	4
FIGURE 1.3; SCHEMATIC OF ENDOTHELIAL DYSFUNCTION, FATTY-STREAK LESION, ADVANCED LESION AND LESION RUPTURE IN ATHEROSCLEROSIS ADAPTED FROM (EPSTEIN AND ROSS, 1999)	12
FIGURE 1.4; SCHEMATIC OF BYPASS GRAFT	15
FIGURE 1.5; SCHEMATIC OF FOREIGN BODY RESPONSE	20
FIGURE 1.6; SCHEMATIC OF THE STRUCTURE OF COLLAGEN AND ELASTIN.....	23
FIGURE 1.7; SCHEMATIC OF ELECTROSPINNING. REPRODUCED FROM (BADAMI ET AL., 2006).	24
FIGURE 1.8; SCHEMATIC OF CELL SHEET FORMATION OF REPLACEMENT BLOOD VESSEL.....	26
FIGURE 1.9; SCHEMATIC OF CELL PRINTING	28
FIGURE 1.10; SCHEMATIC OF DECELLULARISATION PROCESS	30
FIGURE 1.11; SCHEMATIC OF INTRINSIC AND EXTRINSIC PATHWAYS IN BLOOD CLOT FORMATION.....	42
FIGURE 1.12, SCHEMATIC OF THE ACTION OF HEPARIN ON THE FORMATION OF THROMBIN-ANTI-THROMBIN COMPLEX; HEPARIN BINDS TO ANTI-THROMBIN AND CATALYSES THE REACTION WITH THROMBIN, THE AFFINITY OF ANTI-THROMBIN FOR HEPARIN IS REDUCED AND HEPARIN IS RELEASED.....	46
FIGURE 1.13; HIERARCHY OF β -SHEET SELF-ASSEMBLY.....	56
FIGURE 1.14; (A) SCHEMATIC OF FOLDING AND SUBSEQUENT SELF-ASSEMBLY WHEN MAX1 AND MAX8 PEPTIDES ARE PLACED IN PHYSIOLOGICAL SOLUTION. (B) PEPTIDE SEQUENCES OF MAX1 AND MAX8. REPRODUCED FROM HAINES-BUTTERICK ET AL (HAINES-BUTTERICK ET AL., 2007).....	57
FIGURE 1.15, LEFT: FMOC-FF β -SHEETS, BINDING THROUGH π - π -STACKED PHENYL (ORANGE) AND FMOC GROUPS (PURPLE); RIGHT: SIDE VIEW OF FMOC-FF AGGREGATE. ADAPTED FROM SMITH ET AL (SMITH ET AL., 2008).	57
FIGURE 1.16, SCHEMATIC OF ALPHA HELIX FORMING PEPTIDE COILED COIL ARCHITECTURE. REPRODUCED FROM BANWELL ET AL (BANWELL ET AL., 2009).	58
FIGURE 1.17, LEFT) SCHEMATIC MODLE OF PH CONTROL OVER P_{11-4} SELF-ASSEMBLY. RIGHT) SELF-ASSEMBLY OF 6.3 MOL.M^{-3} OF P_{11-4} UNDER DIFFERENT CONDITIONS. (A) PERCENTAGE β -SHEET OF P_{11-4} AS A FUNCTION OF pD IN D_2O (BY FTIR). (B) PERCENTAGE β -SHEET OF P_{11-4} AS A FUNCTION OF pD IN 130 MOL.M^{-3} NaCl IN D_2O (BY FTIR). MODIFIED FROM (AGGELI ET AL., 2003B, CARRICK ET AL., 2007).....	64
FIGURE 2.1; SCHEMATIC OF CLSM AND MPLSM EXCITATION.....	85
FIGURE 2.2; SCHEMATIC OF AREA CELLS ARE COUNTED ON A HAEMOCYTOMETER.....	87
FIGURE 2.3; SCHEMATIC OF CHANDLER LOOP MODEL SET UP	92
FIGURE 2.4, SCHEMATIC OF SERIAL DILUTION OF SERUM FOR CH50 TEST	96
FIGURE 2.5, SCHEMATIC OF SET UP OF CH50 ASSAY	97
FIGURE 2.6; SCHEMATIC OF SET UP OF MODIFIED CH50 COMPLEMENT INHIBITION ASSAY	98
FIGURE 2.7, CROSS-SECTION SCHEMATIC OF FLOW CELL.....	105
FIGURE 3.1; STICK IMAGE OF PEPTIDE P_{11-4} WITH AMINO ACIDS LABELLED, CREATED USING HYPERCHEM 7.	110
FIGURE 3.2; HISTOLOGY IMAGES OF FRESH AND DECELLULARISED PORCINE INTERNAL CAROTID ARTERY, IMAGES 1&2 STAINED USING H&E, IMAGES 3&4 STAINED USING DAPI; 1&3 FRESH PORCINE INTERNAL CAROTID ARTERY, 2&4 DECELLULARISED PORCINE INTERNAL CAROTID ARTERY. S = SUBENDOTHELIAL LAYER, M = MEDIAL LAYER, A = ADVENTITIAL LAYER.	117
FIGURE 3.3; CROSS SECTION IMAGE OF FLUORESCENTLY TAGGED PEPTIDE P_{11-4} (RATIO 1:30 FLUORESCHEIN TAGGED P_{11-4} TO UNTAGGED P_{11-4}) IN DECELLULARISED PORCINE INTERNAL CAROTID ARTERY WITH CONTROL DECELLULARISED PORCINE INTERNAL CAROTID ARTERY AT 10X AND 20X MAGNIFICATION. S = SUBENDOTHELIAL LAYER, M = MEDIAL LAYER, A = ADVENTITIAL LAYER.	120

FIGURE 3.4; FTIR SPECTRUM IN THE AMIDE I AND II REGION (1500 – 1900 cm^{-1}) SHOWING DIFFERENCE BETWEEN TWO AVERAGED SPECTRA; BLUE) COMBINED SPECTRA OF DECELLULARISED PORCINE INTERNAL CAROTID ARTERY, RED) COMBINED SPECTRA OF DECELLULARISED PORCINE INTERNAL CAROTID ARTERY AND 30 MG.ML^{-1} (18.8 MOL.M^{-3}) OF P_{11-4}	121
FIGURE 3.5; FEGSEM IMAGES OF DECELLULARISED PORCINE INTERNAL CAROTID ARTERY WITH SELF-ASSEMBLED P_{11-4} ; A) NO PEPTIDE, B) 1 MG.ML^{-1} (0.63 MOL.M^{-3}), C) 5 MG.ML^{-1} (3.13 MOL.M^{-3}), D) 10 MG.ML^{-1} (6.26 MOL.M^{-3}), IMAGES TAKEN AT 3 KEV AT 60,000X MAGNIFICATION.	123
FIGURE 3.6; CLSM IMAGES OF (A) PEPTIDE GEL, 10 MG.ML^{-1} (6.3 MOL.M^{-3}) OF FLUORESCENTLY TAGGED P_{11-4} MIXED WITH P_{11-4} AT A RATIO OF 1:50, (B) DECELLULARISED PORCINE INTERNAL CAROTID ARTERY WITH 10 MG.ML^{-1} (6.3 MOL.M^{-3}) OF FLUORESCENTLY TAGGED P_{11-4} MIXED 1:50 WITH P_{11-4} , PEPTIDE GEL, (C & D) Z-AXIS STACK OF DECELLULARISED PORCINE CAROTID ARTERY WITH 10 MG.ML^{-1} (6.3 MOL.M^{-3}) OF FLUORESCENTLY TAGGED P_{11-4} MIXED 1:50 WITH P_{11-4} , PEPTIDE GEL; HIGHLIGHTED REGION SHOWS PEPTIDE COATING OF A HORIZONTAL STRUCTURE TAKEN AT DIFFERENT DEPTHS (Z-AXIS). MAGNIFICATION 40X	125
FIGURE 3.7; MULTI-PHOTON IMAGES OF DECELLULARISED PORCINE INTERNAL CAROTID ARTERY COATED IN 30 MG.ML^{-1} (18.8 MOL.M^{-3}) OF FLUORESCENTLY TAGGED P_{11-4} PEPTIDE AT A RATIO OF 1:50 WITH UNTAGGED P_{11-4} . IMAGES SHOW THE SAME AREA WITH THE TWO FLUORESCENT SIGNALS SEPARATED AND COMBINED. TOP IMAGES ARE AT 63X MAGNIFICATION BOTTOM IMAGES ARE AT 20X MAGNIFICATION.	127
FIGURE 3.8; Z-AXIS STACK OF MULTI-PHOTON IMAGES OF DECELLULARISED PORCINE INTERNAL CAROTID ARTERY COATED IN 30 MG.ML^{-1} (18.8 MOL.M^{-3}) OF FLUORESCENTLY TAGGED P_{11-4} PEPTIDE AT A RATIO OF 1:50 WITH UNTAGGED P_{11-4} . IMAGES SHOW FLUORESCENCE AT 2 μM INTERVALS IN THE SAME X,Y, LOCATION. IMAGES TAKEN AT 63X MAGNIFICATION.	128
FIGURE 3.9; IMAGES SHOWING EFFECTS OF CONCENTRATION ON PEPTIDE SELF-ASSEMBLY IN DECELLULARISED PORCINE INTERNAL CAROTID ARTERY. FLUORESCENT CROSS SECTION IMAGES OF DECELLULARISED PORCINE INTERNAL CAROTID ARTERY AND DECELLULARISED PORCINE INTERNAL CAROTID ARTERY COATED IN 30 MG.ML^{-1} (18.8 MOL.M^{-3}), 15 MG.ML^{-1} (9.4 MOL.M^{-3}), 7.5 MG.ML^{-1} (4.7 MOL.M^{-3}), 3.75 MG.ML^{-1} (2.35 MOL.M^{-3}) AND 1.87 MG.ML^{-1} (1.18 MOL.M^{-3}) OF FLUORESCENTLY TAGGED P_{11-4} PEPTIDE AT A RATIO OF 1:50 WITH UNTAGGED P_{11-4} . 10X MAGNIFICATION. S = SUBENDOTHELIAL LAYER, M = MEDIAL LAYER, A = ADVENTITIAL LAYER.....	130
FIGURE 3.10; EFFECT OF SELF-ASSEMBLED STATE ON PEPTIDE PENETRATION INTO DECELLULARISED PORCINE INTERNAL CAROTID ARTERY. FLUORESCENT CROSS SECTION IMAGES OF DECELLULARISED PORCINE INTERNAL CAROTID ARTERY AND DECELLULARISED PORCINE INTERNAL CAROTID ARTERY COATED IN 30 MG.ML^{-1} (18.8 MOL.M^{-3}), 15 MG.ML^{-1} (9.4 MOL.M^{-3}), 7.5 MG.ML^{-1} (4.7 MOL.M^{-3}), 3.75 MG.ML^{-1} (2.35 MOL.M^{-3}) AND 1.87 MG.ML^{-1} (1.18 MOL.M^{-3}) OF FLUORESCENTLY TAGGED P_{11-4} PEPTIDE AT A RATIO OF 1:50 WITH UNTAGGED P_{11-4} . 20X MAGNIFICATION. S = SUBENDOTHELIAL LAYER, M = MEDIAL LAYER, A = ADVENTITIAL LAYER.	132
FIGURE 3.11; STABILITY OF PEPTIDE P_{11-4} AT 0, 1, 2, 3, 4, 7 AND 14 DAYS IN A MODEL OF FLUID FLOW IN A BLOOD VESSEL SHOWING PEPTIDE STABILITY UNDER FLOW CONDITIONS. FLUORESCENT CROSS SECTION IMAGES OF DECELLULARISED PORCINE INTERNAL CAROTID ARTERY AND DECELLULARISED PORCINE INTERNAL CAROTID ARTERY COATED IN 30 MG.ML^{-1} (18.8 MOL.M^{-3}) OF FLUORESCENTLY TAGGED P_{11-4} PEPTIDE AT A RATIO OF 1:50 WITH UNTAGGED P_{11-4} . 10X MAGNIFICATION. ARROWS INDICATES SUBENDOTHELIUM/LUMEN SURFACE.....	134
FIGURE 3.12; STABILITY OF PEPTIDE P_{11-4} AT 0, 1, 2, 3, 4, 7 AND 14 DAYS IN A MODEL OF FLUID FLOW IN A BLOOD VESSEL SHOWING PEPTIDE STABILITY UNDER FLOW CONDITIONS. FLUORESCENT CROSS SECTION IMAGES OF DECELLULARISED PORCINE INTERNAL CAROTID ARTERY AND DECELLULARISED PORCINE INTERNAL CAROTID ARTERY COATED IN 30 MG.ML^{-1} (18.8 MOL.M^{-3}) OF FLUORESCENTLY TAGGED P_{11-4} PEPTIDE AT A RATIO OF 1:50 WITH UNTAGGED P_{11-4} . 20X MAGNIFICATION. ARROWS INDICATES SUBENDOTHELIUM/LUMEN.	135
FIGURE 3.13; AVERAGE FLUORESCENT INTENSITY OF SECTIONED DECELLULARISED PORCINE INTERNAL CAROTID ARTERY (DPICA) COATED IN 30 MG.ML^{-1} P_{11-4} (FLUORESCENTLY TAGGED P_{11-4} 1:50 WITH P_{11-4}) AT 0, 1, 2, 3, 4, 7 AND 14 DAYS. DATA IS PRESENTED AS THE MEAN (N=6) \pm 95 % CONFIDENCE INTERVALS. BLUE 10X MAGNIFICATION, RED 20X MAGNIFICATION	136
FIGURE 4.1; SCHEMATIC OF PATHWAYS OF COMPLEMENT ACTIVATION	150

- FIGURE 4.2; ATP LEVELS IN CELLS CULTURED IN THE PRESENCE AND ABSENCE OF PEPTIDES; NEGATIVE CONTROL DMEM FOR 3T3 CELLS, GMEM FOR BHK CELLS, POSITIVE CONTROL 40 % DMSO IN, DMEM FOR 3T3 CELLS, GMEM FOR BHK CELLS. DATA IS PRESENTED AS THE MEAN (N=6) \pm 95 % CONFIDENCE INTERVALS. DATA WAS ANALYSED BY ONE WAY ANALYSIS OF VARIANCE FOLLOWED BY DETERMINATION OF THE MSD ($p < 0.05$). * = SIGNIFICANT DIFFERENCE FROM NEGATIVE CONTROL. 158
- FIGURE 4.3; ATP LEVELS IN CELLS CULTURED IN THE PRESENCE AND ABSENCE OF PEPTIDES; NEGATIVE CONTROL DMEM FOR 3T3 CELLS, GMEM FOR BHK CELLS, POSITIVE CONTROL 40 % DMSO IN, DMEM FOR 3T3 CELLS, GMEM FOR BHK CELLS. DATA IS PRESENTED AS THE MEAN (N=6) \pm 95 % CONFIDENCE INTERVALS. DATA WAS ANALYSED BY ONE WAY ANALYSIS OF VARIANCE FOLLOWED BY DETERMINATION OF THE MSD ($p < 0.05$). * = SIGNIFICANT DIFFERENCE FROM NEGATIVE CONTROL 160
- FIGURE 4.4; ATP LEVELS IN CELLS CULTURED IN THE PRESENCE AND ABSENCE OF PEPTIDES; NEGATIVE CONTROL DMEM FOR 3T3 CELLS, GMEM FOR BHK CELLS, POSITIVE CONTROL 40 % DMSO IN DMEM FOR 3T3 CELLS, GMEM FOR BHK CELLS. DATA IS PRESENTED AS THE MEAN (N=6) \pm 95 % CONFIDENCE INTERVALS. DATA WAS ANALYSED BY ONE WAY ANALYSIS OF VARIANCE FOLLOWED BY DETERMINATION OF THE MSD ($p < 0.05$). * = SIGNIFICANT DIFFERENCE FROM NEGATIVE CONTROL, ** = SIGNIFICANT DIFFERENCE FROM NEGATIVE CONTROL AND NO SIGNIFICANT DIFFERENCE FROM POSITIVE CONTROL. 162
- FIGURE 4.5; WEIGHTS OF THROMBUS FORMED IN THE PRESENCE OR ABSENCE OF PEPTIDE IN THE CHANDLER LOOP MODEL; NEGATIVE CONTROL 100 μ L OF WATER, POSITIVE CONTROL 2 μ L OF HUMAN α -THROMBIN IN 98 μ L OF WATER. DATA IS PRESENTED AS THE MEAN (N=6) \pm 95 % CONFIDENCE INTERVALS. DATA WAS ANALYSED BY ONE WAY ANALYSIS OF VARIANCE FOLLOWED BY DETERMINATION OF THE MSD ($p < 0.05$). * = SIGNIFICANT INCREASE FROM NEGATIVE CONTROL, ** = SIGNIFICANT REDUCTION COMPARED TO NEGATIVE CONTROL, *** = NO SIGNIFICANT DIFFERENCE FROM POSITIVE CONTROL. 164
- FIGURE 4.6; WEIGHTS OF THROMBUS FORMED IN THE PRESENCE OR ABSENCE OF PEPTIDE IN THE CHANDLER LOOP MODEL; NEGATIVE CONTROL 100 μ L OF WATER, POSITIVE CONTROL 2 μ L OF HUMAN α -THROMBIN IN 98 μ L OF WATER. DATA IS PRESENTED AS THE MEAN (N=6) \pm 95 % CONFIDENCE INTERVALS. DATA WAS ANALYSED BY ONE WAY ANALYSIS OF VARIANCE FOLLOWED BY DETERMINATION OF THE MSD ($p < 0.05$). * = SIGNIFICANT INCREASE FROM NEGATIVE CONTROL, ** = SIGNIFICANT DECREASE COMPARED TO NEGATIVE CONTROL, *** = NO SIGNIFICANT DIFFERENCE FROM POSITIVE CONTROL. 166
- FIGURE 4.7; HAEMOLYTIC EFFECTS OF PEPTIDES AFTER A; 6 HOURS, B; 12 HOURS. POSITIVE CONTROL WATER, NEGATIVE CONTROL RINGER'S SOLUTION. DATA IS PRESENTED AS THE MEAN (N=6) \pm 95 % CONFIDENCE INTERVALS. DATA WAS ANALYSED BY ONE WAY ANALYSIS OF VARIANCE FOLLOWED BY DETERMINATION OF THE MSD ($p < 0.05$). * = SIGNIFICANT DIFFERENCE FROM NEGATIVE CONTROL, ** = SIGNIFICANT DIFFERENCE FROM NEGATIVE CONTROL AND NO SIGNIFICANT DIFFERENCE FROM POSITIVE CONTROL. 168
- FIGURE 4.8; HAEMOLYTIC EFFECTS OF PEPTIDES AFTER A; 24 HOURS, B; 28 HOURS; POSITIVE CONTROL WATER, NEGATIVE CONTROL RINGER'S SOLUTION. DATA IS PRESENTED AS THE MEAN (N=6) \pm 95 % CONFIDENCE INTERVALS. DATA WAS ANALYSED BY ONE WAY ANALYSIS OF VARIANCE FOLLOWED BY DETERMINATION OF THE MSD ($p < 0.05$). * = SIGNIFICANT DIFFERENCE FROM NEGATIVE CONTROL, ** = SIGNIFICANT DIFFERENCE FROM NEGATIVE CONTROL AND NO SIGNIFICANT DIFFERENCE FROM POSITIVE CONTROL. 169
- FIGURE 4.9; HAEMOLYTIC EFFECTS OF PEPTIDES AFTER 72 HOURS; POSITIVE CONTROL WATER, NEGATIVE CONTROL RINGER'S SOLUTION. DATA IS PRESENTED AS THE MEAN (N=6) \pm 95 % CONFIDENCE INTERVALS. DATA WAS ANALYSED BY ONE WAY ANALYSIS OF VARIANCE FOLLOWED BY DETERMINATION OF THE MSD ($p < 0.05$). * = SIGNIFICANT DIFFERENCE FROM NEGATIVE CONTROL, ** = SIGNIFICANT DIFFERENCE FROM NEGATIVE CONTROL AND NO SIGNIFICANT DIFFERENCE FROM POSITIVE CONTROL. 170
- FIGURE 4.10; HAEMOLYTIC EFFECTS OF PEPTIDES; POSITIVE CONTROL WATER, NEGATIVE CONTROL RINGER'S SOLUTION; DATA IS PRESENTED AS THE MEAN (N=6) \pm 95 % CONFIDENCE INTERVALS. DATA WAS ANALYSED BY ONE WAY ANALYSIS OF VARIANCE FOLLOWED BY DETERMINATION OF THE MSD ($p < 0.05$). COLOURED STARS DENOTE A SIGNIFICANT DIFFERENCE FROM THE NEGATIVE CONTROL, RED STARS DENOTE NO SIGNIFICANT DIFFERENCE FROM THE POSITIVE CONTROL. 171

FIGURE 4.11; COMPLEMENT INHIBITION BY PEPTIDES; CH50 NEGATIVE CONTROL, HI (HEAT INACTIVATED) SERUM POSITIVE CONTROL. DATA IS PRESENTED AS THE MEAN (N=6) \pm 95 % CONFIDENCE INTERVALS. DATA WAS ANALYSED BY ONE WAY ANALYSIS OF VARIANCE FOLLOWED BY DETERMINATION OF THE MSD ($p < 0.05$). * = SIGNIFICANT DIFFERENCE FROM NEGATIVE CONTROL.	174
FIGURE 4.12; COMPLEMENT INHIBITION BY PEPTIDES; CH50 NEGATIVE CONTROL, HI (HEAT INACTIVATED) SERUM POSITIVE CONTROL. DATA IS PRESENTED AS THE MEAN (N=6) \pm 95 % CONFIDENCE INTERVALS. DATA WAS ANALYSED BY ONE WAY ANALYSIS OF VARIANCE FOLLOWED BY DETERMINATION OF THE MSD ($p < 0.05$). * = SIGNIFICANT DIFFERENCE FROM NEGATIVE CONTROL.	176
FIGURE 5.1; WEIGHTS OF THROMBUS FORMED WHEN PEPTIDE COATED OR UNCOATED (DPICA) DECELLULARISED VESSEL WAS EVALUATED IN THE CHANDLER LOOP MODEL; DATA IS PRESENTED AS THE MEAN (N=6) \pm 95 % CONFIDENCE INTERVALS. DATA WAS ANALYSED BY ONE WAY ANALYSIS OF VARIANCE FOLLOWED BY DETERMINATION OF THE MSD ($p < 0.05$). BLUE * = SIGNIFICANT DIFFERENCE BETWEEN COATED AND UNCOATED VESSELS, RED * = SIGNIFICANT DIFFERENCE BETWEEN PEPTIDE COATED VESSELS.	196
FIGURE 5.2; INVERTED MICROSCOPE IMAGES OF CULTURED OVINE ARTERIAL CELLS FOLLOWING ISOLATION. A & B; FRESHLY ISOLATED ENDOTHELIAL CELLS AFTER 1 DAY OF CULTURE AT 10 X MAGNIFICATION, C; CONFLUENT ENDOTHELIAL CELLS 4 X MAGNIFICATION, D; CONFLUENT ENDOTHELIAL CELLS 10 X MAGNIFICATION.	197
FIGURE 5.3; CONFOCAL LASER SCANNING MICROSCOPE IMAGES OF ANTIBODY LABELLING OF ISOLATED OVINE ENDOTHELIAL CELLS, A; ANTI-CD31 AND DAPI STAINING, B; ANTI-VWF AND DAPI STAINING, C; ANTI-CD31 ISOTYPE CONTROL AND DAPI STAINING, D; ANTI-VWF ISOTYPE CONTROL AND DAPI STAINING. 10 X MAGNIFICATION.	198
FIGURE 5.4; CONFOCAL LASER SCANNING MICROSCOPE IMAGES OF ANTIBODY LABELLING OF ISOLATED OVINE ENDOTHELIAL CELLS, A; ANTI-SMOOTH MUSCLE CELL α -ACTIN AND DAPI STAINING, B; ANTI-SMOOTH MUSCLE CELL MYOSIN HEAVY CHAIN AND DAPI STAINING, C; ANTI-SMOOTH MUSCLE CELL α -ACTIN ISOTYPE CONTROL AND DAPI STAINING, D; ANTI-SMOOTH MUSCLE CELL MYOSIN HEAVY CHAIN ISOTYPE CONTROL AND DAPI STAINING. 10 X MAGNIFICATION.	198
FIGURE 5.5; CONFOCAL LASER SCANNING MICROSCOPY IMAGES OF LIVE/DEAD STAIN OF OVINE ENDOTHELIAL CELLS AFTER 4, 24 AND 72 HOURS ATTACHED TO DECELLULARISED PORCINE INTERNAL CAROTID ARTERY, DECELLULARISED PORCINE INTERNAL CAROTID ARTERY WITH 30 MG.ML ⁻¹ (18.8 MOL.M ⁻³) P ₁₁₋₄ AND DECELLULARISED PORCINE INTERNAL CAROTID ARTERY WITH 30 MG.ML ⁻¹ (18.8 MOL.M ⁻³) P ₁₁₋₄ -CRGD MIXED WITH P ₁₁₋₄ AT A RATIO OF 1:50. 10 X MAGNIFICATION.	200
FIGURE 5.6; NUMBER OF LIVE CELLS PER MM ² AT 4, 24 AND 72 HOURS. DATA IS PRESENTED AS THE MEAN (N=4) \pm 95 % CONFIDENCE INTERVALS. DATA WAS ANALYSED BY TWO WAY ANALYSIS OF VARIANCE FOLLOWED BY DETERMINATION OF THE MSD ($p < 0.05$) FOR EACH TIME POINT AND EACH TEST CONDITION. BLACK * = SIGNIFICANT INCREASE IN ATTACHED CELLS BETWEEN TEST CONDITIONS AT SET TIME POINT, COLOURED * = SIGNIFICANT INCREASE IN ATTACHED CELLS BETWEEN TIME POINTS FOR CORRESPONDING TEST CONDITION, COLOURED ** = SIGNIFICANT DECREASE IN ATTACHED CELLS BETWEEN TIME POINTS FOR CORRESPONDING TEST CONDITION.	201
FIGURE 5.7; PERCENTAGE OF CELLS COUNTED THAT WERE VIABLE OVER 4, 24 AND 72 HOURS. DATA IS PRESENTED AS THE MEAN (N=4) \pm 95 % CONFIDENCE INTERVALS. DATA WAS ANALYSED BY TWO WAY ANALYSIS OF VARIANCE FOLLOWED BY DETERMINATION OF THE MSD ($p < 0.05$) FOR EACH TIME POINT AND EACH TEST CONDITION. BLACK * = SIGNIFICANT INCREASE IN ATTACHED CELL VIABILITY BETWEEN TEST CONDITIONS AT SET TIME POINT, BLACK ** = SIGNIFICANT DECREASE IN ATTACHED CELL VIABILITY BETWEEN TEST CONDITIONS AT SET TIME POINT, COLOURED * = SIGNIFICANT INCREASE IN ATTACHED CELL VIABILITY BETWEEN TIME POINTS FOR CORRESPONDING TEST CONDITION, COLOURED * * = SIGNIFICANT DECREASE IN ATTACHED CELL VIABILITY BETWEEN TIME POINTS FOR CORRESPONDING TEST CONDITION.	201
FIGURE 5.8; CONFOCAL LASER SCANNING MICROSCOPY IMAGES OF OVINE ENDOTHELIAL CELLS AFTER 24 HOURS SHOWING ALIGNMENT OF CELLS WITH UNDERLYING EXTRACELLULAR MATRIX. A TO C; LIVE CELL STAIN, D TO F; DEAD CELL STAIN AND COLLAGEN AUTO-FLUORESCENCE, A AND D; DECELLULARISED PORCINE INTERNAL CAROTID ARTERY, B AND E; DECELLULARISED PORCINE INTERNAL CAROTID ARTERY WITH 30 MG.ML ⁻¹ (18.8 MOL.M ⁻³) P ₁₁₋₄ , C AND F; DECELLULARISED PORCINE INTERNAL CAROTID ARTERY WITH 30 MG.ML ⁻¹ (18.8 MOL.M ⁻³) P ₁₁₋₄ -CRGD. 10 X MAGNIFICATION.	204
FIGURE A.1; IMAGES OF PEPTIDE P ₁₁₋₄ AT CONCENTRATIONS OF 30 MG.ML ⁻¹ (18.8 MOL.M ⁻³), 15 MG.ML ⁻¹ (9.4 MOL.M ⁻³), 5 MG.ML ⁻¹ (3.13 MOL.M ⁻³) AND 1 MG.ML ⁻¹ (0.63 MOL.M ⁻³) AT PH 8, PH 7 AND PH 5.	218

FIGURE A.2; IMAGES OF PEPTIDE P₁₁₋₄ AT CONCENTRATIONS OF 30 MG.ML⁻¹ (18.8 MOL.M⁻³), 15 MG.ML⁻¹ (9.4 MOL.M⁻³), 5 MG.ML⁻¹ (3.13 MOL.M⁻³) AND 1 MG.ML⁻¹ (0.63 MOL.M⁻³) IN SOLUTIONS OF PBS AND RINGER'S SOLUTION. 219

FIGURE A.3; FLUORESCENT CROSS SECTION IMAGE OF SELF-ASSEMBLED PEPTIDE P₁₁₋₄, 30 MG.ML⁻¹ (18.8 MOL.M⁻³) FLUORESCIN TAGGED P₁₁₋₄ MIXED 1:50 WITH UNTAGGED P₁₁₋₄. A; 10X MAGNIFICATION, B; 20X MAGNIFICATION. 220

FIGURE A.4; RESULTS OF CH50 ASSAY SHOWING PERCENTAGE OF ERYTHROCYTES LYSSED AT DIFFERENT COMPLEMENT DILUTIONS WITH A LINE HIGHLIGHTING THE POINT OF 50 % LYSIS. 220

FIGURE A.5; POSITIVE AND NEGATIVE CONTROLS OF CHANDLER LOOP THROMBOSIS MODEL, * = SIGNIFICANT DIFFERENCE FROM THE POSITIVE CONTROL. 221

List of Tables

TABLE 2-1; CELLS USED THROUGHOUT THE STUDY INCLUDING SUPPLIER.....	70
TABLE 2-2; PRIMARY ANTIBODIES USED THROUGHOUT THE STUDY	71
TABLE 2-3; SECONDARY ANTIBODIES USED THROUGHOUT THE STUDY	72
TABLE 2-4; ISOTYPE CONTROL ANTIBODIES USED THROUGHOUT THE STUDY	72
TABLE 3-1; OBSERVED RESULTS FOR SELF-ASSEMBLY METHOD FOR DIFFERENT CONCENTRATIONS OF P ₁₁ -4.....	118
TABLE 4-1; PEPTIDES USED IN THE STUDY; PEPTIDE NAME, STRUCTURE, CHARGE AND MOLECULAR WEIGHT.....	155
TABLE 4-2; COLLECTED RESULTS OF BIOCOMPATIBILITY AND HAEMOCOMPATIBILITY TESTING	188
TABLE A-1; LIST OF LABORATORY EQUIPMENT USED THROUGHOUT STUDY WITH UK SUPPLIERS.	215
TABLE A-2; LIST OF CHEMICALS AND REAGENTS WITH SUPPLIER.....	217

List of Abbreviations

ADP	Adenosine diphosphate
ANOVA	Analysis of variance
ATP	Adenosine triphosphate
bFGF	Basic fibroblast growth factor
BHK	Baby hamster kidney
BSA	Bovine serum albumin
BSE	Bovine spongiform encephalopathy
CABG	Coronary artery bypass graft
cAMP	Cyclic adenosine monophosphate
CD	Cluster of differentiation
CHAPS	3-[(3-cholamidopropyl)dimethylammonio]-1-propanesulfonate
CH50	50% complement lysis
CLSM	Confocal laser scanning microscope
cRGD	Cyclic RGD (arginine-glycine-aspartic acid)
CVD	Cardiovascular disease
DABCO	1,4-diazabicyclo octane
DAPI	4', 6-diamidino-2-phenylindole
DMEM	Dulbecco's modified Eagles medium
DMSO	Dimethyl sulfoxide
DNA	Deoxyribonucleic acid
DPBSa	Dulbecco's phosphate buffered saline
DPICA	Decellularised porcine internal carotid artery
ECGF	Endothelial cell growth factor
ECM	Extracellular matrix
EDTA	Disodium ethylenediaminetetra acetic acid
ePTFE	Expanded polytera-fluroethylene
FEGSEM	Field emission gun scanning electron microscope

FITC	Fluorescein isothiocyanate
Fmoc	Fluorenylmethyloxycarbonyl
Fmoc-FF	Fmoc-diphenylalanine
FTIR	Fourier transform infrared
<i>gas</i>	Growth arrest specific (gene)
GMEM	Glasgow minimum essential medium
GP	Glycoprotein
HCl	Hydrochloric acid
H&E	Haematoxylin and Eosin
HIV	Human immunodeficiency virus
Ig	Immunoglobulin
IR	Infrared
KGM	Konjac glucomannan
LDL	Low-density lipoprotein
MAC	Membrane attack complex
MBP	Mannan binding protein
MPLSM	Multi-photon laser scanning microscope
MSD	Mean significant difference
M-199	Medium 199
NaOH	Sodium hydroxide
PAD	Peripheral artery disease
PBS	Phosphate buffered saline
PEG	Poly ethylene glycol
PERV	Porcine endogenous retro virus
PGA	Polyglycolic acid
PLA	Polylactic acid
PLGA	Poly(lactic-co-glycolic) acid
POSS-PCU	Polyhedral-oligomeric-silesquioxane-poly(carbonate-urea) urethane
PVC	Polyvinyl chloride

RGD	Arginyl-glycyl-aspartic acid (arginine-glycine-aspartic acid)
RNA	Ribonucleic acid
SD	Standard deviation
SE	Standard error
SEM	Scanning electron microscope
SDS	Sodium dodecyl sulphate
SMC	Smooth muscle cell
TBS	Tris buffered saline
TF	Tissue factor
TFA	Trifluoroacetic acid
TFPI	Tissue factor pathway inhibitor
Tg	Glass transition temperature
TPB	Tryptone phosphate broth
VEGF	Vascular endothelial growth factor
vWF	von Willebrand factor

1 Introduction

1.1 Clinical need

Cardiovascular disease (CVD) is the main cause of mortality in the UK with almost 200,000 deaths a year attributed to CVD (Capewell et al., 2008). Over 100,000 people a year in the UK are diagnosed with peripheral artery disease (PAD), a major indicator of widespread atherosclerosis (Belch et al., 2007). Around 40 % of people who are diagnosed with PAD are symptomatic and require some form of intervention ranging from lifestyle changes to surgical bypass dependent upon the severity of the disease (Belch et al., 2007). Medication and vascular stenting are widely used to control and treat vascular disease; however, in some cases there is no other option than to perform a vascular bypass graft. In the UK over 29,000 coronary artery bypass grafts (CABG) are performed each year (Allender et al., 2008). Medical intervention techniques have had reasonable success with large diameter (>6 mm) grafts maintaining high long term patency rates. However, small diameter (<6 mm) grafts often fail due to thrombosis and occlusion. There is currently a high demand for small diameter grafts which have high patency rates and remain fully functional.

1.2 Blood vessels

1.2.1 Structure

Arteries and veins with a diameter less than 6 mm are taken to be small blood vessels (Zhang et al., 2007). Capillaries whilst small in scale have significantly different structures and functions and are not the target of surgical interventions. The basic structure of an artery and vein is similar (Figure 1.1) with the only differences being related to the elastin content, vessel size and thickness with veins also having valves to prevent the back flow of blood. Arteries handle higher pressures than veins and so have thicker layers of muscle; in a similar manner, the level of elastin in an artery is higher than that found in a vein and reduces the further away from the heart the artery gets as the vessel is required to handle less pressure. The structure of a large blood vessel is the same as the structure of a smaller blood vessel: as the vessel size

decreases, so does the thickness of the layers that make up the blood vessel (Mulvany and Aalkjaer, 1990). The vessel is composed of three layers, the tunica interna (intima), the tunica media (media) and the tunica externa (adventitia) (Zhang et al., 2007). The intima is the inner most layer of the vessel and is constructed of a longitudinal monolayer of vascular endothelial cells that are in contact with the blood flow. The endothelial cells are attached to a subendothelial layer that is comprised of connective tissue that is interlaced with an internal elastic lamina (Bou-Gharios et al., 2004, Zhang et al., 2007). The elastic lamina is a membrane comprised of elastic fibres that anastomose with each other forming a netlike structure that is found in-between each of the layers (Bou-Gharios et al., 2004, Venkatraman et al., 2008). The media is the middle layer of a blood vessel; it is comprised of circumferentially arranged layers of vascular smooth muscle cells (Bou-Gharios et al., 2004, Zhang et al., 2007). The number of smooth muscle cell layers changes with the size of the vessel and the location in the body (Mulvany and Aalkjaer, 1990). The smooth muscle cells are surrounded by extracellular matrix (ECM), made up of collagen, elastin and fibrillin, that is rich in proteoglycans and orientated in the same direction as the cells (Bou-Gharios et al., 2004). The adventitia is comprised of connective tissue, collagen and elastin, separated from the media by an external elastic lamina and primarily contains adventitial fibroblasts (Bou-Gharios et al., 2004, Zhang et al., 2007). Nerves are believed to play a major role in vascular function, however, nerves are sparse in blood vessels and are limited to the adventitia and do not penetrate into the other layers (Mulvany and Aalkjaer, 1990).

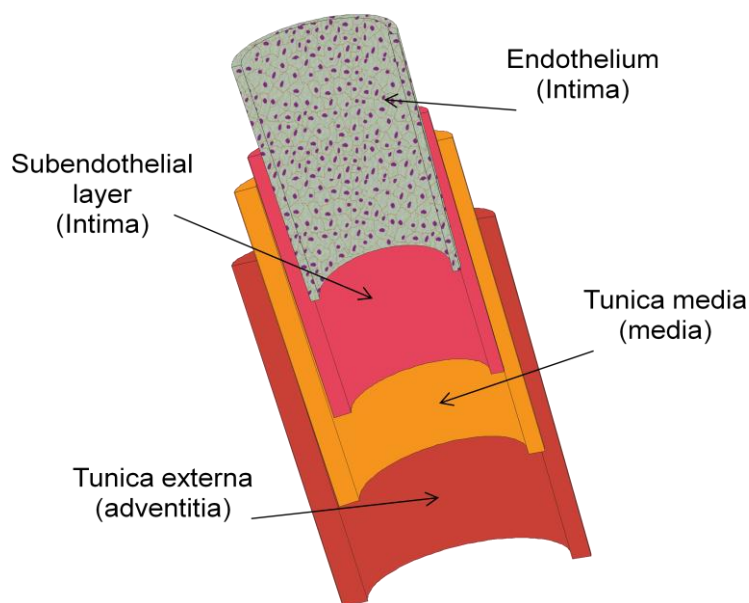


Figure 1.1; Schematic of blood vessel structure

1.2.2 Extracellular matrix

The structure and composition of the ECM is specific to each tissue and location (Nisbet et al., 2009). The ECM of a blood vessel is made of a range of fibrous proteins (collagen and elastin being the most abundant), linker proteins (fibrillin, fibronectin, laminin, etc) and space filling glycosaminoglycans important to normal vessel function. These molecules are ordered into a 3-dimensional network via self-assembly and cell directed assembly/remodelling (Chen and Hunt, 2007). The ECM also acts as a reservoir for soluble macromolecules (growth factors, cytokines etc) and acts to control the diffusion of soluble factors (Chen and Hunt, 2007). The different constituents of the ECM of blood vessels have different turnover rates; overall, the blood vessel ECM has a slow turnover time (Stock et al., 2001, Bou-Gharios et al., 2004). The different layers of a blood vessel have different ECM compositions.

Of the many different types of collagen known to exist in blood vessels, collagen types I and III are the major fibrillar collagens in the vessel representing 60 % and 30 % of the collagen, respectively (Jacob et al., 2001). The remaining collagens found in blood vessels are fibrillar collagen type V, fibril-associated collagens with interrupted triple helices (FACIT) type XII and type XIV, micro-fibrillar collagen type VI, basement-membrane collagen type IV and collagen type VIII (Jacob et al., 2001).

Elastin is the major component that imparts elasticity to tissues. Elastin forms part of an elastic fibre and requires the presence of other extracellular proteins to assemble outside the cell (Wagenseil and Mecham, 2009). Most of the elastin in a blood vessel is found in the medial layer and is arranged in lamellae with collagen fibres and layers of proteoglycan rich ECM with smooth muscle cells in between; the elastic lamellae are connected in 3-dimensions with thin elastic fibres which also connect the lamellae with the smooth muscle cells (Wagenseil and Mecham, 2009).

There is a distinct difference between elastin and elastic fibres: elastin is an amorphous gel like material, whereas elastic fibres are complex structures made of elastin and microfibrils (Rock et al., 2004, Kozel et al., 2005, Wagenseil and Mecham, 2009). Microfibrils are made of fibrillin molecules and are needed for the formation of elastic fibres; microfibrils are present in the body without elastin but rarely is elastin found without microfibrils (Rock et al., 2004, Kozel et al., 2005, Wagenseil and Mecham, 2009). The mammalian elastin gene encodes a protein called tropoelastin which is around 60 -70 kDa; tropoelastin has an arrangement of hydrophobic sequences alternating with lysine-containing cross-linking motifs (Rock et al.,

2004, Kozel et al., 2005, Wagenseil and Mecham, 2009). In the ECM >80 % of the lysine residues in tropoelastin are modified to form covalent cross-links (Rock et al., 2004, Kozel et al., 2005, Wagenseil and Mecham, 2009). It is the cross-linked form of tropoelastin that gives the functional form of the protein. The large number of elastin cross-links is responsible for the recoil properties that contribute to the mechanical properties of a blood vessel; the cross-linking is also responsible for the insolubility and longevity of the protein, where <1 % of total body elastin is turned over in one year (Wagenseil and Mecham, 2009).

It is believed that tropoelastin released from cells is cross-linked by lysyl oxidase to make elastin; elastin is then “chaperoned” to microfibrillar scaffolds where the elastin and microfibrils assemble into elastic fibres (Figure 1.2)(Rock et al., 2004, Kozel et al., 2005, Wagenseil and Mecham, 2009). Other ECM proteins fibronectin, vitronectin, laminin, entactin/nidogen, tenascin and thrombospondin play essential roles in the structure and function of the ECM, comprising a multi-domain structure that could enable the interaction of cells and other ECM components (Jacob et al., 2001).

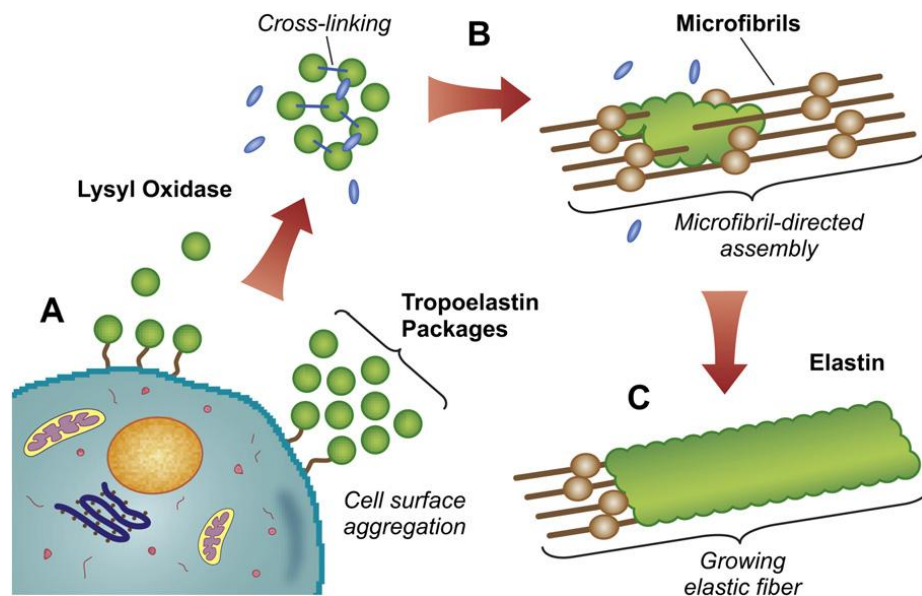


Figure 1.2; Schematic of classical model of elastogenesis, A. Tropoelastin released from cells and cross-linked into elastin. B. Elastin molecules “chaperoned” to microfibrils assembly. C. Elastin and microfibrils assemble to form elastic fibres. Taken from (Moore and Thibeault, 2012).

There are numerous proteoglycans contained in the vascular wall: large aggregating proteoglycans such as aggrecan and versican, small non-aggregating proteoglycans including

biglycan, decorin and fibromodulin and cell associated proteoglycans such as syndecan (Jacob et al., 2001). Aggrecan and versican belong to a family of hyaluronan-binding proteoglycans that play important roles in ECM structure, biomechanical properties and also influence cellular behaviour (Wight, 2002). Versican expression is upregulated in vascular smooth muscle cells by mitogens, such as platelet-derived growth factors which contribute to the expansion of pericellular ECM needed for smooth muscle cell migration and proliferation (Wight, 2002).

It has been reported that biglycan, secreted from endothelial and smooth muscle cells, binds to collagen and is actively involved in the control of collagen deposition. Mutations in biglycan gene expression have been observed to result in abnormal collagen fibrils in tendons; the effect upon the vasculature is unknown. However, high levels of biglycan have been observed in diseased arteries (Shimizu-Hirota et al., 2004). Biglycan has been reported to increase the migration and proliferation of vascular smooth muscle cells and the overexpression of biglycan in transgenic mice has shown resultant thickening of the medial layer (Shimizu-Hirota et al., 2004). Normal arterial media and intima are rich in biglycan but have little to no decorin which is found in the adventitia (Riessen et al., 1994). High levels of biglycan and decorin have been observed in atherosclerotic plaque linked to collagen types I and III. Nonetheless, no biglycan or decorin have been observed linked to collagen type IV, indicating that these proteoglycans are not part of the basement membrane (Riessen et al., 1994).

Fibromodulin regulates collagen fibril formation binding to a different site on collagen than decorin (Hocking et al., 1998). Fibromodulin and decorin interact with collagen to inhibit fibrillogenesis and control fibre diameter resulting in thinner fibre diameters (Hocking et al., 1998). Syndecans are heparin sulphate proteoglycans that can interact with a wide range of growth factors, cytokines, chemokines, and ECM molecules involved in cell growth and attachment (Alexopoulou et al., 2007). Results from experimental models show that syndecans are involved in endothelial cell growth and migration (Alexopoulou et al., 2007).

1.2.3 Cells

The vascular ECM is synthesised by three cell types: intimal endothelial cells, medial smooth muscle cells and adventitial fibroblasts (Jacob et al., 2001). Smooth muscle and endothelial cells show a range of functionality and diverse phenotypes. The cells may exhibit different

characteristics, such as different morphologies, behaviour, biochemical or physiological properties and different development pathways (Bou-Gharios et al., 2004).

The endothelial cells of small arteries form a continuous cover and are reported to project through fenestrations in the elastic lamina and make contact with the smooth muscle cells in the media layer, allowing for endothelial control of vascular contraction (Mulvany and Aalkjaer, 1990). In the intima, the endothelial cells produce and attach to a basal lamina that is supported on the internal elastic lamina (Wagenseil and Mecham, 2009). Vascular endothelial cells produce elastin and so are believed to contribute to the formation and maintenance of the internal elastic lamina (Wagenseil and Mecham, 2009). Whilst endothelial cells maintain some fundamental features regardless of their origin, site-specific differences can be seen between endothelial cells from different locations (Murphy et al., 1998). As well as the different makeup of the ECM affecting the cells, endothelial cells residing in different mechanical environments have been demonstrated to have different characteristics (Topper and Gimbrone Jr, 1999, Nerem, 2000, Chiu et al., 2009, O'Keeffe et al., 2009). The differences between endothelial cells relates not only to their metabolic activity but also to their response to inflammation and tissue damage (Murphy et al., 1998). As such, it is believed that endothelial cell dysfunction is one of the key initiators in CVD.

Around 70 % of the volume of the tunica media comprises mainly smooth muscle cells (SMC) (Mulvany and Aalkjaer, 1990). The number of smooth muscle cell layers in the tunica media decreases with decreasing vessel size (Mulvany and Aalkjaer, 1990). The smooth muscle cells in the tunica media are arranged circumferentially with a slight pitch angle ($< 2^\circ$) and are connected by membranous contacts (Mulvany and Aalkjaer, 1990). It has been reported that the embryonic origins of vascular SMCs arise from different distinct sources dependent upon the vessel location and even from different sources in the same vessel (Wagenseil and Mecham, 2009). Coronary SMCs display a highly differentiated phenotype. However, SMCs from other vascular beds, aorta and Iliac arteries, show greater phenotypic heterogeneity (Patel et al., 2000). Vascular smooth muscle cells can become activated by several mechanical, haemo-dynamic or infectious factors that lead to a change in the cellular composition of the vessel, which in turn is associated with several CVDs (Patel et al., 2000).

The cells found in the adventitia are mainly fibroblasts, mast cells and macrophages with a small number of Schwann cells that are associated with nerve axons (Mulvany and Aalkjaer, 1990). Fibroblasts are the predominant long-lived stromal cell type, the main feature of which is ECM production. Fibroblasts are a heterogeneous cell population and can vary widely in

smooth muscle α -actin content, morphology, and organisation of structures involved in adhesion, *in vitro* (Sartore et al., 2001). Adventitial fibroblasts in models of vessel injury have been observed to be converted into smooth muscle-like cells (Sartore et al., 2001). Activation of fibroblasts induces contraction that correlates to smooth muscle α -actin content and the development of a micro-filamentous cytoplasmic system, fibronexus junctions and other smooth muscle cell properties leading to the formation of hybrid cells called myofibroblasts (Sartore et al., 2001). The tunica adventitia has a high collagen content produced by a heterogeneous population of adventitial myofibroblasts (Wagenseil and Mecham, 2009). Adventitial fibroblasts can migrate and overgrow medial SMCs to become myofibroblasts that display α -SM actin expression (Patel et al., 2000). Stimulation of coronary adventitial fibroblasts resulted in changes typically attributed to “synthetic” SMCs (Patel et al., 2000).

The cells of a blood vessel play a major role in vascular repair with several mechanisms for this proposed. One idea, based on observations of cultured vascular SMCs losing their contractile features and becoming “synthetic” cells, assumes the cells involved in vascular repair are SMCs and that all medial SMCs modulate their phenotype in response to stimulation (Patel et al., 2000). The second concept suggests an heterogeneity of medial SMCs with only a fraction of the cells being able to rapidly respond to stimulation (Patel et al., 2000). The third concept is that vascular repair is due to non-muscle cells, adventitial fibroblasts, that proliferate and migrate from the adventitia into the medial and intimal layers (Patel et al., 2000). Whilst there is much debate as to which concept is correct, they are not mutually exclusive. Regional differences have been observed in arterial repair suggesting that different vessels may repair in different ways dependent upon the function of the different vascular phenotypes (Patel et al., 2000). Medial smooth muscle cells and adventitial fibroblasts have a high capacity to synthesise new ECM and protease inhibitors, although new ECM from repair is never as organised as the ECM synthesised during development (Jacob et al., 2001).

1.2.4 Mechanical properties

The ability of the vasculature to respond to the flow of blood has been well documented. There is conclusive evidence that biomechanical forces have a direct effect on endothelial structure and function (Resnick et al., 2003). Arteries have many different mechanical properties, all of which contribute to the normal health of the vessel. The main mechanical

force placed on the vasculature is stress. Stresses on a vessel wall include shear stresses from the flow of blood across the vessel, longitudinal stresses from surrounding tissue and circumferential stresses from the blood pressure (Wagenseil and Mecham, 2009). Mechanical stimuli can be “sensed” and recognised by a number of different “sensors”. Integrins can be used to transduce mechanical stimuli into biochemical signals. Cell-cell-junction molecules that undergo changes in response to mechanical stimuli can change cell interactions. Adherence junctions in endothelial cells can interact with the cytoskeleton and transfer information intracellularly. Membrane structures such as flow activated ion channels, flow activated receptors, caveolae (cholesterol rich areas of the membrane with high numbers of signalling molecules) and mechanotransducing G proteins can also function as mechano-sensors (Resnick et al., 2003, Chatzizisis et al., 2007).

In healthy individuals a shear stress in the range of 0.5 – 4 Pa is normally experienced by the endothelial cells as a result of blood flow (Resnick et al., 2003, Qiao et al., 2006). Changes in the artery structure can create regions of re-circulated flow where the shear stress can vary greatly. This can lead to vascular remodelling and even disease states such as atherosclerosis (Resnick et al., 2003). Atherosclerosis may be linked with shear stress as atherosclerosis is most likely in areas of the vasculature like branch points, the outer wall of bifurcations and the inner wall of curvatures, where disturbed blood flow occurs (Chatzizisis et al., 2007). It has been reported that endothelial cells require shear stress to adopt the correct characteristics for formation of healthy endothelium and that loss of this shear stress could result in endothelial dysfunction and so trigger atherosclerosis (Resnick et al., 2003, Chatzizisis et al., 2007).

Circumferential stress is important to an artery’s ability to handle the changes in blood pressure as blood moves through the vasculature in a pulsatile fashion. The circumferential stress in a vessel wall is dependent upon the force being applied by the blood, and the thickness, composition and uniformity of the vessel wall. In disease states, such as atherosclerosis and aneurysm, the uniformity of the vessel wall is severely compromised and can lead to changes in the circumferential stresses within the vessel wall (Cheng et al., 1993, Lee et al., 1996). It is believed that one of the factors that can contribute to rupture of atherosclerotic lesions is the build-up of circumferential stress. However, rupture does not always happen at the site of highest stress suggesting that other factors are involved as well (Cheng et al., 1993, Lee et al., 1996).

Vascular distensibility is the resistance presented by a vessel to stretching and swelling. Arterial distensibility is complex. The internal mammary artery has been shown to have a distensibility of between 56 and 47 Pa at pressures between 50 and 150 mmHg (Chamiot-Clerc et al., 1998). When the vessel is relaxed, the distensibility is dependent upon the amount, arrangement and characteristics of the connective tissue. When under pressure the distensibility is dependent upon the amount and type of connective tissue, the fraction volume and activity level of smooth muscle cells all of which is influenced by the intravascular pressure (Mulvany and Aalkjaer, 1990).

The widest reported measure of blood vessels' mechanical properties is the burst pressure. The saphenous vein has a burst pressure of 1599 ± 877 mmHg (n=7) and the internal mammary artery has a burst pressure of 3196 ± 1264 mmHg (n=16), both commonly used in coronary artery bypass surgery, where the coronary artery has a burst pressure > 2300 mmHg (Lamm et al., 2001, Conklin et al., 2002, Konig et al., 2009). Most blood vessels will normally only handle arterial pressures in the range of hundreds of mmHg and so blood vessels can withstand much higher pressures than experienced giving a degree of safety. This means that the vessels are unlikely to burst or plastically deform under normal *in vivo* conditions (Nerem, 2000).

Arterial compliance is the change in blood volume due to a given blood pressure and is an index of the elasticity of arteries. Internal mammary artery and common femoral artery have been shown to have a compliance of 5.4% to 9.8% dilation at pressures between 50 and 2000 mmHg (Chamiot-Clerc et al., 1998, Wilshaw et al., 2011) Endothelial dysfunction can cause a reduction in compliance as can hypertension and aging; some diseases such as diabetes can cause a reduction in compliance as can smoking cigarettes (Cohn, 2001). A reduction in arterial compliance can cause or exacerbate hypertension, can aggravate atherosclerosis and is a risk factor and indicator of CVD (Cohn, 2001). It has been shown that arteries respond to changes in blood flow by remodelling the diameter of the vessel to keep the wall shear stress the same. Where compliance is mismatched in bypass grafts, the flow rate of blood is changed and intimal growth can be stimulated to increase the wall shear stress; this can ultimately lead to the narrowing and occlusion of the vessel, resulting in failure of the graft (Stewart and Lyman, 1992). Compliance mismatch can also cause the degradation of the graft and result in aneurysm formation. The biomechanical properties of an artery are important stimuli for the growth, development, remodelling and maintenance of arteries and are required for normal vessel function.

The mechanical properties of the coronary artery have been shown to change dependent upon age and sex. Below the age of 50 it has been shown that the coronary artery dilates about 10% when subjected to physiological pressure (60 – 140 mmHg) over the age of 50 there is a decrease in compliance (Ozolanta et al., 1998). The elastic modulus of the arterial walls slowly increases with age going from around 1 MPa to around 4 MPa, this increase in elastic modulus is higher after the age of 50 and is higher in men than in women (Ozolanta et al., 1998).

The mechanical properties of bypass grafts are important to the success of the graft. If the bypass graft is not able to match the mechanical properties of the natural vessel this can lead to intimal hyperplasia, aneurysm formation, cellular dysfunction, thrombus formation and graft failure. This can be seen in the failure of early attempts to use synthetic grafts which did not possess the correct mechanical properties. Much of the focus on the design of grafts is on matching the mechanical properties.

1.3 Arterial disease

Cardiovascular disease is the biggest killer in the developed world and has many different forms. Most forms of vascular disease have been linked to or commonly occur as a result of atherosclerosis. Atherosclerosis is the formation of a lesion in the vessel wall. Initially, atherosclerosis was considered to mainly be caused by the accumulation of lipids within the arterial wall as high levels of cholesterol, in particular low-density lipoprotein (LDL) cholesterol, is the primary associated risk factor (Stary et al., 1994, Epstein and Ross, 1999). A second theory linked atherosclerosis to damage: it is believed that atherosclerosis is the result of the vessel's response to injury, in particular the response to damage or dysfunction of the endothelium (Stary et al., 1994, Epstein and Ross, 1999, Libby et al., 2002). There is much debate over the causes of atherosclerosis, however, advances in the understanding of cellular and molecular mechanisms has lead to a wider adoption of the "response to injury" hypothesis.

Atherosclerosis is a series of highly specific cellular and molecular responses and reactions that can be best described as an inflammatory disease. Most of the data available on atherosclerosis is related to the coronary arteries and aorta as this is the area in which major life threatening conditions occur (Stary et al., 1994). The different stages of the disease can be considered as three distinct lesions that represent a stage in the chronic inflammation of the

arterial wall (Epstein and Ross, 1999, Libby et al., 2002). There are many possible causes of atherosclerosis: elevated LDL cholesterol, free radical damage (mainly caused by cigarette smoking), hypertension, diabetes, infectious microorganisms (herpes viruses, *Chlamydia pneumonia* etc), genetic mutations, and combinations of these and other factors (Epstein and Ross, 1999). The damage or dysfunction of the endothelium results in a change in the homeostatic properties of the vessel, allowing the increased adhesion of leukocytes to the vessel wall and causing increased endothelial permeability (Epstein and Ross, 1999, Libby et al., 2002). Endothelial dysfunction also results in a change from the endothelium having anticoagulant properties to pro-coagulant properties. The attachment of these cells and various factors forms the initial lesion most often observed in children or in areas of the vasculature not prone to lesion formation. The lesion initially consists of lipid-laden monocytes and macrophages along with T lymphocytes; as the lesion becomes more distinctly defined it becomes known as a fatty-streak (Figure 1.3) (Stary et al., 1994, Epstein and Ross, 1999).

If the initial response is not effectively neutralised, the secretion of growth factors, cytokines and other inflammatory products from the monocytes, lymphocytes and macrophages can cause the migration and proliferation of SMCs (Epstein and Ross, 1999). The inflammatory response causes medial SMCs to express enzymes that degrade the collagen and elastic fibres of the ECM and permits the penetration of SMCs through the elastic lamina and into the lesion (Libby et al., 2002). The SMCs become intermixed with the area of inflammation to form an intermediate lesion (Epstein and Ross, 1999). There are areas of the vasculature, the coronary arteries for example, where lesion progression is more likely (Stary et al., 1994).

As the SMCs proliferate, the lesion thickens and the artery wall compensates by dilating/remodelling (Epstein and Ross, 1999). Expansion and continued inflammation results in the recruitment of higher numbers of macrophages and lymphocytes which migrate from the blood and multiply within the lesion. These cells release more enzymes, cytokines, chemokines and growth factors which cause further damage. This reaction forms a cycle of mononuclear cell recruitment followed by SMC migration and proliferation that leads to the formation of more fibrous tissue causing the expansion of the lesion into an advanced complicated lesion (Figure 1.3) (Epstein and Ross, 1999). The progress of a fatty-streak lesion into an intermediate and advanced lesion involves the formation of a fibrous cap that walls off the lesion from the lumen and contains a reservoir of leukocytes, lipids, debris and can contain necrotic tissue (Epstein and Ross, 1999). The lesion eventually grows too large and begins to alter and obstruct blood flow as the artery cannot compensate.

The distinctions that separate the individual lesion types are based on constant morphological characteristics that represent a temporary or permanent stabilisation. As the lesions can stabilise at each step, the progression from fatty-streak to intermediate lesion to advanced lesion may require an additional stimulus (Stary et al., 1994). Some lesions are stable and have a uniform dense fibrous cap, while others are unstable and pose a major health risk.

Rupture of the fibrous cap often results from enzymatic action that can be stimulated in many different ways. The most implicated cause is an immune response where activated T cells are known to stimulate macrophages in the lesion to produce metalloproteinases (Epstein and Ross, 1999, Libby et al., 2002). The action of the T lymphocytes on the macrophages causes the heightened expression of pro-coagulant tissue factor (Libby et al., 2002). Rupture of the fibrous cap can lead to haemorrhage from the vasa vasorum, from the lumen of the artery and the release of tissue factor resulting in thrombus formation and occlusion (Figure 1.3). Rupture of the lesion is responsible for the most acute complications of atherosclerosis with as much as 50 % of acute coronary syndromes and myocardial infarctions being caused by plaque rupture and resultant thrombosis (Epstein and Ross, 1999, Libby et al., 2002).

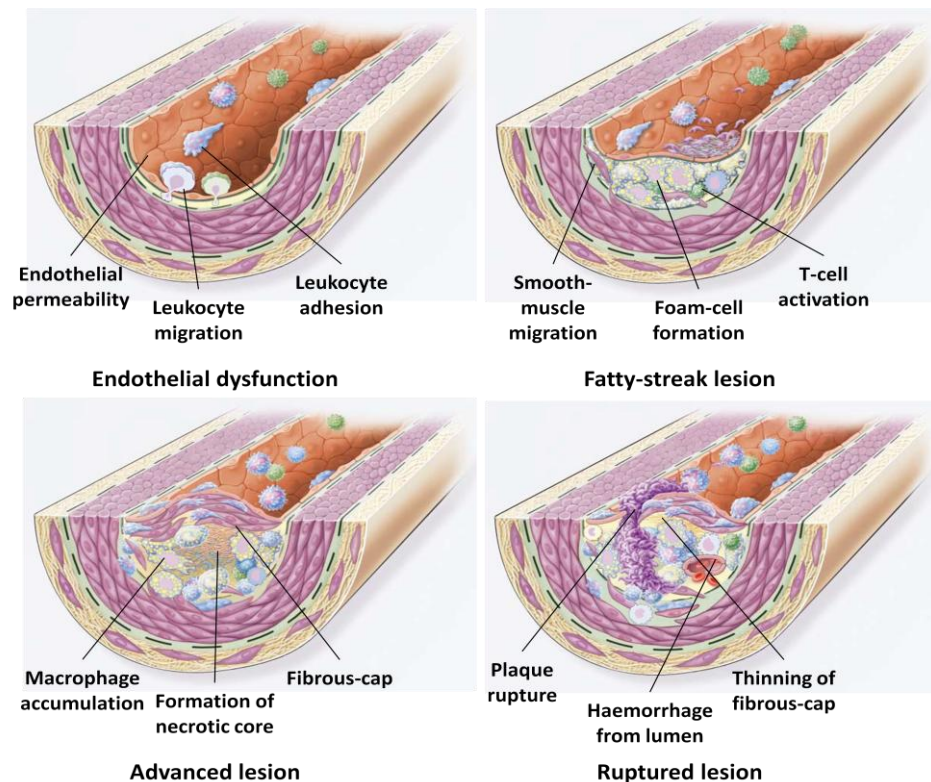


Figure 1.3; Schematic of endothelial dysfunction, fatty-streak lesion, advanced lesion and lesion rupture in atherosclerosis adapted from (Epstein and Ross, 1999)

Aneurysms are a major concern in CVD. Aneurysms can be fatal themselves if they rupture, but they can also be sites for the formation of thrombus that lead to strokes. An aneurysm is a localised swelling or bulging of the blood vessel wall. The most common site for aneurysms to form is in the aorta, but they are widely seen at the base of the brain and can be found in any vasculature (Virmani et al., 1986).

Aneurysm is the result of an injury overcoming the capacity of smooth muscle cells or adventitial fibroblasts to synthesise new ECM and repair the damage to the vessel (Jacob et al., 2001). The balance between proteases and their inhibitors is temporally destroyed by the expression of matrix metalloproteinase genes and the secretion of enzymes from inflammatory cells (Jacob et al., 2001).

Aneurysms of the artery are characterised by abnormal, localised or diffuse dilation of the arterial wall and can be caused by a range of conditions including but not limited to: atherosclerosis, that narrows and hardens the arteries weakening the walls; hypertension, that expands the vessel wall beyond its elastic limit; injury, that thins and weakens the arterial wall; congenital anomalies, where weaknesses are created or exist in the vessel wall as a symptom of a disease or disorder; or by ageing, where the vessel is weakened over time.

Aneurysms can be congenital or acquired; the majority of adults with aneurysm suffer from the acquired condition (Virmani et al., 1986). Acquired aneurysms in children are most commonly due to Kawasaki's disease, a disease that affects the lymph nodes. In adults, arterial aneurysms are commonly found alongside atherosclerosis suggesting that there could be a link between atherosclerosis and arterial aneurysm (Virmani et al., 1986). The cause of arterial dilation and aneurysms is widely debated with suggestions that it is directly caused by atherosclerosis. Others propose that weaknesses in the vessel wall could be present from childhood and that factors such as hypertension and atherosclerosis may only play a role in the rupture of an aneurysm (Virmani et al., 1986, Kamitani et al., 2000).

There are many disease states that are involved in aneurysms. What is not clear is the actual role these different diseases have in aneurysm formation and rupture. This is further complicated by the observable differences dependent upon the location of the aneurysm in the vasculature. Arterial aneurysm is a progressive degenerative disease that, if left uncorrected, can result in rupture and in many cases death.

It is likely that increased production of matrix degrading enzymes such as matrix metalloproteinases plays a key role in the pathogenesis of arterial aneurysm (Raffetto and

Khalil, 2008). The expression of matrix metalloproteinases in patients with aortic aneurysms has been observed to be significantly increased and transgenic animals with deficiencies in matrix metalloproteinases have been shown to be protected from experimentally induced aneurysm (Raffetto and Khalil, 2008).

The most common matrix metalloproteinase, MMP-9, has been shown to be the most abundantly expressed enzyme in aneurysms and is mainly produced by aneurysm-infiltrating macrophages (Raffetto and Khalil, 2008). Matrix metalloproteinases have been observed to prevent the contraction of SMCs; SMC contraction has been shown to contribute to the structural integrity of the arterial wall. Matrix metalloproteinase have also been shown to induce inhibition of SMC contraction and may therefore contribute to further weakening of the arterial wall (Raffetto and Khalil, 2008).

There are a range of treatment methods dependent upon the location of an aneurysm. Aortic or peripheral aneurysms tend to be treated by replacement with bypass grafts. Intracranial aneurysms are treated with surgical clips or endovascular coiling. Endovascular coiling involves placing a platinum coil in the aneurysm via a catheter, resulting in clot formation which, if successful, eliminates the aneurysm.

1.4 Approaches to developing small diameter blood vessel replacements

1.4.1 Autografts

An autograft is the transplantation of a tissue from one area of a patient's body to another. In the case of vascular surgery, an artery or vein is removed from a site of easy access and used for the purposes of a bypass or to repair damage, as in the case of an aneurysm. An autograft is a surgeon's preferred option and is the gold standard to which all other vessel replacements are compared (Reix et al., 2000, Arima et al., 2005, Leask et al., 2005, Wang et al., 2007c). The choice of vessel for autograft is dependent upon the intended use. The standard vessel used for the repair of a popliteal artery aneurysm is the saphenous vein (Reix et al., 2000). In the case of a coronary artery bypass, the graft of choice is the left internal thoracic artery, also known as the internal mammary artery (Figure 1.4) (Arima et al., 2005, Baguneid et al., 2006).

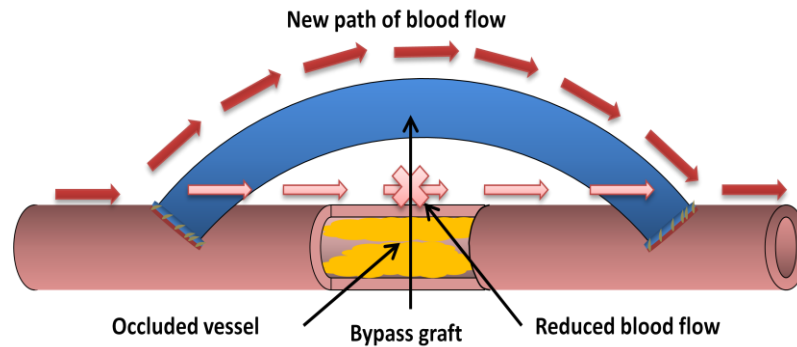


Figure 1.4; Schematic of bypass graft

Bypass grafts are placed at as shallow an angle as is possible when being implanted as to reduce the disturbance to the flow of blood which has been linked to the development of several CVDs. It is possible to use the saphenous vein for coronary bypass surgery but the use of arteries is favoured where possible. Comparison studies have shown that saphenous vein is more prone to intimal thickening and atherosclerosis than arterial grafts, such as the internal mammary artery; arterial grafts also have a higher rate of long-term patency (Uydes-Dogan et al., 1996, Taki et al., 1997). Current saphenous vein autografts suffer from a 30 % to 50 % occlusion rate after ten years, whilst arterial grafts have a failure rate of around 5 % in the same period (Uydes-Dogan et al., 1996, Taki et al., 1997, Wang et al., 2007c). The use of saphenous vein is more complex and prone to failure as the tributaries to the vein have to be tied off and the valves removed (Arima et al., 2005, Leask et al., 2005). Arteries have also been shown to respond to vasodilators, an important medication post-operatively to treat graft spasm that has been related to an increased risk of morbidity and mortality (Uydes-Dogan et al., 1996).

Autografts are known to fail due to surgical difficulties. They are often subject to intimal thickening at the anastomosis due to graft-wall shear stress and surgical trauma at the points of suture (Leask et al., 2005). Autologous vessel transplant still remains the gold standard in vascular surgery; the main problem with autografts is the limited availability of viable grafts as a third of patients are not suitable for autografts due to pre-existing vascular disease or prior graft harvest (Wang et al., 2007c, Cittadella et al., 2013).

1.4.2 Allografts

An allograft is the transplantation of a tissue from a genetically non-identical member of the same species. Allografts are more often thought of in terms of whole organ transplantation. The lack of available autografts means that alternative graft material must be considered for vascular replacement. Allograft transplantation is the next logical step as it provides an endothelium lined human biological conduit with the correct bio-mechanical properties (Carpenter and Tomaszewski, 1998, Fahner et al., 2006).

Fresh vascular allografts are, however, subject to frequent and early failure (Callow, 1996, Bilfinger et al., 1997, Carpenter and Tomaszewski, 1998, Lamm et al., 2001, Fahner et al., 2006). Fresh allografts have been shown to be unusable as they suffer from rapid rejection and failure due to immune rejection (Callow, 1996). One of the main limitations to the use of allografts is tissue sourcing, unlike an autograft that can be collected just before implantation, an allograft has to be collected, transported and possibly stored for long periods of time. Using a range of techniques allografts have been preserved and many have been reported to demonstrate superior performance compared to fresh allografts, but in many cases still suffer from early rejection and failure (Callow, 1996).

Several techniques have been investigated for the storage of allografts, the favoured method being cryopreservation. Cryopreservation unlike cold storage and freezing is intended to maintain cell viability and offer long term storage (Callow, 1996, Fahner et al., 2006). Clinical trials using cryo preserved vascular allografts have highlighted several problems. A number of studies have demonstrated that immune-rejection has a major role in graft failure. Allografts have been demonstrated to produce a strong cell-mediated immune response; endothelial cells being the locus of strong antigenicity (Carpenter and Tomaszewski, 1998). The failure of allografts has been related to the inability of the endothelium to modulate the adherence of leucocytes (Bilfinger et al., 1997).

Even with a great deal of care, the best preservation techniques will not maintain normal cell function (Callow, 1996). Where the endothelium is lost, there is an increased infiltration of T-cells and intimal thickening related to the loss of endothelial cell regulation of smooth muscle cells (Carpenter and Tomaszewski, 1998, Zhou et al., 2009b). It has been suggested that cryopreservation may even accelerate graft occlusion due to non immunogenic mechanisms involved in fibrosis and the loss of contractile function (Miller et al., 1993). Poor patency rates and other associated complications have rendered cryopreserved saphenous vein, human

umbilical artery and other arterial allografts unacceptable for routine use (Baguneid et al., 2006). In whole organ transplantation, great effort is taken to match the histocompatibility antigens of the donor and recipient to reduce the risk of transplant rejection. This has been applied in vascular grafts and has been shown to improve the patency rates of the allografts; this is not practicable due to demand and sourcing restraints (Carpenter and Tomaszewski, 1998, Fahner et al., 2006).

Immunosuppressive drugs have been explored in an attempt to prevent graft rejection. Immunosuppression and antibody cross-matching have been shown to lower the failure rates of allografts but the grafts still suffer from accelerated degradation and failure (Miller et al., 1993, Randon et al., 2010). The problem with these approaches is that immunosuppression does not always eliminate rejection and the economic and health costs of long term immunosuppression make it unjustifiable for use with vascular allografts (Callow, 1996, Fahner et al., 2006).

Initial attempts to overcome the problems of allografts used fixation to maintain ECM integrity and mask immunogenic antigens. This proved to be a problem as it was reported that fixation caused a loss of mechanical properties, in particular compliance, which resulted in aneurismal degradation of the scaffolds (Courtman et al., 2001, Conklin et al., 2002, Schaner et al., 2004). The main issue with fixation is that masking of the antigens does not completely remove the immune response. The antigens are still present, but just inaccessible until the vessel is naturally degraded overtime: this can possibly lead to a long-term inflammatory response (Courtman et al., 2001, Conklin et al., 2002, Schaner et al., 2004).

1.4.3 Xenografts

A xenograft is the transplant of tissue from one species to another. The ability to use animal tissue would remove the complications of graft sourcing. The use of animal tissues would however raise concerns, mainly rejection and interspecies disease transmission (Schaner et al., 2004). Hyperacute rejection of a xenograft is an inevitable consequence of the transplant of tissue between phylogenetically distinct species (Platt et al., 1991). This means that any animal tissue that has foreign antigens will elicit an immune response and suffer rapid rejection. In theory, the immune response can be overcome by decellularising the scaffold to remove all the cells and so remove the antigens that cause the immune response. Decellularised

xenografts have shown potential in animal models as blood vessel replacements as they have been shown to retain the mechanical properties of the vessel once decellularised and are easier to source than auto/allografts (Martin et al., 2005, Roy et al., 2005, Williams et al., 2009). Xenografts which have not been successfully decellularised would however still run the risk of immune rejection and carry the risk of interspecies disease transmission, such as porcine endogenous retroviruses (PERVs) and BSE; this concern may limit or prohibit xenograft use (Prabha and Verghese, 2008).

1.4.4 Synthetic biomaterials

The need for vascular grafts has created an interest in the use of synthetic polymers for tissue engineering such grafts. There are two main potential uses of polymers in vascular bypass grafts. The initial, and most widely reported, use of polymers is as vascular prosthesis devices. In a synthetic polymer vascular prosthesis, a biostable polymer is used to create a conduit that can be used to restore normal blood flow. The prosthesis does not interact with the body and does not allow for the restoration of normal vascular function or eventual integration with the body. The second use of synthetic biomaterials is in the creation of tissue engineering scaffolds that use bio-resorbable polymers that will eventually be replaced by natural ECM and have the potential to eventually restore normal vascular function.

1.4.4.1 Prostheses

The use of synthetic polymer vascular prostheses in the replacement of large blood vessels (>6 mm) has been a success with polyethylene terephthalate (Dacron) and expanded polytetrafluoroethylene (ePTFE) grafts having a high level of patency after ten years (Hoerstrup et al., 2001, Conklin et al., 2002, Bujan et al., 2004, Wang et al., 2007c). Dacron and ePTFE are biostable polymers that are used to create grafts that have a long lifetime in the body. When Dacron and ePTFE are, however, used for small calibre grafts, they occlude due to platelet activation and thrombosis (Hoerstrup et al., 2001, Conklin et al., 2002, Bujan et al., 2004, Wang et al., 2007c, Desai et al., 2011). A wide range of patency rates have been reported for small diameter (<6 mm) Dacron and ePTFE prostheses dependent upon the location the graft was inserted and the use of anti-clotting agents; on average patency rates tend to be below 50 %

after five years (Wang et al., 2007c). Dacron fails due to intimal thickening and thrombosis at the point of attachment causing graft occlusion and failure (Conklin et al., 2002, Venkatraman et al., 2008). ePTFE does not interact well with blood, this has been shown to contribute to the formation of thrombosis and intimal thickening at the point of attachment (Xue and Greisler, 2003).

One of the major problems with synthetic grafts is endothelialisation; most reported results show ePTFE and Dacron grafts fail to develop a full endothelial layer, other reported results show the seeding of cells and the coating of scaffolds with materials such as fibrin allow for the development of an endothelium (Zilla et al., 1993, Bujan et al., 2004, Meinhart et al., 2005, Tatterton et al., 2012). The combination of synthetic and natural materials is addressed later in Section 1.4.4.3. Another major problem with biostable grafts is infection. Prosthetic grafts have been reported to have increased rates of infection compared to autografts that can lead to life threatening situations and can be difficult to treat (Cittadella et al., 2013). Stable synthetic grafts are also a problem in paediatrics as the vessel needs to be able to grow with the patient; this means that children given biostable grafts often need replacement surgery as they grow (Cittadella et al., 2013).

There are a range of other bio-stable polymers that have a history of use in the body, such as polyurethane. Polyurethane has been tested as a vascular graft material as it can be made to match the compliance of a blood vessel, whereas Dacron and ePTFE grafts cannot (Xue and Greisler, 2003, Wang et al., 2007c, Venkatraman et al., 2008). Initial results showed that polyurethanes elongated and degraded over time. Initial attempts at vascular replacements with polyurethane lead to high rates of aneurysm and thrombosis compared to ePTFE and Dacron grafts (Desai et al., 2011). This led to the development of polycarbonate, polyester and silicone based polyurethanes.

It has been reported that polycarbonate based polyurethanes have better mechanical properties and are more resistant to hydrolytic and oxidative damage (Xue and Greisler, 2003, Venkatraman et al., 2008). Polyester based urethanes have been demonstrated to have good mechanical properties and blood compatibility (Soldani et al., 2010). Most polyurethanes, however, suffer from platelet adhesion leading to graft failure and this led to the development of silicone based polyurethanes that are reported to have anti-adhesive properties (Taite et al., 2008, Soldani et al., 2010). These different based polyurethanes have also been mixed together to combine their different properties. It has been demonstrated that

bio-stable polymers tend to elicit a foreign body response by the recipient immune system and are known to cause mild inflammation (Figure 1.5) (Venkatraman et al., 2008).

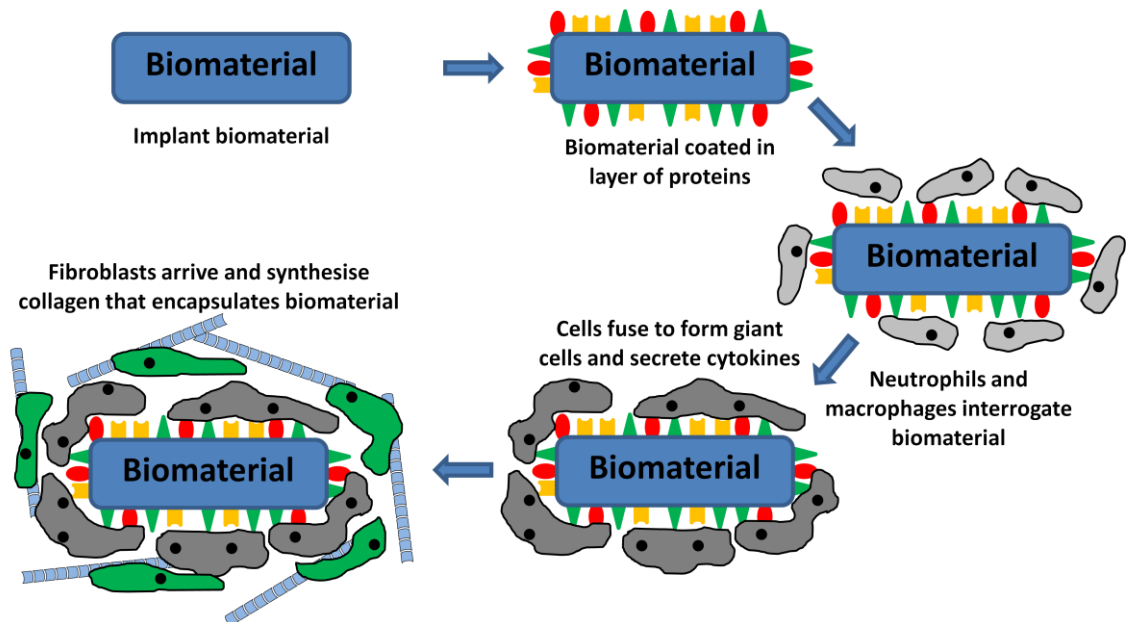


Figure 1.5; Schematic of foreign body response

1.4.4.2 Regenerative

An alternative to a bio-stable polymer is a biodegradable polymer which is broken down by enzymatic and hydrolytic action in the body. As biodegradable polymers are degraded by the body and removed, the source of any long-term foreign body response is eliminated. Biodegradation also allows for the formation of a fully functioning natural ECM which is preferential to a non-responsive polymer.

For a polymer to be used as a tissue engineering scaffold the degradation products produced cannot cause a toxic or inflammatory response (Freed et al., 1994). A range of biodegradable polymers have been used in the lab and in animal models as vascular grafts; the most common biodegradable polymers are polyglycolic acid (PGA), polylactic acid (PLA) and poly(lactic-co-glycolic) acid (PLGA) copolymers. PLA and PGA are broken down into lactic acid and glutamic acid which can then be metabolised by the body, other polymers tested include degradable polyurethanes, polycaprolactone and polydiols (Freed et al., 1994, Gunatillake and Adhikari,

2003, Yang et al., 2005, Martina and Hutmacher, 2007, Guelcher, 2008, Pankajakshan et al., 2008, Pektok et al., 2008). There is concern over the breakdown of biodegradable polymers causing an increase in acidity and the lower pH causing a toxic effect. This lower pH also runs the risk that the degradation rate of the polymers could be increased by autocatalysis (Taylor et al., 1994, Hoerstrup et al., 2001, Hemmrich et al., 2008, Lee et al., 2009).

The biodegradation characteristics of a polymer are affected by the glass transition temperature (T_g); as the T_g decreases, the degradation rate increases. The problem with changing the T_g to improve degradation is that the mechanical properties of a material are heavily influenced by T_g (Wu et al., 2006, Watanabe et al., 2009). Tailoring a polymer for mechanical and degradation properties is therefore complex and often involves compromising one of the resultant material's properties.

This is further complicated by the loss of mechanical properties as the polymer degrades (Xue and Greisler, 2003, Venkatraman et al., 2008). PGA, PLA, PLGA and polyurethanes have been shown to degrade too quickly under physiological conditions: this would lead to aneurismal dilation making them unusable without further modification (Pektok et al., 2008). Polycaprolactone has the required degradation and mechanical properties but suffers from chondrioid metaplasia, calcification, following on from a foreign body immune response (Pankajakshan et al., 2008, Pektok et al., 2008).

There are a range of other polymers which are being explored such as poly (diol citrates) which are biphasic polymers which form tubular scaffolds. Their mechanical properties and compliance closely match that of a natural blood vessel: they are biodegradable and allow for cell attachment (Yang et al., 2005). Anti-thrombogenic materials that biodegrade have also been explored for engineering of vascular grafts; polyurethane based nano-composite polyhedral-oligomeric-silesquioxane-poly(carbonate-urea) urethane (POSS-PCU) is a leading example which has been shown to be biocompatible and have the correct biomechanical properties needed for a blood vessel graft having been used in lower limb vascular bypass grafts (de Mel et al., 2009, Ahmed et al., 2011, Cittadella et al., 2013). Attempts have been made to overcome the limitations of polymers by the addition of growth factors, adhesion ligands and anti-thrombogenic factors (Hoerstrup et al., 2001, Xue and Greisler, 2003, Bujan et al., 2004, Wang et al., 2007c, Venkatraman et al., 2008).

1.4.4.3 Composite materials

There is a large amount of research in the literature in which Dacron has been coated with various combinations of collagen, heparin, fibrin, gelatine, and various growth factors and attachment ligands. There have been some positive experimental results in animals where a fully formed endothelium has been created, resulting in an increase in the patency rate of the grafts (Zilla et al., 1993, Meinhart et al., 2005). Some experimental results showed an increase in the patency of a graft; however, the graft still failed to form an endothelial layer and occluded (Venkatraman et al., 2008). There are cases in which hybrid composite materials have been made with other polymers to improve biocompatibility and to incorporate anti-adhesive properties to improve patency as opposed to the development of an endothelium (He et al., 2005, Pankajakshan et al., 2008, Taite et al., 2008).

1.4.5 Natural biomaterials

Natural biomaterials can be used to create scaffolds for the tissue engineering of vascular grafts. Natural biomaterials have several advantages over synthetically derived biomaterials: they are more responsive to the surrounding environment, allow for easy integration and repair upon implantation, should exhibit little to no foreign body immune reaction and should allow for cellular remodelling of the graft (L'heureux et al., 1998, Boland et al., 2004). Natural biomaterials can contain ligands that can be bound by cell adhesion molecules for the purpose of cellular adhesion and that can act as templates for cell growth, proliferation, migration and function (Schmidt and Baier, 2000).

There are a wide range of natural biomaterials that could be used with the most obvious choices being those materials that comprise the ECM of a natural blood vessel. Collagen and elastin are the main constituents of the vascular ECM. Collagen provides strength against the rupture of the blood vessel and elastin provides the elastic recoil properties that resist elongation and deformation (Figure 1.6) (Buttafoco et al., 2006).

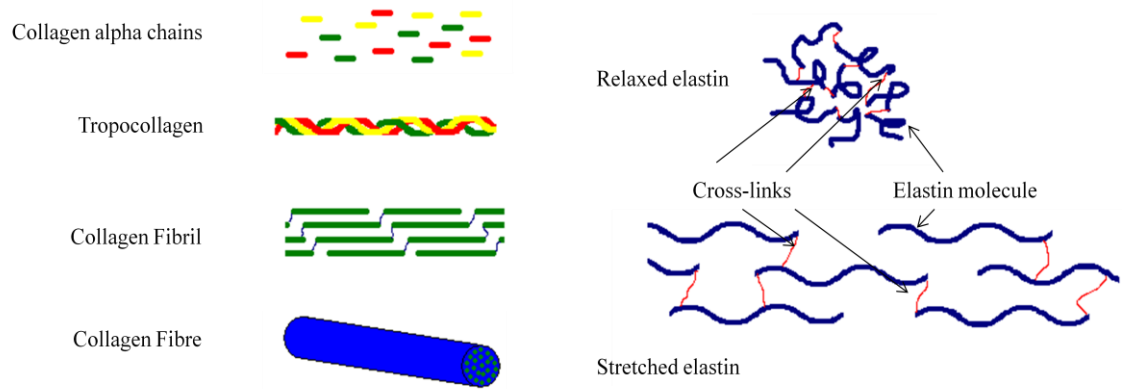


Figure 1.6; Schematic of the structure of collagen and elastin

Fibrin is another obvious choice for use in scaffold creation as it can be derived from a patient's own blood (Jockenhoevel et al., 2001). On their own, natural biomaterials have a limited potential as they lack mechanical strength. This can be overcome by using combinations of natural materials to create composites that more closely resemble the ECM (L'heureux et al., 1998, Buttafoco et al., 2006). Unmodified natural materials are subject to rapid chemical and enzymatic degradation and so require the material to be modified prior to use (Schmidt and Baier, 2000).

Cross-linking the naturally derived biomaterials increases the resistance to enzymatic and chemical degradation. There are several ways in which the natural materials can be cross-linked. Glutaraldehyde has been used extensively for the cross-linking of materials but has several limitations: it can compromise the mechanical properties, it is cytotoxic and the treated material is prone to calcification (Schmidt and Baier, 2000, Buttafoco et al., 2006). Polyepoxy compounds (Denacol) can be used for cross-linking and are less cytotoxic than glutaraldehyde and have a reduced rate of calcification. A preferred method is cross-linking using dye mediated photooxidation. Photooxidation uses a dye photosensitiser, added to the biomaterial, which oxidises amino acids such as tryptophan, histidine, tyrosine, and methionine when exposed to visible light. The dye biomaterial mixture is exposed to the correct wavelength of light to trigger cross-linking; the level of cross-linking in the biomaterial is a result of the exposure time. Photooxidation has no toxic effects, is not known to calcify and has a limited detrimental effect on the properties of natural materials and biomechanical integrity of the vessel (Schmidt and Baier, 2000).

There are various methods by which natural scaffolds can be prepared. Foams, hydrogels and fibrous scaffolds can be created by a range of techniques. Freeze drying, gas expansion, knitting, weaving, and cross-linking can all be used to create scaffolds with different properties and structures. One area of current interest is electrospinning (Figure 1.7). Electrospinning of natural biomaterials creates a non-woven mesh that has fibre dimensions that closely resemble the natural structure of the ECM. It is possible to electrospin multiple materials at the same time and create a composite material. The non-woven mesh can then be modified and cross linked to improve mechanical properties and cellular interactions (Buttafoco et al., 2006).

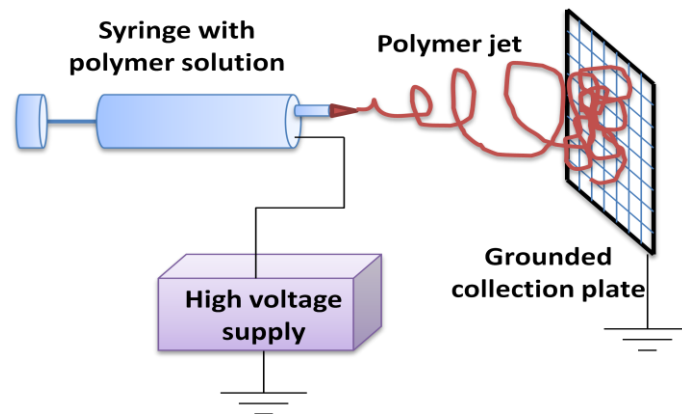


Figure 1.7; Schematic of electrospinning. Reproduced from (Badami et al., 2006).

Random topography is known to enhance cellular attachment, but this is not necessarily an advantage in scaffold design (Badami et al., 2006). Cells that attach to orientated scaffold are influenced by the underlying structure. The organisation, migration, proliferation and activity of cells has been shown to be changed by the orientation of the scaffold (Vitte et al., 2004, Murugan and Ramakrishna, 2007). The natural extracellular matrix in blood vessels is orientated in different directions in the different layers and so this is of importance for normal vessel and cellular function (Boland et al., 2004).

Blood clot and thrombus formation are still a major problem with natural materials as platelets are activated by interaction with a number of these bio-molecules in normal wound healing. As such, a confluent layer of endothelial cells or anti-clotting agents are needed to prevent blood clot formation (Boland et al., 2004). Nonetheless, natural materials have an advantage with regard to cellular interactions: fibronectin, vitronectin and laminin mediate contact between

endothelial cells and collagen. The use of these and other of bio-molecules has been shown to aid in the formation of a confluent endothelium (Dixit et al., 2001). Another method is to seed cells on to the scaffold. Cell seeding of natural scaffolds has been shown to enhance long-term function, prevent thrombus formation and allow the graft to develop into a responsive living tissue (Schmidt and Baier, 2000).

One concern in the use of natural biomaterials is tissue shrinkage. As the cells interact and remodel the biomaterial, it has been shown to contracted and shrink. *In vivo*, this should be less of a problem but for *in vitro*, production and development may prove to be a major concern (Jockenhoevel et al., 2001). Other concerns about the use of biomaterials and cells include: intimal thickening, due to a lack of regulation of smooth muscle cell proliferation; cell sourcing; the sourcing of the natural biomaterial and the time taken to grow sufficient numbers of cells and seed the scaffolds. Many of the biomaterials used in laboratories are derived from animals and could carry disease or elicit an immune response. Some natural biomaterials such as fibrin can easily be isolated from a patient, while the collection of collagen and other materials is more complex (L'heureux et al., 1998, Boland et al., 2004, Hasegawa et al., 2007).

Natural biomaterials can be useful as scaffolds, but a large focus has been placed on their use with synthetic scaffolds to improve cellular interactions and increase cell migration and proliferation (Dixit et al., 2001, Hasegawa et al., 2007). Fibrin is an example of a natural biomaterial that has been added to synthetic polymer scaffolds to create composites, in which the fibrin has been used to promote cell migration and proliferation (Hasegawa et al., 2007, Tschoeke et al., 2009). This method can be used to overcome the problems with mechanical properties but does not address the problems of sourcing and thrombogenesis.

1.4.6 Cell derived replacements

Instead of using a scaffold to tissue engineer a small diameter blood vessel, it has been shown that an alternative is to tissue engineer a scaffold directly from cells. A construct composed of cells surrounded by secreted ECM has the advantage of being highly responsive, of being able to self-repair, remodel and react according to environmental stimuli (L'heureux et al., 1998). Tissue engineered blood vessels using cells have been produced by forming cell sheets or by the template layering of cells. In cell sheet tissue engineering, cells are grown in conditions

that promote the production of ECM, for example, in ascorbic acid to promote collagen synthesis. The cells are cultured until they have formed a sheet of cells bound in ECM proteins. The cell sheets are then rolled on to porous tubes and cultured to allow for fusion into cohesive tissues (Figure 1.8). Many different cells types, different sources of cells, different growth techniques and handling methods have been explored in order to develop cell-based replacements; most follow the similar method of growing and rolling cell sheets to form tubes.

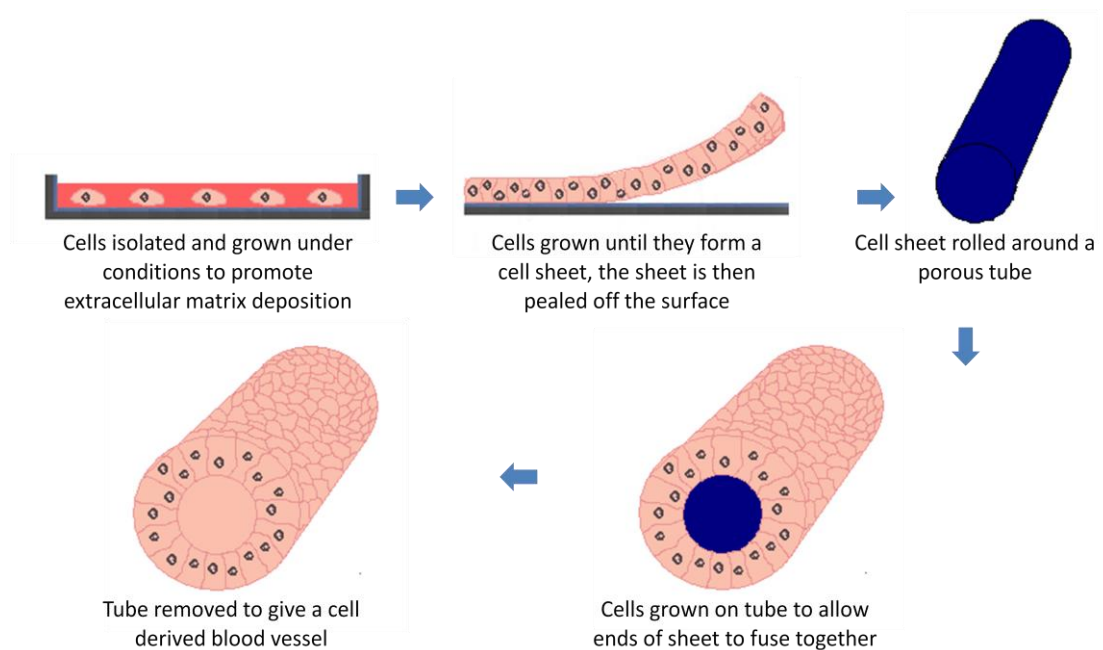


Figure 1.8; Schematic of cell sheet formation of replacement blood vessel

To create an anti-thrombogenic surface, endothelial cells have been seeded on the inner layer of the cell sheets to create the lumen (L'heureux et al., 1998, Isenberg et al., 2006, L'Heureux et al., 2007). Konig et al. and L'Heureux et al. used fibroblasts to create cell sheets (L'heureux et al., 1998, L'Heureux et al., 2007, Konig et al., 2009) Isenberg et al. used both smooth muscle and fibroblast cells to create different cell sheets (Isenberg et al., 2006). L'Heureux et al. demonstrated how multilayered vessels could be created by rolling multiple cell sheets together (L'heureux et al., 1998, L'Heureux et al., 2007). This construct was shown to have burst pressure properties similar to natural arteries. The construct was, however, not ideal as the layers were composed of fibroblasts which are typically not found in the medial layer.

Konig et al. created an internal membrane free of viable cells by drying out the internal fibroblast cell sheet. A new layer of fibroblast cells was then rolled over the initial construct to create the adventitia and endothelial cells were seeded onto the construct to create a confluent endothelium (Konig et al., 2009). At the time of implantation, it was shown that these tissue engineered vessels had burst pressures similar to native arteries. Furthermore, the compliance of the vessels was significantly lower at the time of implantation, but after six months the vessel had achieved a compliance match (Konig et al., 2009).

Isenberg et al. reported the creation of a cell sheet of smooth muscle cells to mimic the media layer and a sheet of fibroblasts to create the adventitia. The two layers were allowed to fuse and endothelial cells seeded to the inside of the vessel to create the lumen (Isenberg et al., 2006). The vessel produced by Isenberg et al. was shown to be anti-thrombogenic and had a similar burst pressure to native arteries. Gauvin et al. showed that the mechanical properties of these cell sheets can be further improved by co-culturing the two cell sheets together into one larger sheet which was then rolled up leading to a denser ECM (Gauvin et al., 2010).

A compliance mismatch between the tissue engineered blood vessels and native artery has been reported for several of the cell-based sheet approaches. In tissue engineered vessels this is a major problem as compliance mismatch has been attributed to the development of intimal hyperplasia (Isenberg et al., 2006, L'Heureux et al., 2007). The major limitation of cell sheet tissue engineering of blood vessels is the quality of the ECM produced. The ECM in the cell sheets lacks the correct fibre alignment that gives native blood vessels some of their biomechanical properties; the ECM produced by the cell sheets is also composed of different amounts of ECM proteins compared to natural tissue, often having lower levels of elastin. This difference is important and is likely the cause of the compliance mismatch (L'heureux et al., 1998, Isenberg et al., 2006, Konig et al., 2009, L'Heureux et al., 2007). The differing levels of different ECM components highlights the importance of the source of cells: the same cell type from different locations may produce different quantities and types of ECM (Gauvin et al., 2010).

Recent studies have focused on cell and tissue culture using biomechanical stimulation. Using bioreactors, Hoerstrup et al demonstrated the acceleration of tissue formation using a pulsatile flow system similar to the native tissue's biomechanical environment (Hoerstrup et al., 2000, Barron et al., 2003). This produced a tissue that when analysed showed histological features closer to the native tissue than when compared to tissue without mechanical stimulation (Hoerstrup et al., 2000, Hoerstrup et al., 2001, Barron et al., 2003).

It has been reported that dynamic mechanical conditioning of tissue cultures leads to an improvement in the mechanical properties and histological organisation of tissues (Seliktar et al., 2000, Sodian et al., 2002, Barron et al., 2003). Dynamic mechanical stimulation may overcome some of the problems associated with cell-based techniques and may even speed up tissue growth. However, the need to create an enclosed bioreactor capable of the correct mechanical stimulation vastly increases the risk of infection and the sensitivity of the culture environment.

The templating methods involve the ordered layering of cells to create small diameter tubes. This method often uses spheroids of cells to layer and create the tissue engineered vessels (Figure 1.9) (Norotte et al., 2009, Mironov et al., 2009). The advantage of using a template to order the cells is that a vessel of varying shape and size can be constructed with in-built branching. The disadvantage is that it is hard to maintain sterility in the templating process (Norotte et al., 2009, Mironov et al., 2009).

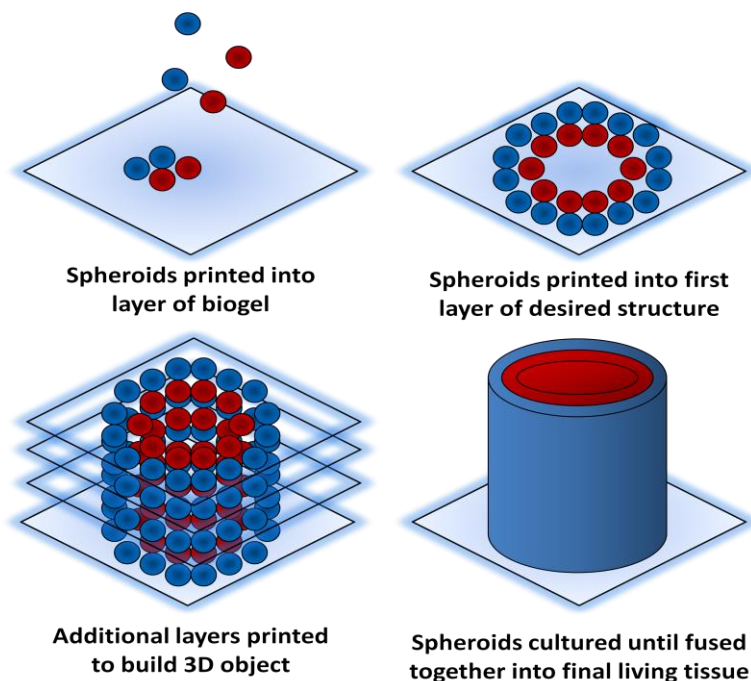


Figure 1.9; Schematic of cell printing

An alternative approach to the creation of arterial bypass grafts is to use the body's natural actions to create an autologous vessel. A foreign material implanted into the body will produce a host response that will result in the formation of a cellular capsule that surrounds the

material (Campbell et al., 1999, L'Heureux et al., 2007). It has been shown that by implanting a silastic tube into the peritoneal cavity of rats that a layer of myofibroblasts, a collagen matrix and a mesothelium monolayer will be formed on the outside of the tube after two weeks (Campbell et al., 1999). It was shown that the tube could be removed and the resultant layer of cells inverted to create an anti-thrombogenic mesothelium. In rats, this approach produced a replacement vessel that remained patent for four months (Campbell et al., 1999). The graft grown in the body potentially overcomes the need to isolate and expand the cells from biopsies. However, the graft is composed of myofibroblasts and mesothelial cells, not smooth muscle and endothelial cells. The resultant vessel also lacks the structure and biomechanical properties found in the native blood vessel (Campbell et al., 1999).

There are two main problems with the use of cell-based tissue engineered constructs. Cell sourcing is a major problem as the availability of autologous vascular cells is limited due to poor vessel quality in patients needing vascular grafts. The isolation and purification of vascular cells is limited by technical ability and the isolated cells have a poor proliferative capacity and have been shown to change phenotype when cultured *in vitro* (Krenning et al., 2008). The isolation of autologous cells also requires that a blood vessel or skin biopsy be taken and this introduces a new site of trauma (Krenning et al., 2008).

The sourcing of cells from bone marrow and the extraction of progenitor cells from the blood is a possible solution to this problem, but this is still in the early stages of investigation (Krenning et al., 2008). The main problem with the *in vitro* use of cells is the time taken to culture and grow the cells needed for any application. The growth of cell sheets takes time as does the development of spheroids. This may be acceptable when time is not an issue but in the case of trauma and emergency situations, where time is a factor, the isolation and growth of cells is not viable (L'heureux et al., 1998, Krenning et al., 2008, Isenberg et al., 2006, L'Heureux et al., 2007, Norotte et al., 2009, Konig et al., 2009).

1.4.7 Decellularised scaffolds

The immunological problems associated with the use of allograft and xenograft tissues and the structural limitations of the biomaterial scaffolds have led to the development of decellularised scaffolds. The idea is that by removing the cells from natural tissue the immunogenic molecules will be removed whilst maintaining the structure of the natural ECM

(Wang et al., 2007c). Since a decellularised vessel will have the same structure as the natural vessel, it should have similar mechanical properties and be resistant to rupture. The ideal vessel for decellularisation and for use in arterial bypass is an artery as its mechanical properties and compliance will most closely match that of the natural vessel (Conklin et al., 2002, Schaner et al., 2004).

Decellularised tissues may also serve as structural supports, providing attachment sites for recellularisation and a reservoir for growth factors and other bio-molecules. It is possible to decellularise a tissue in many ways: chemical, mechanical and enzymatic techniques can be used to remove the cells, most commonly by cell lysis (Figure 1.10) (Schmidt and Baier, 2000). The cellular debris then needs to be removed from the scaffold as cellular components and lipids are known to cause calcification and an inflammatory response (Schmidt and Baier, 2000). Washing procedures are used to remove the cellular debris left following cell lysis; protease inhibitors may be used during washing to prevent degradation of the extracellular matrix and DNase and RNase enzymes are used to remove residual encoding DNA and RNA (Figure 1.10) (Meyer et al., 2006, Wilshaw et al., 2008a).

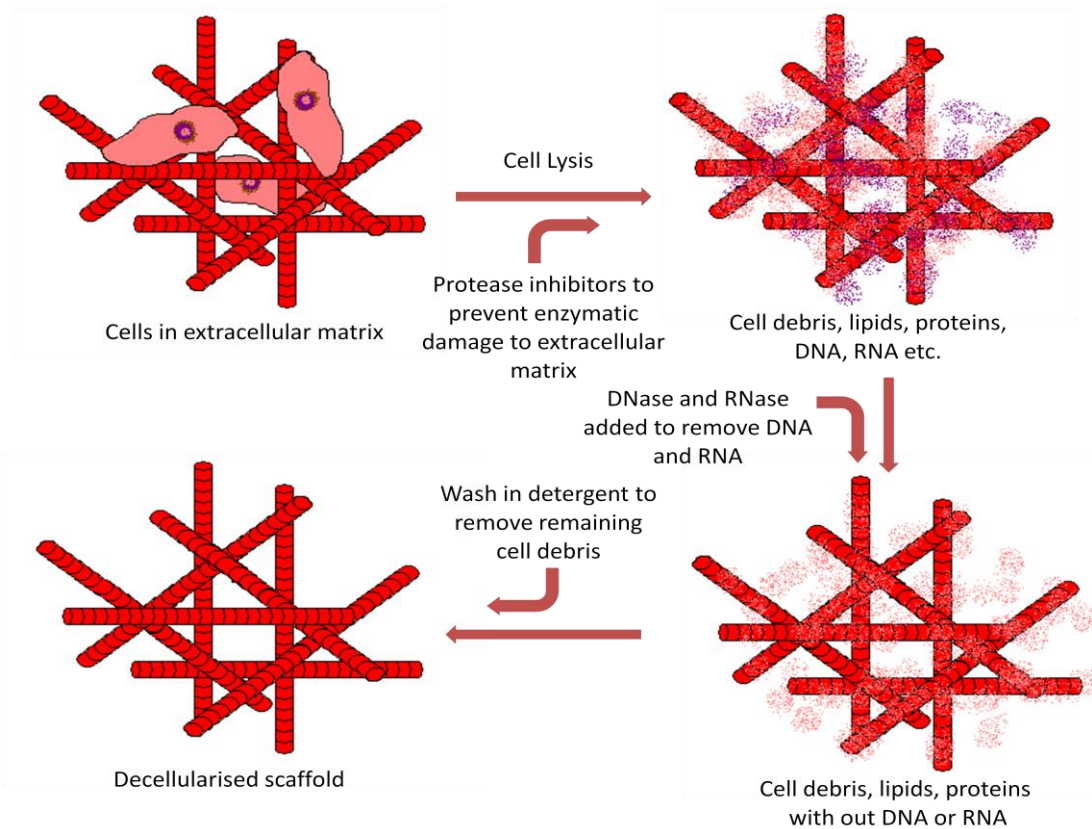


Figure 1.10; Schematic of decellularisation process

Platelet activation, thrombus formation and intimal hyperplasia are problems that have been observed with the use of decellularised scaffolds in animal models (Patel et al., 2007, Wang et al., 2007b, Cai et al., 2009, Zhou et al., 2009b). The lack of an endothelium activates platelets, a natural response to damage to the blood vessel and exposure of the underlying ECM; this causes blood clotting and thrombus formation (Rendu and Brohard-Bohn, 2001, Conklin et al., 2002, Wang et al., 2007b, Zhou et al., 2009b, Zhou et al., 2011).

The lack of endothelial cells and the release of inflammatory products may result in the uncontrolled proliferation of SMCs resulting in intimal hyperplasia (Cai et al., 2009). It has been shown that cells are slow to re-cellularise acellular scaffolds *in vivo*, mainly migrating through the scaffold at its cut edge (Simionescu et al., 2006). It has been reported that the arterial geometry and structure change due to the removal of the cells causing a release in the prestresses present in the normal tissue. This has been shown to be reversed under pressure when the voids left by the removed cells are filled with fluid (Roy et al., 2005).

It has been shown that there is no significant difference between the burst pressure, stress modulus and compliance of decellularised vessels compared to natural vessels (Schaner et al., 2004, Martin et al., 2005, Roy et al., 2005, Wilshaw et al., 2008a, Gui et al., 2009). It has, however, been reported that there may be an increase in the stiffness of the vessels following decellularisation (Roy et al., 2005, Williams et al., 2009). This is likely due to small changes in the ECM geometry and structure as a result of the removal of the cells. An increase in fibre mobility and a loss of collagen crimping has been associated with an increase in vessel stiffness (Williams et al., 2009).

The burst pressure of common femoral arteries decellularised using the same method described in Section 2.2.3 has been shown to have no significant difference compared to the native human arteries with burst pressures of 3214 mmHg and 2562 mmHg respectively (Wilshaw et al., 2011). Using the same method it was also found that following tensile testing there was no significant difference in the transition stress and strain, ultimate tensile strength and failure strain in either circumferential or axial direction between decellularised and native arteries (Wilshaw et al., 2011). The same study also showed there was no significant difference in the compliance of the decellularised and native arteries with dilation of 9.8% and 7.9% respectively at 200 mmHg (Wilshaw et al., 2011). Others have shown that decellularisation of other tissues such as pericardium resulted in no ultrastructure damage and that there was no significant effect on fracture tension and percentage strain at fracture compared to fresh tissue (Wilson et al., 1995). It is believed that the early mechanical failures of decellularise

tissue was due to damage to the ECM and the use of cross-linking agents. It has been demonstrated that cross-linking tissue with glutaraldehyde or other cross linking agents failed to preserve tissue mechanics (Wilson et al., 1995).

There has also been reported a loss of some ECM components due to the different decellularisation methods used (Heine et al., 2011). At the same time, different techniques have been shown not to affect the majority of natural proteoglycans and growth factors present in the scaffold (Courtman et al., 1994, Badylak, 2004).

The source of natural tissue for the creation of a decellularised scaffold is of importance. Arteries and veins can be obtained from allogeneic or xenogeneic donors. It has been reported that allografts elicit little to no immune response once decellularised, as the immune response is instigated by antigens on the cell surfaces (Allaire et al., 1997, Courtman et al., 2001). The response observed once decellularised allografts have been implanted in animals has been reported to be similar to the inflammatory response observed for autografts and to be significantly less than for fresh allografts (Martin et al., 2005, Ketchedjian et al., 2005).

Acellular xenografts have demonstrated a range of different results. Some investigations into the use of xenografts have reported that xenografts elicit an immune response once decellularised due to interspecies differences in the primary structure of the extracellular matrix components (Allaire et al., 1997, Courtman et al., 2001, Takagi et al., 2006, Bergmeister et al., 2008). Once implanted in animal models, decellularised xenografts have been shown to develop deposits of immunoglobulin, IgM and IgG, with the presence of macrophages (Allaire et al., 1997, Courtman et al., 2001, Cai et al., 2009). The monocytes have been shown to cause damage to the elastin and release factors that promote SMC proliferation causing intimal hyperplasia (Courtman et al., 2001, Cai et al., 2009). An immune response to decellularised xenografts in animals has also been shown to result in the formation of mural thrombus and lead to vessel occlusion (Courtman et al., 2001).

It has been reported that the immune response to decellularised xenogeneic tissue can be overcome by cross-linking (Bayrak et al., 2010). Others report a lowering of immune response but attribute it to the cross-linking preventing the penetration of macrophages and other inflammatory cells into the tissue and preventing the degradation (Chang et al., 2005, Bergmeister et al., 2008). It has also been reported that decellularised xenogenic grafts in animal models elicit no immune response (Conklin et al., 2002, Wang et al., 2007b, Bergmeister et al., 2008). Whilst there are reported interspecies differences in the primary

structure of the ECM components, it is also reported that major ECM components such as collagen and elastin are highly conserved in higher species and so should not cause an immune response (Conklin et al., 2002, Wang et al., 2007b).

The range of results obtained in the analysis of decellularised allogenic and xenogenic grafts can be explained by the different efficiencies of the decellularisation protocols used. An inability to remove cellular debris can lead to an immune response and inflammation associated with the danger signals released by the dead cells remaining in the scaffold (Badylak, 2004). Some decellularisation protocols will remove more cellular debris than others, and different species will have slightly different vessel sizes and structures. A vessel harvested from one location will have a different ECM structure and composition compared to a vessel from a different location (Ketchedjian et al., 2005, Rieder et al., 2006, Williams et al., 2009).

Calcification is also a problem associated with inadequately decellularised scaffolds as lipid and cellular remnants provide nucleation sites for the formation of calcium crystals (Courtman et al., 1994). Developments made in tissue engineering have presented an alternative method of producing a decellularised scaffold. Natural vessel like structures can be formed by growing cells on biodegradable polymer scaffolds or by using rolled cell sheets *in vitro* (Quint et al., 2012). This artificially produced scaffold may then be decellularised to leave the extracellular matrix produced by the cells behind (Quint et al., 2012). The artificial scaffolds have the advantage of being produced using human cells to result in allogeneic tissue and so eliminate the problems associated with sourcing allografts.

When implanted into animal models, decellularised scaffolds have been shown to exhibit ECM turnover and the formation of endothelial-like structures on the implant surface (Dahan et al., 2012). Reported attempts to overcome thrombogenesis have involved the re-cellularisation of the grafts *in vitro* and the use of anti-clotting factors to prevent clot formation, growth factors and adhesion ligands to improve cell migration and proliferation, and use of antibodies to catch and bind progenitor cells from the blood stream, all with the aim to improve re-endothelialisation of the scaffold (Patel et al., 2007, Wang et al., 2007b, Cai et al., 2009, Zhou et al., 2009b).

The use of decellularised scaffolds seeded with cells before implantation has been demonstrated in several animal and preclinical studies. The patency and lifetime of the grafts have been significantly improved by the pre-formation of an endothelium (Zhao et al., 2010, Heine et al., 2011). Cell seeding has also been shown to reduce the problem of calcification in

decellularised grafts known to calcify (Koenneker et al., 2010). Anti-clotting agents such as heparin have been added to decellularised grafts and this has the observed effect of lowering the level of platelet adhesion to the graft and slowing the onset of thrombosis formation (Zhou et al., 2011). A major problem facing vascular grafts is post-surgical infection. Decellularised grafts perform well here, having been shown to be more resistant to infection than synthetic materials such as Dacron and ePTFE (Jernigan et al., 2004, Yow et al., 2006).

1.4.8 Advantages and limitations to current approaches to vascular tissue engineering

The search for a viable replacement for small diameter blood vessels has been compared to the search for the “holy grail”. None of the above methods have been successful in producing a graft that is able to match all the requirements of a small diameter vascular graft. Autografts remain the gold standard for blood vessel replacements. However, their limited availability and associated complications has led to the need to develop other sources of graft material. Allografts are the next logical choice but, due to the immune response associated with foreign tissues and the unjustifiable costs and risks of immuno-suppression, are severally limited.

Synthetic materials have potential as materials for future use in vascular tissue engineering; however, there remain significant obstacles that need addressing before any future application. A synthetic material that allows for cell attachment and growth that maintains patency and sterility and has the required mechanical properties is needed but is currently unavailable.

A lack of processability, mechanical strength and tailorability limit any potential use of natural biomaterials. Natural biomaterials have potential when used in conjunction with synthetic materials to provide a composite scaffold for tissue engineering a replacement blood vessel, but problems with thrombus formation and platelet activation still need to be addressed. Cellular derived scaffolds can be made to closely resemble natural blood vessels; the problem is the sourcing of the cells and the time required to construct the artificial blood vessel.

A decellularised scaffold has the required biocompatibility and mechanical properties for a blood vessel replacement, but the lack of an endothelium has been shown to lead to hyperplasia and thrombosis.

Allogeneic sourcing of tissues for decellularisation could pose a problem due to limited availability. This could be overcome by the use of xenogeneic tissue which results suggest, with the correct decellularisation technique, could provide a scaffold that does not elicit an immune reaction. There are also problems to overcome with the use of xenogeneic tissue. Failure to correctly decellularise the scaffold could result in severe immune rejection and interspecies disease transmission is still a concern. As long as a method for preventing thrombus formation and intimal hyperplasia can be found, decellularised scaffolds have the potential to provide “off the shelf” vascular grafts that will maintain functionality and long term patency.

1.5 Development of decellularised small diameter blood vessel grafts

Decellularised grafts are a promising candidate for a viable long-term small diameter blood vessel graft. There are a wide range of decellularisation methods that could be used to develop decellularised small diameter blood vessel grafts. The major problems associated with decellularised materials are disease transmission, sterilisation and thrombosis formation.

1.5.1 Decellularisation methods

Physical, chemical and enzymatic techniques can be used to decellularise a tissue. Physical techniques include sonication and agitation, mechanical compression, high pressure environments and freezing. These techniques are designed to physically cause the lysis of the cells within the natural tissue. Freezing creates ice crystals within the cells to rupture the cell membrane. High pressure and compression cause cell deformation and cell death (Gilbert et al., 2006). Sonication and agitation have been demonstrated to aid and improve the decellularisation of tissues. Chemical and enzymatic techniques rely upon the use of a chemical reaction or enzymatic cleavage that acts to disrupt cell membranes.

Early attempts at decellularisation concentrated on the use of freezing techniques and enzymatic washes. Freezing techniques were shown to be limited as the rate of temperature change had to be very carefully controlled to rupture the cells but not cause extensive damage to the ECM (Gilbert et al., 2006). A number of studies have investigated the use of enzymes such as trypsin for the removal of cells from tissues; whilst the enzymes have been shown to

successfully remove cells, considerable damage to the ECM has been reported (Yang et al., 2005).

One of the most successful techniques uses hypotonic and hypertonic solutions to change the osmotic pressure within the cell, disrupting the cell membrane and killing the cell (Meyer et al., 2006, Wilshaw et al., 2008a). Hypotonic and hypertonic washes are however unable to remove cellular debris and so other washing steps are needed to remove all cell remnants. There are a range of detergents that can be used to aid in the removal of cellular debris; Triton X-100 and sodium dodecyl sulphate (SDS) are common choices for use; Triton X-100 and SDS are used to remove lipids, proteins and DNA (Schaner et al., 2004, Chang et al., 2005, Martin et al., 2005, Roy et al., 2005, Meyer et al., 2006, Rieder et al., 2006, Wilshaw et al., 2008a, Bergmeister et al., 2008, Gui et al., 2009, Williams et al., 2009) other detergents such as N-lauroyl sarcosinate and 3-[(3-cholamidopropyl)dimethylammonio]-1-propanesulfonate (CHAPS) have also been used to remove cellular debris (Ketchedjian et al., 2005, Gilbert et al., 2006).

Triton X-100 is a non ionic detergent that will disrupt lipid-lipid and lipid-protein interactions but not affect protein-protein interactions as such that the ECM should not be affected by its use. Triton X-100 has been used with differing degrees of success in cellular removal dependent upon the tissue being decellularised. Studies have shown that the use of Triton X-100 did not result in a fully decellularised blood vessel even after prolonged treatment (Gilbert et al., 2006).

Ionic detergents, such as SDS, are known to disrupt protein-protein interactions and have been shown to successfully solubilise nuclear and cytoplasmic membranes (Gilbert et al., 2006). This use of SDS has the potential to disrupt and damage the ECM. The action of SDS has been shown to be concentration dependent: damage to the ECM increased as the concentration and time period over which SDS was used increased (Courtman et al., 1994, Grauss et al., 2005). Low concentrations of SDS have been reported to successfully remove cellular debris (Rieder et al., 2004, Gilbert et al., 2006, Koenneker et al., 2010). There are however concerns over residual detergent left in the decellularised material causing cytotoxicity effects (Ketchedjian et al., 2005, Wilshaw et al., 2008a). It has also been argued that damage to the ECM is responsible for poor cell in growth and toxic effects as opposed to detergent toxicity (Gratzer et al., 2006).

Many early stage attempts at decellularisation resulted in damage to the ECM as the solutions used did not contain protease inhibitors. The ECM has the potential to be degraded during

decellularisation by the proteases released from the lysed cells. To overcome protease degradation of the ECM it has been suggested that protease inhibitors such as disodium ethylenediaminetetra acetic acid (EDTA) should be added to the wash solutions used during decellularisation.

1.5.2 Sterilisation & Disease transmission

Transmission of infectious agents is a major risk in the use of any naturally derived biomaterial. The risks can be reduced by screening the tissue source, but the transmission of undetected agents or any contamination from processing requires a terminal sterilisation step and the removal of all coding DNA. There are a number of different techniques that can be used for the sterilisation of soft tissues; gamma-irradiation, ethylene oxide and peracetic acid have been shown to be effective in removing bacteria, viruses, spores and fungi.

Gamma-irradiation has been shown to produce structural damage to biological tissues, causing cross-linking of collagen fibres and a reduction in mechanical properties (Badylak et al., 2009). Ethylene oxide has been observed to cause structural damage, but there are major concerns about the safety of its reportedly mutagenic reaction products (Lucas et al., 2003, Badylak et al., 2009). Both gamma-irradiation and ethylene oxide have been widely used in the sterilisation of medical products and devices.

Peracetic acid, also known as peroxyacetic acid, is a colourless liquid that has the chemical formula $\text{CH}_3\text{CO}_3\text{H}$. Peracetic acid is ideal for use as an antimicrobial agent as it has a high oxidising potential (Fraise, 1999, Lomas et al., 2003, Freytes et al., 2004, Kitis, 2004, Hodde et al., 2007, Zanetti et al., 2007). Microorganisms are killed by oxidation and the subsequent disruption of their cell membrane, via the hydroxyl radical ($\bullet\text{OH}$). The radical will react with any oxidisable compound in its vicinity and can damage virtually all types of macromolecules: carbohydrates, nucleic acids, lipids and amino acids (Fraise, 1999, Hodde et al., 2007, Vandekinderen et al., 2009a). This means that peracetic acid has the potential to damage the ECM. It has been reported that peracetic acid will not remove or affect collagen; it has also been reported that peracetic acid will affect or remove collagen in particular collagen IV, and elastin in the ECM (Huang et al., 2004, Derham et al., 2008).

The antimicrobial properties of peracetic acid have been known for some time, but recently there has been an increasing interest in the potential for peracetic acid as a sterilising agent. This is due to its potential for easy use with limited residual contamination. Peracetic acid breaks-down into hydrogen peroxide and acetic acid both of which are non-toxic and can be metabolised by the body (Fraise, 1999, Kitis, 2004). This makes peracetic acid a preferred choice over other sterilising agents that have toxic break-down products (Cowan et al., 1993, Maffei et al., 2005, Vandekinderen et al., 2009a, Vandekinderen et al., 2009b).

One major concern in the use of decellularised tissue is the potential for the transmission of diseases, such as HIV, or cross species transmission of viruses such as porcine endogenous retro viruses (PERVs)(Kallenbach et al., 2004). Some studies have shown that up to 2 % of vascular DNA can survive some decellularisation processes (Kallenbach et al., 2004, Gilbert et al., 2009). To prevent the transmission of viruses or the risks associated with leaving encoding DNA and RNA behind, DNase and RNase enzymes are used in decellularisation processes to breakdown and destroy any coding DNA or RNA (Brody and Pandit, 2007). The removal of RNA and DNA also removes a potential nucleation point that can lead to calcification.

1.6 Thrombus formation

Thrombosis can be caused by the composition of the blood, changes to the blood vessel wall or by changes to the flow of blood. Hypercoagulability or thrombophilia is caused by congenital/genetic disorders or by acquired disorders such as or in the case of autoimmune conditions that change the composition of the blood and cause increased blood clotting. Disturbances in the flow of blood, particularly at points of injury and vessel compression, can cause stagnant blood to coagulate. Damage or dysfunction of the endothelium is the major cause of thrombus formation following injury or surgical interventions and is associated with several disease states (Kroll and Schafer, 1989, Wu and Thiagarajan, 1996, McNicol and Israels, 2003).

Blood clotting is one of the most complex events in nature with a careful balance needing to be found between the prevention of blood clotting in healthy blood vessels and the need to trigger rapid haemostasis in the result of injury or trauma. Blood coagulation is a highly conserved process throughout biology. Mammals all have a blood coagulation pathway that involves both a cellular (platelet) and protein (coagulation factor) component. Blood clotting

involves a wide range of cellular, protein and enzymatic actions to result in the formation and maintenance of a blood clot: the human blood clotting pathway is one of the most widely studied in biology and yet is still not fully understood.

In a healthy individual, the main concern regarding the implantation of any foreign material is the formation of a thrombus. Thrombosis is also the major concern regarding those with CVD. There are two independent pathways to platelet activation that can work together or separately to result in thrombus formation. The main trigger for haemostatic thrombus is the loss or dysfunction of the endothelial cell barrier. Platelets also become activated by minimal stimulation from the sub-endothelium and artificial surfaces (Ruggeri, 2002, Gorbet and Sefton, 2004).

Coagulation begins almost immediately at the site of platelet activation where platelets come into contact with different ECM components or associated secreted molecules; von Willebrand factor (vWF), laminin, collagen and fibulin (Ruggeri, 2002). Platelets tend to bind directly to collagen with collagen-specific glycoprotein Ia/IIa surface receptors which are further strengthened by binding to vWF. The vWF is an adhesive glycoprotein synthesised by endothelial cells, it is secreted and stored in α -granules of platelets and in the ECM (Andrews et al., 1997). The glycoprotein Ib-IX-V complex on the platelet plasma membrane mediates the initial deposition of platelets on the sub-endothelium via the binding of the glycoprotein with vWF on the ECM or in high shear stress with vWF in the plasma (Andrews et al., 1997). There are many different platelet adhesion receptors, glycoprotein Ib and IIb/IIIa have the highest densities; glycoprotein Ib binds to immobilized vWF where glycoprotein IIb will bind to both mobile and immobilized vWF (Gorbet and Sefton, 2004). Platelets respond to an antagonist in three integrated phases that involve adhesion, activation and aggregation (Andrews et al., 1997, Ruggeri, 2002, Gorbet and Sefton, 2004, Mackman, 2008).

Platelet activation results in the release of intracellular granules that contain platelet factor 4, thrombospondin, β -thromboglobulin, ADP and serotonin. P-selectin, a glycoprotein that mediates adhesion of platelets with neutrophils, monocytes and lymphocytes, is expressed on the membrane after α granule secretion, and platelet micro-particles form that are rich in factor Va and platelet factor 3 (Gorbet and Sefton, 2004). This initial primary binding state is then accelerated to form a plug at the site of activation.

Activation changes the shape of the platelets through the release of ADP, a weak antagonist that directly induces only shape changes and reversible platelet aggregation (Ruggeri, 2002,

Gorbet and Sefton, 2004, Mackman, 2008). This shape change promotes platelet-platelet contact and adhesion and releases prothrombinase complexes on phospholipids; additional platelets then bind through receptor mediated binding to the attached platelets resulting in platelet aggregation (Ruggeri, 2002, Gorbet and Sefton, 2004, Mackman, 2008).

Platelet aggregation in the secondary state is caused by ADP induced synthesis of thromboxane A₂ and acts as the amplification step that within minutes leads to the accumulation of platelets into a thrombus (Ruggeri, 2002). Platelet activation involves the cleavage and activity of G protein-linked platelet receptor PAR1, thrombin receptor, by the protease α -thrombin generated on the membrane of stimulated platelets (Ruggeri, 2002). These newly activated platelets then release the contents of granules that further promote platelet recruitment, adhesion, aggregation and activation (Mackman, 2008). Platelet binding to adhesive ligands causes enhanced adhesive and pro-coagulant properties through signalling pathways (Ruggeri, 2002). The binding of vWF to platelets triggers an intracellular signalling pathway and a calcium flux that activates a calcium dependent membrane aggregation receptor for fibrinogen (Andrews et al., 1997). The cross-linking with fibrinogen aids in platelet aggregation and completes the primary stage of haemostasis.

The secondary stage of haemostasis occurs simultaneously with the primary stage and has two protein based pathways that lead to the formation of fibrin strands that strengthen and help maintain the platelet plug. The intrinsic, contact activation pathway, and extrinsic, tissue factor pathway, are activated in different ways and involve different proteins found in the serum.

The intrinsic pathway is a series of stepwise reactions that convert proteins in the plasma into serine proteases by proteolysis and is involved in the growth and formation of fibrin in the coagulation cascade (Figure 1.11) (Davie et al., 1991). The intrinsic or contact activation pathway is activated by contact with negatively charged surfaces and the formation of primary complexes on collagen types I and III and other ECM components or artificial materials. Factor XII is auto-activated and undergoes a conformational change due to cleavage and binding upon auto-activation (Colman and Schmaier, 1997). Contact with negatively charged surfaces and ECM also results in the activation of prekallikrein and the cleavage of kininogen (Gailani and Rennè, 2007).

These processes are involved in the activation of several plasma host-defences, in fibrin formation, complement activation and thrombus stability (Gailani and Rennè, 2007). Factor XII becomes factor XIIa that acts on factor XI to convert it into factor XIa. Factor XIa then acts on

factor IX and produces factor IXa (Davie et al., 1991, Colman and Schmaier, 1997, Gailani and Rennè, 2007). Factor IXa and its cofactor factor VIIIa form a tenase complex that binds to factor X and in the presence of Ca^{2+} ions and converts factor X into factor Xa as shown in Figure 1.11 (Davie et al., 1991, Colman and Schmaier, 1997, Gailani and Rennè, 2007).

The physiological and pathological importance of the intrinsic coagulation pathway is not fully understood with no evidence of factor XII deficiencies being related to bleeding disorders. However, other studies have shown that the intrinsic pathway is involved in several vascular diseases (Gailani and Rennè, 2007). Deficiencies in factor XI in mice does not cause a loss of haemostasis whereas factor IX deficiency does. Still, comparisons of factor XI null mice and IX null mice in arterial injury show similar protection from thrombus formation. This finding suggests that the intrinsic pathway is not critically involved with haemostasis but is critical to thrombus formation (Gailani and Rennè, 2007).

The main role of the extrinsic pathway or tissue factor pathway is to rapidly form large amounts of thrombin that is important for the initial activation of blood clotting and is used as a feedback mechanism in coagulation activation (Davie et al., 1991, Gorbet and Sefton, 2004, Gailani and Rennè, 2007). Tissue factor (TF) forms the other pathway of platelet activation and involves thrombin generated by the action of tissue factor found in the vessel wall or free in the blood. The release of tissue factor is one of the ways atherosclerotic plaque rupture is believed to trigger thrombosis (Epstein and Ross, 1999, Libby et al., 2002, Furie and Furie, 2008).

The extrinsic pathway involves the formation of a tenase complex that converts factor X into factor Xa (Figure 1.11). The tenase complex is produced when factor VIIa, from the circulation, comes in contact with and forms a complex with TF as shown in Figure 1.11. TF is found on the membrane of cells in the subendothelial layers of blood vessels, is expressed on the surface of damaged cells at the site of vascular injury and can be found free in the blood (Gorbet and Sefton, 2004, Gailani and Rennè, 2007). TF activates clotting when blood vessels are damaged and the underlying cells are exposed to blood flow (Gailani and Rennè, 2007). The extrinsic pathway is believed to be short lived due to the presence of a lipo-protein-associated coagulation inhibitor or extrinsic pathway inhibitor that inactivates the factor VIIa-tissue factor complex (Davie et al., 1991, Gailani and Rennè, 2007). The short lived nature of the extrinsic pathway means that the intrinsic pathway becomes the primary mode for the continued growth of fibrin clots (Davie et al., 1991, Gailani and Rennè, 2007).

The intrinsic and extrinsic pathways converge at the common pathway where factor X is activated and is converted to factor Xa. Factor Xa activates pro-thrombin conversion to thrombin in the presence of cofactor Va and subsequently the conversion of fibrinogen into fibrin by thrombin (Gailani and Rennè, 2007). The fibrin that is formed in the common pathway is then cross-linked by factor XIII to stabilise the clot (Figure 1.11) (Gorbet and Sefton, 2004).

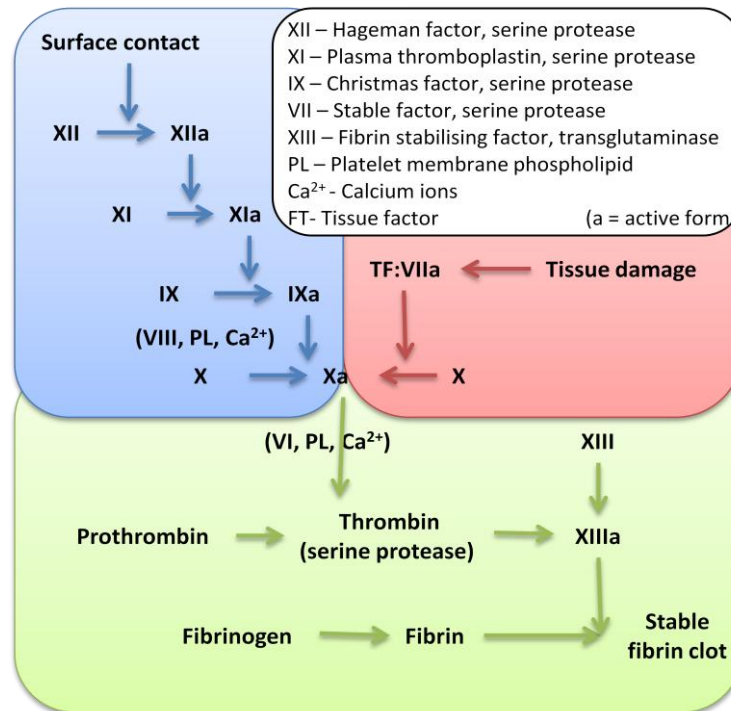


Figure 1.11; Schematic of intrinsic and extrinsic pathways in blood clot formation

There are a number of cofactors that are involved in several of the blood clotting cascades. Calcium is a key cofactor and is involved in the binding of several factors to platelets and the action of the tenase complexes formed by the extrinsic and intrinsic pathways (Mann et al., 1990, Gorbet and Sefton, 2004, Gailani and Rennè, 2007). Removal of calcium from collected blood by the addition of citrate is a widely used method to prevent blood coagulation. Blood coagulation can be restored to citrated blood by the addition of excess calcium. Vitamin K is an important cofactor involved in many different metabolic pathways. Several of the complexes involved in the blood coagulation pathway, most notably the tenase complexes from the intrinsic and extrinsic pathways, involve vitamin K-dependent enzymes to create the appropriate serine proteases (Mann et al., 1990). Warfarin, an anti-clotting agent, works by

reducing the level of available vitamin K and its effects can be reversed by the addition of excess vitamin K to treated blood.

There are many different mechanisms that are used to regulate blood coagulation. Protein C is a major physiological anticoagulant that degrades factor Va and VIIIa (Esmon, 1989). Protein C is activated by the binding of Protein C and thrombin to a thrombomodulin receptor; the receptor vastly accelerates the activation of Protein C (Esmon, 1989). Activated Protein C forms a complex with Protein S and several lipids to form a serine protease that inactivates factors Va and VIIIa by proteolysis of several peptide bonds in activated factor Va and VIIIa (Esmon, 1989).

The majority of coagulation factors are serine proteases. Plasma contains several protease inhibitors, α 1-protease inhibitor, α 2-macroglobulin, heparin cofactor II and antithrombin III, which are involved in the modulation and inhibition of coagulation in healthy vasculature *in vivo* (Gorbet and Sefton, 2004). Antithrombin is the most common serine protease inhibitor that inhibits the action of thrombin and the factors involved in the intrinsic pathway, factors Xa, IXa, XIa and XIIa (Davie et al., 1991). Antithrombin forms a one-to-one complex with these factors and blocks the site of enzymatic activity. In the presence of heparin or similar sulphated glycosaminoglycans, the inhibitory effect of antithrombin is greatly increased (Davie et al., 1991). Antithrombin plays an important part in preventing thrombosis. Deficiency in antithrombin can be inherited or acquired but leads to hypercoagulable diseases and often death from thrombophilia if not carefully treated (Van Boven and Lane, 1997).

The main regulator of the extrinsic or tissue factor pathway is the tissue factor pathway inhibitor (TFPI). TFPI inhibits the activity of the factor VIIa-TF complex towards factor X and, to a lesser extent, to factor IX in what is believed to be a two step mechanism (Broze Jr, 1995, Panteleev et al., 2002). TFPI binds to factor Xa near or on the active site of the enzyme and inhibits further progression through the common pathway. It is believed that the TFPI-Xa complex then binds to the factor VIIa-TF complex and blocks its activity rapidly deactivating the extrinsic pathway (Broze Jr, 1995, Panteleev et al., 2002). Platelets carry around 10 % of the total TFPI in the blood and release it following stimulation by antagonists such as thrombin (Broze Jr, 1995).

Several of the regulatory mechanisms target platelet activity. Prostacyclin is released from platelets upon activation and is involved in the negative feedback regulation of platelet activity (Ruggeri, 2002). Prostacyclin is a potent stimulator of cyclic adenosine monophosphate (cAMP)

accumulation in platelet rich serum. cAMP inhibits platelet activation in many different ways; preventing granule release, preventing the exposure of a pro-coagulant phospholipid surface and preventing platelet adhesion and aggregation (Krishnamurthi et al., 1984, Zwaal et al., 1984). It is believed that this is brought about by the lowering of cytoplasmic calcium in the platelets that has been shown to be critically involved, directly or indirectly, with platelet activation (Krishnamurthi et al., 1984).

Fibrinolysis is one of the key maintenance mechanisms involved in blood clotting and starts to degrade a clot within a few hours. In the presence of newly generated fibrin tissue, plasminogen activators catalyze plasminogen into plasmin, which breaks down fibrin (Davie et al., 1991). Slow fibrin turnover allows for tissue remodelling and repair and the intrinsic pathway likely acts as an antagonist against fibrinolysis to create a slow rate of fibrin turnover (Davie et al., 1991). This adds to the belief that the intrinsic pathway is more closely involved with thrombus formation.

Thrombi formed in arteries and veins differ in their composition. Venous thrombi tend to be fibrin and red blood cell rich and relatively poor in platelets where arterial thrombi tend to have high levels of platelets. The intrinsic pathway is involved in fibrin formation in venous thrombosis. The role of the intrinsic pathway in arterial thrombosis is not as clear (Gailani and Rennè, 2007). As such arterial thrombi differ from venous thrombi in their target of action, anti-arterial thrombosis treatments target platelets and anti-venous thrombosis treatments target the proteins of the coagulation cascade (Mackman, 2008).

1.6.1 Thrombus prevention

There are two main ways by which to prevent thrombus formation. In a healthy blood vessel, thrombus formation is prevented by a layer of endothelial cells that form an anti-thrombogenic layer (Nerem, 2000, Rémy-Zolghadri et al., 2004, Williamson et al., 2007, Yin et al., 2009). In the case of medical intervention, blood clot formation is often prevented by treatment with anti-clotting agents such as heparin, dipyridamole and warfarin, or by the use of anti-fouling surfaces (Uyama et al., 1998, Aldenhoff et al., 2001, Liem et al., 2001, Crowther et al., 2002, Knetsch et al., 2004, Fittkau et al., 2005, Wang et al., 2007b).

1.6.2 Non-fouling surfaces

There are a wide range of non-fouling materials, mainly synthetic polymers, which have been produced for use in biomedical applications. Polyacrylamide has been shown to have a low level of platelet interaction. Polyvinylpyrrolidone has been used to coat surfaces to reduce the adsorption of fibronectin and poly N, N-dimethylacrylamide has been shown to work as a coating that will remain unfouled for extended periods of time (Uyama et al., 1998). Poly ethylene glycol (PEG) has been the main focus of anti-fouling surfaces in vascular graft replacements. PEG has been incorporated into a wide range of materials and extensive testing has revealed a short, four subunit long PEG that has been found to be the most inert form in interactions with blood; PEG has also been modified with RGD and other ligands to allow for the attachment of cells to the surface (Uyama et al., 1998, Fittkau et al., 2005).

The use of anti-fouling surfaces works but is not an ideal solution for preventing thrombus formation since the modification of the surfaces can lead to changes in chemical and mechanical properties. Degradation of the surface will naturally occur in the long-term use of a vascular replacement and the loss of the anti-fouling coating will allow for the formation of blood clots if a fully functional endothelial layer has not formed. Natural extracellular matrix regulates the binding and release of proteins and various factors from the blood. The loss of this function could negatively impact on cellular interactions and negate one of the reasons for using naturally derived scaffolds as vascular grafts.

1.6.3 Anti-clotting agents

In thrombotic disorders such as deep vein thrombosis, blood clots are formed and lead to thrombus that occlude the blood vessel and cause serious problems. Blood clotting disorders are treated with anti-clotting agents to prevent the initial blood clot formation. In the same manner, anti-clotting agents could be used to prevent thrombus formation in vascular grafts. There has been much interest in the use of anti-coagulants that are released from or attached to vascular replacements. Anti-clotting agents that are used systemically can often lead to complications, especially as patients requiring vascular grafts often have some form of vascular disease making long term treatment with anti-clotting agents undesirable (Saltzman and Olbricht, 2002, Nagai et al., 2006).

Controlled delivery or immobilisation is a preferable method of treatment as it is more efficient, being able to directly deliver to the required site means that lower overall doses are needed and there are lower potential risks (Wissink et al., 2000, Fattori and Piva, 2003, Luong-Van et al., 2006). Heparin is a highly-sulphated glycosaminoglycan that is a naturally occurring anti-clotting agent. Commercially available heparin has a molecular weight of around 12 kDa – 15 kDa (native heparin is between 3 kDa and 50 kDa) and is highly negatively charged.

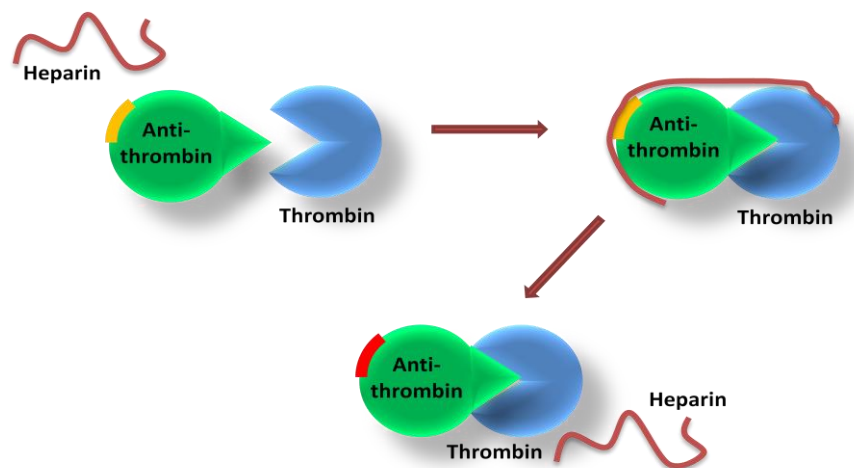


Figure 1.12, Schematic of the action of heparin on the formation of thrombin-anti-thrombin complex; Heparin binds to anti-thrombin and catalyses the reaction with thrombin, the affinity of anti-thrombin for heparin is reduced and heparin is released.

It has been demonstrated that heparin works by accelerating the action of anti-thrombin, an inhibitor that neutralizes thrombin, by increasing the rate at which thrombin and anti-thrombin complex (Rosenberg, 1974, Bjork and Lindahl, 1982). Once the thrombin-anti-thrombin complex has been created, the heparin is released from the complex as it is not consumed in the reaction (Figure 1.12) (Bjork and Lindahl, 1982).

The use of heparin on Dacron has been extensively explored as a method of improving patency. Heparin has been shown to increase the lifetime of vascular grafts by reducing the rate of thrombus formation without affecting mechanical properties (Wang et al., 2007b). The use of heparin has been shown to have no effect on the attachment of endothelial cells and has also been demonstrated to significantly increase endothelial cell density (Knetsch et al., 2004). This could be caused by direct stimulation of endothelial cell growth or by the potentiation of growth factors, where under the right conditions heparin binds such growth

factors as vascular endothelial growth factor or basic fibroblast growth factor, increasing the proliferation of the endothelial cells (Knetsch et al., 2004).

Heparin increases the time a graft remains patent, but the loss of heparin as this is released or lost from the surface of the graft eventually leads to thrombus formation (Xue and Greisler, 2003, Venkatraman et al., 2008). Dipyridamole is an anti-platelet drug. Dipyridamole is believed to act in two possible ways. One way is blocking the uptake of adenosine into platelets. The other mechanism is by inhibiting the enzyme phosphodiesterase, that breaks down cAMP, leading to higher levels of cAMP, so preventing platelet coagulation (Moncada and Korbust, 1978, Gresele et al., 1986). Dipyridamole has been shown to reduce thrombus formation and platelet activation, increasing the lifetime of vascular grafts (Aldenhoff et al., 2001). An endothelial cell layer can attach and survive on dipyridamole, but dipyridamole has been shown to significantly slow cell growth by reducing the rate of DNA synthesis which could cause problems with re-endothelialisation and long term patency (Aldenhoff et al., 2001, Liem et al., 2001).

Warfarin has been used for the treatment of thrombus formation. For this purpose, low levels of warfarin are used as it has been shown to carry a high risk of haemorrhage (Crowther et al., 2002). Warfarin works by inhibiting peroxide reductase that diminishes the level of vitamin K and therefore prevents the synthesis of vitamin K dependent clotting factors (Bell et al., 2002). Warfarin has been shown to increase the lifetime of grafts but does not prevent eventual failure due to thrombosis (Crowther et al., 2002). It has been shown that the presence of warfarin has no significant effect upon the attachment and normal function of endothelial cells (Liem et al., 2001).

Recently, there has been increased interest in the use of DNA aptamers in the prevention of thrombus formation. On screening a collection of randomly synthesized DNA segments, it was found that a single strand of DNA will bind to thrombin with high affinity (Raviv et al., 2008). The DNA segment GGTGGTGTGGTTGG is able to bind to exosite 1, the fibrin binding site, of thrombin and prevent thrombin catalyzed fibrin clot formation (Bock et al., 1992, Dougan et al., 2003). The DNA aptamer has been shown to fully displace pre-bound thrombin from preformed clots and aid in, but not directly cause, the breaking up and removal of blood clots (Raviv et al., 2008). The aptamer has also been shown to prevent the binding of thrombin to protease-activated receptors and so prevent platelet activation (Raviv et al., 2008). The main problem concerning the use of DNA aptamers is the lifetime of free DNA in the blood due to serum nucleases that will destroy the aptamer within a matter of minutes (Dougan et al.,

2000). The lifetime of the aptamers can be extended by adding caps to the end of the DNA sequence to prevent enzymatic degradation (Dougan et al., 2000).

The use of slow release anti-coagulants and anti-coagulant coatings allows for the prevention of clot formation and platelet activation. The problem with using anti-clotting agents is that they do not replace the natural endothelial layer. Additionally, if the anti-coagulant is fully released or removed from the surface of a scaffold by degradation and a fully formed endothelial layer has not formed, platelets will become activated and blood clots will form. This is the reason for the number of reported cases in which anti-clotting agents were able to increase the lifetime of the vascular graft, but unable to prevent eventual thrombus formation and failure.

1.6.4 Endothelium formation

Another approach to deal with thrombus formation is the creation of an endothelial layer. This is the approach taken when scaffolds are cellularised *in vitro* and the presence of a fully formed endothelium is used to prevent platelet activation and thrombus formation. *In situ* cellularisation attempts to increase the speed and efficiency at which a fully formed and functional endothelial layer is created in order to prevent thrombus formation. This can be achieved by the use of cell attachment ligands and growth factors.

1.6.4.1 Growth factors

There are a range of different growth factors that have been identified to be involved with endothelial cell maintenance. Basic fibroblast growth factor (bFGF) belongs to the family of fibroblast growth factors and is involved in angiogenesis and wound healing. bFGF is found in a membrane bound form on the basement membrane and subendothelial layers of blood vessels (Thomas, 1987, Ornitz and Itoh, 2001). It has been reported that bFGF is a mitogen for fibroblasts, endothelial and smooth muscle cells (Asahara et al., 1995, Dixit et al., 2001). An increase in the penetration of cells into scaffolds and in endothelial cell proliferation has been observed with the use of bFGF, and it has been demonstrated to work in a dose dependent manner (Chen et al., 1997, Wissink et al., 2000, Simionescu et al., 2006). The lifetime of

fibroblast growth factors have been shown to be increased by the introduction of heparin which increases resistance of fibroblast growth factors to thermal degradation (Thomas, 1987, Wissink et al., 2000, Ornitz and Itoh, 2001).

Vascular endothelial growth factor (VEGF) is a subset of the platelet derived growth factor family; it is a key regulator of angiogenesis and vasculogenesis and has been implicated in wound healing, endothelium maintenance and endothelial cell survival (Zachary, 1998, Luo et al., 1998, Dorafshar et al., 2003, Ferrara et al., 2003, Matsuno et al., 2003, Cursiefen et al., 2004, Zhou et al., 2009b). VEGF has been reported to be a powerful mitogen and chemo-attractant of endothelial cells, working on endothelial cells to increasing their rates of proliferation and migration (Asahara et al., 1995, Zachary, 1998, Luo et al., 1998, Matsuno et al., 2003, Zhou et al., 2009b).

There are different forms of VEGF: factor A has been associated with migration and proliferation of endothelial cells and linked to the creation of the blood vessel lumen; factor B has been shown to be involved with embryonic angiogenesis; factor C has been reported to be linked to lymphangiogenesis; and factor D has been linked to angiogenesis (Zachary, 1998, Ferrara et al., 2003, Matsuno et al., 2003, Cursiefen et al., 2004, Bhardwaj et al., 2005).

VEGF is highly specific to endothelial cells and acts by promoting the expression of plasminogen activators, metalloproteinase and interstitial collagenase which provide the environment needed for cell migration and proliferation (Dvorak et al., 1995, Asahara et al., 1995, Luo et al., 1998, Ferrara et al., 2003, Matsuno et al., 2003). Cellular invasion and vascular remodelling is also promoted by the expression of urokinase receptors triggered by VEGF (Ferrara et al., 2003). VEGF has been shown to accelerate the re-endothelialisation of vascular scaffolds and prevent thrombus formation (Asahara et al., 1995, Lemstrom et al., 2002, Drury and Mooney, 2003, Ferrara et al., 2003, Zhou et al., 2009b).

A variant of VEGF, VEGF₁₆₅, has been found to have the highest mitogenic activity and to promote faster re-endothelialisation (Zhou et al., 2009b). High local levels of VEGF are needed to promote re-endothelialisation because of the short lifetime of VEGF in the blood. The lifetime of VEGF can be increased by the presence of heparin which improves stability and bioactivity (Drury and Mooney, 2003, Matsuno et al., 2003, Zhou et al., 2009b).

The use of growth factors has been shown to greatly improve the re-endothelialisation of vascular grafts. However, there are several problems associated with the use of growth factors. Fibroblast growth factors are able to promote the proliferation of endothelial cells but,

as they are not cell specific, they also promote the proliferation of smooth muscle cells which is linked to intimal hyperplasia. VEGF is cell specific but is reported to be closely linked with tumour pathogenicity and spreading (Zachary, 1998, Dorafshar et al., 2003, Ferrara et al., 2003, Cursiefen et al., 2004).

1.6.4.2 Attachment ligands

For in situ re-endothelialisation, it is important not only to stimulate cell proliferation but also cell migration and attachment. Migration can be triggered by growth factors, but this is heavily dependent upon the presence of attachment ligands to facilitate attachment and retention; this is of particular importance in flow conditions.

RGD (Arginine-Glycine-Aspartic acid) is a naturally occurring attachment motif; it is often in the form of RGD, PRGDS or YRGDS and is known to enhance cell attachment to a surface (Drury and Mooney, 2003, Chen and Hunt, 2007, Wang et al., 2008). The inclusion of RGD on vascular scaffolds such as Dacron and POSS-PCU, has been shown to enhance cell migration, attachment and retention; it has been suggested that RGD could have catch and hold characteristics (Patel et al., 2007, Wang et al., 2008, de Mel et al., 2009). RGD sequences are reported to be easily incorporated into scaffolds either by direct binding of the amino acid groups, the physical adsorption of the RGD peptide sequence onto the scaffold or the incorporation of RGD into the structure of synthetic grafts (Walluscheck et al., 1996, Fittkau et al., 2005, Patel et al., 2007).

Studies using RGD motifs have highlighted the importance of distribution and density on cell function. It has been demonstrated that the presence and density of attachment ligands can control cell growth and function. Low concentrations of RGD result in poor cell migration, retention and function. High levels of RGD have been shown to significantly increase cell attachment but have been reported to have a detrimental effect upon cell migration and proliferation. At the appropriate concentrations RGD has been shown to enhance cell attachment and retention whilst stimulating cell migration and proliferation; it has also been shown to increase the cells resistance to shear stresses (Walluscheck et al., 1996, Chen and Hunt, 2007, Norman et al., 2008).

Other naturally derived attachment ligands have been investigated, such as YIGSR and RYVVLPR from laminin and TAGSCLRKFSTM from collagen. All have been shown to improve the

attachment and migration of endothelial cell to scaffolds, but not as well as RGD (Drury and Mooney, 2003, Genové et al., 2005). YIGSR has been found to increase cell migration whilst not causing blood clotting (Jun and West, 2004). A mixture of RGD and YIGSR has been reported to have a higher rate of cell adhesion and retention, than either of the two ligands individually, without affecting the cell spreading behaviour (Fittkau et al., 2005). This indicates that a combination of different attachment ligands may yield the best results.

There has been interest in the possible use of antibodies for the selective capture and retention of cells from the blood stream. Endothelial progenitor cells are a bone-marrow derived subset of CD34+ cells that can differentiate into endothelial type cells (Urbich and Dimmeler, 2004, Aoki et al., 2005, Rotmans et al., 2005, Patel et al., 2007, Yin et al., 2009). In normal vascular biology, endothelial progenitor cells contribute to re-endothelialisation, but only to a small extent (Urbich and Dimmeler, 2004). It has been reported that antibodies against CD34+ cells may be used to capture and attach endothelial progenitor cells from the blood stream. Using antibodies the number of progenitor cells attached to the scaffold has been increased; the progenitor cells then contribute to, and accelerate, re-endothelialisation (Aoki et al., 2005, Patel et al., 2007, Yin et al., 2009). This technique has been used to attach cells and form a layer of cells on the surface of a replacement blood vessel. The antibodies have been shown not to adversely affect the metabolic activity of the endothelial cells, and normal growth and differentiation has been observed (Aoki et al., 2005, Yin et al., 2009).

There are possible problems with the use of antibodies against CD34+ cells; endothelial progenitor cells are just one subset of CD34+ cells. Because of this, the attached cell has the potential to differentiate into other cells rather than endothelial cells, such as smooth muscle cells (Urbich and Dimmeler, 2004, Rotmans et al., 2005). As the antibodies used must be anti-human CD34+ antibodies, they could elicit an immune response if they have been developed in animals, as in the case of mice (Aoki et al., 2005).

Due to the immune response and range of cells that can be attached to antibodies against CD34+ cell markers there is research into the development of aptamers that are specifically targeted to one cell type. An example is a DNA aptamer developed by Hoffman et al. that binds endothelial progenitor cells. Similarly, Veleva et al. have developed a peptide aptamer, with amino acid sequence of TPSLEQRTVYAR, that selectively binds to blood outgrowth endothelial cells (Hoffmann et al., 2008, Veleva et al., 2008). Cell ligand interactions are complex and the function of the ligand is dependent upon the ligand environment (Barker, 2011).

Proteolysis and mechanical stimulation of the ECM has been shown to potentially expose or alter conformationally-sensitive ligand domains that have different effects in different conformations (Barker, 2011). Proteolytic fragments of the ECM have been shown to have an enhanced mitogenic activity; this effect results in a new class of bio-molecules called “matrikines” (Barker, 2011). The inclusion of cell attachment ligands has the potential to aid and accelerate the formation of an endothelial cell layer to aid in the prevention of thrombus formation. It is worth noting that, even though the addition of the attachment ligands will accelerate endothelialisation, there is a time period before the fully functional endothelial layer is formed where the vessel will be prone to blood clot formation and thrombosis.

1.6.5 Advantages and limitations of current methods associated with thrombus prevention

There are many different ways of preventing thrombosis that have been researched, yet no ideal approach has been found. The use of non-fouling surfaces has been well explored for the creation of a range of medical devices. Non-fouling surfaces have been shown to successfully prevent thrombus formation, but, due to the properties of the materials that make them non-fouling, these materials are unable to facilitate normal cellular function. The controlled release of anti-clotting drugs and their coating of surfaces has been shown to increase the life-time and patency of vascular grafts. The use of anti-clotting drugs should allow for normal cellular attachment and function; however, coatings and controlled release devices have a limited lifetime until the drug has worn off the surface or has been fully released. If a fully formed and functional endothelium is not present then thrombosis can occur. It is also not desirable to use anti-clotting agents unless necessary as their use can lead to complications. The idea of forming a fully functional endothelium on a scaffold *in vitro* should mimic the natural method of thrombosis prevention. The sourcing of the patient’s own cells, the time and cost of growing the endothelium and the risks of infection limit the potential application of this technique.

The idea of forming an endothelium *in vivo* is very attractive and, if successful, it should provide a natural anti-thrombogenic barrier which will allow for long-term graft patency and lifetime. The problem with *in vivo* recellularisation is that the endothelium will take time to form and before the endothelium is fully formed the graft will be highly susceptible to

thrombosis formation. To prevent thrombogenesis, it is desirable to have an endothelium that can interact and regulate blood clotting.

Because of the issues with *in vitro* recellularisation, it is preferable to use *in situ* recellularisation to form the endothelium. To prevent thrombosis formation before the endothelium can be grown *in situ*, some form of anti-clotting function is needed. As non-fouling surfaces tend to disrupt or prevent cell attachment and migration, their use would be counterproductive to the formation of an endothelium layer. The use of anti-clotting agents is one possible method of preventing thrombogenesis; however, their use is not ideal due to the possibility of associated complications. The ideal situation would be the addition of a material or coating to the decellularised vessel that acts to passivate the surface and aids in cell attachment and migration.

1.7 Self-assembled peptides as biomaterials for tissue engineering

1.7.1 Self-assembly

Self-assembly is the spontaneous organisation of molecules into well ordered and structurally defined arrangements that are stabilised through non-covalent interactions. Self-assembly is a major field of research in nanotechnology and is the basis of bottom-up nanotechnology. The best examples of self-assembly can be found in biology. The cell membrane is a double layer of lipid molecules that self-assemble into a membrane due to hydrophobic interactions. Similarly, the proteins that constitute the capsid of a virus are synthesised by the host cell and then self-assemble around the viral nucleic acids. Self-assembly is possible with a wide range of polymers, lipids, DNA, peptides and proteins; the structures of these molecules can be rationally designed to control the structures that are formed and the conditions that will trigger self-assembly (de Loos et al., 2005). The most basic form of self-assembly is self-complementary; where two identical molecules, designed to have alternating charges, align alongside each other in a parallel or anti-parallel arrangement and are joined by hydrogen bonds (Aggeli et al., 2001).

1.7.2 Nucleated and non-nucleated 1D self-assembly

The most basic form of self-assembly is the organisation of molecules in one direction/dimension into an ordered structure. Self-assembly can either be nucleated or non-nucleated. Non-nucleated self-assembly otherwise known as isodesmic equilibrium is where monomers are added together in a step-wise fashion and the addition of every monomer is governed by a single equilibrium (Smulders et al., 2009). Nucleated or cooperative self-assembly has an unfavourable activation step requiring the formation of a nucleus from which chain elongation and growth happens (Chen, 2005, Smulders et al., 2009). The formation of a nucleus occurs by self-association and will only happen above a critical concentration. Below this concentration, the molecules will be monomeric with the presence of unstable seeds (Chen, 2005). Isodesmic self-assembly is a slow and gradual process with an increase in concentration resulting in an increase in chain length and number. Nucleated self-assembly has a bimodal distribution of monomer and elongated chains, this can be seen as a steady increase in chain length with concentration (Smulders et al., 2009).

1.7.3 Complementary self-assembly

Complementary self-assembly happens when two different molecules combine together to create an ordered structure. Two molecules that have the opposite electrostatic charge that self-assemble when mixed are an example of complementary self-assembly. The molecules that will self-assemble complementarily have a 1:1 stoichiometric ratio and will only self-assemble if they are correctly charged under the same conditions (Aggeli et al., 2003a). Complementary self-assembly most commonly happens due to Coulombic attraction between the two oppositely charged monomers; when mixed, the monomers will spontaneously self-assemble. Complementary self-assembly is attractive due to the ease of triggering self-assembly and the increased stability of the structures formed. Self-complementary self-assembled structures are mainly held together by hydrogen bonding; complementary self-assembled structures are held together by electrostatic interactions as well as hydrogen bonds increasing the stability (Aggeli et al., 2003a).

1.7.4 Peptide self-assembly

Peptides have great potential as biomaterials for tissue engineering. The use of the natural material, amino acids, in peptide design should allow for the creation of a biocompatible, biodegradable and non-immunogenic biomaterial. As with natural protein folding, the two main conformations that peptides can assume are α -helix and β -sheet. Peptides can self-assemble to form a wide range of different structures including β -sheets, β -hairpins, α -helices, monolayers, nanotubes (vesicles) and there are peptides that can switch between a β -sheet and α -helix conformation (Zhang and Altman, 1999, Zhang, 2002). The wide range of amino acids that can be used to make a peptide sequence mean that a range of material properties can be achieved by varying the peptide sequence and length. It has been found that the most important factor when designing a peptide to be either α -helix or β -sheet is periodicity; an alternating sequence of polar and non-polar amino acids will preferentially form a β -sheet structure (Xiong et al., 1995).

1.7.4.1 β -Sheet

Due to their biological relevance, peptides that form β -sheets are of particular interest for the formation of biomaterials, but also for their pathological significance in the misfolding of proteins and the formation of amyloid plaques. β -sheet forming peptides can be considered as chiral rods that self-assemble in one dimension to create elongated peptide β -sheet tapes (Aggeli et al., 2001, Aggeli et al., 2003b, Carrick et al., 2007).

The surfaces of a β -sheet forming peptide have differences in hydrophobicity. This causes tapes to stack, one on top of the other, above a certain concentration to create a range of higher ordered structures (Zhang and Altman, 1999, Aggeli et al., 2001). The concentration dependence of peptide self-assembly results in a hierarchy of structures being formed (Aggeli et al., 2001, Carrick et al., 2007). As the peptides are chiral, a twist is induced in the peptide tape. As the concentration is increased the ribbons stack to create a fibril, the fibril size is limited by the twisting of the ribbons (Figure 1.13). Fibrils then interact edge to edge and twist together to create fibres (Aggeli et al., 2001, Aggeli et al., 2003b, Carrick et al., 2007). Fibril size and width is related to the competition between the free energy gain and the elastic cost of

untwisting, since a fibril has to untwist slightly to permit further stacking (Aggeli et al., 2001, Carrick et al., 2007).

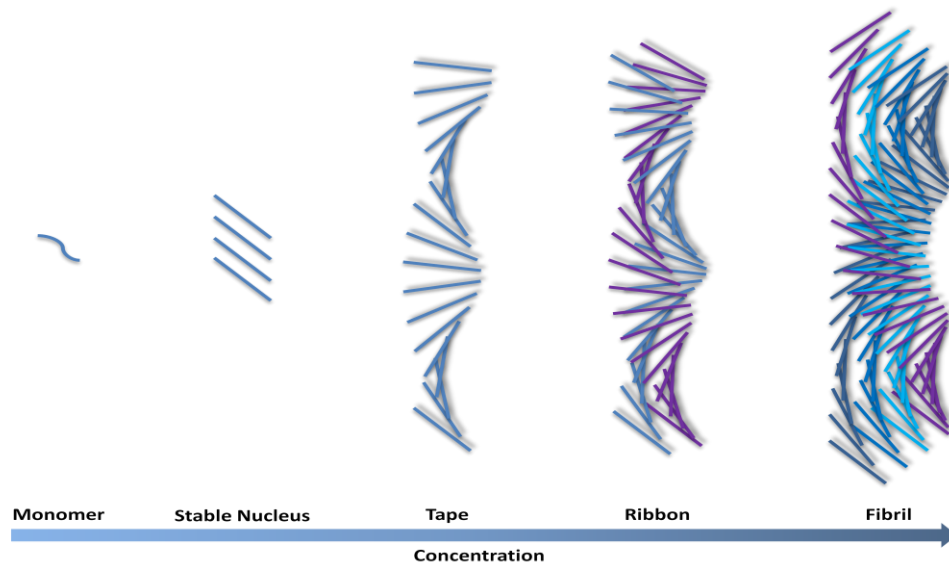


Figure 1.13; Hierarchy of β -sheet self-assembly

1.7.4.2 β -Hairpin

β -Hairpin peptides are formed from two β -sheet strands joined together by a β -turn. The strands are made of alternating hydrophobic and hydrophilic amino acids, such as lysine and valine. The formed peptide will fold into an amphiphilic β -hairpin when the electrostatic repulsion between strands is reduced. The amphiphilic hairpin will then self-assemble via hydrophobic interactions to form a fibrillar structure that excludes the hydrophobic amino acids from aqueous solution (Figure 1.14). The lessening of the electrostatic repulsive forces on hydrophilic amino acids can be achieved in basic conditions, deprotonating and neutralising the charged side chains (Schneider et al., 2002, Ozbas et al., 2004). The electrostatic charge on the hydrophilic amino acids can also be screened by the presence of salt, as in physiological conditions (Ozbas et al., 2004, Haines-Butterick et al., 2007). The amphiphilic β -hairpins naturally form non-covalent cross-links between fibrils. These cross-links are semi-permanent and are formed by both hydrogen bonding and hydrophobic interactions (Ozbas et al., 2004).

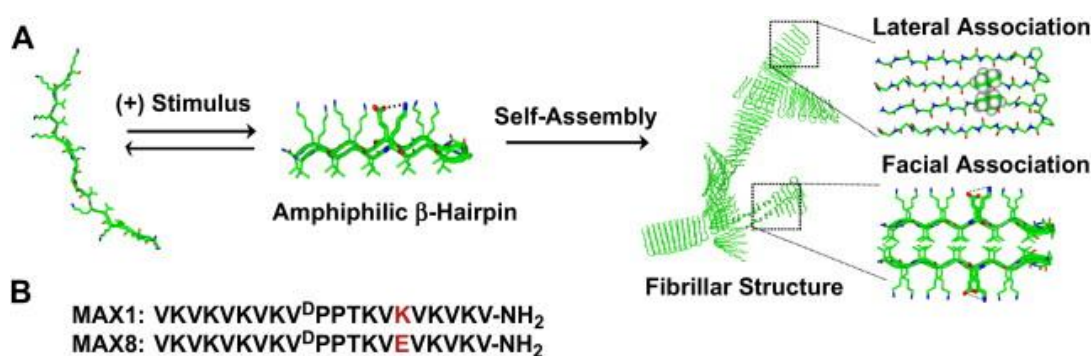


Figure 1.14; (A) Schematic of folding and subsequent self-assembly when MAX1 and MAX8 peptides are placed in physiological solution. (B) Peptide sequences of MAX1 and MAX8. Reproduced from Haines-Butterick *et al* (Haines-Butterick *et al.*, 2007).

1.7.4.3 π - π Stabilised β -sheet

Fmoc-dipeptides have been demonstrated to self-assemble and form stable self-supporting gels with a reduction of solution pH. Fmoc-dipeptides self-assemble in two ways; Fmoc-dipeptides form anti-parallel β -sheets but also form anti-parallel π - π stacks. The only conformation that allows for both states to exist is the formation of cylindrical structures formed by the interlocking of anti-parallel β -sheets through lateral π - π interactions with aromatic groups on adjacent sheets (Figure 1.15); these cylindrical structures then align to form a flat ribbon (Smith *et al.*, 2008). Work on Fmoc-AA peptides has shown that Fmoc-group π - π stacking plays the key role in stabilizing the fibril structure of the self-assembled peptides (Mu *et al.*, 2012).

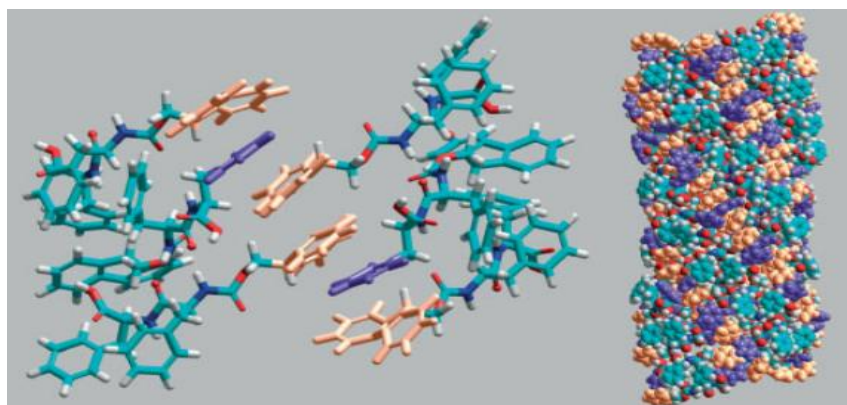


Figure 1.15, Left: Fmoc-FF β -sheets, binding through π - π -stacked phenyl (orange) and Fmoc groups (purple); Right: side view of Fmoc-FF aggregate. Adapted from Smith *et al* (Smith *et al.*, 2008).

1.7.4.4 α -Helix coiled coils

A coiled coil is made up of two or more supercoiled α -helices. These comprise two or more peptide chains designed to co-assemble resulting in an offset α -helix dimer with complementary ends (Figure 1.16). The complementary ends allow dimers to assemble longitudinally into a fibril. Through careful design, the fibrils are made to align by hydrophobic and hydrogen bonding interactions into thick fibres. The use of hydrophobic interactions favours the hydrogelation of these peptides when mixed. As long as these peptide are mixed in the correct conditions, self-assembly follows the complementary self-assembly pathway and no additional trigger is needed except for the mixing of the peptides (Banwell et al., 2009).

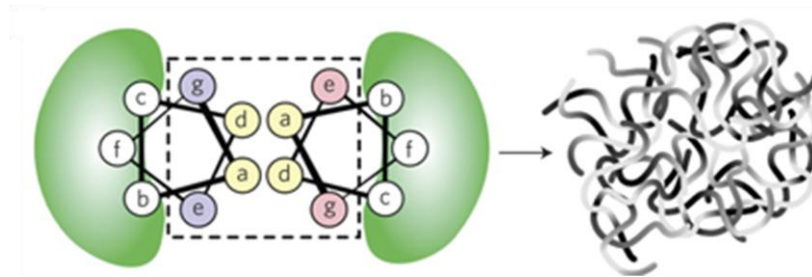


Figure 1.16, Schematic of Alpha helix forming peptide coiled coil architecture. Reproduced from Banwell et al (Banwell et al., 2009).

1.7.5 Peptide biocompatibility

1.7.5.1 RAD-based peptides

At the time of writing RAD-based peptides, developed by Zhang and co-workers, are the subject of the majority of the literature on peptide self-assembly. The RAD-based peptides are modelled on a peptide sequence from a yeast protein and undergo hydrophobic stacking into β -sheets. These β -sheets then stack further into ribbons and fibrils (Zhang et al., 1993). Whilst several variations of the RAD-based peptide have been developed, the main interests lies in RAD16-1, Ac-(RADA)₄-CONH₂, which has been commercialised under the name PuraMatrix.

Several applications for RAD16-1 have been investigated. RAD16-1 has been shown to support the growth of neural cells and the formation of new functional synapses (Holmes et al., 2000,

Ellis-Behnke et al., 2006). RAD-based peptides have been demonstrated to support the growth of endothelial and myocardial cells, and have been shown to be better for recellularisation than Matrigel (Davis et al., 2005). It is reported that RAD16-1 has immediate haemostatic properties and has been shown to support favourable tissue growth and repair in a wound site due to the 3-dimensional matrix formed as the peptides self-assemble (Meng et al., 2009). RAD16-1 has also been shown to increase tissue repair by lowering the number of macrophages and astrocytes at the wound, cells known to be causes of secondary injury (Guo et al., 2009).

The immunological properties of RAD16-1 have been tested. When injected into rats, rabbits and goats RAD16-1 showed no inflammatory or immune response even having been conjugated with a carrier protein (Holmes et al., 2000). Attempts have been made to enhance the biological properties of RAD16-1 by the addition of functional groups YIGSR and RYVVLPR. Attachment ligands shown to promote cell adhesion, migration and tubular formation have been added onto the end of RAD16-1 and have been shown to increase the number of attached cells and increase cell growth (Genové et al., 2005).

1.7.5.2 P₁₁ series of peptides

The P₁₁ peptides are a range of around 30 peptides developed by Aggeli and co-workers at the University of Leeds. This series of peptides are all 11 amino acids in length and are designed to form anti-parallel β -sheet structures following the hierarchy of nucleated self-assembly (Figure 1.13). Some of these peptides have been designed to self-assemble by a change in pH or ionic concentration (Aggeli et al., 2003b, Carrick et al., 2007). Several of the peptides have also been designed to remain monomeric and self-assemble by complementary self-assembly (Aggeli et al., 2003a).

The main focus of the work around the P₁₁ series of peptides has been on the development of design criteria to produce superior peptides for the purpose of tissue engineering and regenerative medicine. It has been found that for this class of peptides a ± 2 charge is needed for self-assembly in physiological solutions (Maude et al., 2011a) (Personal communication from Dr D. Miles, University of Leeds). It has been shown that serine and threonine based P₁₁ peptides interact with model cell membranes and that amino acid sequence is important to peptide/phospholipid membrane interactions (Protopapa et al., 2009). It has been reported

that the positively charged peptides P₁₁-8, P₁₁-12, P₁₁-16 and P₁₁-18 are non cytotoxic to L929 murine fibroblasts. However, only P₁₁-8 supports cell growth and proliferation in 3-dimensional culture (Maude et al., 2011a). It is believed that this is due to the stability of the different peptide gels as P₁₁-8 remains stable where the other peptides degrade preventing cell attachment and normal cell function (Maude et al., 2011a). All of the positively charged peptides show inferior levels of cell growth and proliferation when compared to a collagen gel (Maude et al., 2011a). This could be due to the higher levels of trifluoro acetic acid (TFA) in the positively charged peptides.

It has been shown that the negatively charged peptides P₁₁-4, P₁₁-9, P₁₁-15, P₁₁-17 and P₁₁-20 are non cytotoxic to L929 murine fibroblasts (Personal communication from Dr D. Miles, University of Leeds). Peptides P₁₁-4, P₁₁-15, P₁₁-17 and P₁₁-20 appeared to have supported the growth and proliferation of the cells: most noticeably, P₁₁-4 supported similar levels of growth to the collagen control. Testing with primary human fibroblasts has been reported to show no cytotoxic effect for P₁₁-4 and P₁₁-8 (Wilshaw et al., 2008b). It has been shown that lymphocytes from mice immunised with peptide showed no response to P₁₁-4 or P₁₁-8, however, when the peptides were conjugated with keyhole limpet hemocyanin an antibody titre of 1/64 was measured against both peptides (Wilshaw et al., 2008b).

1.7.5.3 β -Hairpin

Several self-assembling β -hairpin peptides have been developed by Schneider and co-workers. Most widely reported in the literature at the time of writing are MAX1 and MAX8. MAX1 and MAX8 are very similar with one of the lysine residues in MAX1 being replaced with glutamic acid to reduce the gelation time (Haines-Butterick et al., 2007). MAX1 and MAX8 are both designed to self-assemble in cell culture medium (Haines-Butterick et al., 2007).

It has been reported that MAX1 is non-cytotoxic to fibroblasts, and allows for cell attachment and proliferation whilst maintaining its mechanical properties (Kretsinger et al., 2005). The capacity for a pro-inflammatory response has been assessed; it is reported that macrophages will grow on MAX1 and MAX8 gels and show no significant secretion of pro-inflammatory cytokine TNF- α indicating that the peptide gels are non-inflammatory (Haines-Butterick et al., 2008). It has been suggested that MAX1 may be of increased interest as it shows antibacterial properties against both Gram positive and negative bacteria (Salick et al., 2007). MAX1 has

been shown to inhibit the growth and proliferation of *E.coli* below a certain concentration, above this concentration the surface of the gel is covered and the cell remnants allow for the shielding and attachment of other microorganisms (Salick et al., 2007).

MAX1 and MAX8 have been reported as possible cell encapsulation gels for cell delivery. With a reduced gelation time, MAX8 has been reported to be able to entrap cells throughout the gel without the cells settling to the bottom (Haines-Butterick et al., 2007).

1.7.5.4 Fmoc-dipeptides

There are a range of Fmoc-dipeptides that will form self-assembled structures. Of particular interest is Fmoc-diphenylalanine (Fmoc-FF) as it will form gels at low concentrations at a physiological relevant pH (Zhou et al., 2009a). The first reported use of Fmoc-FF was by Gazit and co-workers; the majority of the work on biological use of Fmoc-FF has been reported by Ulijn and co-workers.

Fmoc-FF has been reported to have a wide range of mechanical properties. It is believed that these observed differences are due to different preparation methods and solution pH used to achieve a gel (Helen et al., 2011). A number of different cells have been grown in and on Fmoc-FF peptide gels. It has been reported that chondrocytes grow and proliferate on the surface of Fmoc-FF gels and can be encapsulated in a 3D gel (Jayawarna et al., 2009, Zhou et al., 2009a, Yan et al., 2010). It has been shown that other cells, 3T3 and human dermal fibroblasts, die when grown on the surface of Fmoc-FF peptide gels (Jayawarna et al., 2009). It was reported that when Fmoc-FF was mixed with other Fmoc-protected peptides these problems could be overcome. The addition of other Fmoc-amino acids and Fmoc-RGD can allow growth of 3T3 and human dermal fibroblasts (Jayawarna et al., 2009, Zhou et al., 2009a). Fmoc-FF has been suggested as a possible drug delivery mechanism; konjac glucomannan (KGM) has reportedly been mixed with Fmoc-FF in solution and self-assembly triggered to form an Fmoc-FF-KGM peptide-polysaccharide composite that is able to be tailored to give different release profiles (Huang et al., 2011).

1.7.5.5 α -Helix

An example of coiled coils reported by Woolfson and co-workers uses a pair of 28 amino acids long peptides, hSAF_{AAA-W}, to form α -helix coiled coils. This pair of peptides can be used to form hydrogels that are stable in physiological solutions (Banwell et al., 2009). Neural cells grown in hSAF_{AAA-W} peptide gel have been reported to show cell growth, proliferation, differentiation and neurite outgrowth but cells grown on Matrigel showed better results (Banwell et al., 2009).

Other peptides that self-assemble into coiled coils have been developed, modified and explored for biological use. It has been reported that adding an RGD containing region into the helix destabilises the peptide gel; when the peptide was used to coat other materials the RGD containing peptide was able to increase cell adhesion (Villard et al., 2006). However, RGD containing α -helices in solution were shown to bind to RGD receptors and inhibit the binding of other ligands to the receptor (Villard et al., 2006). This binding could prove problematic as the peptide gel breaks down; the binding could also be used as a potential method for slow release, targeted drug delivery (Villard et al., 2006). This has implications in the development of α -helix functionalised peptide gels.

1.7.5.6 Peptide amyloidogenicity

One of the major concerns about fibrillar forming peptides is their similarity to pathological amyloid fibrils. Fibrillation of amyloid proteins is associated with the pathogenicity of amyloid diseases. Fibrillation is a two-step process involving a slow initial lag phase where nucleation seeds are formed followed by comparatively rapid fibril propagation from the seeds (Wu et al., 2008). The same as what is observed in peptide nucleated self-assembly. There is an increased risk that self-assembling peptides could cause increased amyloid deposition by acting as nucleating seeds. There are a number of tests for amyloid deposition; basic *in vitro* tests use Congo red and thioflavin staining which can be tested for using microscopy or spectroscopic techniques, while animal models of amyloidosis have also been developed for *in vivo* testing.

A mouse model of AA-amyloidosis which is triggered by the injection of silver nitrate has been used to study the deposition of amyloid fibers in the presence of a range of peptide gels

(Westermarck et al., 2009). Testing of RAD16-1 in the mouse model showed the potential for these peptides to reduce the time taken for amyloid development; it should however, be noted that not all the mice in the test developed amyloid formations (Westermarck et al., 2009).

A wide range of materials have been shown to reduce amyloid deposition time; natural amyloid-like fibrillar materials such as Bombyx mori silk, curli from *E.coli* and artificial materials such as nano-particles have all been shown to reduce the lag time of amyloid fibrillar formation (Linse et al., 2007, Wu et al., 2008, Westermarck et al., 2009). It should also be noted that stains such as thioflavin and Congo red not only bind to amyloid like structures but also bind to connective tissues such as elastic fibers, mucopolysaccharides and RNA and DNA, an increased detection of these stains does not necessarily indicate amyloidogenicity (Khurana et al., 2005).

1.7.6 Rational design and modification of peptides

The design of a peptide will be dependent upon the desired properties and responsiveness. Peptides can be designed to be responsive to different stimuli. An example is a peptide that has side-chains that are able to be protonated and de-protonated: the peptide will respond to changes in the pH as the side chains are protonated and de-protonated, such that self-assembly can be triggered and reversed by changing the pH (Figure 1.17) (Aggeli et al., 2003b, Carrick et al., 2007, Maude et al., 2011b). A peptide can be designed that responds to ionic concentration; a peptide designed not to self-assemble at neutral pH due to repulsive charge interactions will self-assemble when the ionic concentration is changed as the ions shield the repulsive charges (Chen, 2005, Carrick et al., 2007, Maude et al., 2011b).

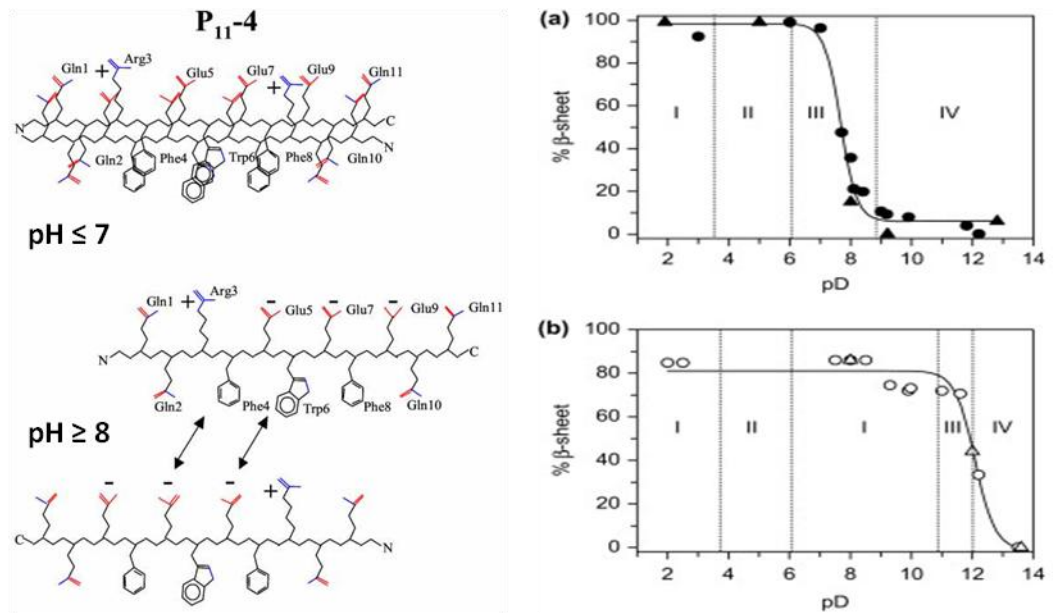


Figure 1.17, Left) Schematic model of pH control over P₁₁-4 self-assembly. Right) Self-assembly of 6.3 mol.m⁻³ of P₁₁-4 under different conditions. (a) Percentage β-sheet of P₁₁-4 as a function of pD in D₂O (by FTIR). (b) Percentage β-sheet of P₁₁-4 as a function of pD in 130 mol.m⁻³ NaCl in D₂O (by FTIR). Modified from (Aggeli et al., 2003b, Carrick et al., 2007)

Varying the length of the peptide and the amino-acid sequence allows for control over the energetics and dynamics of the peptide; this control allows the tailoring of a peptide to have specific physical and chemical properties (Aggeli et al., 1997, Chen, 2005).

Peptides can be obtained in a number of different ways. They can be cleaved from naturally obtained proteins, synthesised chemically or can be recombinantly expressed. The advantage of peptide self-assembly is the ease with which functional groups can be added to the peptide sequence. As β-sheet peptides self-assemble face to face the C and N termini are exposed on the outside of the peptide tape and make the ideal location for modification (Genové et al., 2005, Gelain et al., 2006, Gelain et al., 2007, Jung et al., 2009). Other peptide conformations can be modified by the inclusion of functional groups into the peptide sequence, as they are found in nature, or by modification of exposed side chains.

The addition of the motif can impact upon the self-assembly and mechanical properties of the peptide (Jung et al., 2009), in some cases there is no noticeable effect (Gelain et al., 2006) and in others the self-assembly of the peptide is affected (Genové et al., 2005, Villard et al., 2006). The modified peptide can then be mixed with unmodified peptide and self-assembled; as long as the addition of the motif does not interfere with the self-assembly the modified peptide will be incorporated into the self-assembled structure and will not leach out (Jung et al., 2009).

This ability to mix modified peptide and unmodified peptide allows for the inclusion of multiple functional groups.

1.7.7 Advantages and limitations of peptides as biomaterials for tissue engineering

There are a wide range of different self-assembling peptides that have potential as scaffolds for tissue engineering. The most widely used peptide in tissue engineering is RAD16-1 with results showing good cellular growth and function for a range of different cell types. One possible complication with the use of RAD16-1 is the reported haemostatic properties of the peptide. An effect upon the blood clotting pathway will make a peptide unsuitable for use in contact with blood, especially in the development of a tissue engineered blood vessel.

Fmoc-FF is attractive due to it being cheap to make. However, difficulty with controlling gelation and material properties coupled with the mixed results for the growth of different cell types on and in Fmoc-FF gels severely limits the potential applications and raise concerns over long term toxicity and peptide-cell interactions. Alpha helix coiled coils show good compatibility but are not as good at supporting cell growth and function as commercial products like Matrigel. The cost and difficulty of synthesising two 28 amino acid long peptides also makes coiled coils less commercially desirable.

The antibacterial properties of β -hairpin peptides MAX1 and MAX8 make them very attractive peptide for tissue engineering applications, especially with problems associated with post-operative infection. The mechanism of this antibacterial activity needs to be better understood. Testing is needed on the antibacterial properties as several possible mechanisms could impair normal cellular function. The size and associated cost of the β -hairpin peptides could potentially limit their application.

The P₁₁ series of peptides have a wide range of potential due to the different material properties expressed by the range of peptide sequences. The shorter size of the P₁₁ series compared to the β -hairpin and α -helix peptides makes them more desirable commercially but less so than the cheaper/shorter Fmoc-FF. The limited data on the immuno-compatibility of some of the P₁₁ series of peptides and the results showing good cell growth and proliferation show the potential of some of these peptides. A large amount of work is needed on self-

assembled peptides to develop peptides that are optimised for specific tissue engineering applications. Whilst the majority of peptides have demonstrated potential, more detailed work is needed with comparisons to biologically and commercially relevant controls to truly assess self-assembling peptides for potential application.

1.8 Hypothesis

A fully decellularised vascular graft will be free from problems of infection, immune response, calcification, mechanical mismatch and aneurysm, but will still suffer from thrombus formation. A self-assembling peptide could be self-assembled within the decellularised tissue to passivate the surface and prevent initial thrombus formation. The re-endothelialisation of the decellularised graft could be aided and enhanced by the addition of functionalised peptides designed to aid in cell attachment and retention.

1.9 Aims and objectives

The aim of the work undertaken in this thesis is to test the hypothesis that decellularised vascular tissue and self-assembling peptides can be combined to overcome the limitations of both materials in the application of blood vessel tissue engineering.

Objectives

- Investigate the possible self-assembly of peptide with a decellularised vascular conduit
- Assuming that self-assembly in decellularised vessel works, develop a protocol for the production of vessel peptide hybrid materials
- Test a range of peptides for biocompatibility
- Test a range of peptides for haemocompatibility
- Analyse results of biocompatibility and haemocompatibility testing to assess for any design criteria for biocompatible peptides
- Test anti-thrombogenic properties of self-assembled peptide
- Test attachment of cells to functionalised self-assembled peptide

2 Materials and methods

2.1 Materials

2.1.1 Equipment

A list of laboratory equipment used throughout the study and UK suppliers is presented in Appendix Table A-1.

2.1.2 Glassware

All laboratory glassware was obtained from Fisher Scientific (Loughborough, UK) unless otherwise stated. Glassware was cleaned by immersion in a 1 % (v/v) solution of Neutracon® for one hour and was then rinsed with tap water and dried or sterilised using dry heat.

2.1.3 Plastic ware

All sterile and non-sterile disposable plastic ware was purchased from Scientific Laboratory Supplies Ltd. (Nottingham, UK) unless otherwise stated. All plastic ware was stored as per suppliers' instruction.

2.1.4 Chemicals

A list of all Chemicals and reagents used in this study can be found in Appendix Table A-2.

2.1.5 Cell biology reagents and solutions

2.1.5.1 Dulbecco's phosphate buffered saline (DPBSa)

One tablet of DPBS per 100 ml was dissolved in distilled water and the pH adjusted to pH 7.6. The DPBSa was sterilised by autoclaving and stored at room temperature for up to one month.

2.1.5.2 Ringer's solution

Four Ringer's tablets were dissolved in 500 ml of distilled water and the pH adjusted to pH 7.6. The Ringer's solution was sterilised by autoclaving and stored at room temperature for up to one month.

2.1.5.3 Tris buffered saline (TBS)

Trizma base, 6.05 g to achieve a final concentration of 50 mol.m^{-3} , and 8.76 g of sodium chloride to achieve a final concentration of 150 mol.m^{-3} were dissolved in 1 L of distilled water and the pH adjusted to pH 7.6. The TBS was sterilised by autoclaving and stored at room temperature for up to one month.

2.1.5.4 Tryptone phosphate broth 50 % stock solution (TPB)

Tryptone phosphate, 50 mg, was dissolved in 100 ml of distilled water and filter sterilised in a class II safety cabinet and stored in aliquots of 10 ml at -20°C .

2.1.5.5 3T3 culture medium

Foetal bovine serum, 20 ml, 2 ml of L-glutamine to achieve a final concentration of 200 mol.m^{-3} and 4 ml of penicillin/streptomycin to achieve a final concentration of 100 U.ml^{-1} were added

to 174 ml of Dulbecco's modified Eagles medium (DMEM) and mixed. Once prepared the medium was stored for up to one week at 4°C.

2.1.5.6 2X 3T3 culture medium

Foetal bovine serum, 20 ml, 2 ml of L-glutamine to achieve a final concentration of 400 mol.m⁻³ and 4 ml of penicillin/streptomycin to achieve a final concentration of 200 U.ml⁻¹ were added to 74 ml of DMEM and mixed. Once prepared the medium was stored for up to one week at 4°C.

2.1.5.7 BHK culture medium

Foetal bovine serum, 10 ml, 10 ml of tryptone phosphate broth stock solution to achieve a final concentration of 2.5 % TPS, 2 ml of L-glutamine to achieve a final concentration of 200 mol.m⁻³ and 4 ml of penicillin/streptomycin to achieve a final concentration of 100 U.ml⁻¹ were added to 174 ml of Glasgow minimum essential medium (GMEM) and mixed. Once prepared the medium was stored for up to one week at 4°C.

2.1.5.8 2X BHK culture medium

Foetal bovine serum, 10 ml, 10 ml of tryptone phosphate broth stock solution to achieve a final concentration of 5 % TPB, 2 ml of L-glutamine to achieve a final concentration of 400 mol.m⁻³ and 4 ml of penicillin/streptomycin to achieve a final concentration of 200 U.ml⁻¹ were added to 74 ml of GMEM and mixed. Once prepared the medium was stored for up to one week at 4°C.

2.1.5.9 Endothelial cell culture medium

Foetal bovine serum, 40 ml, 4 ml of penicillin/streptomycin to achieve a final concentration of 100 U.ml⁻¹, 30 U.ml⁻¹ of heparin sulphate and 75 µg.ml⁻¹ of endothelial cell growth factor (ECGF) were added to 156 ml of Medium-199 (M-199) and mixed. Once prepared the medium was stored for up to one week at 4°C.

2.1.6 Cells and biological tissues

2.1.6.1 Cells

All mammalian cell lines used in biocompatibility assays are shown below in Table 2-1 and were received as frozen cultures. Cells were expanded, subcultured and cryopreserved in liquid nitrogen until use unless otherwise stated.

Cell	Type	Origin	Isolation method	Supplier
3T3	Fibroblast	Swiss Mouse Embryo Tissue	Trypsin digestion	Health Protection Agency Culture Collections
BHK-21	Epithelial	Baby Syrian Hamster Kidneys	Trypsin digestion	Health Protection Agency Culture Collections

Table 2-1; Cells used throughout the study including supplier

2.1.6.2 Biological tissue

Porcine internal carotid arteries were procured from Graystone Ltd (Hull). Vessels arrived frozen and were defrosted, dissected and washed in DPBSa. DPBSa was passed through the vessels using a syringe to remove remaining blood before use. Vessels not used immediately were wrapped in tissue soaked in DPBSa and stored at -80°C.

Ovine legs were procured from John Penny and Sons abattoir (West Yorkshire). All legs arrived fresh having been slaughtered that morning. All procedures involving the ovine legs were carried out on the day of arrival.

Citrated sheep blood was obtained from Harlan Laboratories. Blood was mixed with trisodium citrate 10% (w/v) upon harvesting and shipped under refrigerated conditions. Blood was received, stored at 4°C and used within 5 days.

Normal human serum from pooled normal clotted human blood, tested for *Hepatitis* associated antigen and HIV, was purchased from MP Biomedicals Europe. Serum arrived as a frozen sample, was stored at -20°C and was defrosted at room temperature before use.

All animal tissue and biological fluids were disposed of following established procedures in place at the time of experimentation.

2.1.7 Antibodies

A list of antibodies used throughout the study and suppliers information is presented in Table 2-2, Table 2-3 and Table 2-4.

Antigen	Type	Clone number	Isotype	Dilution	Supplier
Red Blood Cell Stroma	Rabbit anti- sheep	-	IgG1	1:200	Sigma Aldrich
Von Willebrand Factor	Rabbit anti- human	-	Polyclonal	1:200	Dako UK Ltd
α Smooth Muscle Actin	Mouse anti- human	1A4	IgG2a	1:400	Sigma Aldrich
Smooth Muscle Myosin Heavy Chain	Mouse anti- human	N1/5	IgG1	1:100	Chemicon International
Endothelial Cell CD31:FITC	Mouse anti- sheep	CO.3E1D4	IgG2a	1:100	AbD Serotec

Table 2-2; Primary antibodies used throughout the study

Antigen	Type	Conjugate	Dilution	Supplier
Mouse Whole antibody	Goat anti-Mouse	Alexa Fluor 488	1:200	Invitrogen Ltd
Rabbit F(ab') ₂ fragment	Goat anti-rabbit	Alexa Fluor 488	1:200	Invitrogen Ltd

Table 2-3; Secondary antibodies used throughout the study

Antigen	Host	Isotype	Dilution	Supplier
<i>Aspergillus niger</i> glucose oxidase	Mouse	IgG2a	As Primary	Dako UK Ltd
<i>Aspergillus niger</i> glucose oxidase	Mouse	IgG1	As Primary	Dako UK Ltd
-	Rabbit	Immunoglobulin fraction	As Primary	Dako UK Ltd
<i>Aspergillus niger</i> glucose oxidase	Mouse	IgG2a-FITC	As Primary	MBL international

Table 2-4; Isotype control antibodies used throughout the study

2.1.8 Peptides

All P₁₁ series peptides and peptides hSAF_{AAA-W} P1 and P2 were purchased from Polypeptide group, Fmoc-diphenylalanine was purchased from BACHEM and the homo-polypeptides were purchased from Sigma Aldrich; all peptides were tested for purity on arrival using elemental analysis and were over 95 % pure.

2.2 General Methods

2.2.1 Sterilisation

2.2.1.1 Dry heat sterilisation

Items to be sterilised were placed in suitable containers or wrapped in tinfoil and placed into a hot air oven at a temperature of 190°C for 4 hours. Items were allowed to cool and then removed from the oven taking care to maintain sterile conditions.

2.2.1.2 Moist heat/ autoclave sterilisation

Solutions and items not suitable for dry heat sterilisation were sterilised using an autoclave. Items were placed into suitable containers or placed into autoclave bags and labelled with autoclave tape. Items were autoclaved at 15 psi at 121°C for 20 minutes. Items were allowed to cool and were then removed from the autoclave taking care to maintain sterility.

2.2.1.3 Gamma irradiation sterilisation

The peptides used in biological experiments were weighed out into glass vials and sterilised as a dry powder as the peptides could not be autoclaved or sterilised using dry heat. Gamma sterilisation at 25 kGy was carried out by Synergy Health using standard methods developed for the sterilisation of medical products.

2.2.2 Measurement of pH

The pH meter was calibrated using purchased solutions of pH 4, 7, and 10. The pH of solutions was measured at room temperature using temperature compensation. The pH of solutions was changed by the drop-wise addition of 6 M hydrochloric acid (HCl) or 6 M sodium hydroxide (NaOH) whilst stirring unless otherwise stated.

2.2.3 Decellularisation of porcine arterial conduits

Reagents

- Disinfection solution** Vancomycin hydrochloride, 50 mg to achieve a final concentration of 0.05 mg.ml⁻¹, 500 mg Gentamicin sulphate to achieve a final concentration of 0.5 mg.ml⁻¹ and 200 mg polymyxin B to achieve a final concentration of 0.2 mg.ml⁻¹ were added to 100 ml of DPBSa and the pH adjusted to pH 7.4. The solution was passed through a 0.2 µm pore size filter and made up to 1 L using sterile DPBSa.
- EDTA solution** Disodium ethylenediaminetetra acetic acid (EDTA), 74.4 g to achieve a final concentration of 200 mol.m⁻³, was dissolved in 1L of distilled water and the pH adjusted to pH 7.4. The EDTA solution was sterilised by autoclaving and stored at room temperature for up to one month.
- Hypotonic buffer** Trizma base, 1.21 g to achieve a final concentration of 10 mol.m⁻³ and 1 g of EDTA to achieve a final concentration of 2.7 mol.m⁻³ were added to 1 L of distilled water and the pH adjusted to pH 8.2. The hypotonic buffer was sterilised by autoclaving and stored at room temperature for up to one month. Aprotinin, 1 ml to achieve a final concentration of 10 KIU.ml⁻¹, was added before use.
- SDS solution** Sodium dodecyl sulphate, 10 g to achieve a final concentration of 10 % (w/v), was dissolved in 100 ml of distilled water and was passed through a 0.2 µm pore size filter. The solution was stored at room temperature for up to six months.
- SDS hypotonic buffer** SDS solution, 10 ml to achieve a final concentration of 0.1 % (w/v), was added to 990 ml of autoclaved hypotonic buffer and stored for one week at 4°C if opened aseptically.
- Washing buffer** Ten Oxoid Dulbecco's PBS tablets and 1 g of EDTA to achieve a final concentration of 2.7 mol.m⁻³ were dissolved in 1 L of distilled water and the pH adjusted to pH 7.4. The wash buffer was sterilised by autoclaving and stored at room temperature for up to one month.

Nuclease solution	Trizma base, 6.1 g to achieve a final concentration of 50 mol.m^{-3} and 2 g magnesium chloride to achieve a final concentration of 20 mol.m^{-3} were dissolved in 990 ml of distilled water and the pH adjusted to pH 7.6. The nuclease solution was sterilised by autoclaving and stored at room temperature for up to one month. Bovine serum albumin, to achieve $50 \text{ }\mu\text{g.ml}^{-1}$, DNAase to achieve 50 U.ml^{-1} and RNAase to achieve 1 U.ml^{-1} were added and the solution used within 10 minutes.
Hypertonic solution	Trizma base, 6.06 g to achieve a final concentration of 50 mol.m^{-3} and 87.66 g sodium chloride to achieve a final concentration of $1.5 \times 10^3 \text{ mol.m}^{-3}$ were dissolved in 1 L of distilled water and the pH adjusted to pH 7.6. The hypertonic solution was sterilised by autoclaving and stored at room temperature for up to one month.
Sterilising solution	Peracetic acid, 3.14 ml to achieve a final concentration of 0.1 % (v/v), was added to 1 L of autoclaved DPBSa and the pH adjusted to pH 7.4. The solution was used within one hour of production.

Procedure

Following dissection of the vessel from surrounding tissue or defrosting, 15 cm lengths of the porcine arteries were placed in plastic pots and washed using 150 ml of the disinfection solution for 30 minutes at 37°C . All washes were carried out with agitation on a shaking table at 110 rpm. Following disinfection the vessels were washed in 150 ml of EDTA solution at 4°C for 24 hours. The arteries were then removed and washed in 150 ml of hypotonic buffer at 4°C for 24 hours. To further remove cells and cellular debris the arteries were washed in 150 ml of SDS hypotonic solution at 37°C for 24 hours then washed in 150 ml of hypotonic buffer at 4°C for 24 hours. The vessels were washed in 150 ml of washing buffer containing 10 KIU.ml^{-1} of aprotinin over the weekend (48-56 hours) at 4°C followed by a further wash in 150 ml SDS hypotonic buffer at 37°C for 24 hours. The vessels were washed three times using 150 ml of DPBSa at 37°C for 30 minutes each and then washed using 150 ml of the nuclease solution at 37°C for 3 hours. The vessels were washed three times in 150 ml of washing buffer containing 10 KIU.ml^{-1} of aprotinin at 37°C for 30 minutes each. The vessels were added to 150 ml of the hypertonic solution at 37°C for 24 hours then washed three times in 150 ml of the washing buffer containing 10 KIU.ml^{-1} of aprotinin for 30 minutes each. The vessels were sterilised using

150 ml of the sterilising solution at 27°C for 3 hours; further manipulations were carried out aseptically in a class II safety cabinet. The vessels were washed using 150 ml of the washing buffer containing 10 KIU.ml⁻¹ of aprotinin at 37°C for 30 minutes each then washed with 150 ml of DPBSa at 4°C for 24 hours. The decellularisation of the vessels was assessed using histological techniques described in Section 2.2.4 and the vessels were stored in 150 ml of DPBSa at 4°C for up to three months.

2.2.4 Analysis of decellularisation

2.2.4.1 Paraffin wax embedding of tissue samples

Samples were placed into small plastic cassettes (Histosette®) and dehydrated using an automated tissue processor. The automated tissue processor sequentially immersed the samples in 70% (v/v) alcohol for 1 hour, 90% (v/v) alcohol for 1 hour and three changes of 100% (v/v) alcohol for 1 hour each. The samples were then immersed in two changes of xylene for 1 hour each. The cassettes were then immersed in molten paraffin wax for 1 hour then transferred to fresh paraffin wax for a further hour. Once the processor had finished the samples were kept in molten paraffin wax until removed. Wax block moulds were filled with molten paraffin wax and the samples quickly removed from the cassettes and orientated in the wax block moulds using heated forceps. The molten paraffin wax was allowed to cool and once fully hardened the moulds were removed and the excess wax trimmed.

2.2.4.2 Sectioning of paraffin wax embedded samples

The paraffin wax blocks were sectioned at 5 – 10 µM using a microtome. The sections were floated in a water bath at 40°C for mounting on a glass slide. The glass slide with three sections on was placed on a rack to dry. The slides were then placed on a hot plate for 20 minutes to further dry and melt the wax, fixing the sections to the slide. After drying the slides were left to cool and then placed in a slide holder for storage.

2.2.4.3 De-waxing and rehydration of sectioned paraffin wax embedded samples

The slides were de-waxed by submersion in two changes of xylene for ten minutes each to remove all the wax. The slides were then placed in three changes of 100 % (v/v) ethanol for three, two and two minutes respectively. The slides were then submerged in 70 % (v/v) ethanol for two minutes and washed under running water for three minutes.

2.2.4.4 Haematoxylin and Eosin staining

Haematoxylin stains cell nuclei and eosin is used to stain cytoplasm, collagen and muscle fibres. The de-waxed and rehydrated sections on slides were placed into a metal slide holder and immersed in haematoxylin for one minute. The slides were then removed and washed under running water until it ran clear and all excess stain had been removed. The sections were then immersed in eosin stain for three minutes. Sections were then immediately mounted as is Section 2.2.4.6.1.

2.2.4.5 DAPI staining

Reagents

- Dye Buffer** Trizma base, 1.211g to achieve a final concentration of 10 mol.m^{-3} , 0.3724 g of EDTA to achieve a final concentration of 1 mol.m^{-3} and 5.8 mg of sodium chloride to achieve a final concentration of 1 mol.m^{-3} were dissolved in 1 L of distilled water and sterilised by autoclaving. The solution was stored at room temperature in the dark for up to six months the pH was adjusted to pH 7.4 before use.
- DAPI dye stock** DAPI, 10 mg, was added to 10 ml of nuclease free water and stored in 20 μl aliquots at -25°C for up to six months
- Working dye** DAPI dye stock solution, 40 μl to achieve a final concentration of $0.1 \mu\text{g.ml}^{-1}$, was mixed with 400 ml of Dye buffer in a dark bottle and used immediately.

Procedure

DAPI or 4', 6-diamidino-2-phenylindole forms fluorescent complexes that bind strongly with A-T base rich regions within DNA. The sections having been de-waxed and rehydrated (Section 2.2.4.3) were placed in a metal slide holder and immersed in DAPI solution for ten minutes in the dark then washed three times using DPBSa for ten minutes each in the dark. The sections were mounted using DABCO:glycerol (Section 2.2.5), then imaged under a fluorescent microscope using a DAPI filter.

2.2.4.6 Mounting of sections

2.2.4.6.1 Mounting of stained sections using DPX mountant

Following staining sections were submerged in 70 % (v/v) ethanol for five seconds and taken through three changes of 100 % (v/v) ethanol for one, two and three minutes respectively. The slides were then submerged in two changes of clean xylene for ten minutes each and the sections mounted using DPX mountant and glass cover slips. Slides were left to dry for a minimum of four hours and imaged using an upright microscope and images captured using a digital camera and Image-Pro Plus v 5.1.

2.2.5 Mounting of sections using DABCO:glycerol

Reagents

Mounting solution	DABCO (1,4-diazabicyclo octane) 2.5 % (w/v), 10 ml, was added to 90 ml of glycerol and mixed. The solution was stored in the dark at 4°C for up to 3 months.
--------------------------	--

Procedure

Following cryostat sectioning or staining the sections were mounted using the mounting solution. A small drop of mounting solution was placed in proximity to each section and a glass cover slip placed on top. Slides could be immediately imaged or left on the dark for a

maximum of 24 hours. Samples were imaged using an upright microscope and images captured using a digital camera and Image-Pro Plus v 5.1.

2.2.6 Triggering peptide self-assembly

Rationale

Peptide self-assembly can be triggered in a number of different ways. One dimensional nucleated self-assembly is a concentration dependent reaction thus self-assembly can be triggered by changing the concentration of peptide in solution, however, it is difficult to control concentration when switching between a monomeric and self-assembled state. By using peptides that are charged and can be protonated and de-protonated it is possible to trigger self-assembly by a pH change or change in ionic concentration. Dependent upon the amino acids used in the peptide sequence and their associated pKa values high or low pH can trigger self-assembly or disassembly. A concentration of 18.8 mol.m^{-3} , approximately 30 mg.ml^{-1} of P₁₁ peptide, was used as a standard concentration for the formation of a self-supporting peptide gel.

2.2.6.1 Peptide monomer solution

To ensure the peptide formed a uniform gel upon self-assembly the peptide first had to be monomeric in solution to ensure an even distribution of peptide. A monomeric/soluble aggregate solution of peptide was made by increasing the pH of the solution to pH 8 using 1 M NaOH or by decreasing the pH to pH 5 using concentrated HCl dependent upon the designed responsiveness of the peptide. For example P₁₁₋₄ was monomeric at pH 8 and self-assembled at pH 5 where P₁₁₋₈ was designed for the opposite response and was monomeric at pH 5 and self-assembled at pH 8. The peptide solution was vortexed after each addition. The pH of the solution was then changed to pH 7.6 using concentrated HCl or 1M NaOH, vortexing after each addition. A new pH reading was taken using a pH meter after every acid or base addition.

2.2.6.2 Self-assembly triggers

2.2.6.2.1 pH trigger

As the pH is changed amino acids are protonated or de-protonated removing or restoring the repulsive forces between the peptide monomers triggering self-assembly or disassembly. A monomeric solution of peptide was made in water as in Section 2.2.6.1. To use pH as a trigger for self-assembly the pH of the solution was decreased using concentrated HCl to pH 5 or increased to pH 8 using 1M NaOH, dependent upon the designed responsiveness of the peptide, vortexing after each addition. The peptide solution was left overnight to allow for self-assembly to fully occur.

2.2.6.2.2 Ionic trigger

As the ionic concentration is increased a screening effect removes the repulsive forces between the peptide monomers triggering self-assembly. There are a number of biologically relevant salt solutions in which peptide should self-assemble. PBS is a very common salt solution that was chosen for use as it is widely used in biological applications, another solution that was chosen for use is Ringer's solution, since it is a physiological solution.

Water, 0.9 ml (9/10 final volume) was added to peptide to make a monomeric solution as in Section 2.2.6.1. Self-assembly was triggered by the addition of 0.1 ml (1/10 final volume) of a 10X solution of PBS or Ringer's solution to create 1 ml of peptide in standard PBS or Ringer's solution. The peptide solution was left overnight to allow for self-assembly to fully occur.

2.2.7 Peptide self-assembly in decellularised porcine internal carotid artery

Rationale

The self-assembly of peptide within the decellularised porcine internal carotid artery first required that the peptide was able to penetrate the material. The artery was naturally porous, however, to ensure that the peptide penetrated into the acellular vessel the peptide was added to the decellularised artery in a monomeric form unless otherwise stated. This was the

same whether the self-assembly was triggered by a pH change or by an increase in ionic concentration.

Procedure

A monomer solution of peptide was made (Section 2.2.6.1) the acellular vessel was added to the solution and left overnight to allow the peptide to fully penetrate into the vessel. Self-assembly was then triggered as described in Section 2.2.6.2 or in Section 2.2.6.2.2 dependent upon which trigger was being used. The vessel was left in the peptide solution overnight to allow for self-assembly to occur.

2.2.8 Inclusion of fluorescently labelled peptide for fluorescent microscopy

Peptide P₁₁₋₄ was labelled with a fluorescein tag using a β -alanine spacer to show the presence of the peptide within the decellularised vessel (Fluorescein- β A-Q-Q-R-F-E-W-E-F-E-Q-Q-NH₂). It was found that a ratio of 1:30 of fluorescein tagged P₁₁₋₄ to untagged P₁₁₋₄ gave strong high quality fluorescent images. Following self-assembly within decellularised vessel as described in Section 2.2.7 the samples were left in the dark until use.

2.2.9 Fourier transform infrared (FTIR) spectroscopy

Rationale

The Born-Oppenheimer approximation allows molecular rotational, translational and vibrational motion to be considered separately (Hollas, 2004, Griffiths and De Haseth, 2007). FTIR spectroscopy works on the principle that the differences between vibrational energy levels are in the range of infra-red radiation (IR). The IR frequency absorbed by a bond is influenced by the vibrational frequency of the bond; the vibrational frequency of the bond is in turn influenced by the mass of the atoms and nature of the bonds. This means that for a particular molecule the precise absorbance of a bond is governed by the affect different atoms in the molecule have on the bonding and on inter/intra-molecular effects, such as hydrogen bonding and π - π stacking.

As β -sheet and α -helix both have different hydrogen bonding patterns the secondary structures observed in peptide self-assembly can be identified using FTIR. There are significant differences in the hydrogen bonding in a α -helix structure compared to a β -sheet structure; this gives rise to the characteristic amide I ($1600 - 1700 \text{ cm}^{-1}$) and the amide II ($1500 - 1600 \text{ cm}^{-1}$) absorption bands (Seshadri et al., 1999). The amide I band is mainly due to C=O stretching where amide II is mainly due to N-H bending.

The key component of an FTIR spectrometer is the interferometer. The interferometer is an optical device with a beam splitter used to split and recombine the beams produced by the source. After being split the incident radiation hits one of two mirrors; both mirrors are at right angles to each other and one is fixed in position and one moves position. As the radiation beam hits the mirror it is reflected back and re-enters the beam splitter, part of the beam is then reflected back at the source and part is directed towards a detector. As the movable mirror is moved an interference pattern is produced as the waves from the fixed and movable mirrors are recombined. The recombined beam is then passed through a sample before it reaches a detector. An interferogram of the sample is produced as the intensity of the IR radiation reaching the detector is measured as the mirror is moved. This interferogram is then analysed using Fourier analysis which splits a curve into its component wavelengths, this analysis gives a spectrum which is the Fourier transform of the interferogram (Griffiths and De Haseth, 2007).

Procedure

To provide quantitative evidence that the peptide was self-assembling in the acellular vessel FTIR analysis was carried out. Decellularised porcine internal carotid artery sections were placed in 10 ml of deuterium oxide and left over night. The decellularised vessel was removed from the deuterium oxide and placed in 10 ml of new deuterium oxide and left over night. This was repeated once more to remove any residual water that could affect the FTIR scan. Peptide was self-assembled within half of the decellularised vessel sections using the method described in Section 2.2.6.2 replacing water in all solutions with deuterium oxide. The remaining decellularised vessel sections were kept in deuterium oxide and taken through the same pH changes as the vessels added to the peptide solutions. The peptide coated vessel sections and decellularised vessel sections without peptide as a control were compressed between two calcium fluoride optical disks and an FTIR spectrum taken. The sample was then

moved between the disks to take a spectrum of a different area of the vessel. The spectra from the random locations of the samples were combined into a single spectrum and analysed.

2.2.10 Field emission gun scanning electron microscope (FEGSEM) imaging

Rationale

A scanning electron microscope (SEM) works by scanning a high intensity beam of electrons over the surface of a sample using magnetic coils to control the beam of electrons. When the electron beam hits the target secondary electrons, backscattered electrons and X-rays are produced. The main imaging in the SEM uses secondary electrons, which are electrons from the sample that have been ionised by the interaction with the electron beam. X-rays and backscattered electrons are used to gather data on the composition of the sample. FEGSEM refers to the method by which the electron beam is produced; a field emission gun uses a large potential gradient to pull electrons from a tungsten tip. The field emission gun produces a beam of electrons that is smaller in diameter and is more coherent with up to three orders of magnitude greater current density (brightness) than a normal SEM.

ECM will collapse and lose its structure when the water is removed; normally biological tissue is dried by changes of organic solvents like methanol and ethanol, however, the use of peptide prevents the use of organic solvents as the peptide would be removed in these solvents.

Procedure

In order to maintain the structure of the ECM sections of vessel decellularised as described in Section 2.2.3 were fixed in neutral buffered formalin for 4 hours and washed in three changes of 20 ml of sterile PBS. Peptide was then self-assembled within the samples (Section 2.2.7). The peptide coated fixed vessels were dried in vacuum overnight to ensure the removal of all water before imaging in the FEGSEM. The samples were attached to SEM stubs using double sided stick carbon pads and coated in a 5 nm layer of platinum and palladium (50:50) using a Cressington 108 sputter coater. The samples were then imaged using a Gemini LEO 1530 FEGSEM at 3 KeV.

2.2.11 Fluorescent microscopy imaging

2.2.11.1 Sectioning of fluorescent samples

The samples were embedded in cryostat embedding solution (Cryoembed, Bios Europe Ltd) at -30°C. Once the embedding solution had fully set the samples were sectioned at 7 µm using a cryostat. Three sections were collected on a glass slide, covered and allowed to air dry in the dark. Sections were mounted with DABCO:glycerol mountant (Section 2.2.5) and kept in the dark until imaged.

2.2.11.2 Fluorescent imaging

Sectioned samples were imaged within 24 hours of sectioning using an inverted fluorescent microscope with a FITC filter. Images were captured in black and white using a digital camera and colour added using Image-Pro Plus v 5.1.

2.2.12 Confocal laser scanning microscopy (CLSM) and multi-photon laser scanning microscopy (MPLSM)

The key feature of both the CLSM and the MPLSM is the ability to acquire in-focus images from different depths, a process known as optical sectioning. The CLSM does this by using a laser that is focused onto a small area of the sample. The fluorescent and reflected light is recollected by the objective lens and part of the light is split off into the photo-detector using a light splitter. The light passes through a filter that blocks the reflected light but not the fluorescence. After passing through a pinhole aperture the light intensity is measured using a photo-detector. The pinhole aperture blocks out light not coming from the focal point; out of focus light is suppressed meaning that the CLSM provides sharper images than conventional fluorescent microscope techniques and is capable of gathering Z-axis stacks through the sample. MPLSM works by using red-shifted excitation light; this means that for a fluorophore to emit light, two photons have to be absorbed. The probability of absorbing two photons at the focal point of the microscope is significantly higher than for any other area in the sample and as single stray photons will not cause fluorescence the area that is imaged in a multi-

photon microscope has less background noise and higher resolution (Figure 2.1). One advantage of the use of MPLSM and CLSM is the imaging of live wet samples.

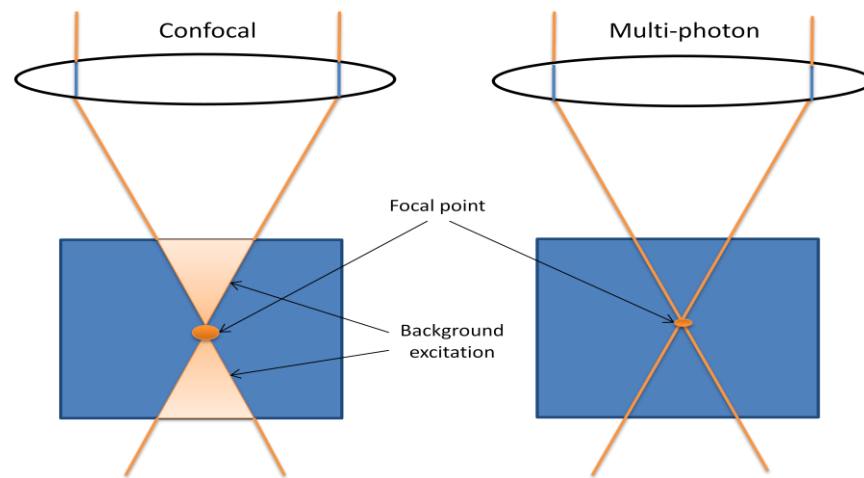


Figure 2.1; Schematic of CLSM and MPLSM excitation

2.2.12.1 Confocal laser scanning microscopy (CLSM) imaging

Decellularised vessel was coated in fluorescein tagged P₁₁-4 as described in Section 2.2.8. Self-assembly was triggered using an ionic trigger as in Section 2.2.6.2.2. The peptide coated decellularised vessel was left in the excess peptide gel in a hydrated state until use. The samples were imaged in a wet state and were placed on a glass slide with a cover slip on top. To reduce the refractive index mismatch and improve the image quality an oil immersion objective lens was used rather than a dry objective lens (Frisken Gibson and Lanni, 1991). The samples were imaged using a Zeiss LSM 510 META inverted confocal microscope using a FITC filter. Images were collected using the associated image software (Carl Zeiss ZEN) and were analysed using LSM image browser.

2.2.12.2 Multi-photon laser scanning microscopy (MPLSM) imaging

Decellularised vessel was coated in fluorescein tagged P₁₁-4 as described in Section 2.2.8. Self-assembly was triggered using a change in ionic concentration as in Section 2.2.6.2.2. The peptide coated decellularised vessel was left in the excess peptide gel in a hydrated state until use. Samples were imaged by technicians at the University of York using a Zeiss LSM 510 NLO

on an Axiovert 200M microscope stand with a coherent Chameleon Ultra TiSa tuneable laser. Images were taken and analysed using LSM image browser.

2.2.13 Cell culture

2.2.13.1 Resurrection and culture of primary cells and cell lines

Cells were removed from liquid nitrogen storage and rapidly defrosted at 37°C in a water bath. Supplemented cell culture medium (10 ml) pre-warmed to 37°C was added drop wise to the cells. The cells were centrifuged at 150 g for ten minutes, the supernatant discarded and the cell pellet resuspended in 5 ml of supplemented cell culture medium. The cell suspension was transferred to a 25 cm² tissue culture flask and incubated in 5 % (v/v) CO₂ in air at 37°C. The medium was removed and replaced with 5 ml of supplemented cell culture medium every 48 hours until the cells became confluent.

2.2.13.2 Sub-culture of primary cells and cell lines

The culture medium was removed from the flask and the cell layer was washed using 10 ml of Hank's balanced salt solution without calcium and magnesium. After 2 – 5 minutes the Hanks balanced salt solution was removed and replaced with trypsin/EDTA solution (1 ml in a 25 cm² tissue culture flask, 2.5 ml in a 75 cm² tissue culture flask and 5 ml in a 175 cm² tissue culture flask) and incubated in 5 % (v/v) CO₂ in air at 37°C for no more than five minutes. The cells were dislodged from the surface of the flask by gently tapping the surface. The trypsin was neutralised by the addition of 5 ml of supplemented medium, containing at least 10 % (v/v) foetal calf serum. The cell suspension was transferred to a sterile universal tube and centrifuged at 150 g for ten minutes. The supernatant was removed and the cells resuspended in 5 ml of supplemented medium. The total number of viable cells was determined using the trypan blue method (Section 2.2.13.3). The cells were seeded into a larger tissue culture flask or split 1:3 into the same size tissue culture flasks with 5ml of supplemented cell culture medium for a 25 cm² tissue culture flask, 10 ml of medium in a 75 cm² tissue culture flask and 15 ml of medium in a 175 cm² tissue culture flask. The cells were incubated in 5 % (v/v) CO₂ in air at 37°C with the medium changed every 48 hours.

2.2.13.3 Trypan blue estimation of cell viability and number

Rationale

The trypan blue exclusion test works on the principle that a viable cell will have an intact membrane and is therefore not permeable to the dye. When cell death occurs the membrane begins to lose integrity and becomes permeable to the dye. The cells that remain unstained are viable whilst unviable cells are stained blue.

Procedure

The cell suspension (90 μ l) was mixed with the trypan blue dye (10 μ l). The stained suspension was loaded onto a haemocytometer (Figure 2.2) and was observed under an inverted microscope. The number of unstained cells was counted and in order to make the counts accurate the cell suspension was diluted such that the total number of cells in each chamber was between 30 and 300 cells.

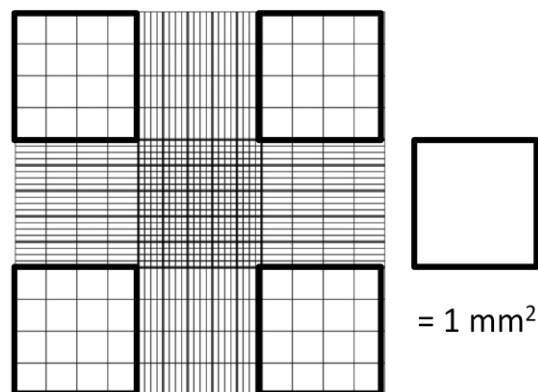


Figure 2.2; Schematic of area cells are counted on a haemocytometer

The mean cell count was calculated by dividing the number of cells counted by the number of 1 mm² squares counted. The total number of viable cells per ml was calculated using the following:

$$\text{Number of cells.ml}^{-1} = \text{Mean cell count} \times 10^4 \times \text{Original dilution (10/9)}$$

2.2.13.4 Cryopreservation of primary cells and cell lines

Cells were harvested from culture as described in Section 2.2.13.2. The cell suspension was transferred to a sterile universal tube and centrifuged at 150 g for ten minutes. The supernatant was removed and the cells resuspended in 5 ml of supplemented medium. The total number of viable cells was determined and the cell suspension was transferred to a sterile universal tube and centrifuged at 150 g for ten minutes. The supernatant was removed and the cells resuspended in medium containing 20 % (v/v) foetal calf serum and 10 % (v/v) dimethyl sulfoxide (DMSO), which was filtered before use, at a density appropriate for the growth of the cell type in a 25 cm₂ tissue culture flask. Aliquots of 1 ml the cell suspension were placed into cryovials then placed in a Mr Freezy pot containing isopropanol. The Mr Freezy pot was placed in a -80°C freezer overnight and the vials then transferred to liquid nitrogen for long-term storage.

2.2.14 Biocompatibility testing

Rationale

Cells will not grow in a toxic environment; hence by growing cells in contact with a material or in an extract of a material, the material may be tested for any potential toxic effects. Cell growth is easily measured in a number of ways. A simple method, used here, was the ATPLite-M[®] assay. When the level of ATP from the cells grown in the presence of the extract was compared to the negative and positive controls it was possible to assess for any toxic effects. Toxic effects would be shown by a reduction in the level of ATP produced by the cells in comparison with the negative control. As not all the peptides could be tested by contact cytotoxicity testing, the assessment of biocompatibility was based on extract cytotoxicity testing.

Procedure

Each peptide was weighed and following sterilisation was added to GMEM and DMEM to create test solutions that would give a final concentration of 0.3 mol.m⁻³ of each peptide during the cytotoxicity testing.

Two cell lines, 3T3 and BHK cells, were sub-cultured and resuspended in cell culture medium; DMEM based medium for 3T3 cells (Section 2.1.5.5) and GMEM based medium for BHK cells (Section 2.1.5.7). Cells were seeded at an appropriate cell density to achieve 80 % confluence in a 96 well plate. The cell suspension (200 μ l) was added to the wells of a 96 well plate and incubated for 48 hours at 37°C in 5 % (v/v) CO₂ in air. The cell culture medium was aspirated from the cells and replaced with 100 μ l of fresh 3T3 and BHK cell culture medium with double the concentration of additives (Sections 2.1.5.6 and 2.1.5.8). To this, 100 μ l of test solution or control (positive, standard cell culture medium with 40 % DMSO; negative, standard cell culture medium) was added and incubated at 37°C in 5 % (v/v) CO₂ in air for 72 hours. Six samples of each peptide were tested. The level of ATP was then measured using the ATPLite-M[®] assay described in Section 2.2.14.1. The results were collected and graphed as the mean value with 95 % confidence limits (Section 2.2.21.1). Data was analysed for significant difference by one-way ANOVA.

2.2.14.1 ATPLite-M[®] assay

Rationale

Adenosine triphosphate plays a key role in energy exchanges in all living cells; cell injury or nutrient depletion results in a rapid decrease in cytoplasmic ATP (Crouch et al., 1993). ATP can be measured using a luminescence assay. The ATPLite-M[®] assay uses the luciferase enzyme from fireflies that reacts with luciferin to produce light. MgATP₂₋ converts the luciferin into a form that is oxidised by luciferase in a high yield chemiluminescent reaction (Crouch et al., 1993). Cellular ATP can be measured by lysis of the cells and reaction with luciferin-luciferase leading to luminescence emission (Crouch et al., 1993).

Procedure

ATPLite-M[®] assay reagents, lyophilised substrate solution, substrate buffer and mammalian cell lysis solution, were allowed to equilibrate to room temperature. The vial of lyophilised substrate solution was reconstituted by the addition of 5 ml of substrate buffer.

The medium was aspirated from each well of the 96 well plate and replaced with 100 μ l of fresh cell culture medium. To each well 50 μ l of mammalian cell lysis solution was added and

shaken at 500 rpm for five minutes. To each well 50 μ l of substrate solution was added; the wells were covered to prevent photo-bleaching and shaken at 500 rpm for five minutes. The luminescence was determined using TopCount™. A printed copy of the data was taken, recorded and the results transcribed into Microsoft® Excel 2007.

2.2.15 Chandler loop thrombosis model

Rationale

The Chandler loop model was developed to create a model thrombus *in vitro* that could be used to understand thrombus formation and test “clot busting” drugs for their action (Chandler and Jacobsen, 1967, Mutch et al., 2009). There are many different variations on the Chandler loop model but the basic model uses a loop of plastic tubing to model a blood vessel. Whole blood is added to the loop and rotated at a rate to model normal blood flow in a vessel. This produces a standardised thrombus that can easily be removed from the plastic tubing and analysed. The Chandler loop forms thrombi that are very similar in morphology to arterial thrombi formed *in vivo* comprising dense platelet and leukocyte rich upstream sections, white heads, and red blood cell and fibrin rich downstream sections, red tails (Stringer et al., 1994, Robbie et al., 1997). It has been shown by electron microscopy that the platelets in thrombi formed in the Chandler loop contained only mitochondria, indicating that platelet degranulation had occurred and that there was a polarised distribution of leukocytes predominantly in the white heads of the thrombi similar to the distribution seen in arterial thrombi (Stringer et al., 1994). Thrombosis in the Chandler loop model is characterised by the formation of small platelet aggregates followed by the formation of fibrin and larger platelet aggregates that eventually will occlude the loop (McClung et al., 2007b). Thrombogenesis in the Chandler loop model has been attributed to the formation of thrombin in the loop (Hornstra, 2009). This model can also be modified to test the interactions of materials with blood and the effect this has upon thrombus formation. The modified Chandler loop model is widely used to test stents and bypass grafts by introducing the stents to the tubing or by adding in a graft material as part of the loop (Christensen et al., 2001, Weber et al., 2002, Tepe et al., 2006, McClung et al., 2007a).

2.2.15.1 Chandler loop model for testing addition of material to blood

Rationale

In this study the Chandler loop model was modified to test the effect of a solution containing peptide monomer or soluble aggregate on thrombus formation. The Chandler loop model creates a thrombus of uniform size but normally does not involve total clotting of all the blood added to the loop. Adding a clotting agent such as α -thrombin will cause total clotting of the blood and produce a significantly larger thrombus. As the thrombus normally produced is uniform in size the effect of a material on thrombus formation can be observed by a difference in the mass of the thrombus produced. If a material has an anti-clotting effect no thrombus or a smaller thrombus will be produced. If a material is thrombogenic the size of the thrombus will be larger and similar to the thrombus produced with the clotting agent. If the material has no to little effect on thrombus formation then no difference in the size of the thrombus produced will be observed.

Reagents

Calcium chloride solution Calcium chloride dihydrate, 3.68 g to achieve a final concentration of 250 mol.m^{-3} , was dissolved in 100 ml of distilled water and the pH adjusted to pH 7.4. The calcium chloride solution was sterilised by autoclaving and stored at room temperature for up to one month.

Dilute α -thrombin solution Human α -thrombin, 20 μl , was added to 980 μl of distilled water and mixed by inversion.

Procedure

Medical grade polyvinyl chloride (PVC) tubing with an internal diameter of 3 mm and an external diameter of 4mm was cut to 33 cm lengths. The tubing was cut at both ends using a scalpel to leave straight cut edges which joined together leaving no visible gaps. Lengths, 2 cm, of medical grade PVC tubing with an internal diameter of 4 mm and an external diameter of 5 mm were cut and used to connect the ends of the 3 mm tubing together. Peptide was dissolved in distilled water at a concentration to achieve a final concentration of 0.3 mol.m^{-3}

when added to the blood. Distilled water was used as the negative control and diluted human α -thrombin as the positive control. TBS, 0.6 ml, (Section 2.1.5.3) and 50 μ l of calcium chloride solution were mixed together with 0.9 ml of citrated sheep blood and 100 μ l of the peptide test solution or controls. The blood mixture was then added by syringe, using a large gauge needle to prevent damage to the blood cells, to the loop of PVC tubing. The tubing was then placed on a rotator and spun at room temperature (27°C) at 30 rpm to achieve a shear rate of 428s^{-1} (Figure 2.3).

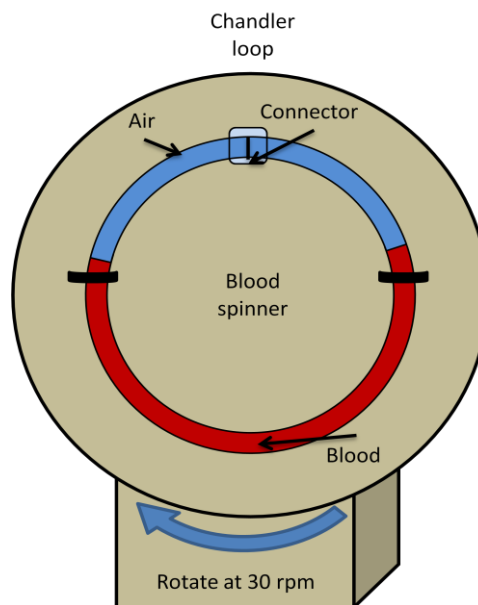


Figure 2.3; Schematic of Chandler loop model set up

This shear rate modelled flow in a blood vessel; the loop was spun for 90 minutes. Six samples of each peptide were tested. At the end of 90 minutes the loops were immediately emptied and the thrombus removed using smooth tipped forceps and weighed on a 7 figure balance. The results were recorded in Microsoft® Excel 2007, averaged and graphed as the mean value with 95% confidence limits (Section 2.2.21.1). Data was analysed for significant difference by one-way ANOVA.

2.2.15.2 Modified Chandler loop model for testing the thrombogenicity of the decellularised artery

Rationale

The modified Chandler loop model is widely used to test stents and bypass grafts by introducing the stents to the tubing or by adding in a graft material as part of the loop (Christensen et al., 2001, Weber et al., 2002, Tepe et al., 2006, McClung et al., 2007a). The Chandler loop model was used to test the ability of the peptide coating to passivate the surface of the decellularised vessel and reduce or prevent thrombus formation.

Procedure

Porcine internal carotid artery with an internal diameter of 5 mm was decellularised (Section 2.2.3). The decellularised vessel was cut into 5 cm lengths and 18.8 mol.m^{-3} of peptide was self-assembled within the vessel (Section 2.2.6.2.2). A loop of PVC tubing with an internal diameter of 3 mm and an external diameter of 4 mm was cut to 33 cm lengths; 5 cm was removed from the middle of each loop. The tubing was cut at both ends using a scalpel to leave straight cut edges which joined together leaving no visible gaps. Decellularised vessel controls and peptide coated vessels were placed over the ends where the 5 cm length of tubing had been removed and secured in place using silk sutures. Lengths, 7 cm, of medical grade PVC tubing with an internal diameter of 4 mm and an external diameter of 5 mm were cut and split down the middle so that they could be opened out. The larger tubing was placed over the decellularised vessel to maintain the loops shape and secured in place with cable ties. Lengths, 2 cm, of medical grade PVC tubing with an internal diameter of 4 mm and an external diameter of 5 mm were cut and used to connect the ends of the 3 mm tubing together to form the loop. The 5 cm length of PVC tubing removed from the loop was reinserted in the controls in place of the decellularised vessel. TBS, 0.6 ml, (Section 2.1.5.3) and 50 μl of calcium chloride solution were mixed together with 0.9 ml of citrated sheep blood. Human α -thrombin, 2 μl , was also added for the positive control. The blood mixture was then added by syringe, using a large gauge needle to prevent damage to the blood cells, to the loop of PVC tubing. The tubing was then placed on a rotator and spun at room temperature (27°C) at 30 rpm to achieve a shear rate of 428s^{-1} . The loop was spun for 90 minutes. At the end of 90 minutes the loops were then immediately emptied and the produced clot removed using smooth tipped forceps

and weighed on a 7 figure balance. The results were recorded in Microsoft® Excel 2007, averaged and graphed as the mean value with 95% confidence limits (Section 2.2.21.1). Data was analysed for significant difference using one-way ANOVA.

2.2.16 Haemolysis assay

Rationale

Haemolysis is the rupturing of erythrocytes and the subsequent release of their contents into the surrounding environment. Haemolysis can be caused by the interaction of erythrocytes with foreign materials. This lysis action is not limited to erythrocytes but can affect different cells; erythrocytes are used to test for this destructive membrane interaction as the release of haemoglobin into solution is easily detected. The principle behind the haemolysis test is simple; the erythrocytes are incubated in contact with a test material. If the materials cause haemolysis then high levels of free haemoglobin will be detected in solution; if the material has no haemolytic activity then no excess haemoglobin will be detected.

2.2.16.1 Washed erythrocytes

Erythrocytes were obtained from citrated sheep blood which was washed with Ringer's solution at a ratio of 2 parts blood to 3 parts Ringer's solution. The blood was mixed by inversion and centrifuged at 600 g for 10 minutes. The supernatant was discarded and the erythrocytes washed a further two times. After the final wash the erythrocyte mixture was centrifuged at 900 g for 10 minutes to pack the cells. The erythrocytes were resuspended in Ringer's solution to make a 10 % (v/v) solution of washed erythrocytes, i.e. 5 ml of packed erythrocytes resuspended in 45 ml of Ringers solution. Washed erythrocytes were kept at 4°C for a maximum of 24 hours.

2.2.16.2 Haemolysis assay

Peptide was dissolved in Ringer's solution at a concentration to achieve a final concentration of 0.3 mol.m^{-3} of peptide in each test. Test solutions, 500 μl , of peptide solution, Ringer's solution (negative control) and distilled water (positive control) were added to 500 μl of washed erythrocytes. The erythrocyte suspensions were mixed by inversion and the mixture was incubated at 37°C . Samples, 160 μl , were taken at 6, 12, 24, 48 and 72 hours and centrifuged at 1500 g for 5 minutes to pellet any intact erythrocytes. Supernatant, 100 μl , from each test sample was added to 100 μl of distilled water in a flat bottomed optical 96 well plate and the absorbance of the samples measured at 540 nm using a microplate spectrophotometer. Six replicates of each peptide were tested and the results exported to Microsoft® Excel 2007 and saved as a worksheet. The results were averaged and graphed as the mean value with 95% confidence limits (Section 2.2.21.1). Data was analysed for significant difference using one-way ANOVA.

2.2.17 Complement inhibition assay

Rationale

The principle behind the complement assay is that when complement containing serum is incubated in contact with antibody sensitised erythrocytes the classical complement pathway is activated and haemolysis occurs. The level of haemolysis is easily detected and is dependent upon the concentration of complement present in the serum. A standard test to determine the level of complement in serum is the 50 % complement haemolysis (CH50) assay. In the CH50 assay serum is diluted and incubated with sensitised erythrocytes; as the serum becomes more dilute there is less complement present to cause haemolysis. Serial dilution of the serum allows the dilution at which 50 % of the erythrocytes are lysed to be determined.

2.2.17.1 CH50 assay

Reagents

Antibody solution Lyophilized anti-sheep red blood cell stroma antibody was reconstituted with 2 ml of sterile deionised water. Reconstituted antibody, 2 ml, was added to 18 ml of sterile Ringer's solution (1:10 dilution) and stored at -20°C in 2 ml aliquots.

Procedure

The assay used washed sheep erythrocytes which were prepared as described in Section 2.2.16.1. Erythrocytes were sensitised by adding, drop-wise, an equal volume of antibody solution to washed erythrocytes all the time mixing the solutions together to prevent agglutination. The erythrocyte antibody mixture was incubated at 37°C for 30 minutes, mixing the cells after 15 minutes. Sensitised erythrocytes were kept at 4°C for a maximum of 24 hours.

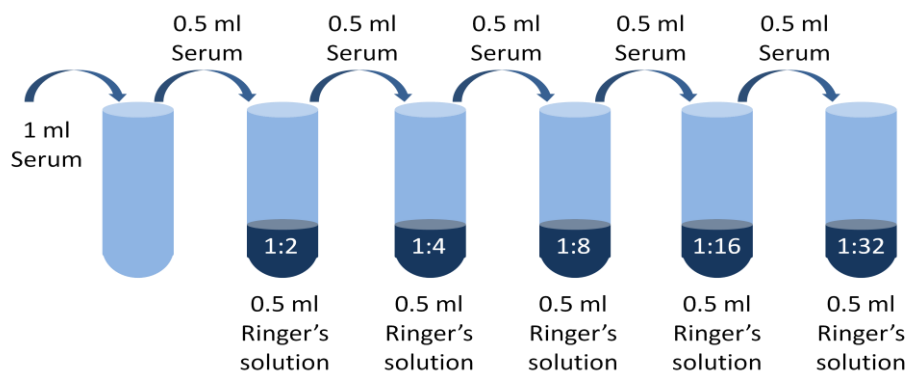


Figure 2.4, Schematic of serial dilution of serum for CH50 test

Normal human serum from pooled blood was serially diluted as in Figure 2.4. Diluted serum, $100\ \mu\text{l}$, $100\ \mu\text{l}$ of water as a total lysis control (positive control), $100\ \mu\text{l}$ of Ringer's solution as a blank control (negative control) and $100\ \mu\text{l}$ of serum incubated for 180 minutes at 60°C to heat inactivate the complement (negative control) were added to test tubes with $100\ \mu\text{l}$ of sensitised erythrocytes as in Figure 2.5 and were gently mixed. The samples were incubated at

37°C for 30 minutes gently mixing after 15 minutes. Six samples of each serum dilution and control were tested. The samples were then centrifuged at 1500g for 5 minutes to sediment the erythrocytes. Supernatant, 100 µl, was added to 100 µl of distilled water in a flat bottomed optical 96 well plate and the absorbance of the samples measured at 540 nm using a microplate spectrophotometer. The results were imported into Microsoft® Excel 2007 and converted into a line graph. From the graph the dilution of serum needed to achieve 50 % lysis of the sensitised erythrocytes was calculated.

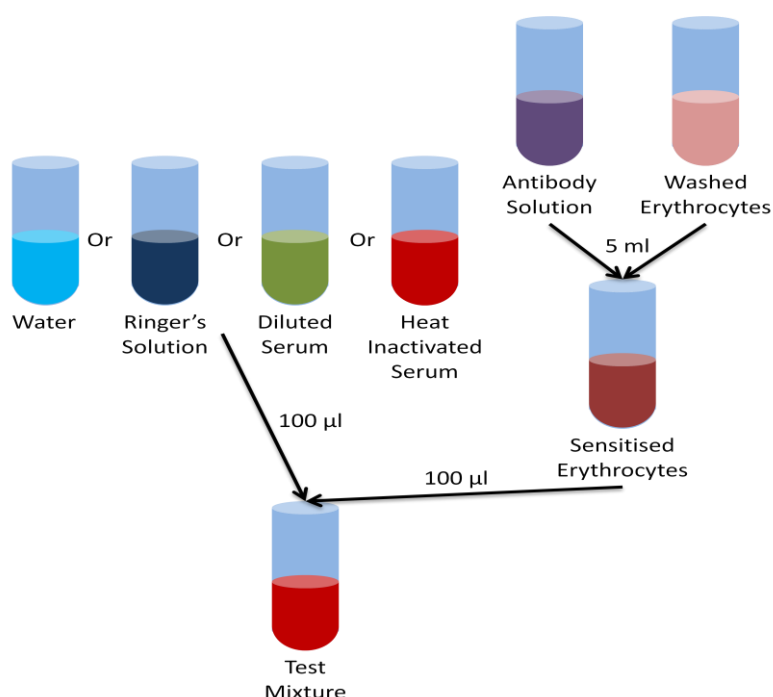


Figure 2.5, Schematic of set up of CH50 assay

2.2.17.2 Modified CH50 complement inhibition assay

Rationale

The principle of the CH50 assay can be modified in order to test for the inhibition of complement activation. When sensitised erythrocytes, serum diluted to give 50 % lysis and a test material are mixed together the effect of the material on the complement system can be assessed. If the test material has no effect on the complement system then 50 % cell lysis will still be observed, however, if the test material inhibits the complement system the level of

lysis in the sample will be below 50 %. Since the level of haemolysis observed was dependent upon the concentration of complement in the serum it was not possible to test for complement activation using this assay.

Procedure

The assay used washed sheep erythrocytes which were prepared as described in Section 2.2.16.1. Peptide was dissolved in Ringer's solution to achieve a final concentration of 0.3 mol.m^{-3} in the test mixture. The peptide solution, 1 ml, was added to 1 ml of antibody solution and mixed by inversion. Erythrocytes were sensitised by adding, drop-wise, an equal volume of antibody-peptide solution to washed erythrocytes all the time mixing the solutions together to prevent agglutination. The erythrocyte antibody-peptide mixture was incubated at 37°C for 30 minutes, mixing the cells after 15 minutes. Sensitised erythrocytes were kept at 4°C for a maximum of 24 hours. Sensitised erythrocytes for the controls were prepared as in the CH50 assay (Section 2.2.17.1).

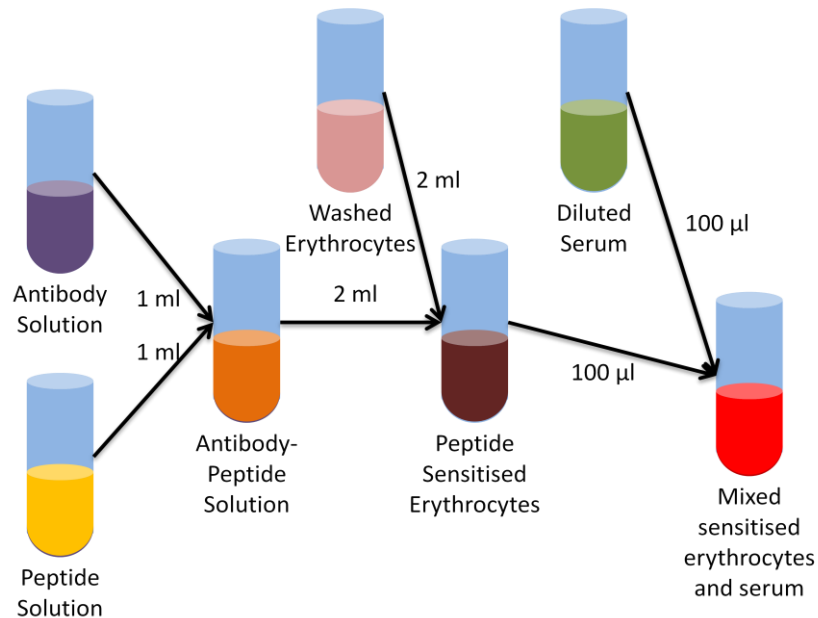


Figure 2.6; Schematic of set up of modified CH50 complement inhibition assay

Normal human serum from pooled blood was serially diluted as in Figure 2.4 to the dilution determined using the CH50 assay. Diluted serum, 100 µl, was added to 100 µl of antibody-

peptide sensitised erythrocytes and gently mixed as in Figure 2.6. Diluted serum (dilution determined by CH50 assay), 100 µl, as a 50 % lysis control, 100 µl of water as a total lysis control (positive control), 100 µl of Ringer's solution as a blank control (negative control) and 100 µl of serum incubated for 180 minutes at 60°C to heat inactivate the complement (negative control) were added to test tubes with 100 µl of sensitised erythrocytes as in Figure 2.6 and were gently mixed. Six replicates of each mixture were made and the samples were incubated at 37°C for 30 minutes gently mixing after 15 minutes. The samples were then centrifuged at 1500g for 5 minutes to sediment the erythrocytes. Supernatant, 100 µl, was added to 100 µl of distilled water in a flat bottomed optical 96 well plate and the absorbance of the samples measured at 540 nm using a microplate spectrophotometer. The results were imported into Microsoft® Excel 2007 and saved as a worksheet. The results were graphed as the mean value with 95% confidence limits (Section 2.2.21.1). Data was analysed for significant difference using one-way ANOVA.

2.2.18 Isolation and growth of ovine endothelial cells

2.2.18.1 Isolation of ovine arterial endothelial cells

Reagents

Antibiotic solution	Penicillin streptomycin, 6 ml to achieve a final concentration of 300 U.ml ⁻¹ , was added to 100 ml of sterile PBS with calcium and magnesium. The solution was made aseptically and used within 24 hours of production.
Collagenase stock solution (1%)	Collagenase type II (2273 U.ml ⁻¹), 50 mg, was reconstituted in 5 ml sterile PBS without calcium and magnesium. Solution was made aseptically and was stored at -20°C.
Working collagenase solution (0.1%)	Collagenase type II stock solution (1% w/v), 1 ml, was added to 9 ml of PBS without Calcium and magnesium. The solution was made aseptically and was used immediately

Procedure

All procedures were carried out in a class II safety cabinet to reduce the chance of infection. Ovine legs delivered fresh from slaughter that morning were placed in the class II safety cabinet. The legs were dissected to find the end of the superficial femoral artery. The ends of the vessels were clamped to reduce the chance of infection. The branches of the vessels were tied off with sutures or surgical clips as the vessel was removed. Once fully dissected from the ovine legs the superficial femoral arteries were placed in antibiotic solution and incubated at 37°C for one hour. The vessels were washed through with antibiotic solution using a syringe to remove any blood or blood clots. One end of the vessel was closed with a clip or silk suture and a blunt ended needle was placed in the other end and secured with a silk suture. A syringe containing working collagenase solution (0.1% w/v) was attached to the needle and used to fill the vessel. The needle was then removed and the suture tightened to contain the collagenase solution. The vessel containing the collagenase was then incubated at 37°C for 30 minutes. Following incubation the vessel contents were emptied into a sterile universal tube and the vessel washed through using 10 ml of sterile PBS without calcium or magnesium added. The cell suspension was centrifuged at 250 g for ten minutes. The supernatant was removed and the cells washed with 20 ml M-199. The cells were then resuspended in 5 ml of endothelial cell culture medium (Section 2.1.5.9) and placed in a 25 cm² tissue culture flask. The cells were incubated at 37°C in 5 % (v/v) CO₂ in air changing the culture medium every 48 hours.

2.2.18.2 Subculture of ovine arterial endothelial cells

The culture medium was removed from the flask and the cell layer was washed using Hank's balanced salt solution without calcium and magnesium. After 2 – 5 minutes the Hanks balanced salt solution was removed and replaced with trypsin/EDTA solution (1 ml in a 25 cm² tissue culture flask, 2.5 ml in a 75 cm² tissue culture flask and 5 ml in a 175 cm² tissue culture flask) and incubated in 5 % (v/v) CO₂ in air at 37°C for no more than three minutes. Having isolated the cells there is a need to purify the cell population. It has been observed that after 3 minutes trypsin digestion small polygonal endothelial cells detached whereas larger flatter smooth muscle cells were still attached (Ryan, 1984). Others have reported that endothelial cells were subcultured in trypsin for 2-3 minutes as that is all the time endothelial cells needed to detach in trypsin (Gimbrone et al., 1974). After three minutes the endothelial cells detached but any smooth muscle or fibroblast cells remained attached to the bottom of the tissue

culture flask. The trypsin was neutralised by the addition of 5 ml of supplemented medium, containing at least 10 % (v/v) foetal calf serum. The cell suspension was transferred to a sterile universal tube and centrifuged at 180 g for ten minutes. The supernatant was removed and the cells resuspended in 5 ml of supplemented medium. The total number of viable cells was determined using the trypan blue method (Section 2.2.13.3). The cells were seeded into a larger tissue culture flask or split 1:3 into the same size tissue culture flasks with 5ml of supplemented cell culture medium for a 25 cm² tissue culture flask, 10 ml of medium in a 75 cm² tissue culture flask and 15 ml of medium in a 175 cm² tissue culture flask. The cells were incubated in 5 % (v/v) CO₂ in air at 37°C changing the medium every 48 hours. Isolated cells were purified by successive subculture, taking advantage of the difference in detachment times for endothelial cells, short 2 – 3 minutes, and smooth muscle cells, longer 4 -5 minutes (Ryan, 1984).

2.2.18.3 Cryopreservation of ovine endothelial cells

Isolated endothelial cells were cryopreserved as described in Section 2.2.13.4 using medium M199.

2.2.18.4 Characterisation of ovine arterial endothelial cells

Ovine arterial endothelial cells were subcultured (Section 2.2.18.2). Cell suspension, 20 µl, was added to the spots of a multi-spot glass slide and incubated for 4 hours. The medium was then aspirated and the slide covered in 5 ml of endothelial cell culture medium and incubated for 48 hours at 37°C in 5 % (v/v) CO₂ in air. Cell culture medium was removed and the cells fixed for one minute in 1:1 acetone and methanol. The slides were air dried for five minutes and washed in running tap water for 10 minutes. The slides were washed with TBS for five minutes and tapped to remove excess saline.

2.2.18.4.1 Indirect immunofluorescent antibody method

Reagents

BSA stock solution	Bovine serum albumin (BSA), 2.5 g, was dissolved into 50 ml sterile PBS. The solution was passed through a 0.2 μm pore size filter and stored at -20°C for up to six months.
Antibody diluent	Sodium azide (1%), 6 ml, 300 μl of BSA stock solution and 40 ml sterile TBS were mixed together. The pH of the solution was adjusted to pH 7.6 and the volume made up to 60 ml using sterile TBS. The solution was stored at 4°C for up to three months.
TBS-Tween 20	Tween 20, 500 μl , was added to 1 L of sterile TBS. The pH of the solution was adjusted to pH 7.6. The solution was stored at room temperature for up to three months.
Dye buffer	Trizma base, 1.211g to achieve a final concentration of 10 mol.m^{-3} , 0.3724 g of EDTA to achieve a final concentration of 1 mol.m^{-3} and 5.8 mg of sodium chloride to achieve a final concentration of 1 mol.m^{-3} were dissolved in 1 L of distilled water and sterilised by autoclaving. The pH of the solution was adjusted to pH 7.4 before use and stored at room temperature in a dark bottle for up to six months.
DAPI dye stock	DAPI (10 mg) was added to 10 ml of nuclease free water and stored in 20 μl aliquots at -25°C for up to six months
DAPI working solution	DAPI dye stock solution, 40 μl , to achieve a final concentration of $0.1\text{ }\mu\text{g.ml}^{-1}$, was mixed with 400 ml of Dye buffer and was used immediately.

Procedure

Primary antibody solutions against von Willebrand factor, smooth muscle cell α -actin and myosin heavy chain were made at the manufacturers recommended dilutions in antibody diluent; Anti-vWF 1:200, anti- α -actin 1:400 and anti-myosin 1:100. Primary antibody, 20 μl , was added to each spot of cells on a multi-spot slide and incubated in a moist environment for

one hour at room temperature. The slides were washed twice in TBS-Tween 20 for 10 minutes each on an orbital shaker at 40 rpm. The slides were then washed in TBS for 10 minutes on an orbital shaker at 40 rpm. Secondary fluorescently labelled antibody solutions were made using antibodies against the primary antibodies host species. Alexa Fluor 488 labelled goat anti-mouse antibody (whole antibody) diluted 1:200 against anti- α -actin and anti-myosin primary antibodies and Alexa Fluor 488 labelled goat anti-rabbit antibody (F(ab')₂ fragment) diluted 1:200 against anti-vWF antibody. Fluorescently labelled secondary antibody, 20 μ l, was added to each spot and incubated in a moist environment for 30 minutes in the dark. The slides were washed twice in TBS-Tween 20 for 10 minutes each on an orbital shaker at 40 rpm. The slides were then washed in TBS for 10 minutes on an orbital shaker at 40 rpm. Slides were then immersed in DAPI working solution and incubated at room temperature for 10 minutes in the dark. The slides were washed with DPBSa three times for 10 minutes each in the dark. Slides were mounted with a glass slide and DABCO: glycerol mountant (Section 2.2.5) and stored in the dark for a maximum of 24 hours then imaged using an upright fluorescent microscope and appropriate filters. Images were captured using a digital camera and image-Pro Plus v 5.1.

2.2.18.4.2 Direct immunofluorescent antibody method

Reagents

Reagents as above in Section 2.2.18.4.1

Procedure

Primary antibody solution against CD31 was made at the manufacturers recommended dilution, 1:100, in antibody diluent. Primary antibody, 20 μ l, was added to the each spot of cells and incubated in a moist environment for one hour at room temperature. The slides were washed twice in TBS-Tween 20 for 10 minutes each on an orbital shaker at 40 rpm. The slides were then washed in TBS for 10 minutes on an orbital shaker at 40 rpm. Slides were then immersed in DAPI working solution and incubated at room temperature for 10 minutes in the dark. The slides were mounted and visualised as above in Section 2.2.18.4.1.

2.2.19 Endothelial cell attachment and proliferation

Porcine internal carotid artery was decellularised (Section 2.2.3). Following histological assessment (Section 2.2.4) the decellularised vessel was cut into 1.5 cm lengths and cut horizontally to open the vessel and create sections of vessel with the intimal layer exposed. Peptide P₁₁-4, 60 mg (18.8 mol.m⁻³), and 60 mg (18.8 mol.m⁻³) P₁₁-4 mixed at a ratio of 1:50 with P₁₁-4-cRGD was weighed and added to 1.8 ml of sterile water and a monomer solution made. The sections of decellularised vessel were added to the peptide monomer and left overnight. Peptide self-assembly was triggered by the addition of 0.2 ml of 10X Ringer's solution (Section 2.2.6.2.2). Sections of decellularised vessel were added to 1.8 ml of sterile water and left overnight, 0.2 ml of 10X Ringer's solution was added and the vessels left overnight as a control. Four samples of the control and each peptide coated vessel sections were placed at the bottom of 6 wells of a 12 well plate for each time point and a seeding ring placed on the vessel section and pressed down to create a seal. Endothelial cell growth medium without ECGF, 300 µl, was added to each seeding ring and incubated for 24 hours at 37°C. The endothelial cell growth medium without ECGF was aspirated from each seeding ring.

Endothelial cells were subcultured as described in Section 2.2.18.2. Cell numbers were estimated (Section 2.2.13.3) and the cells resuspended in endothelial growth medium at 25,000 cells per ml. Endothelial cell suspension, 200 µl, was added to each seeding ring to give 5000 cells per seeding ring and incubated at 37°C in 5 % CO₂ (v/v) in air for 4 hours. After 4 hours the medium was aspirated and the seeding rings removed. Sterile PBS, 1 ml, was added to each well and removed after 1 minute to remove any unattached cells. Endothelial cell growth medium, 1 ml, was added to each well and incubated at 37°C changing the medium every 48 hours. Four samples for each test condition were removed at 4 hours, 24 hours and 72 hours for analysis. A solution of 1 mol.m⁻³ calcein AM and 2 mol.m⁻³ ethidium homodimer-1 was made in sterile PBS (2 µl of calcein AM and 8 µl of ethidium homodimer-1 in 8 ml of PBS). The culture medium was aspirated from each well and replaced with 0.5 ml of PBS containing calcein AM and ethidium homodimer-1 and incubated at 27°C in the dark for 40 minutes. The PBS containing calcein AM and ethidium homodimer-1 was removed and replaced with 1 ml of sterile PBS which was removed after 1 minute. Each sample of decellularised vessel was turned over and stored in the dark until imaged. Samples were imaged using an inverted confocal fluorescent microscope (Section 2.2.12.1). Six images were taken of each sample at random and the number of live and dead cells present counted, recorded and analysed using Microsoft® Excel 2007. Results were shown as representative images and graphed as the mean

value with 95% confidence limits (2.2.21.1). Data was analysed for significant difference by two-way ANOVA.

2.2.20 Flow cell model of flow over luminal surface in small diameter blood vessels used to test peptide stability under flow

Rationale

The peptide stability under flow in a small diameter blood vessel was judged by the design and use of a flow cell system that modelled the flow rate of blood over the luminal surface of the vessel. A flow cell was designed such that a section of peptide coated vessel could be placed in a well with a lamina flow of salt solution being passed over the top of the luminal face of the vessel. The flow cell used a reservoir that was the same width as the test well; the reservoir filled up with test solution to be level with the surface of the test material and test solution flowed over the whole sample surface and down into a second reservoir at the end of the test well resulting in lamina flow.

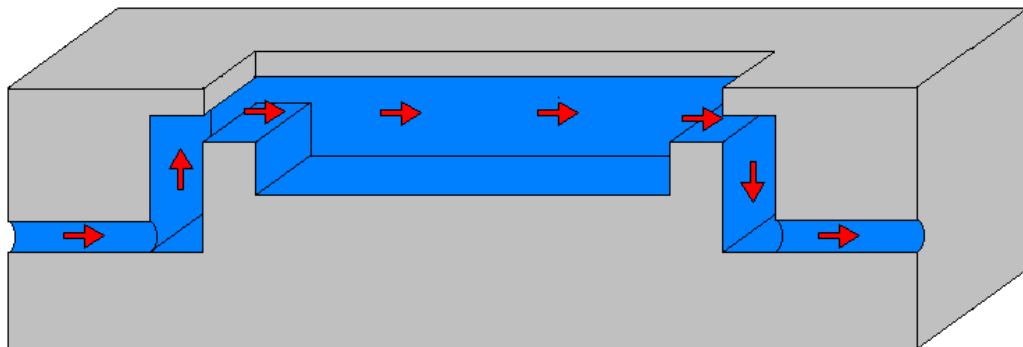


Figure 2.7, Cross-section schematic of flow cell

Reagents

Test solution Ringers solution with 0.02 % (W/V) sodium azide (NaN_3)

Procedure

Decellularised vessel was cut in half to expose the luminal face of the vessel and fluorescently tagged peptide self-assembled within the vessel as described in Section 2.2.7. The peptide coated vessel was placed in the bottom of the flow cell. A peristaltic pump was used to circulate test solution through the flow cell. The normal flow rate of blood over the surface of the vessel could be modelled in the flow cell by setting the pump to a revolution speed of 65 rpm and using tubing with an internal diameter of 5 mm. The flow cell system was covered and set running in a dark room as not to photo-bleach the fluorescently tagged peptide. A separate flow cell was set up for each sample of vessel being tested. After 1, 2, 3, 4, 7 and 14 days the vessel was removed from the flow cell, sectioned and imaged as described in Section 2.2.11.1 and Section 2.2.11.2. The intensity of fluorescence for three different locations for each image was determined and recorded in Microsoft® Excel. The fluorescent intensity was averaged for each time point at each magnification, 95% confidence limits determined as in Section 2.2.21.1 and the mean value and 95 % confidence limits graphed.

2.2.21 Statistical analysis

2.2.21.1 Confidence limits

Confidence limits were calculated at 95 % for all applicable data with a minimum of three replicates using the equation;

$$\text{Confidence limit} = SE \times t$$

$$\text{SE (Standard error)} = \frac{SD}{\sqrt{n}}$$

$$\text{SD} = \text{Standard deviation of a sample}$$

$$(t) = t\text{-value}$$

Confidence limits were determined using statistical package on Microsoft® Excel 2007.

2.2.21.2 Statistical analysis

For the comparison of data for one test condition with more than two groups a one way analysis of variance (ANOVA) was carried out using data analysis tools. For the comparison of data for two test conditions with more than two groups a two way analysis of variance (ANOVA) was carried out using data analysis tools. Individual differences between means were then determined by calculating the minimum significant difference (MSD) at $p=0.05$ using the T-method.

$$\text{MSD} = \text{Critical value} \times \text{SE}$$

$$\text{SE} = \sqrt{\frac{\text{mean square within groups}}{n}}$$

$$\text{Critical value} = [K,v] \text{ from table of studentized range at } Q=0.05$$

$$K = \text{Number of groups}$$

$$V = \text{Degrees of freedom of MS within}$$

3 Development of methodologies and testing of peptide self-assembly in decellularised arterial conduits

3.1 Introduction

Peptide β -sheet self-assembly and arterial decellularisation have been extensively studied. Previous work done within the Institute of Medical and Biological Engineering (iMBE) at the University of Leeds has developed and tested a patented method of decellularising tissues that has been adapted and applied to blood vessels (Wilshaw et al., 2011, Owen et al., 2012). The peptide group at the University of Leeds has studied the self-assembly properties of a range of peptides and has started to apply these peptides in biological applications (Aggeli et al., 2001, Kirkham et al., 2007, Maude et al., 2011a). The purpose of this work was to study the self-assembly of a model peptide within decellularised porcine internal carotid artery, to ascertain if the peptide would self-assemble within the acellular scaffold.

3.1.1 Peptide self-assembly

The peptides developed at the University of Leeds are eleven amino acids long and self-assemble by a one dimensional nucleated process. The effects of the environment upon the energetics of the self-assembling process have been explored in depth in order to develop design characteristics for the production of self-assembling peptides. Knowledge from protein folding has shown that an alternating sequence of hydrophobic and hydrophilic residues will create a β -sheet structure regardless of the propensity of the amino acids in the chain to form α -helix or β -sheet (Xiong et al., 1995). It has been identified that peptides self-assembled in antiparallel β -sheet tapes when there were an odd number of amino acids in the peptide sequence as this encouraged a more complete register and better spatial positioning of the adjacent strands and hydrogen bonds (Maude et al., 2011a).

The structures formed by the self-assembling peptides have been explored and found to be the result of the concentration of peptide in solution forming a hierarchy of self-assembled structures which resulted in the formation of peptide hydrogels (Aggeli et al., 2001). The effect of changing, pH and ionic concentration on a range of different peptides was studied for the

effect on the nucleation, gelation and the hierarchy of the self-assembled structures formed (Aggeli et al., 2003b, Carrick et al., 2007). The pKa of the different amino acids in the peptide allows for switchable self-assembly as the residues are protonated and de-protonated, this behaviour has been well documented (Zhang et al., 1993, Schneider et al., 2002, Carrick et al., 2007). It has also been reported that the natural repulsive charges between the peptides can be overcome by charge screening from an increase in ionic concentration (Carrick et al., 2007, Maude et al., 2011a). It was reported that the change in the Debye length when the ionic concentration was altered resulted in the self-assembly of the peptide at lower energies and did not affect the structure of the peptide aggregates formed (Carrick et al., 2007).

Design characteristics that have been found for the peptides developed at the University of Leeds that showed a net charge was needed to stabilise fibril formation (Aggeli et al., 2003a). It was further established that in biological conditions a net charge of +/- 2 produced the most stable self-assembled peptide gels (Maude et al., 2011a)(Personal communication, Dr D. Miles, University of Leeds).

3.1.2 Peptide P₁₁₋₄

Self-assembling peptides lie between two material classes, they are not natural proteins such as collagen and elastin but are comprised of natural amino acids (Maude et al., 2013). The primary difference between a peptide and a protein is size; peptides are typically less than 50 amino acids long where proteins consist of several polypeptide chains. Unlike proteins that can fold to form complex tertiary and quaternary structures the P11 series of peptides are limited to secondary structure β -sheets; consequently self-assembled peptides are held together, predominantly, by hydrogen bonding where the tertiary structured proteins are held together by other bonds such as disulphide bridges. The main difference between the β -sheets found in proteins and self-assembled peptides are the β -sheets found in proteins tend to be connected together and be part of the same protein chain where the β -sheet structures formed by peptides are made up of individual monomers.

The peptide selected to test self-assembly within acellular scaffolds was P₁₁₋₄ (Figure 3.1). This peptide is a rationally designed peptide comprising eleven amino acids (CH₃CO-Q-Q-R-F-E-W-E-F-E-Q-Q-NH₂). The P11 series of peptides typically use alternating polar and aromatic residues to drive anti-parallel β -sheet self-assembly (Maude et al., 2013). It has been shown that

peptides of 7 -40 amino acids will have a propensity towards β -sheet formation (Bell et al., 2006). It is believed that an odd number of amino acids allows for maximisation of the enthalpy of the peptide subunits aiding in self-assembly (Personal communication from Dr Robert Davies University of Leeds). Peptide P₁₁-4 was designed to form fibrils and gels at low pH and is converted to a monomeric state at high pH; this material change is driven by the protonation and deprotonation of glutamic acid (Carrick et al., 2007). Self-assembly of peptide P₁₁-4 can also be triggered by a change in ionic concentration. Repulsive charges interactions prevent peptide association and self-assembly, when the ionic concentration is changed self-assembly occurs as the ions shield the repulsive charges (Chen, 2005, Carrick et al., 2007, Maude et al., 2011b). P₁₁-4 was designed to have a resultant charge of -2 in physiological conditions; this has been identified as the ideal charge for self-assembly to occur (Personal communication, Dr D. Miles, University of Leeds).

P₁₁-4 was chosen as it has been studied for biological applications and found to be biocompatible (Protopapa et al., 2009, Maude et al., 2011a). P₁₁-4 was designed to form fibril structures with a left hand twist at low pH and to be monomeric at high pH. In solutions with a concentration of 6.3 mol.m⁻³ of P₁₁-4 self-supporting gels were observed between pH 2.0 and pH 3.2, at pH 3.2 to pH 5.0 flocculation occurred and at pH 5.0 to pH 7.0 viscous nematic fluids were found. This could be changed by changing the concentration of peptide, for example at 12.6 mol.m⁻³, twice the concentration, nematic gels were found at pH 5.0 to pH 7.0 (Aggeli et al., 2003a).

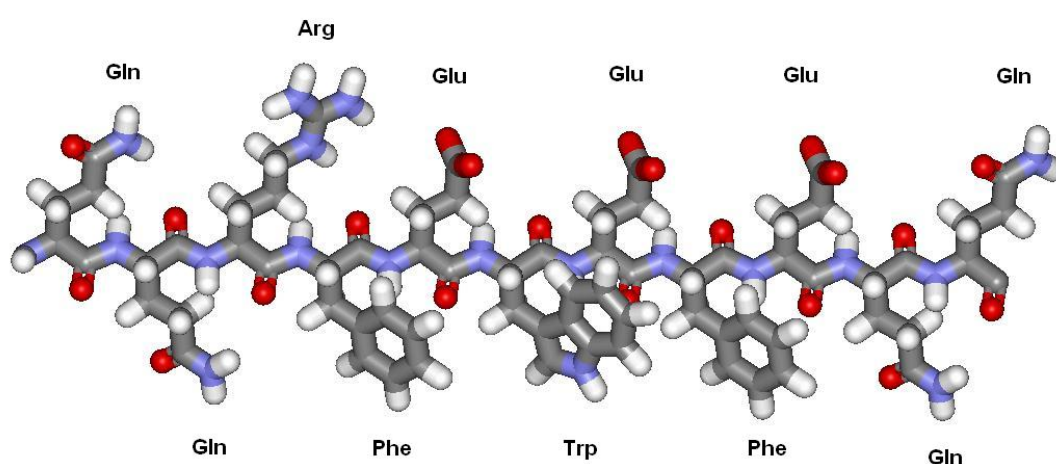


Figure 3.1; Stick image of peptide P₁₁-4 with amino acids labelled, created using HyperChem 7.

3.1.3 Decellularisation

Decellularisation is a logical progression in the development of immunocompatible biological scaffolds from allogenic and xenogenic grafts. The idea behind decellularisation is that by removing all the cells, cellular debris and coding DNA and RNA the antigens that cause immune rejection are removed whilst leaving the ECM. The ECM retains the same biomechanical and structural properties as the native tissue. Cellular debris needs to be removed as it may be immunogenic. Cellular debris has also been shown to be a potential site for calcification to occur (Courtman et al., 1994). The removal of all coding DNA and RNA is important in the prevention of possible disease transmission. If DNA is not removed from a decellularised tissue it is possible that coding fragments of retroviruses might be present (Prabha and Verghese, 2008). The response of a host to a decellularised scaffold has been shown to be largely dependent upon the decellularisation method and the decellularised tissue (Badylak, 2004, Badylak et al., 2009). Methods that resulted in the removal of the majority of cells and cellular debris have shown the best results as there was little to no immune reaction. Where immune and detrimental reactions were seen a large amount of debris was present in the tissue following less successful decellularisation. Decellularisation has been explored in more detail in Section 1.4.7. Blood vessel is a naturally porous material but in theory the vessel is more porous following decellularisation as voids will remain where the cells have been removed.

3.1.4 Aims and objectives

The aims of this chapter were to investigate the self-assembly of a model peptide P₁₁₋₄ within decellularised porcine internal carotid artery.

Specific objectives:

- a) To determine if P₁₁₋₄ will self-assemble within the decellularised vessel
- b) Should the peptide self-assemble in the decellularised vessel;
 - I. To develop a protocol for the self-assembly of peptides within an acellular vessel
 - II. To evaluate how P₁₁₋₄ self-assembles within the acellular vessel
 - III. To test the stability of the peptide structures formed

3.2 Methods

3.2.1 Histological evaluation of decellularised porcine internal carotid artery

Porcine internal carotid artery was decellularised as described in Section 2.2.3. After decellularisation a 1 cm length sample from the ends and middle of all the vessels were taken and processed for standard histological evaluation as described in Section 2.2.4, each sample was sectioned at 5 μm , and sections were air dried overnight. Three sections were placed on each slide and a minimum of 4 slides were made for each sample. Two slides for each sample were stained using haematoxylin and eosin (Section 2.2.4.4) or were stained using DAPI (Section 2.2.4.5) and imaged.

3.2.2 Evaluation of peptide self-assembly triggers

The affect of different self-assembly triggers was assessed at 4 different concentrations of peptide P₁₁₋₄. Monomer solutions of peptide, 0.5 ml, were made in deionised water at 30 $\text{mg}\cdot\text{ml}^{-1}$ (18.8 $\text{mol}\cdot\text{m}^{-3}$), 15 $\text{mg}\cdot\text{ml}^{-1}$ (9.4 $\text{mol}\cdot\text{m}^{-3}$), 5 $\text{mg}\cdot\text{ml}^{-1}$ (3.13 $\text{mol}\cdot\text{m}^{-3}$) and 1 $\text{mg}\cdot\text{ml}^{-1}$ (0.63 $\text{mol}\cdot\text{m}^{-3}$), as described in Section 2.2.6.1, for testing the effects of changing the pH. The samples were adjusted to pH 8 by the addition of 1 $\text{mol}\cdot\text{dm}^{-3}$ NaOH and left overnight before making observations and capturing images. The pH of the samples was then lowered to pH 7 by the addition of concentrated HCl and left overnight before making observations and capturing images. The pH of the samples was then lowered to pH 5 by the addition of concentrated HCl and left overnight before making observations and capturing images. To test the effects of changing ionic concentration monomer solutions of peptide were made in deionised water at 9/10 final wanted volume (0.45 ml = 9/10 final volume of 0.5 ml) to achieve a final concentration of 30 $\text{mg}\cdot\text{ml}^{-1}$ (18.8 $\text{mol}\cdot\text{m}^{-3}$), 15 $\text{mg}\cdot\text{ml}^{-1}$ (9.4 $\text{mol}\cdot\text{m}^{-3}$), 5 $\text{mg}\cdot\text{ml}^{-1}$ (3.13 $\text{mol}\cdot\text{m}^{-3}$) and 1 $\text{mg}\cdot\text{ml}^{-1}$ (0.63 $\text{mol}\cdot\text{m}^{-3}$) as in Section 2.2.6.1. The different concentration samples for testing of biological salt solutions were made as described in Section 2.2.6.2.2 using PBS or Ringer's solution. The samples were left overnight to allow for self-assembly and were then imaged and observations recorded. Inversion of the glass vials allowed for visual assessment of the peptide state. Visual inspection of the peptides with a polarised light allowed for the assessment of self-assembly by the presence of birefringence.

3.2.3 Cross sectioning and imaging of fluorescent peptide penetration into decellularised vessel

A monomer solution at 9/10 the final volume was made to achieve a final concentration of 30 mg.ml⁻¹ (18.8 mol.m⁻³) of P₁₁₋₄ at a ratio of 1:30 of fluorescein tagged P₁₁₋₄ to untagged P₁₁₋₄ as described in Section 2.2.8. One end of three 5 cm lengths of decellularised vessel were sealed using silk sutures and 0.45 ml of peptide monomer solution was placed inside the vessel. The other ends of the vessels were sealed with a silk suture and each vessel was left overnight in 15 ml of deionised water to cover the vessel. Observations were made of the vessels and the surrounding deionised water. Each vessel was opened at one end and self-assembly was triggered by the addition of 0.05 ml of 10X Ringer's solution (Section 2.2.6.2.2). The vessels were then sealed again and placed in 15 ml of Ringer's solution and left overnight to allow for self-assembly too occur. The vessels were removed from solution, emptied of excess peptide gel and 1 cm length samples were taken from the middle of the vessels and sectioned using a cryostat as in Section 2.2.11. The sections were stored in the dark and imaged. Controls of decellularised porcine internal carotid artery were put through the same pH and solution changes without any peptide present.

3.2.4 FTIR spectroscopy and analysis of peptide presence in decellularised vessel

Decellularised porcine internal carotid artery was cut into three 1 cm² sections and taken through three changes of deuterium oxide (10 ml) as described in Section 2.2.9. Peptide P₁₁₋₄ at a concentration of 30 mg.ml⁻¹ (18.8 mol.m⁻³) in deuterium oxide was self-assembled within decellularised vessel using pH as a trigger (Section 2.2.6.2.1). Three sections of decellularised vessel were taken through the same pH and solution changes without any peptide present. The control vessel and peptide coated vessel sections were compressed between calcium fluoride optical lenses and spectra taken of different areas of the control vessels and P₁₁₋₄ coated vessels as described in Section 2.2.9. Three samples of each test condition were used and the calcium fluoride optical lenses cleaned using methanol in between the collection of each spectra.

3.2.5 Field emission gun scanning electron microscopy (FEGSEM) imaging of peptide in decellularised vessel

Six 1 cm² sections of decellularised porcine internal carotid artery were fixed in neutral buffered formalin for 4 hours. Peptide P₁₁₋₄ at concentrations of 10 mg.ml⁻¹ (6.26 mol.m⁻³), 5 mg.ml⁻¹ (3.13 mol.m⁻³) and 1 mg.ml⁻¹ (0.63 mol.m⁻³) in deionised water were self-assembled in samples of the fixed decellularised porcine internal carotid artery, using pH as a trigger (Section 2.2.6.2.1). The peptide coated vessel along with uncoated vessel as a control was dried under vacuum overnight and processed for imaging as described in Section 2.2.10. Samples were placed in the Zeiss LEO 1530 Gemini FEGSEM and imaged using secondary electron imaging at 3 KeV. Images were recorded using the associated software and analysed using Image J.

3.2.6 Confocal laser scanning microscopy (CLSM) imaging of peptide in decellularised vessel

Peptide P₁₁₋₄ in deionised water at a concentration of 30 mg.ml⁻¹ (18.8 mol.m⁻³) at a ratio of 1:30 of fluorescein tagged P₁₁₋₄ to untagged P₁₁₋₄ was self-assembled within three 1 cm² sections of decellularised porcine internal carotid artery using Ringer's solution as a trigger (Section 2.2.6.2.2). Three controls of decellularised porcine internal carotid artery were put through the same pH and solution changes without any peptide present. Samples for imaging in the CLSM were removed from the peptide gel and placed on a glass slide and a cover slip placed on top. An oil emersion objective lens was used as described in Section 2.2.12.1. A range of scans were taken of the samples and several z-axis stacks that allowed for images to be taken at different depths within the sample. Images were collected and recorded using ZEN v7.1 and analysed using LSM image browser.

3.2.7 Multi-photon laser scanning microscopy (MPLSM) imaging of peptide in decellularised vessel

Peptide P₁₁₋₄ in deionised water at a concentration of 30 mg.ml⁻¹ (18.8 mol.m⁻³) at a ratio of 1:30 of fluorescein tagged P₁₁₋₄ to untagged P₁₁₋₄ was self-assembled within a 1 cm² section of decellularised porcine internal carotid artery using Ringer's solution as a trigger (Section 2.2.6.2.2). A control of decellularised porcine internal carotid artery was put through the same pH and solution changes without any peptide present. The samples were stored in the dark and transported to the University of York where they were imaged as described in Section 2.2.12.2. Images were taken using secondary harmonic auto-fluorescence and an FITC filter; images were then analysed using LSM image browser.

3.2.8 The effect of concentration on peptide distribution throughout decellularised vessel

Three 1 cm² sections of decellularised vessel were added to monomer solutions of P₁₁₋₄ at a ratio of 1:30 of fluorescein tagged P₁₁₋₄ to untagged P₁₁₋₄ in deionised water at concentrations of 30 mg.ml⁻¹ (18.8 mol.m⁻³), 15 mg.ml⁻¹ (9.4 mol.m⁻³), 7.5 mg.ml⁻¹ (4.7 mol.m⁻³), 3.75 mg.ml⁻¹ (2.35 mol.m⁻³) and 1.87 mg.ml⁻¹ (1.18 mol.m⁻³) made as described in Section 2.2.6.1. Decellularised vessel was left in the monomer solutions overnight and self-assembly triggered using Ringer's solution (Section 2.2.6.2.2). Samples were then stored in the dark until sectioning using a cryostat and imaged as described in Section 2.2.11. Three 1 cm² controls sections of decellularised porcine internal carotid artery were put through the same pH and solution changes without any peptide present; this control was used to check for vessel auto-fluorescence.

3.2.9 The effect of self-assembled state on peptide penetration into decellularised vessel

Monomer solutions of peptide P₁₁₋₄ in deionised water at a ratio of 1:30 of fluorescein tagged P₁₁₋₄ to untagged P₁₁₋₄ were made at concentrations of 30 mg.ml⁻¹ (18.8 mol.m⁻³), 15 mg.ml⁻¹

(9.4 mol.m^{-3}), 7.5 mg.ml^{-1} (4.7 mol.m^{-3}), 3.75 mg.ml^{-1} (2.35 mol.m^{-3}) and 1.87 mg.ml^{-1} (1.18 mol.m^{-3}) as described in Section 2.2.6.1. Self-assembly was triggered by the addition of Ringer's solution (Section 2.2.6.2.2). Three 1 cm^2 sections of decellularised vessel were added to the peptide gel/solutions and left overnight. Samples were then stored in the dark until sectioning using a cryostat and imaged as described in Section 2.2.11. Three 1 cm^2 sections of decellularised porcine internal carotid artery as controls were put through the same pH and solution changes without any peptide present; this control was used to check for vessel auto-fluorescence.

3.2.10 Evaluation of peptide stability in decellularised vessel under flow

Decellularised porcine internal carotid artery was cut into sections to fit the flow cell chamber (2 cm by 1.5 cm) and added to a monomeric solution of P_{11-4} in deionised water at a ratio of 1:30 of fluorescein tagged P_{11-4} to untagged P_{11-4} at a concentration of 30 mg.ml^{-1} (18.8 mol.m^{-3}) made as described in Section 2.2.6.1. Peptide self-assembly was triggered by the addition of Ringer's solution as described in Section 2.2.6.2.2. Peptide stability was tested as described in Section 2.2.20 using the flow apparatus. The peristaltic pump was switched on and the flow cell experiment covered and placed in a dark room. Vessel was removed from the flow cell and sectioned using a cryostat after 1, 2, 3, 4, 7 and 14 days. Sections ($7 \mu\text{m}$) were taken from the middle of the sample to discount any effects due to the edges of the flow cell. Decellularised vessel and peptide coated vessel that had not been in the flow cell were used as controls of the vessel with and without self-assembled peptide.

3.3 Results

3.3.1 Histological evaluation of decellularised porcine internal carotid artery

Following staining sections were imaged, recorded and analysed to assess the success of decellularisation. Results of histological analysis of decellularised vessel are presented in Figure 3.2 along with images of control fresh vessel.

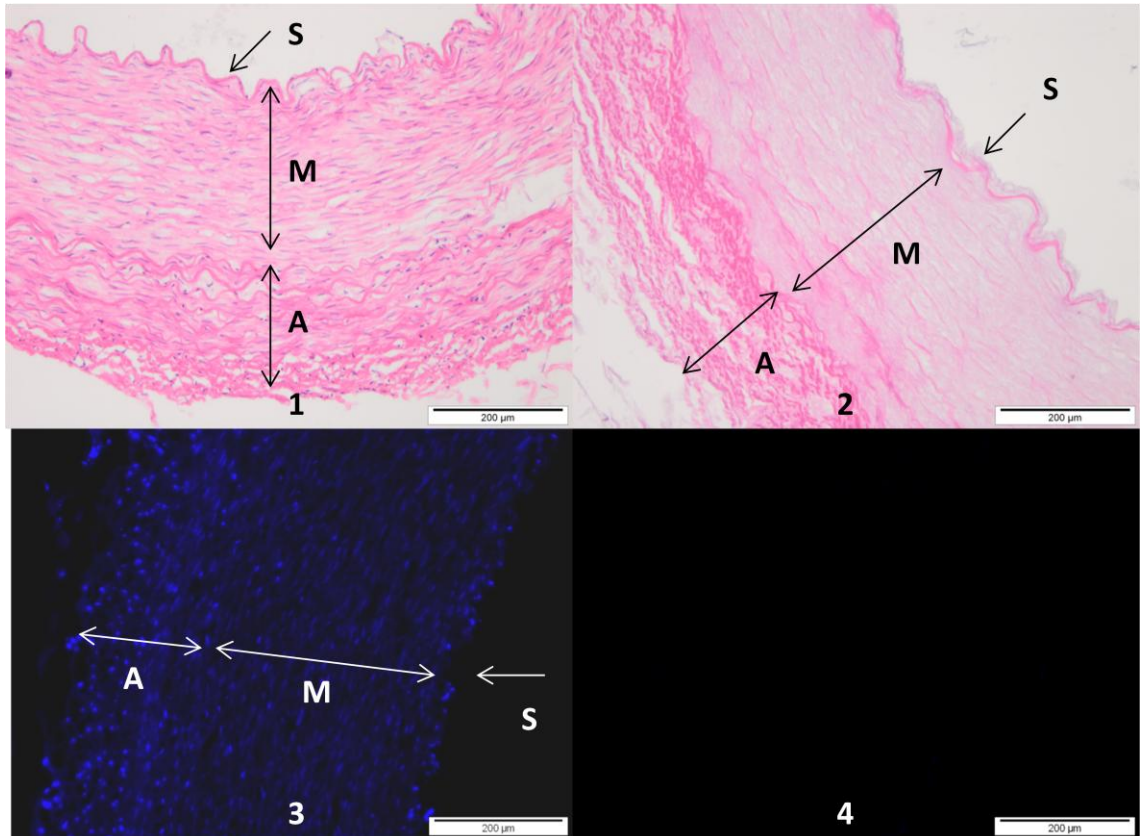


Figure 3.2; Histology images of fresh and decellularised porcine internal carotid artery, Images 1&2 stained using H&E, images 3&4 stained using DAPI; 1&3 Fresh porcine internal carotid artery, 2&4 Decellularised porcine internal carotid artery. S = subendothelial layer, M = medial layer, A = adventitial layer.

Imaging of the sections in Figure 3.2 showed the presence of the characteristic three layered structure of a blood vessel. An endothelial layer should not be present on the decellularised vessel but should be present on the fresh vessel; however, no endothelium could be seen on either the fresh or decellularised vessels. The subendothelial layer could be seen on both the fresh and decellularised sections in Figure 3.2 images 1 and 2. The presence of a densely packed and organised ECM in the medial layer could be seen in the both the fresh and decellularised vessel sections. The adventitia can be distinguished from the medial layer by the presence of less dense and less organised ECM.

Haematoxylin and eosin staining of tissue sections showed the presence of cells throughout the different layers in the fresh vessel. The DAPI staining in Figure 3.2 image 3 showed the presence of DNA in the fresh vessel; the location of the staining suggested that the DNA was located in the cell nuclei. The presence of cells or DNA could not be seen in the sections of the decellularised vessel suggesting that the removal of all cells and visually detectable DNA had

been successful. Haematoxylin and eosin staining showed there had been no visual effect upon the structure of the ECM within the subendothelial, medial and adventitial layers following successful decellularisation. Having been decellularised the different layers of the vessel could still be easily distinguished with no obvious defects present in the ECM. These results showed that decellularisation appeared to have been successful with no detrimental effects.

3.3.2 Evaluation of peptide self-assembly triggers

Observations of peptide self-assembly at a range of concentrations at different solution pH and in different biological salt solutions were made and images recorded (Appendix Figure A.1 and Figure A.2). Results and observations are summarised and presented in Table 3-1.

Solution Condition	30 mg.ml ⁻¹ 18.8 mol.m ⁻³	15 mg.ml ⁻¹ 9.4 mol.m ⁻³	5 mg.ml ⁻¹ 3.13 mol.m ⁻³	1 mg.ml ⁻¹ 0.63 mol.m ⁻³
pH 8	Clear fluid	Clear fluid	Clear fluid	Clear fluid
pH 7	Self-assembled gel	Self-assembled gel	Cloudy fluid	Clear fluid
pH 5	Self-assembled gel	Self-assembled gel	Part assembled gel/Cloudy fluid	Cloudy fluid
PBS	Self-assembled gel	Cloudy fluid	Clear fluid	Clear fluid
Ringer's solution	Self-assembled gel	Self-assembled gel	Part assembled gel/Cloudy fluid	Clear fluid

Table 3-1; Observed results for self-assembly method for different concentrations of P₁₁₋₄

The results showed that in deionised water at pH 8 peptide P₁₁₋₄ was a monomer or soluble aggregate at all concentrations tested. At pH 7 in deionised water P₁₁₋₄ formed a stable self-supporting gel at concentrations of 30 mg.ml⁻¹ (18.8 mol.m⁻³) and 15 mg.ml⁻¹ (9.4 mol.m⁻³). Peptide P₁₁₋₄ at a concentration of 5 mg.ml⁻¹ (3.13 mol.m⁻³) in deionised water at pH 7 started to form visible aggregates but failed to form a self-assembled gel and at a concentration of 1 mg.ml⁻¹ (0.63 mol.m⁻³) P₁₁₋₄ appeared to be a monomer or soluble aggregate in solution. Peptide P₁₁₋₄ at a concentration of 30 mg.ml⁻¹ (18.8 mol.m⁻³) and 15 mg.ml⁻¹ (9.4 mol.m⁻³) in

deionised water at pH 5 formed a stable self-supporting peptide gel; at a concentration of 5 mg.ml⁻¹ (3.13 mol.m⁻³) P₁₁₋₄ formed a viscous flowing peptide gel that was not self-supporting. At a concentration of 1 mg.ml⁻¹ (0.63 mol.m⁻³) at pH 5 P₁₁₋₄ started to form visible aggregates in solution but failed to form a peptide gel.

At physiological pH peptide P₁₁₋₄ made in phosphate buffered saline (PBS) formed a self-supporting gel at 30 mg.ml⁻¹ (18.8 mol.m⁻³). At 15 mg.ml⁻¹ (9.4 mol.m⁻³) P₁₁₋₄ started to form visible aggregates in PBS but did not form a gel. P₁₁₋₄ in PBS at 5 mg.ml⁻¹ (3.13 mol.m⁻³) and 1 mg.ml⁻¹ (0.63 mol.m⁻³) remained as monomers or soluble aggregates in solution. Peptide P₁₁₋₄ at physiological pH made in Ringer's solution formed self-assembled gels at 30 mg.ml⁻¹ (18.8 mol.m⁻³) and 15 mg.ml⁻¹ (9.4 mol.m⁻³). P₁₁₋₄ in Ringer's solution at 5 mg.ml⁻¹ (3.13 mol.m⁻³) formed a self-assembled viscous fluid/gel which was not self-supporting and remained as monomers or soluble aggregates in solution at 1 mg.ml⁻¹ (0.63 mol.m⁻³)

These results showed that at high pH P₁₁₋₄ was a monomer or soluble aggregate in solution at all tested concentrations. At low pH peptide P₁₁₋₄ started to self-assemble in a concentration dependent manner and formed a self-supporting peptide gel above a concentration of 15 mg.ml⁻¹ (9.4 mol.m⁻³) just below physiological pH. The results showed that ionic concentration could be used to trigger self-assembly of model peptide P₁₁₋₄; the addition of PBS triggered the formation of self-supporting gels at 30 mg.ml⁻¹ (18.8 mol.m⁻³) and the addition of Ringer's solution triggered the formation of self-supporting gels at 30 mg.ml⁻¹ (18.8 mol.m⁻³) and 15 mg.ml⁻¹ (9.4 mol.m⁻³).

From the results it was decided a standard concentration of 30 mg.ml⁻¹ (18.8 mol.m⁻³) of peptide would be used in further studies unless otherwise stated. At this concentration the peptide has been shown to form a stable self-supporting gel when self-assembly is triggered, above this concentration the peptide will self-assemble above neutral pH due to the concentration dependence of peptide self-assembly and be difficult to make a monomer solution (Aggeli et al., 2001, Carrick et al., 2007). As low pH is known to adversely affect the components of the ECM it was decided self-assembly would be triggered in further studies by the addition of Ringer's solution. It was decided that pH would be used as a trigger in the sample preparation for FTIR and FEGSEM analysis where excess salt had greater potential to interfere with the observed results.

3.3.3 Cross sectioning and imaging of fluorescent peptide penetration into decellularised vessel

Following sectioning images were collected and analysed. For all peptide coated sections there was a distinct difference compared to the control decellularised vessel. Results are presented as representative images in Figure 3.3 at different magnifications.

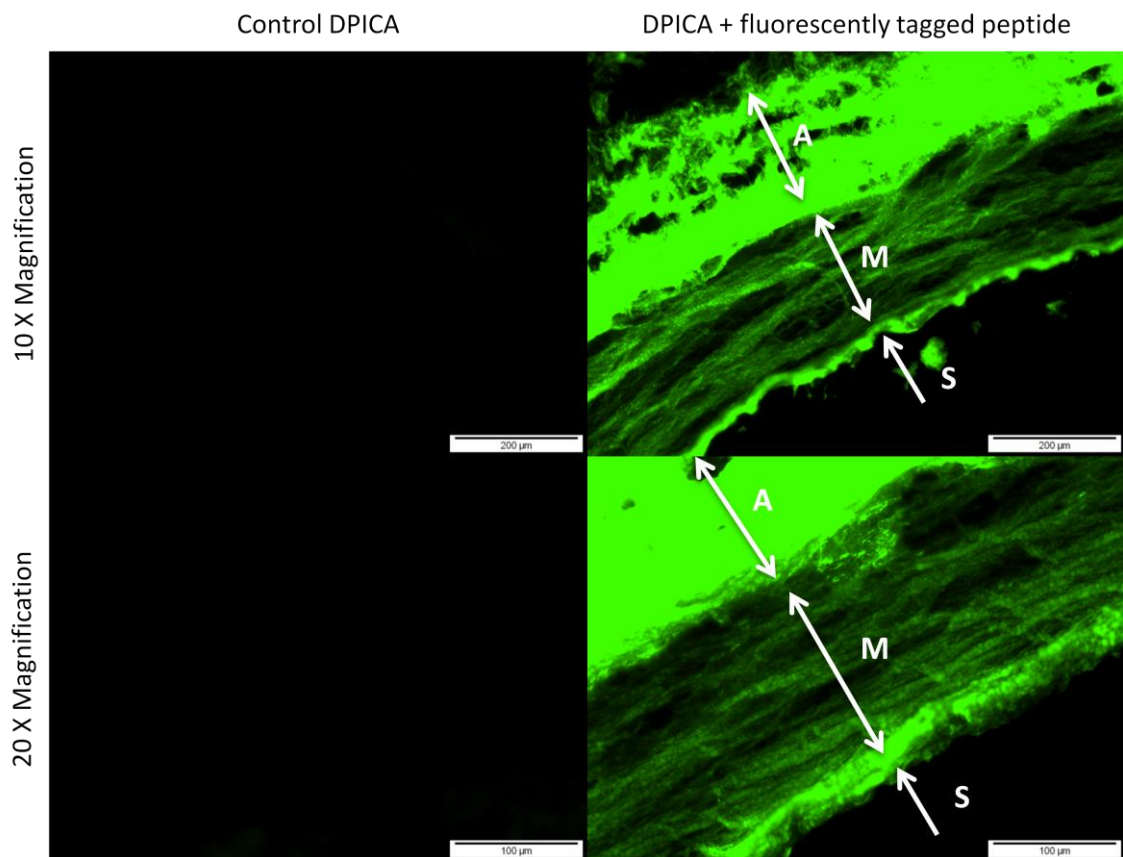


Figure 3.3; Cross section image of fluorescently tagged peptide P₁₁₋₄ (ratio 1:30 fluorescein tagged P₁₁₋₄ to untagged P₁₁₋₄) in decellularised porcine internal carotid artery with control decellularised porcine internal carotid artery at 10X and 20X magnification. S = subendothelial layer, M = medial layer, A = adventitial layer.

Having been left overnight, following the addition of the monomer solution of peptide, the deionised water around the outside of the vessel had changed colour taking on a yellow tint. The fluorescently tagged peptide solution was optically yellow in appearance suggesting that some of the peptide from the inside of the vessel had penetrated through the vessel and out into solution. The images in Figure 3.3 showed that the decellularised porcine internal carotid

artery was not auto-fluorescent in the same range as the fluorescein tagged P₁₁-4. The images of the cross-sections through peptide coated vessels showed that in a monomeric state the peptide had fully penetrated through the subendothelial, medial and adventitial layers of the vessel and self-assembled. A greater fluorescence was observed at the luminal surface and in the adventitia. The peptide on the medial layer appeared to show the fibrous structure of the ECM.

3.3.4 FTIR spectroscopy and analysis of peptide in decellularised vessel

Following the collection of spectra from different areas of the samples the spectra were combined into a single average spectrum and graphed. Results are presented in Figure 3.4 as absorbance against wavelength with selected peaks highlighted and labelled.

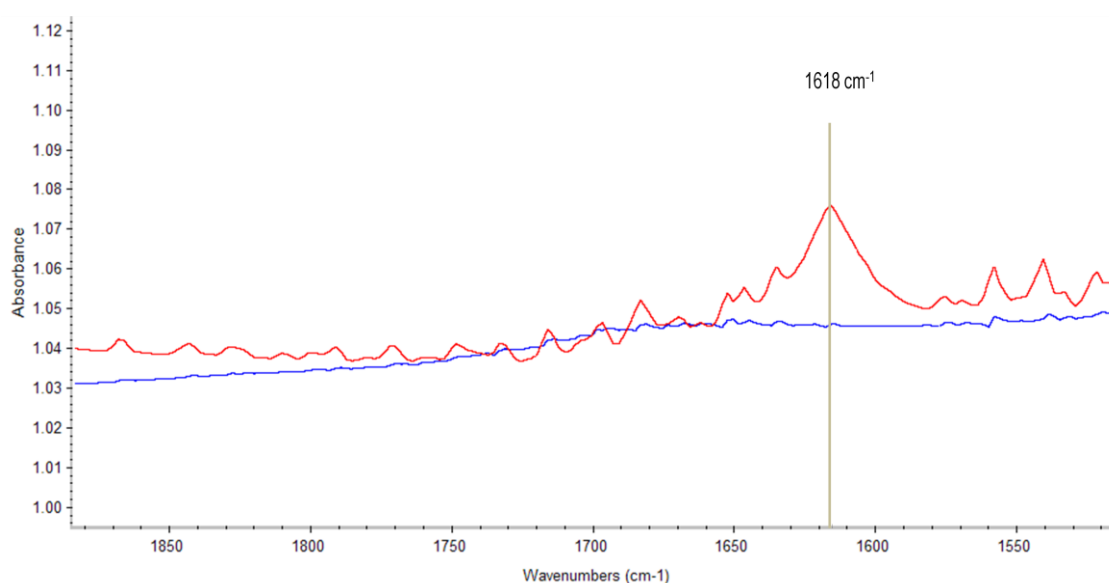


Figure 3.4; FTIR spectrum in the amide I and II region ($1500 - 1900 \text{ cm}^{-1}$) showing difference between two averaged spectra; Blue) combined spectra of decellularised porcine internal carotid artery, Red) combined spectra of decellularised porcine internal carotid artery and 30 mg.ml^{-1} (18.8 mol.m^{-3}) of P₁₁-4.

The average FTIR spectrum for decellularised porcine internal carotid artery is compared to the average FTIR spectrum for decellularised porcine internal carotid artery with 30 mg.ml^{-1} (18.8 mol.m^{-3}) self-assembled P₁₁-4 in the region of amide I ($1600 - 1700 \text{ cm}^{-1}$) and amide II ($1500 -$

1600 cm^{-1}). As shown in Figure 3.4 a difference can be seen between the two spectra with a peak for the peptide coated vessel at 1618 cm^{-1} . This corresponded to the region where β -sheet hydrogen bonds are known to absorb between 1615 and 1642 cm^{-1} . The majority of β -sheet globular proteins absorb between 1625 and 1643 cm^{-1} in an FTIR spectrum, a lower value between 1615 and 1625 cm^{-1} is believed to represent anti-parallel β -strand pairing/self-assembly as they have shorter hydrogen bonds than typically found in β -sheet globular proteins (Seshadri 1999).

The FTIR spectrum shown in Figure 3.4 provided evidence that the peptide was present in the decellularised vessel and was forming an anti-parallel β -sheet structure that is known to be formed by P₁₁-4 when self-assembled. This demonstrated that the peptide was not only in the vessel but was also self-assembling in the vessel and not just forming a coating on the vessel ECM.

3.3.5 FEGSEM imaging of peptide on the surface of decellularised vessel

Following drying and coating in platinum and palladium (50:50) the uncoated and P₁₁-4 coated samples of decellularised vessel were imaged and the secondary electron images recorded and analysed. Results are presented as representative images in Figure 3.5 at the same magnification.

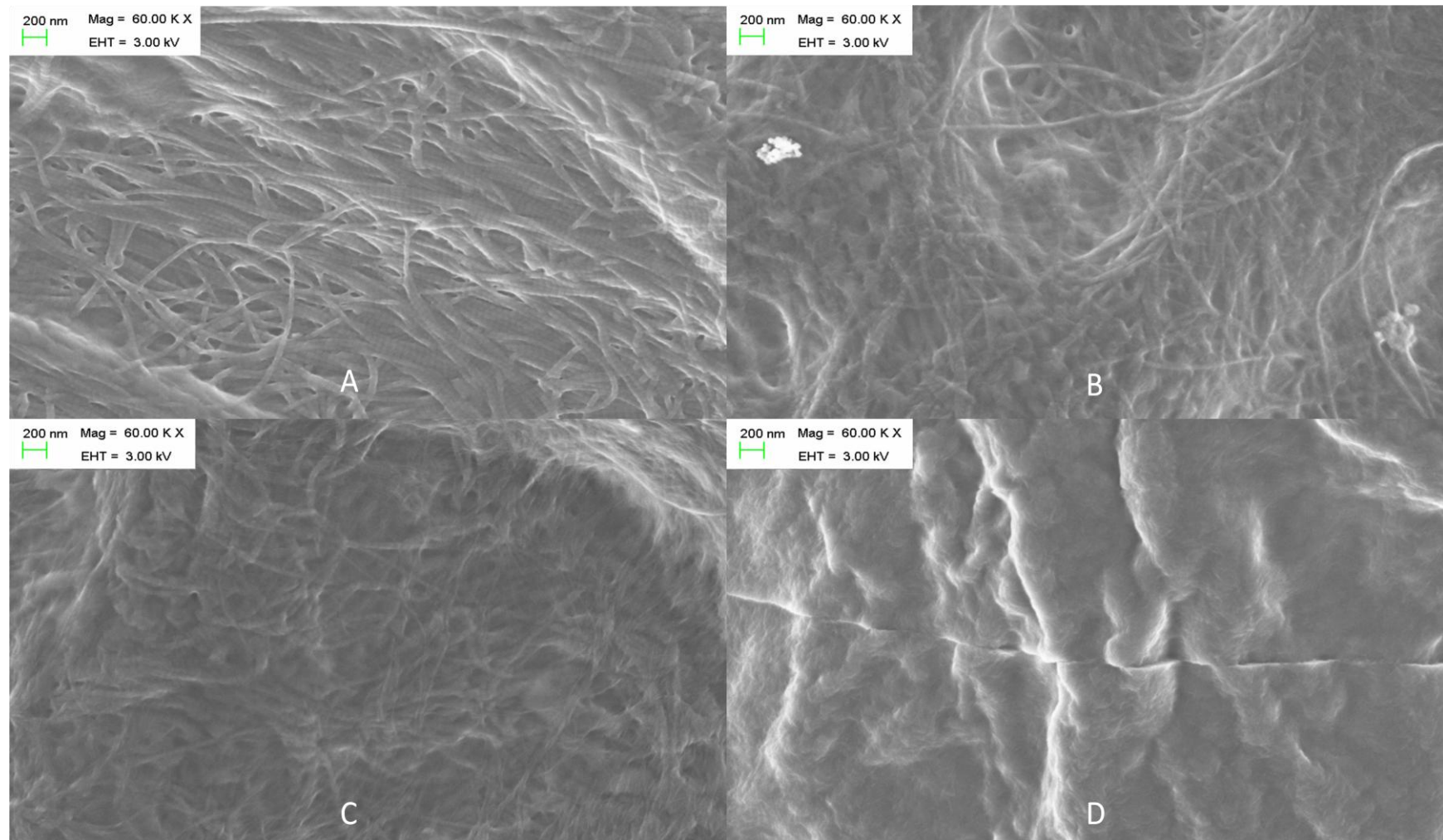


Figure 3.5; FEGSEM images of decellularised porcine internal carotid artery with self-assembled P₁₁₋₄; A) No peptide, B) 1 mg.ml⁻¹ (0.63 mol.m⁻³), C) 5 mg.ml⁻¹ (3.13 mol.m⁻³), D) 10 mg.ml⁻¹ (6.26 mol.m⁻³), images taken at 3 KeV at 60,000X magnification.

Fixed decellularised porcine internal carotid artery without peptide, showed the structure of the ECM in the decellularised vessel (Figure 3.5 image A). The collagen fibre bundles could be identified by the characteristic banding structure seen in the image. The fibrous nature of the ECM could be seen. Fixed decellularised porcine internal carotid artery with 1 mg.ml^{-1} (0.63 mol.m^{-3}) of self-assembled peptide P₁₁₋₄ showed the collagen fibre bundles but the characteristic collagen banding was no longer present (Figure 3.5 image B). Fixed decellularised porcine internal carotid artery with 5 mg.ml^{-1} (3.13 mol.m^{-3}) of self-assembled peptide P₁₁₋₄ showed fewer collagen fibre bundles on the surface of the vessel (Figure 3.5 image C). Fixed decellularised porcine internal carotid artery with 10 mg.ml^{-1} (6.26 mol.m^{-3}) of self-assembled peptide P₁₁₋₄ showed a relatively thick surface coating (Figure 3.5 image D).

The different surface coatings that were present on the surface of the vessel formed by the different concentrations of peptide P₁₁₋₄ were clearly evident in Figure 3.5. The fibre arrangements present in images A to C were not present in image D. The loss of fibre characteristics and definition appeared to be related to peptide concentration; as peptide concentration increased a thicker layer of peptide was observed on the surface of the decellularised vessel until only the peptide surface coating was seen and none of the fibre arrangements underneath.

3.3.6 CLSM imaging of peptide in decellularised vessel

Following peptide self-assembly samples of acellular vessel were removed from the excess peptide gel and imaged in the confocal laser microscope. The peptides coated sections were distinctly different compared to the control decellularised vessel and control peptide gel. Results are presented as representative images in Figure 3.6.

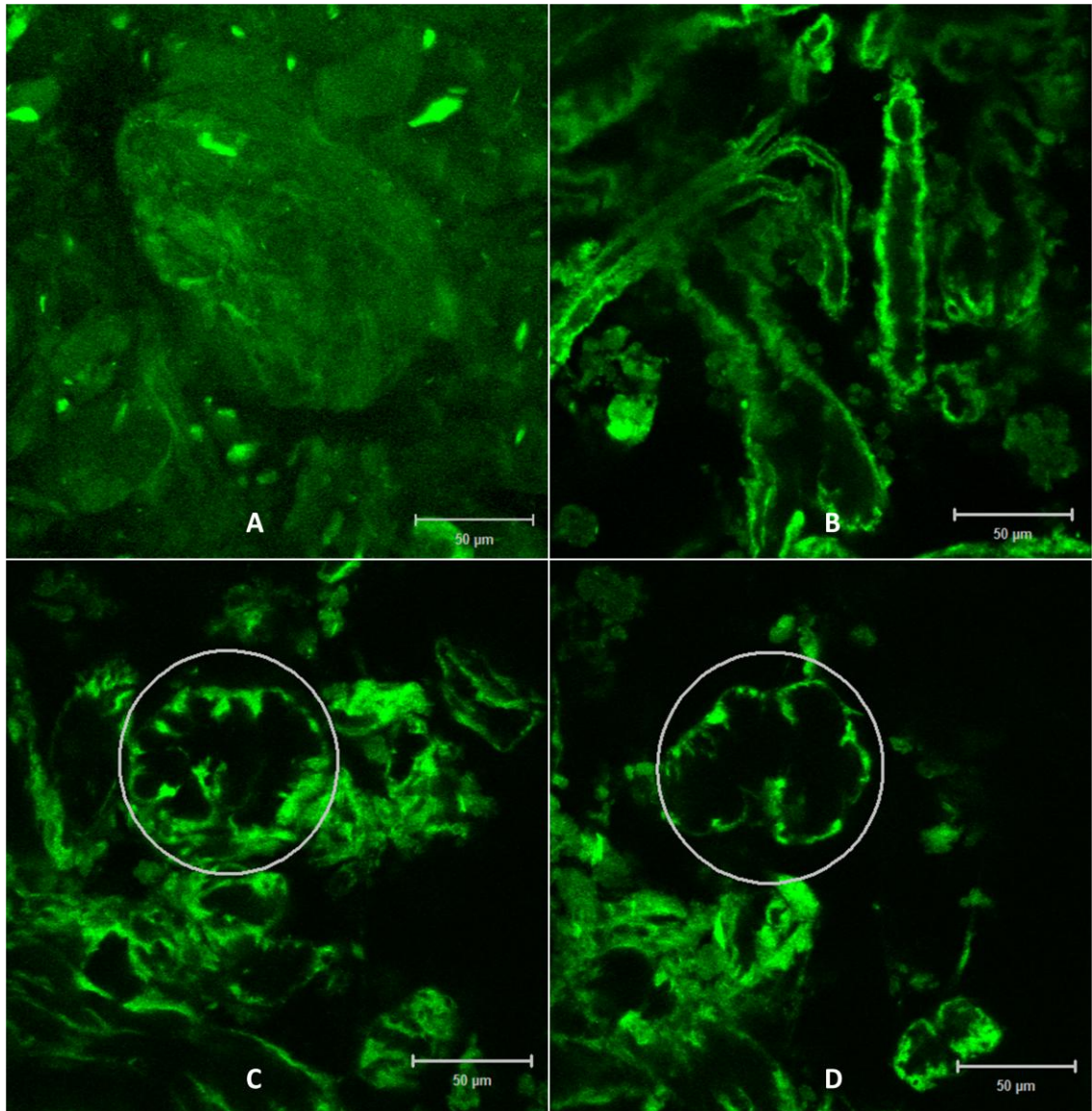


Figure 3.6; CLSM images of (A) Peptide gel, 10 mg.ml^{-1} (6.3 mol.m^{-3}) of fluorescently tagged P_{11-4} mixed with P_{11-4} at a ratio of 1:50, (B) Decellularised porcine internal carotid artery with 10 mg.ml^{-1} (6.3 mol.m^{-3}) of fluorescently tagged P_{11-4} mixed 1:50 with P_{11-4} , peptide gel, (C & D) Z-axis stack of decellularised porcine carotid artery with 10 mg.ml^{-1} (6.3 mol.m^{-3}) of fluorescently tagged P_{11-4} mixed 1:50 with P_{11-4} , peptide gel; highlighted region shows peptide coating of a horizontal structure taken at different depths (z-axis). Magnification 40X

As shown in Figure 3.6 image A, fluorescently tagged peptide control, the fluorescently tagged peptide gel formed a randomly ordered gel that had little visible structure. As shown in image B the fluorescently tagged peptide appeared to have self-assembled around the outer surface of the ECM coating the bundles of fibres. As shown in the images C and D the fluorescently tagged peptide appeared to have coated the ECM, the highlighted region of the image show a Z-axis stack through a horizontal bundle of fibres, it was apparent that the peptide had acted

to fill the gaps in between the fibres in the bundle and appeared to have then formed a coating of similar thickness over the whole surface of the bundle. This coating whilst not smooth appeared to be nearly uniform over the surface, it was not possible determine whether the coating covered all the fibre bundles or not as the presence of the bundles was only inferred by the outline created by the peptide coating.

3.3.7 MPLSM imaging of peptide in decellularised vessel

Following peptide self-assembly samples of decellularised vessel were removed from the excess peptide gel and imaged in the multi-photon laser microscope. The peptides coated sections were distinctly different compared to the control decellularised vessel. Results are presented as representative images in Figure 3.7 and Figure 3.8.

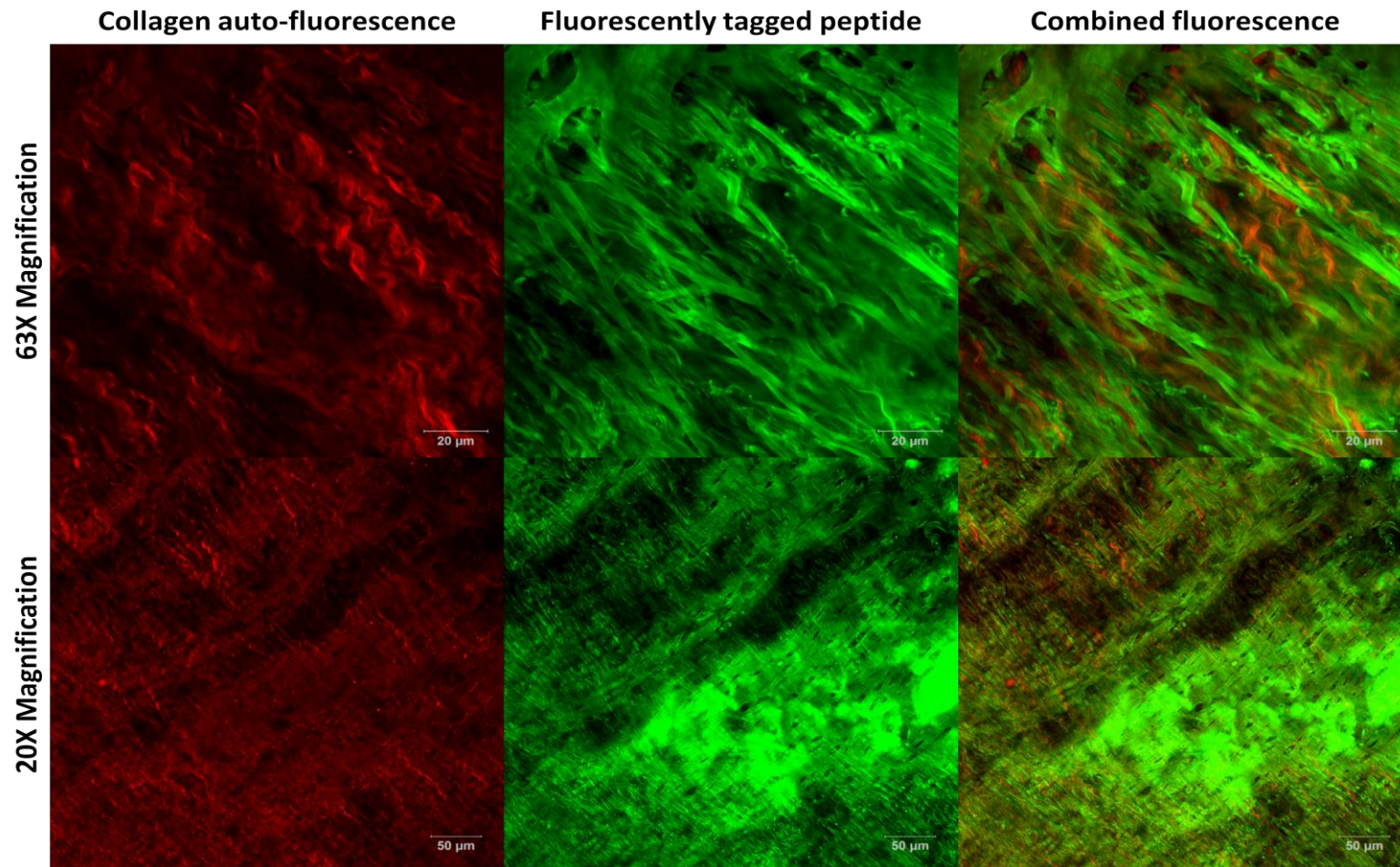


Figure 3.7; Multi-photon images of decellularised porcine internal carotid artery coated in 30 mg.ml^{-1} (18.8 mol.m^{-3}) of fluorescently tagged P_{11-4} peptide at a ratio of 1:50 with untagged P_{11-4} . Images show the same area with the two fluorescent signals separated and combined. Top images are at 63X magnification bottom images are at 20X magnification.

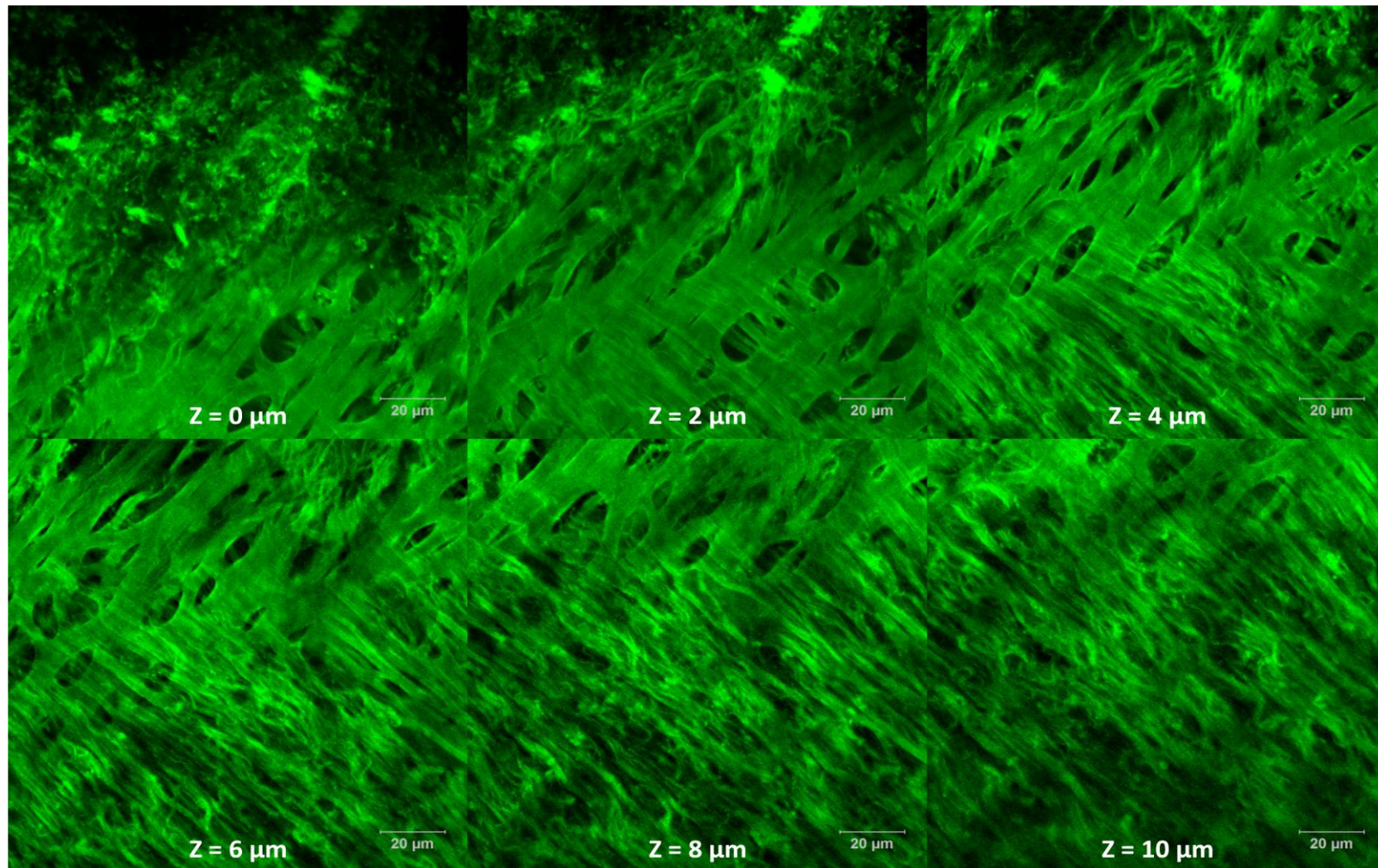


Figure 3.8; Z-axis stack of multi-photon images of decellularised porcine internal carotid artery coated in 30 mg.ml^{-1} (18.8 mol.m^{-3}) of fluorescently tagged P_{11-4} peptide at a ratio of 1:50 with untagged P_{11-4} . Images show fluorescein fluorescence at $2 \mu\text{m}$ intervals in the same x,y, location. Images taken at 63X magnification.

The secondary harmonic auto-fluorescence from collagen, the fluorescence from the fluorescein labelled P₁₁-4 peptide and the two images combined are seen in Figure 3.7. The 20X magnification image shows a scan near the surface of the sample that covered a large area. The collagen auto-fluorescence showed the characteristic coiled structure associated with collagen and showed the fibre bundles were aligned in the same direction as seen in a blood vessel. The image of the fluorescein tagged P₁₁-4 showed that the collagen fibre bundles appeared to have been coated in self-assembled peptide. The peptide also appeared to have coated other extracellular structures in the vessel. A mesh like layer, likely the elastic lamina, was seen on top of the collagen fibre bundles. An area of high intensity fluorescence that lacked any clear structure was seen on the surface of the vessel, this was most likely excess peptide gel on the surface of the vessel. The combined image showed that the majority of the collagen auto-fluorescence was covered by the fluorescein fluorescence; however, the collagen auto-fluorescence showed through in some areas. The high (63X) magnification images from within the vessel showed that the peptide did not form a space filling gel in the ECM but rather self-assembled around the ECM structures. The image of the fluorescein tagged P₁₁-4 showed the clear coating of the ECM structures with self-assembled peptide and provided better evidence that not only the collagen but other extracellular components were coated with self-assembled peptide as an ECM structure could be seen coated in peptide but showed no collagen auto-fluorescence. The comparison of the two images showed that not all of the collagen fibre bundles were coated in self-assembled peptide.

A Z-axis stack through the vessel is shown in Figure 3.8. The z-axis stack showed the presence of an extracellular net-like structure on the surface of the vessel, most likely the elastic lamina. As the z-axis went deeper into the vessel the presence of orientated fibre bundles could be seen below the net-like structure.

3.3.8 Effect of concentration on peptide distribution throughout decellularised vessel

Following peptide self-assembly samples of acellular vessel were sectioned and imaged. The images were recorded and analysed. The peptides coated sections were distinctly different compared to the control decellularised vessel. Results are presented as representative images in Figure 3.9.

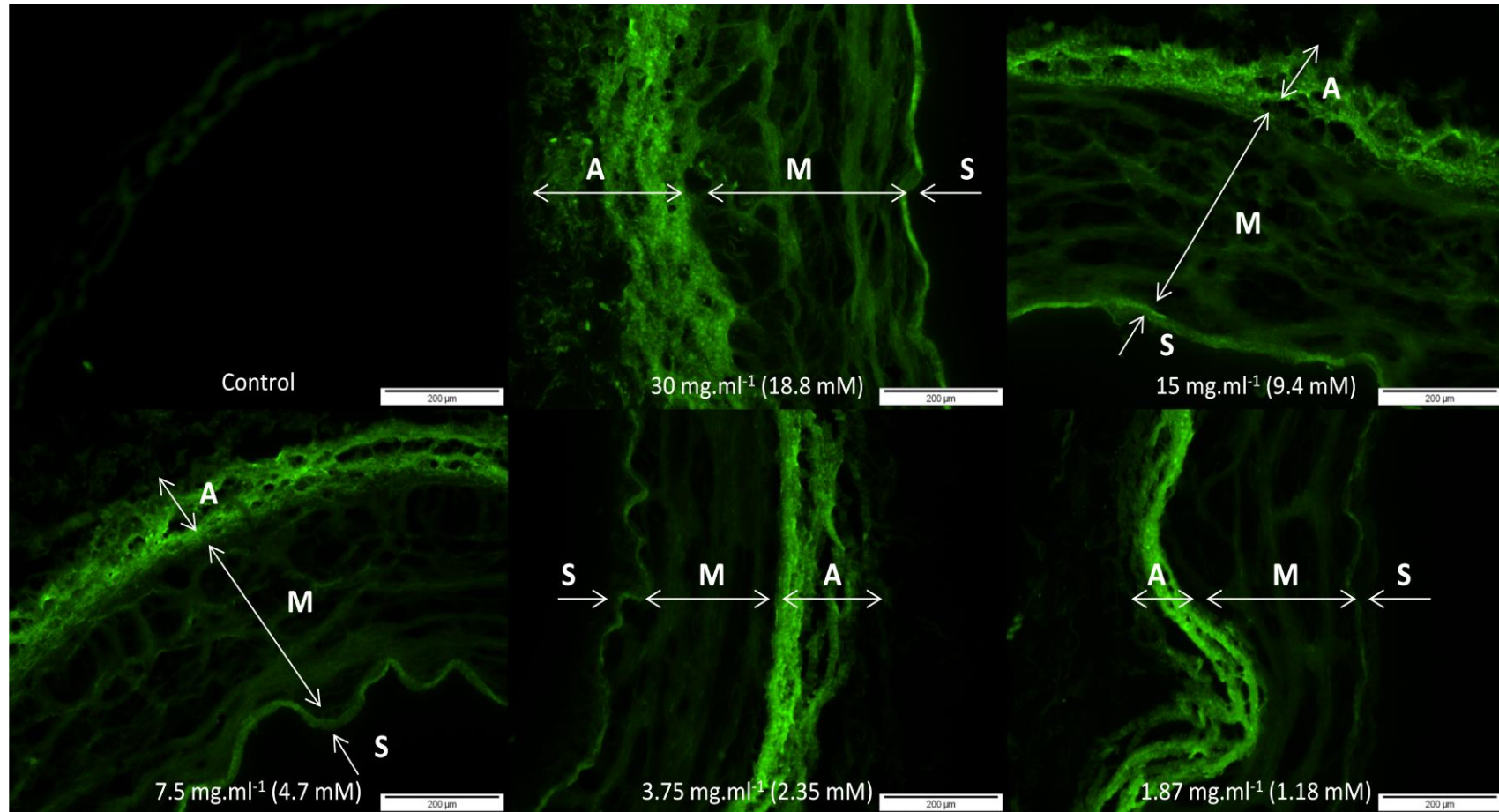


Figure 3.9; Images showing effects of concentration on peptide self-assembly in decellularised porcine internal carotid artery. Fluorescent cross section images of decellularised porcine internal carotid artery and decellularised porcine internal carotid artery coated in 30 mg.ml⁻¹ (18.8 mol.m⁻³), 15 mg.ml⁻¹ (9.4 mol.m⁻³), 7.5 mg.ml⁻¹ (4.7 mol.m⁻³), 3.75 mg.ml⁻¹ (2.35 mol.m⁻³) and 1.87 mg.ml⁻¹ (1.18 mol.m⁻³) of fluorescently tagged P₁₁-4 peptide at a ratio of 1:50 with untagged P₁₁-4. 10X magnification.

S = subendothelial layer, M = medial layer, A = adventitial layer.

The control image in Figure 3.9 showed that the vessel had little to no auto-fluorescence at the wavelengths associated with fluorescein. At all concentrations high fluorescence intensity was observed in the adventitial layer of the vessel. A high level of fluorescence was also observed on the subendothelium at peptide concentrations between 30 mg.ml^{-1} (18.8 mol.m^{-3}) and 3.75 mg.ml^{-1} (2.35 mol.m^{-3}). At a concentration of 30 mg.ml^{-1} (18.8 mol.m^{-3}) P₁₁₋₄ had penetrated throughout the vessel and had coated the ECM of the media layer with the structure of the coated ECM visible in the fluorescent image. At a concentration of 15 mg.ml^{-1} (9.4 mol.m^{-3}) and 7.5 mg.ml^{-1} (4.7 mol.m^{-3}) peptide P₁₁₋₄ was seen coating the ECM of the media layer. As the concentration was decreased the fluorescent intensity decreased and less of the vessel structure could be seen. At a concentration of 3.75 mg.ml^{-1} (2.35 mol.m^{-3}) P₁₁₋₄ was seen on the outside, subendothelium and adventitia layer, of the vessel but not clearly on the inside of the vessel. Peptide P₁₁₋₄ at a concentration of 1.87 mg.ml^{-1} (1.18 mol.m^{-3}) was seen in the adventitia but not through the rest of the vessel.

3.3.9 Effect of self-assembled state on peptide penetration into decellularised vessel

The state of the peptide when the decellularised porcine internal carotid artery was introduced could significantly affect the observed results. The decellularised vessel is porous in nature. The penetration of the peptide into the vessel will be dependent upon the size and stability of the hierarchy of structures formed when self-assembly is triggered. The stability and size of the hierarchy of structures will predominantly be controlled by the concentration of peptide present (Aggeli et al., 2001). The energetics of the system will also have an effect such that pH and ionic concentration will also affect which structures are formed and their stability (Aggeli et al., 2003b, Carrick et al., 2007). The self-assembly of peptide P₁₁₋₄ is a concentration dependent reaction. The effect of different concentrations of self-assembled peptide P₁₁₋₄ within decellularised porcine internal carotid artery was explored by adding sections of decellularised vessel to self-assembled peptide P₁₁₋₄. Images were taken, recorded and analysed. The peptide coated sections were distinctly different compared to the control decellularised vessel. Results are presented as representative images in Figure 3.10.

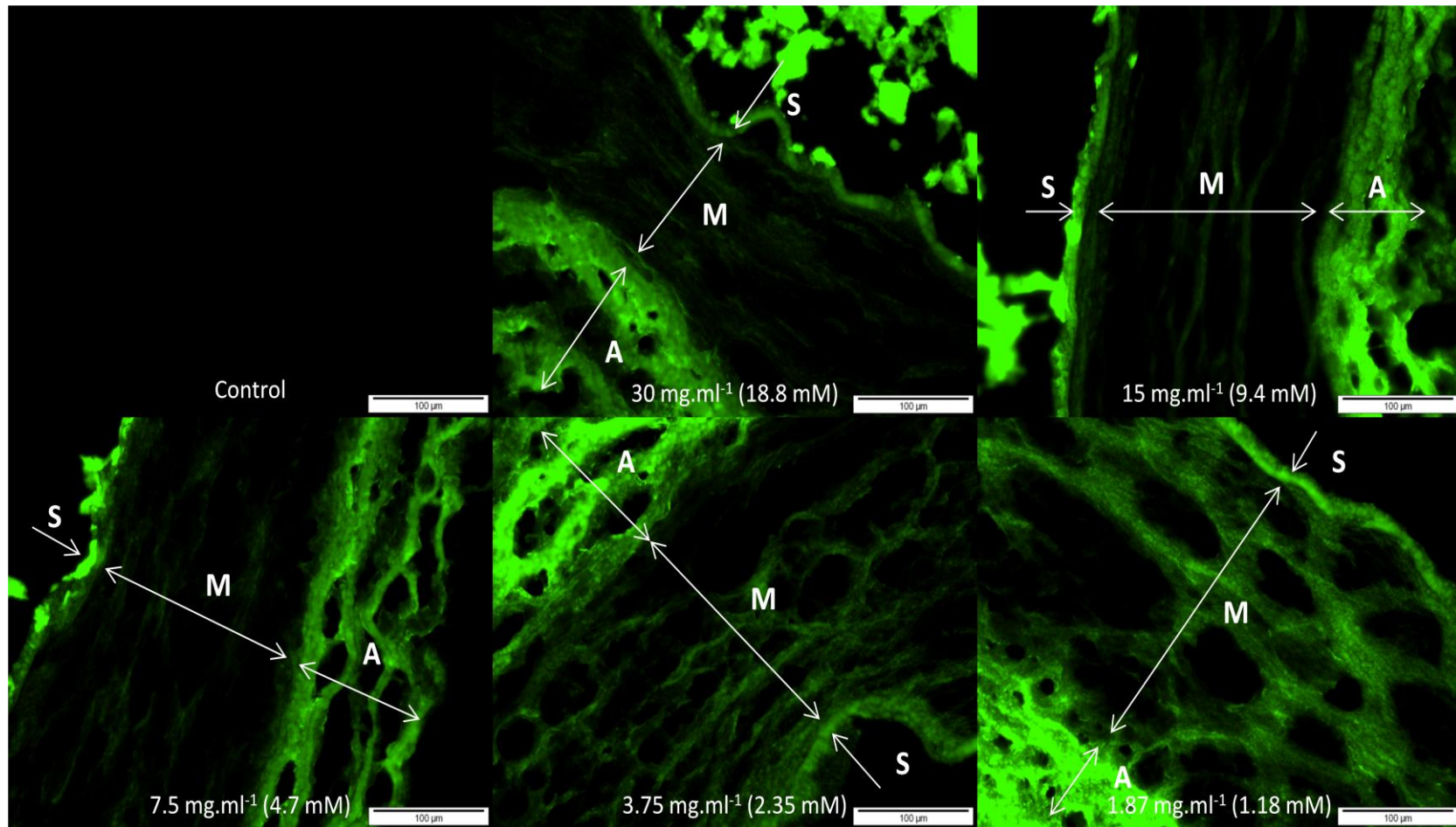


Figure 3.10; Effect of self-assembled state on peptide penetration into decellularised porcine internal carotid artery. Fluorescent cross section images of decellularised porcine internal carotid artery and decellularised porcine internal carotid artery coated in 30 mg.ml^{-1} (18.8 mol.m^{-3}), 15 mg.ml^{-1} (9.4 mol.m^{-3}), 7.5 mg.ml^{-1} (4.7 mol.m^{-3}), 3.75 mg.ml^{-1} (2.35 mol.m^{-3}) and 1.87 mg.ml^{-1} (1.18 mol.m^{-3}) of fluorescently tagged P_{11} -4 peptide at a ratio of 1:50 with untagged P_{11} -4. 20X magnification. S = subendothelial layer, M = medial layer, A = adventitial layer.

The control image in Figure 3.10 showed that the vessel had little auto-fluorescence at the wavelengths associated with fluorescein. It was known that at 30 mg.ml^{-1} (18.8 mol.m^{-3}) P_{11-4} would form a stable self-supporting gel; as the concentration decreased the stability of the gel decreased as the length of the β -sheet tapes formed decreased. A large amount of peptide was observed on the outside of the vessel in the cross-section of the 30 mg.ml^{-1} (18.8 mol.m^{-3}) sample. A relatively small amount of the peptide appeared to have penetrated into the vessel. As the concentration of the peptide and as accordingly the size of the self-assembled peptide aggregates, decreased more of the vessel structure became clear as more peptide was present in the media layer of the vessel. At 15 mg.ml^{-1} (9.4 mol.m^{-3}) and 7.5 mg.ml^{-1} (4.7 mol.m^{-3}) of P_{11-4} a large amount of peptide was observed on the outside edges of the vessel with significantly less peptide in the media layer. At 3.75 mg.ml^{-1} (2.35 mol.m^{-3}) and 1.87 mg.ml^{-1} (1.18 mol.m^{-3}) of P_{11-4} the peptide appeared to be evenly distributed throughout the vessel.

The results in Figure 3.10 showed that when a stable P_{11-4} peptide gel was formed the peptide was unable to fully penetrate the vessel wall. As the peptide concentration was decreased, the self-assembled structures became less supported and smaller in size meaning the peptide was able to penetrate into the decellularised vessel.

3.3.10 Peptide stability in decellularised vessel under flow

Following removal from the flow cell samples of decellularised vessel were sectioned and imaged. The images were recorded and analysed. The peptides coated sections were distinctly different compared to the control decellularised vessel. Results are presented as representative images in Figure 3.11 and Figure 3.12. The average fluorescent intensity of the collected images are shown as a graph for each magnification in Figure 3.13.

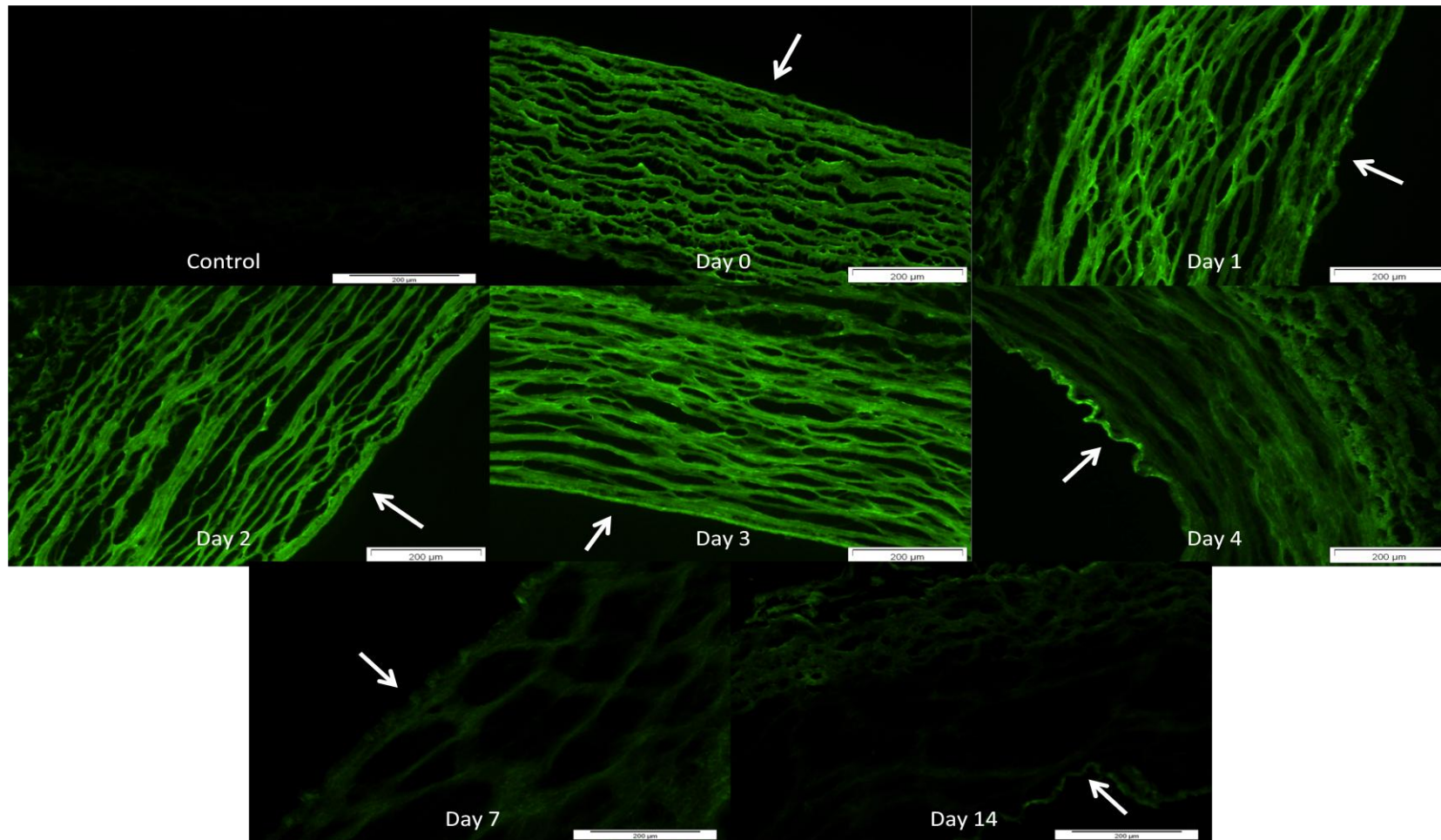


Figure 3.11; Stability of peptide P₁₁₋₄ at 0, 1, 2, 3, 4, 7 and 14 days in a model of fluid flow in a blood vessel showing peptide stability under flow conditions. Fluorescent cross section images of decellularised porcine internal carotid artery and decellularised porcine internal carotid artery coated in $30 \text{ mg}\cdot\text{ml}^{-1}$ ($18.8 \text{ mol}\cdot\text{m}^{-3}$) of fluorescently tagged P₁₁₋₄ peptide at a ratio of 1:50 with untagged P₁₁₋₄. 10X magnification. Arrows indicates subendothelium/lumen surface.

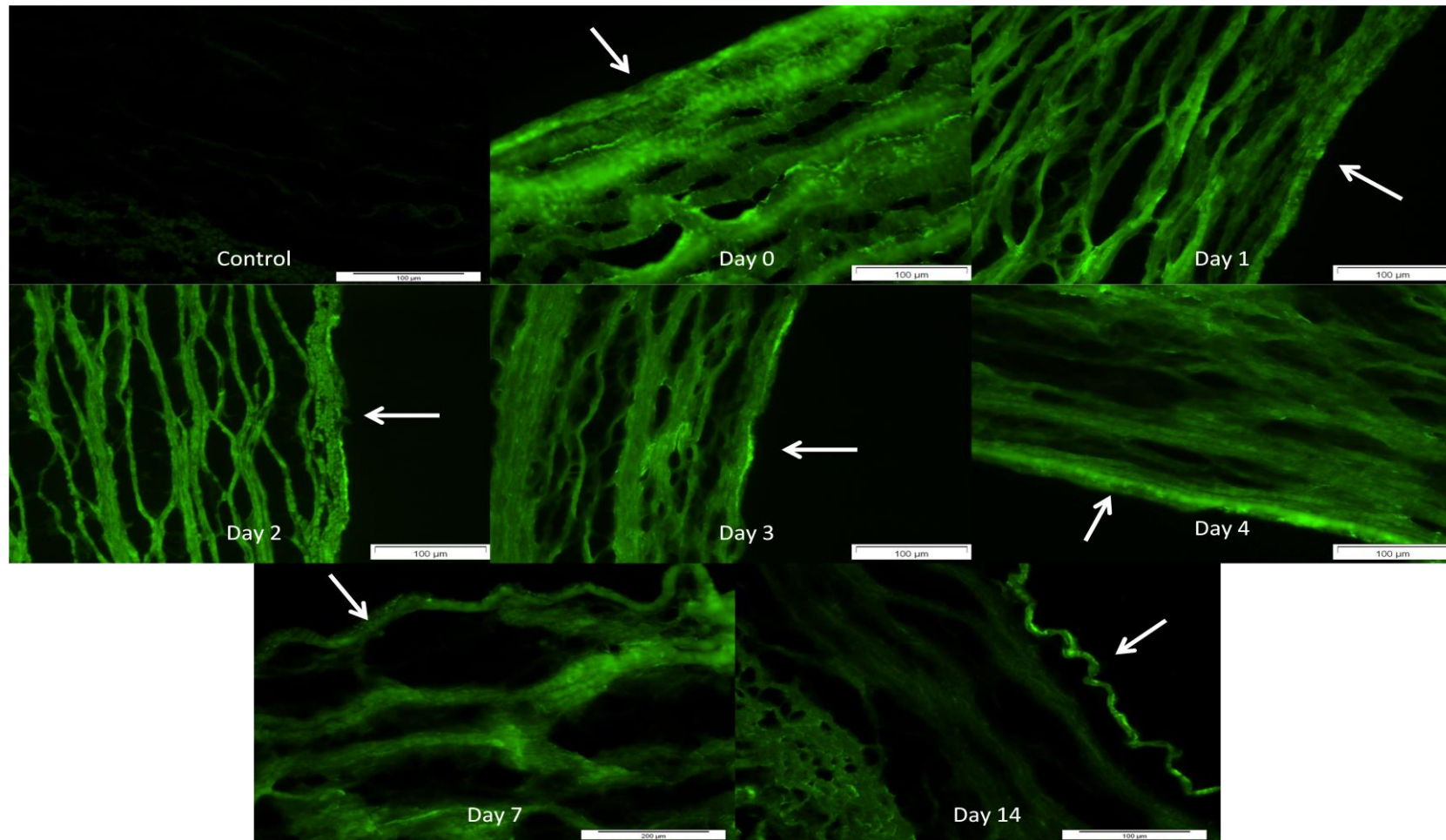


Figure 3.12; Stability of peptide P11-4 at 0, 1, 2, 3, 4, 7 and 14 days in a model of fluid flow in a blood vessel showing peptide stability under flow conditions. Fluorescent cross section images of decellularised porcine internal carotid artery and decellularised porcine internal carotid artery coated in 30 mg.ml^{-1} (18.8 mol.m^{-3}) of fluorescently tagged P₁₁-4 peptide at a ratio of 1:50 with untagged P₁₁-4. 20X magnification. Arrows indicates subendothelium/lumen.

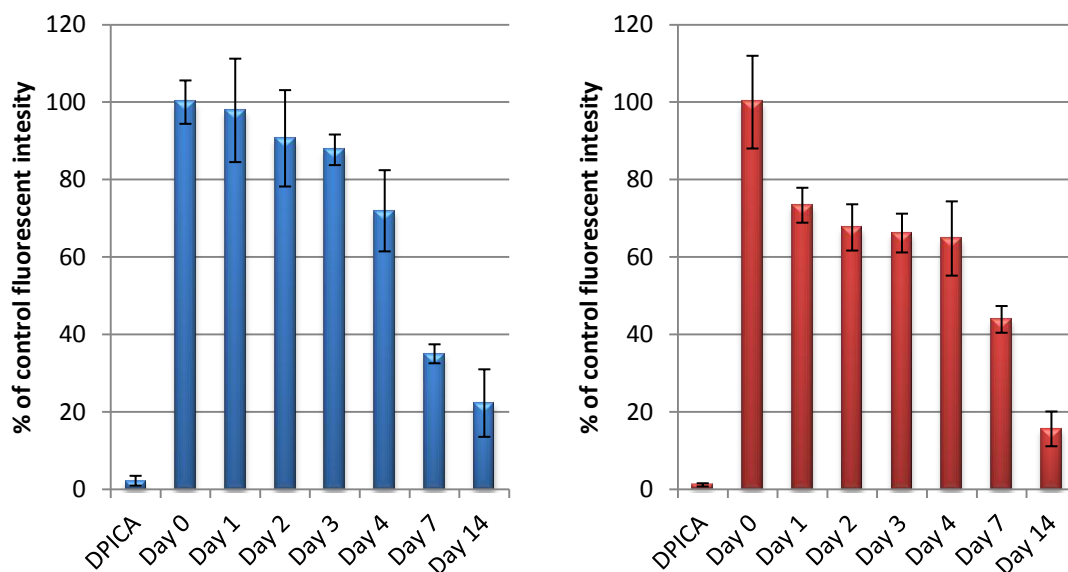


Figure 3.13; Average fluorescent intensity of sectioned decellularised porcine internal carotid artery (DPICA) coated in 30 mg.ml^{-1} P_{11-4} (fluorescently tagged P_{11-4} 1:50 with P_{11-4}) at 0, 1, 2, 3, 4, 7 and 14 days. Data is presented as the mean ($n=6$) \pm 95 % confidence intervals. Blue 10X magnification, Red 20X magnification

The control images of decellularised vessel in Figure 3.11 and Figure 3.12 showed that the vessels had no visual auto-fluorescence. In the images in Figure 3.11 and Figure 3.12 the subendothelial/luminal surface that was in direct contact with the fluid flow is indicated by white arrows. The sections from the vessel are shown at 10X magnification and 20X magnification respectively in Figure 3.11 and Figure 3.12. Comparing the images of peptide present in the vessel before testing (Figure 3.11; Day 0) and after 1 day (Figure 3.11; Day 1) there was a noticeable reduction in peptide present in the vessel yet a large amount of peptide was still present as the peptide coated ECM structures could still be seen. Little difference was seen between the day 1, day 2 and day 3 images (Figure 3.11). After 4 days there was a noticeable reduction in fluorescent intensity, however, the vessel structure could be seen with a clear fluorescence from the medial layer. At day 7 there was a further reduction in fluorescent intensity, however, peptide was clearly still present throughout the vessel. After day 14 there was little fluorescence left in the vessel and the majority of the fluorescence left in the vessel came from deeper in the vessel that was further away from the fluid flow.

The fluorescent cross-sections at day 0 shown in Figure 3.12 indicated that the peptide had formed a thick layer of self-assembled peptide around the ECM components in the vessel. It was observed that after 1 day in flow conditions a large amount of the peptide had been

washed away, however, there was still clearly a coating of peptide present throughout the decellularised vessel. At day 2 the peptide was still present on the surface of the ECM. The fluorescently tagged P₁₁-4 coating at day 2 looked to be less uniform with clear areas of higher intensity fluorescence. At days 3, 4 and 7 the peptide was still present throughout the vessel however the fluorescence intensity decreased over time. At day 14 there was little peptide left within the vessel however a noticeable fluorescence was observed in the adventitial layer and on the luminal surface of the vessel. Comparing the images in Figure 3.11 and Figure 3.12 it was clear that the peptide was being removed by the flow of solution over the luminal surface over time. This loss of peptide appeared to affect the whole vessel and not just the luminal surface.

The average fluorescence intensity averaged from the images of the cross section samples at each time point is presented in Figure 3.13. The graphs showed that there was a steady reduction in the fluorescent intensity over time even when the images shown in Figure 3.11 and Figure 3.12 were indistinguishable from each other. The comparison of the intensity at day 14 with the negative decellularised porcine internal carotid artery control showed that there was still peptide left in the vessel after 14 days but around 80 % of the peptide had been removed.

3.4 Discussion

3.4.1 Histological analysis of decellularised porcine internal carotid artery

The results of the haematoxylin & eosin and DAPI staining showed that all visible cells, cellular debris and DNA had been removed from the arteries. The results showed the decellularisation process developed at the University of Leeds worked on porcine internal carotid artery; this result has also been reported by others on different allogenic and xenogenic arterial matrices (Wilshaw et al., 2011, Owen et al., 2012).

3.4.2 Evaluation of self-assembly triggers

Testing of peptide self-assembly triggers demonstrated that peptide P₁₁₋₄ responded to varying pH; at high pH P₁₁₋₄ was a monomer or soluble aggregate at the concentrations tested. At low pH peptide P₁₁₋₄ self-assembled in a concentration dependent manner and formed a self-supporting peptide gel above a concentration of 15 mg.ml⁻¹ (9.4 mol.m⁻³) just below physiological pH.

The results showed that ionic concentration could be used to trigger self-assembly. The addition of PBS triggered self-assembly and the formation of a self supporting gel at 30 mg.ml⁻¹ (18.8 mol.m⁻³). The addition of Ringer's solution triggered self-assembly and formed a self supporting gel at 30 mg.ml⁻¹ (18.8 mol.m⁻³) and 15 mg.ml⁻¹ (9.4 mol.m⁻³). The self-assembly of peptide P₁₁₋₄ in solutions of varying pH and ionic concentrations corresponded to previously observed results (Aggeli et al., 2003b, Carrick et al., 2007).

An unusual effect was observed when comparing the use of PBS and Ringer's solution to trigger self-assembly. Ringer's solution and PBS both had similar concentrations of salts but had different compositions. Ringer's solution contained slightly higher levels of sodium chloride and contained calcium; PBS contained phosphate salts. The difference between Ringer's solution and PBS lead to a difference in the efficiency of the ionic trigger. It is possible that the slightly higher level of sodium chloride salt in the Ringer's solution lead to more charge screening and so the formation of a self-supporting gel at a lower concentration. The presence of the calcium in the Ringer's solution could also have increased the charge screening effect. It is possible that the presence of the phosphate in PBS could have interfered with the self-assembly of the peptide. It is also possible that a mixture of these possible effects could have happened and so triggered self-assembly at a lower concentration in Ringer's solution.

The concentration, electronic structure, valence and hydration of counter ions have all been shown to have a significant effect upon self-assembly (Stendahl et al., 2006, Cui et al., 2010). Taking the conditions of the counter ions in both the Ringer's solution and PBS it is likely that the different concentrations and compositions were responsible for the observed difference in self-assembly.

3.4.3 Peptide penetration into decellularised vessel

The fluorescent cross sectioning of the vessel showed that the peptide had fully penetrated throughout the decellularised vessel. The observed colour change in the water surrounding the vessel indicated that the peptide was able to diffuse through the decellularised vessel. The vessel was naturally porous and the peptide, as a monomeric solution, was very small in comparison hence the peptide was free to diffuse through the vessel. The removal of the cells from the artery will have increased the permeability of the conduit as the endothelium that normally limits and controls vascular permeability had been removed (Fukumura et al., 2001). Vessel thickness has to be taken into account when self-assembling peptide into a vessel as the diffusion rate will decrease as the vessel thickens increases.

3.4.4 FTIR analysis of peptide self-assembly

An FTIR spectrum of the decellularised vessel showed no discernible peaks in the amide I ($1600 - 1700 \text{ cm}^{-1}$) and the amide II ($1500 - 1600 \text{ cm}^{-1}$) absorption bands. As these bands are where absorbance peaks associated with the hydrogen bonding, observed in β -sheet self-assembly, are seen it was possible to use FTIR analysis to assess if the peptide within the decellularised vessel was self-assembled (Seshadri et al., 1999). The peak absorbance observed at 1618 cm^{-1} in the decellularised vessel with P₁₁-4 has been identified as the peak associated with anti-parallel β -sheet self-assembly. This peak has been observed and reported in FTIR spectra using the same and similar peptides (Aggeli et al., 2003a, Aggeli et al., 2003b, Carrick et al., 2007, Maude et al., 2011a). This result and previous corresponding results showed that the peptide had self-assembled within the decellularised vessel.

3.4.5 FEGSEM imaging of peptide on decellularised vessel surface

The results of the FEGSEM imaging showed the build up of a surface coating on the decellularised vessel as the peptide concentration was increased. As the only difference between the samples imaged was the concentration of the peptide; it could be assumed that the surface coating was made up of self-assembled peptide. The FEGSEM images did not allow

for verification that the peptide had self-assembled as the peptide could have dried around the ECM. This assumption was based on the excess peptide in solution forming a self-assembled gel and the FTIR results. The build up of peptide was first observed on the FEGSEM images at low peptide concentrations, seen by the loss of the characteristic banding typically attributed to collagen fibres (Ottani et al., 2001).

As the peptide concentration increased a thicker layer of peptide was observed on the surface of the decellularised vessel until only the peptide surface coating could be seen and none of the fibre arrangements underneath. The initial loss of fibre definition and structure likely resulted from the presence of self-assembled peptide around the ECM; as the peptide concentration increased the more peptide was present in the decellularised vessel and so the peptide coating became thicker obscuring more and more of the ECM structure. The thick surface coatings observed at higher concentrations were likely the result of excess peptide gel on the surface of the decellularised vessel that had collapsed down into a thick layer when dried in vacuum.

3.4.6 CLSM and MPLSM imaging of peptide within decellularised vessel

Confocal laser scanning microscopy and multi-photon laser scanning microscopy allowed for the imaging of the peptide within the decellularised vessel in a wet state. The CLSM and MPLSM images showed the ECM had been coated in a layer of peptide. In the CLSM images it could be inferred that the ECM fibre bundles had been coated in a layer of peptide. It was not possible to see the ECM as there was no observable auto-fluorescence, however, structures could clearly be seen in the negative space surrounded by fluorescently tagged peptide. The CLSM images demonstrated that the ECM was coated in an evenly distributed peptide layer. The peptide coating appeared to have filled the gaps between the ECM fibre bundles and formed a coating over the whole surface of the bundles. In the MPLSM images it was possible to see that the collagen fibre bundles and other ECM components had been coated in a layer of self-assembled peptide gel. The auto-fluorescence of the collagen fibres could clearly be seen in the MPLSM images and the corresponding presence of the peptide coating could be seen when the fluorescently tagged peptide was imaged. Combining the two images it is possible to see that not all the collagen was coated in peptide and that other extracellular structures were also present that could not be seen in the auto-fluorescence images.

The peptide self-assembled on the ECM forming a peptide coating and not in solution forming a space filling gel. It is, however, possible that a self-assembled network of peptide fibres formed between the ECM but was too small to be seen in the CLSM and MPLSM images. The self-assembled peptide coatings on the ECM were likely due to the difference in the energetics of the self-assembling system in solution and at a solid-liquid interface. When the peptide and surface could interact and the charge on the peptide and surface was correct self-assembly would have started on the surface as the attraction to the surface became larger than the repulsive force (Wattenbarger et al., 1990).

The surface interface could have acted as a template for nucleation by lowering the energy barrier that needed to be overcome for self-assembly to start. Thus the peptide would preferentially self-assemble at the surface of a material as the energetics of the system are lower than in solution (Taylor and Osapay, 1990, Wattenbarger et al., 1990). This would explain why the majority of the ECM was coated in self-assembled peptide. The filling of gaps between the bundles of fibres seen on the CLSM can also be explained by this as the peptide would have preferentially self-assembled between the two surface interfaces rather than in solution or on just the one surface interface.

The presence of uncoated collagen bundles could be explained by the close packed nature of the ECM where the surrounding bundles of fibres protected some bundles from being coated in peptide. It was also possible that some property of the uncoated ECM was preventing the initial association of the peptide with the surface of those fibres. Different collagen types have been shown to have different physical and chemical structures with differences in properties, functions, structure and composition, for example the distribution of hydrophobic residues in the protein sequence (Bornstein and Sage, 1980). These differences could have caused differences in the interaction of the peptide with the ECM; this could have prevented the self-assembly of the peptide on those ECM fibres.

3.4.7 Effect of concentration on peptide distribution in decellularised vessel

The results demonstrated that the concentration of the peptide in solution affected the coating of the peptide in the decellularised vessel. High concentrations of peptide, 30 mg.ml⁻¹ (18.8 mol.m⁻³), formed a peptide coating throughout the vessel; as the concentration was decreased the peptide was observed in the adventitia and luminal surface layers but

decreasingly in the medial layer. The adventitia and subendothelium being on the outside of the vessel could have come into more contact with the peptide in solution. This could be the result of preferential self-assembly on the different surfaces. The adventitia and luminal surface were more open structures whereas the medial layer had a more compact and organised structure (Bou-Gharios et al., 2004, Zhang et al., 2007). A less dense structure could have been surrounded by more of the peptide allowing for preferential self-assembly around the adventitial and subendothelial layers. It is also possible that the different ECM components of the different layers allowed for preferential peptide self-assembly.

3.4.8 Effect of the self-assembled state of peptide on distribution in the decellularised vessel

The need to add the decellularised vessel to monomeric peptide then trigger self-assembly was ascertained by studying the effect that the self-assembled state had on the diffusion of the peptide throughout the vessel. It was shown that in a self-assembled state the peptide was unable to fully penetrate into the decellularised vessel. As the peptide concentration was decreased it was observed that the peptide was able to start to penetrate into the vessel and a more even distribution of peptide was seen. This was the result of the concentration dependence of the hierarchy of structures formed when the peptide self-assembled (Aggeli et al., 2001). At high concentrations larger longer peptide structures were formed which were unable to penetrate into the decellularised vessel. As the concentration was decreased these structures decreased in size and length allowing the peptide to diffuse into the vessel.

3.4.9 Peptide stability in decellularised vessel under flow

Peptide stability will be of key importance to any potential application. Having self-assembled the peptide within the decellularised vessel the results showed that the peptide was slowly lost from the decellularised vessel over time but that peptide still remained in the vessel after 14 days in a model system. The results showed that peptide was primarily lost from the luminal face of the vessel but peptide was also lost from the whole vessel as well. This suggests that whilst peptide removed by the force of the flow of solution over the surface may account for some of the peptide loss that this is not the whole picture.

The loss of peptide from the whole vessel was likely the result of the way in which the peptide self-assembled. In nucleated self-assembly there is a concentration of peptide that remains monomer in solution; above the critical concentration for self-assembly the same concentration of peptide remains as monomer in solution (Aggeli et al., 2001, Maude et al., 2011a). As the monomer was removed by the flow the self-assembled peptide disassembled to maintain the concentration of monomer in solution and so slowly disassembled throughout the vessel. This means that the time the peptide remained in the vessel was dependent upon the critical concentration of self-assembly and the concentration of the peptide present in the vessel.

As the peptide self-assembled with preference at the surface interface the critical concentration for self-assembly was lower at the interface and therefore the peptide would be lost in a staggered manner. Excess peptide would first be lost from the surface of the vessel where the critical concentration for self-assembly was lower. Once the peptide started to disassemble from around the ECM the only limiting factor would be the diffusion rate of the peptide through the vessel and out into the solution. *In vivo* this effect would undoubtedly become more complex with the involvement of serum proteins.

3.4.10 Summary

Peptide P₁₁-4 was shown to self-assemble within decellularised porcine internal carotid artery. It was shown that the peptide preferentially self-assembled around the ECM of the vessel. It was established that the peptide had to be added to the decellularised vessel as a monomeric solution for the peptide to fully penetrate throughout the vessel. It was shown that the thickness of the peptide coating on the decellularised vessel could be controlled by varying the concentration of peptide introduced into the vessel. It was also established that the peptide was still present in the decellularised vessel for over 14 days under flow conditions that modelled the situation in a small diameter blood vessel.

4 Systematic study of peptide biocompatibility and haemocompatibility

4.1 Introduction

Peptide self-assembly has been widely studied and design characteristics have been developed enabling peptides to be intelligently designed to have certain materials properties once self-assembled. Peptides are of great interest as potential materials for use in tissue engineering applications and many groups have explored the potential of peptides as tissue engineering scaffolds. Zhang et al, have shown that PuraMatrix (RAD16-1) supports the growth of a range of different cell types and Allen et al, demonstrated that PuraMatrix supported blood vessel development *in vitro* (Zhang et al., 2005, Allen et al., 2011). Jayawarna et al presented results showing that Fmoc-diphenylalanine (Fmoc-FF) hydrogels supported the growth of chondrocytes and Banwell et al have demonstrated that alpha-helix forming peptide hSAF_{AAA-W} P1 & 2 will support the growth and differentiation of PC12 cell lines (Banwell et al., 2009, Jayawarna et al., 2009). These results show the potential of peptides however there have been no reported attempts to define design characteristics for the haemocompatibility and biocompatibility of self-assembling peptides.

If a self-assembling peptide is used in a medical application it will exist in two forms in the body. The peptide will exist at the site of implantation as a gel but will also disseminate as a monomer or soluble aggregate carried away from the site of implantation in the blood or lymph. The monomer or soluble aggregate exists at a concentration below the critical concentration for self-assembly in all peptide gels that self-assembly using nucleated self-assembly (Aggeli et al., 2001). The monomer or soluble aggregate exists at equilibrium with the peptide gel and will be removed by the movement of fluids in the body and by diffusion.

Testing a peptide as a monomer has several advantages; it reduces the cost of the testing as less peptide is needed and monomer can be added to standard test solutions with no need to modify tests to allow for the testing of gels. Whilst it is possible that both the monomeric form and the gel form of the peptide could be toxic it is unlikely that a peptide would be toxic as a gel but not as a monomer. In Alzheimer's disease it is widely accepted that the self-assembled fibrils made up of Amyloid β (A β) peptides are toxic, however, it has also been shown that the soluble smaller amyloid aggregates are also toxic and could represent the primary pathological

mechanism in amyloid disease (Klein et al., 2001, Lacor et al., 2007, Glabe, 2008). If a peptide monomer is toxic and non-haemocompatible the peptide will not be suitable for biomedical application.

4.1.1 Biocompatibility

Biocompatibility can be defined as “the ability of a material, device or system to perform without a clinically significant host response in a specific application” (Blass, 1999). Biocompatible materials should not be toxic nor have an injurious effect on a biological system. Biocompatibility is the corner stone of biomedical research; if materials are not biocompatible then there is no potential for these materials to be used in any biomedical application. The testing of biocompatibility has been standardised in ISO 10933-5, Biological evaluation of medical devices Part 5: Tests for *in vitro* cytotoxicity.

4.1.2 Haemocompatibility

Haemocompatibility is the ability of a material or device to interact with blood and have no detrimental effect on blood clotting and the complement system. Haemocompatibility also refers to the ability of a material or device to be in contact with blood cells and not cause significant damage. Haemocompatibility is of vital interest when attempting to introduce artificial materials into the human body. If a material is not haemocompatible then the range of potential medical uses for that material will be limited. Materials that are non-haemocompatible can still be used in medical applications that are non-blood contacting. Testing of haemocompatibility has been standardised in ISO 10993-4, Biological evaluation of medical devices Part 4: Selection of tests for interactions with blood.

4.1.3 Thrombus formation/blood clotting

A thrombus is formed in flowing blood and differs from a blood clot found in stagnant blood. Thrombi formed in flowing blood have a distinct organised structure and constituents; clotted

stagnant blood has a more random arrangement and is made up of all the constituents of blood in their normal concentrations (Chandler, 1969). Thrombus formation has been explored in Section 1.6.

When considering the haemostatic response to biomaterials it is important to know how these materials in general can lead to thrombosis. The presence of a foreign surface in contact with blood results in a complex interlinked series of events involving protein adsorption, platelet and leukocyte activation and adhesion, activation of complement and coagulation (Gorbet and Sefton, 2004). Immediately following contact between the blood and biomaterial a boundary layer of proteins from the plasma is formed that is deposited and displaced; the amount of bound individual proteins varies on different biomaterials dependent upon the materials surface properties (Basmadjian et al., 1997, Hong et al., 1999). Protein adsorption is the first event in blood material interactions and may result in the activation of the intrinsic pathway, suggesting that the intrinsic pathway plays a role in the thrombotic activity of materials (Gorbet and Sefton, 2004). An important protein involved in this is factor XII which binds to the surface of the biomaterials and in an active state converts factor XI into factor XIa (Basmadjian et al., 1997, Gorbet and Sefton, 2004). No matter how inert a surface is trace amounts of bound factor XII will lead to a significant initiation of the intrinsic pathway (Basmadjian et al., 1997).

Platelets will bind or “bounce off” a layer of adsorbed proteins, adhesion is mediated by glycoprotein GPIIb/IIIa interaction with fibrinogen and GPIb/IIa and von Willebrand factor, however, absence of adhesion does not preclude platelet activation (Gorbet and Sefton, 2004). Adherent platelets generated by contact with biomaterials have been shown to be pro-coagulant (Gorbet and Sefton, 2004). It is often presumed that platelet activation by biomaterials is caused by the generation of thrombin due to the activation of the intrinsic pathway, however the inability of thrombin inhibitors to reduce platelet activation suggests that activation is in part mediated by other antagonists (Gorbet and Sefton, 2004). The thrombogenic consequences of platelet attachment and activation have been explored in greater detail in Section 1.6.

Material characteristics and adsorbed proteins modulate the level of leukocyte adhesion and activation; as the biomaterial is larger than can be phagocytised the leukocytes release an array of oxygen metabolites and proteolytic enzymes (Gorbet and Sefton, 2004). Leukocytes are efficient cells in the vasculature that initiate and amplify coagulation through a regulated change in disparate membrane proteins and the release of tissue factor (TF) (Altieri, 1993,

Gorbet and Sefton, 2004). Circulating leukocytes will adhere to adherent platelets and further contribute to localized thrombogenesis (Gorbet and Sefton, 2004). The presence of leukocytes in a thrombus has been shown to significantly contribute to fibrin formation (Altieri, 1993, Gorbet and Sefton, 2001). Studies on leukocyte expression of TF in patients with ventricular assist devices, in baboon-shunt models and *in vitro* clotting assays have shown material-induced TF expression results in fibrin formation enhancing coagulation (Gorbet and Sefton, 2001).

In addition to TF leukocytes possess alternative pathways to initiate coagulation and generate thrombin; this allows the assembly of co-factors IXa/VIII that form a tenase complex and activate the common pathway (Altieri, 1993). Leukocyte activation has been shown to be surface area dependent, however, TF expression has been shown to be stimulated by a biomaterial regardless of surface area (Gorbet and Sefton, 2001). TF expressed by monocytes and platelets has been suggested to represent a possible activation of the extrinsic pathway (Gorbet and Sefton, 2004). Results show leukocytes could be required for the activation of the coagulation cascade; suggesting the TF dependent extrinsic pathway of activation may apply to biomaterials (Hong et al., 1999). Inflammatory conditions have often been linked to fibrin deposits, leukocytes and complement proteins. It has been demonstrated that activation of complement, in particular C5, causes a marked increase in TF released by activated leukocytes (Muhlfelder et al., 1979). As discussed in Section 4.1.4 the presence of foreign materials can activate the complement system leading to increased thrombosis.

Mass transport is important to consider in thrombosis as flow enhances the transport of coagulation factors or inhibitors to the surface. As flow increases, the conversion of factor XI into XIa increases and conversion then decreases as flow exceeds a critical value (Basmadjian et al., 1997). Surface reactivity and flow are intertwined and have to be considered in unison when dealing with the intrinsic pathway (Basmadjian et al., 1997). The effects of flow on mass transfer and cell phenotype mean that different flow conditions will favour thrombosis by either the extrinsic or intrinsic pathway (Basmadjian et al., 1997, Gorbet and Sefton, 2004). Protein adsorption occurs within a few seconds/minutes whereas tissue factor synthesis takes over one hour (Gorbet and Sefton, 2004). This means the relative roles between extrinsic and intrinsic pathways in the thrombogenic activity of a material are likely to depend upon both the time frame and flow rate.

The common pathway takes place at platelet and leukocyte membranes and involves feedback loops that act to increase the levels of thrombin; thrombin levels are affected by flow

rate as levels of thrombin are increased with increasing flow rate but decrease as flow exceeds a critical value (Basmadjian et al., 1997). The dependence of flow rate on thrombus formation in contact with biomaterials explains why large diameter grafts with higher flow rates are observed not to occlude as fast as small diameter grafts with lower/intermediate flow rates. The understanding needed for biomaterial application is limited by a lack of understanding of how much of an inflammatory and thrombotic response is tolerable or if any changes in normal haemostasis results in harmful consequences.

There are a number of different ways to test for thrombogenicity. Testing can be done *in vivo* or *in vitro* with materials being implanted in animal models or blood being extracted from animals or humans for lab based testing. Thrombi can be formed in static or dynamic conditions; given the distinct structure of thrombi, dynamic conditions such as in the Chandler loop model are preferred. Thrombi can be analysed in a number of ways, the simplest method is gravimetric analysis in which the thrombi formed are weighed in a wet or dried state.

Microscopic analysis of thrombi along with the use of immuno-labelling can be used to assess the constituents, structure and morphology of the thrombi. Experiments can be set up to analyse the effects of reduction in flow, the percentage occlusion and the time taken for thrombogenesis. The ideal *in vitro* test is a dynamic model that does not adversely affect the blood constituents and allows for the flow of blood. The Chandler loop model allows for the flow of blood through a closed loop of tubing partly filled with air; this limits the possible flow rate and potentially introduces artefacts due to the air interface (van Oeveren et al., 2012).

The roller pump model uses a closed loop of tubing with no air and circulates the blood using a roller pump; this compresses the blood and can lead to haemolysis but higher rotation speeds can be used (van Oeveren et al., 2012). The Hemobile model uses a ball valve placed in a closed loop of tubing filled with blood; this model has high flow rates and does not induce damage to the blood but only achieves semi-circular movement (van Oeveren et al., 2012).

Another method of testing thrombosis is the use of a thromboelastograph (TEG). The TEG mimics sluggish venous flow to activate coagulation (Essell et al., 1993). The TEG can test coagulation function testing as well as platelet function, clot strength and fibrinolysis (Peng, 2010). The TEG gives more data than the other methods described, however, it does not model arterial flow which is of interest in this study. The most widely used model for the generation of thrombi and the testing of bypass grafts is the Chandler loop model. Given the

limited flow rates possible the Chandler loop model is more suited to modelling smaller diameter blood vessels with lower flow rates.

4.1.4 Complement system

The complement system is a component of the immune system that consists of more than 20 proteins found in the blood and fluids surrounding tissues; it can be activated by microorganisms, a variety of disease states and by contact with medical devices and foreign materials. The complement proteins circulate in an inactive form but become activated in response to the presence of foreign materials or antigen/antibody complexes. Activation of the complement system generates several different molecular pathways, enhancing opsonisation, acting as chemotaxins that attract macrophages and neutrophils, being involved in the inflammatory response and causing lysis of cell membranes (Ward et al., 1965, Ruddy et al., 1972, Ehlenberger and Nussenzweig, 1977, Fearon and Austen, 1980). The complement system can be activated by three pathways.

The classical pathway is antibody dependent; the antibodies bind to an antigen, C1 (C1q, C1r and C1s) then binds to the Fc portion of the antibody. Complement C1 is able to cleave C4 into C4b, which attaches to the antigen and C4a that is released. Complement C1 cleaves C2 into C2a, which attaches to the antigen and C2b that is released. The C4bC2a complex then functions as a C3 convertase cleaving C3 into C3a and C3b (Figure 4.1) (Kerr, 1980, Muller-Eberhard, 1988). In the lectin pathway mannan-binding protein (MBP) binds to mannose groups on the membrane of microbes, two proteins called MASP1 and MASP2 bind to MBP and function in the same way as C1 to create an C4bC2a convertase causing the cleavage of C3 into C3a and C3b (Figure 4.1) (Muller-Eberhard, 1988, Carroll, 2004).

The alternative pathway is different from the lectin and classical pathways. Complement C3 undergoes spontaneous hydrolysis into C3a and C3b, C3a and C3b will naturally decay unless C3b binds to the surface components of a cell. Once bound Factor B, an alternative pathway protein, binds to C3b and is split by Factor D into Bb and Ba. Factor Bb remains bound to C3b forming a C3bBb complex, this C3bBb complex is stabilised by Properdin and functions as a C3 convertase cleaving C3 into C3a and C3b (Figure 4.1) (Fearon and Austen, 1980, Muller-Eberhard, 1988, Carroll, 2004). As such the alternative pathway can become involved in the amplification of the classical and lectin pathways.

After C3 is cleaved the pathway for complement activation is the same as for the classical, lectin and alternative pathways. Complement fragment C3b can incorporate as a subunit in the existing convertases and form the C5 convertase of the classical/lectin pathway (C4b2b3b) or the alternative pathway (C3bBbC3b) (Medicus et al., 1976, Józsi, 2011). Upon activation of the complement system C5 is cleaved into C5a and C5b by the C5 convertase; C6 binds to a labile binding site on C5b which is followed by association with C7 exposing a hydrophobic site on C7 that binds to the cell membrane. C8 is then bound and the complex inserts into the cell membrane (Hadders et al., 2012). Up to 16 C9 molecules can bind to the complex and form a β -barrel pore in the membrane (Figure 4.1) (Muller-Eberhard, 1988). The complex of C6 to C9 is called the membrane attack complex (MAC).

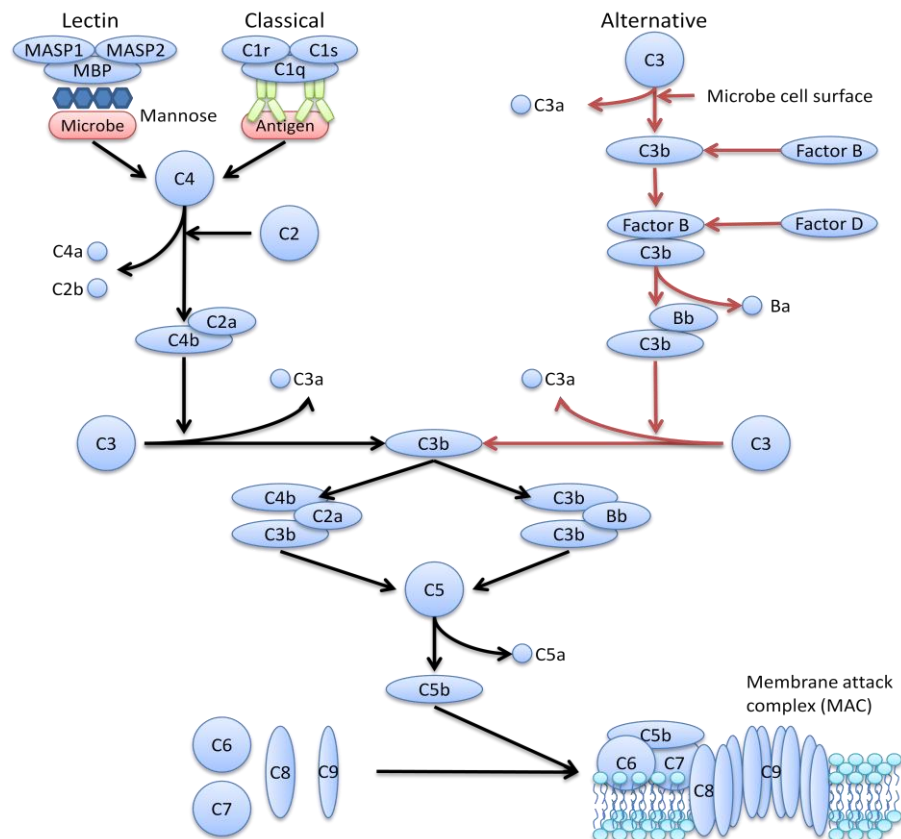


Figure 4.1; Schematic of pathways of complement activation

The presence of biomaterials is conventionally believed to activate complement by the alternative pathway. The alternative pathway is triggered by the binding of C3b to surfaces that do not provide adequate down-regulation of the C3 and C5 convertase; C3b is able to bind

to proteins and carbohydrates via free hydroxyl or amino groups (Andersson et al., 2005). Complement C3b has been shown to bind to serum proteins, in particular albumin and IgG and that these proteins support binding, convertase assembly and amplification of the alternative pathway (Andersson et al., 2005).

Both the classical and alternative pathway are involved in complement activation in the presence of biomaterials; at normal complement concentration in serum activation is mainly driven by the alternative pathway with little contribution by the classical pathway, as the complement concentration levels in serum decrease the contribution of the classical pathway increases as the alternative pathway decreases (Andersson et al., 2005). This supports the theory that the alternative pathway is being activated on biomaterials by the adsorption of serum proteins. This means that in most biological applications complement activation will be by the alternative pathway. Hydroxyl rich surfaces have been shown to cause substantial complement activation and deposition; amine and carboxyl surfaces have been shown to trigger only slight activation of the complement system (Tang et al., 1998). Non-activating materials tend to have negatively charged groups such as sulphate, sialic acid and bound heparin (Gorbet and Sefton, 2004). However, not all known activators of the complement system conform to this observation suggesting that the mechanism is more complex.

There are numerous reported methods to test for complement activation. Immunoelectrophoresis has been used to assess the presence and levels of complement fractions C3a and Bb produced by complement activation (Craddock et al., 1977). Immunofluorescence and radiolabelling have also been used to assess complement activation (Atkinson et al., 2005). ELISA assays and radioimmunoassay using antibodies against specific complement fractions or complexes, for example C3a, have been used to test for the levels of complement components only produced following complement activation (Rogers et al., 1992, Bruins et al., 1997).

Animal erythrocytes have been used to test for total complement and C1 and C3 activity using haemolysis assays (Craddock et al., 1977, Rogers et al., 1992). Complement inhibition can also be tested for using these methods by mixing a known trigger and test material together and testing for a reduction in the level of detected complement or complexes compared to a control of activated complement (Atkinson et al., 2005, Hammel et al., 2007). A modification of the CH50 assay described in Section 2.2.17.2 was chosen for testing complement activity over the other methods discussed above. This method was chosen as the CH50 assay is less specific and includes the whole complement activation pathway where Immunofluorescence,

radiolabelling and ELISA assays are more specific and target only part of the pathway; e.g. an ELISA assay against C3a uses antibodies only against C3a. This means that if a material has an inhibitory effect elsewhere on the complement system this effect may not be noticed using a more targeted test.

4.1.5 Animal models

All new medical devices and materials have to be tested in animal models in order to get approval for sale and any medical use. Whilst there is no one ideal candidate for comparison to human tests dogs, sheep and pigs are the most widely used. Sheep are the favoured animal model for vascular research as their blood vessels are similar in size to human vessels, their coagulatory system is closer to humans than dogs or pigs and the rate that sheep form an endothelium most closely approximates the situation in humans (Narayanaswamy et al., 2000, Ueberrueck et al., 2005). Since sheep are the likely animal model for further testing of the concepts developed in this study all tests carried out using blood utilised sheep blood.

4.1.6 Peptides

A number of different peptides have been developed at the University of Leeds. These peptides were based on an initial design characteristic of 11 amino acids in the peptide sequence to ensure an anti-parallel β -sheet conformation. The peptides were designed to investigate the effect of changing charge, polarity and hydrophobicity of amino acid residues upon the self-assembling properties of the peptides under various conditions. The same library of developed peptides were utilised to test the effect of charge, polarity and hydrophobicity of the amino acid residues on biocompatibility and haemocompatibility.

4.1.7 Peptides from the literature

In order to ascertain if any observed design characteristics were limited to the library of peptides developed at the University of Leeds or apply to all peptides it was necessary to

include several peptides from the literature. The widest used and reported peptide in the literature is PuraMatrix developed by Dr Shuguang Zhang and co-workers at Massachusetts Institute of Technology. PuraMatrix is the trade name of peptide RAD16-1 that has the amino acid sequence (RADA)₄. PuraMatrix forms anti-parallel β -sheet structures and has been shown to be biocompatible. Fmoc-FF has been explored for tissue engineering applications by Dr Rein V. Ulijn and co-workers and comes from a family of simple Fmoc-di-peptides that have been shown to self-assemble into hydrogels via π - π interlocking β -sheets (Smith et al., 2008). As the peptides developed at the University of Leeds, PuraMatrix and Fmoc-FF all self-assemble via a β -sheet pathway a peptide that self-assembles using a α -helix pattern was chosen. The peptides hSAF_{AAA-W} P1 and P2 were developed by Professor Derek Woolfson and co-workers at the University of Bristol; the peptides are 28 residues in length and are designed to co-self-assemble when mixed together. Self-assembly happens longitudinally and forms an α -helix coiled fibril, fibrils can then bundle together to form fibres (Banwell et al., 2009). A range of homo-polypeptides were also chosen as they are larger in size and allow for the demonstration of any effects that are due to particular amino acids.

4.1.8 Aims and objectives

The aims of this chapter were to screen a library of self-assembling peptides developed at the University of Leeds, self-assembling peptides from the literature and homo-polypeptides for haemocompatibility and biocompatibility in order determine suitable candidate peptides for use in vascular tissue engineering applications. A secondary aim was to determine design characteristics allowing for the intelligent design of peptides for a range of biological applications.

Specific objectives;

- a) To determine the biocompatibility of a range of peptides
- b) To evaluate the capacity of a range of peptides to induce thrombus formation
- c) To evaluate the haemolytic capacity of a range of peptides
- d) To determine the capacity of the range of peptides for inhibition of the complement system
- e) To determine if a set of design characteristics can be found for future design of self-assembling peptides for a range of biological applications

4.2 Methods

4.2.1 Peptides

The sequences, charge (at physiological pH) and molecular weights of the peptides used throughout these studies are given in Table 4-1.

Peptide Name	Sequence	Charge	Molecular weight
P ₁₁ -1	CH ₃ CO-Q-Q-R-Q-Q-Q-Q-E-Q-Q-NH ₂	0	1497
P ₁₁ -2	CH ₃ CO-Q-Q-R-F-Q-W-Q-F-E-Q-Q-NH ₂	0	1593
P ₁₁ -3	CH ₃ CO-Q-Q-R-F-Q-W-Q-F-Q-Q-Q-NH ₂	+1	1593
P ₁₁ -4	CH ₃ CO-Q-Q-R-F-E-W-E-F-E-Q-Q-NH ₂	-2	1596
P ₁₁ -5	CH ₃ CO-Q-Q-O-F-O-W-O-F-Q-Q-Q-NH ₂	+3	1522
P ₁₁ -7	CH ₃ CO-S-S-R-F-S-W-S-F-E-S-S-NH ₂	0	1348
P ₁₁ -8	CH ₃ CO-Q-Q-R-F-O-W-O-F-E-Q-Q-NH ₂	+2	1567
P ₁₁ -9	CH ₃ CO-S-S-R-F-E-W-E-F-E-S-S-NH ₂	-2	1432
P ₁₁ -10	CH ₃ CO-N-N-R-F-N-W-N-F-E-N-N-NH ₂	0	1510
P ₁₁ -12	CH ₃ CO-S-S-R-F-O-W-O-F-E-S-S-NH ₂	+2	1401
P ₁₁ -13	CH ₃ CO-E-Q-E-F-E-W-E-F-E-Q-E-NH ₂	-6	1571
P ₁₁ -14	CH ₃ CO-Q-Q-O-F-O-W-O-F-O-Q-Q-NH ₂	+4	1508
P ₁₁ -16	CH ₃ CO-N-N-R-F-O-W-O-F-E-N-N-NH ₂	+2	1511
P ₁₁ -17	CH ₃ CO-T-T-R-F-E-W-E-F-E-T-T-NH ₂	-2	1487.6
P ₁₁ -18	CH ₃ CO-T-T-R-F-O-W-O-F-E-T-T-NH ₂	+2	1457.6
P ₁₁ -19	CH ₃ CO-Q-Q-R-Q-O-Q-O-Q-E-Q-Q-NH ₂	+2	1469.6
P ₁₁ -20	CH ₃ CO-Q-Q-R-Q-E-Q-E-Q-E-Q-Q-NH ₂	-2	1499.5
P ₁₁ -22	CH ₃ CO-T-T-R-F-T-W-T-F-E-T-T-NH ₂	0	1431.6
P ₁₁ -24	CH ₃ CO-S-S-R-Q-E-Q-E-Q-E-S-S-NH ₂	-2	1335.3
P ₁₁ -25	CH ₃ CO-S-S-R-S-E-S-E-S-E-S-S-NH ₂	-2	1212.2
P ₁₁ -26	CH ₃ CO-Q-Q-O-Q-O-Q-O-Q-O-Q-Q-NH ₂	+4	1412.8
P ₁₁ -27	CH ₃ CO-Q-Q-E-Q-E-Q-E-Q-E-Q-Q-NH ₂	-4	1474.4

P ₁₁ -28	CH ₃ CO-O-Q-O-F-O-W-O-F-O-Q-O-NH ₂	+6	1481.4
P ₁₁ -29	CH ₃ CO-Q-Q-E-F-E-W-E-F-E-Q-Q-NH ₂	-4	1569.6
P ₁₁ -30	CH ₃ CO-E-S-E-F-E-W-E-F-E-S-E-NH ₂	-6	1488.5
P ₁₁ -31	CH ₃ CO-S-S-O-F-O-W-O-F-O-S-S-NH ₂	+4	1344.5
RAD16-1	CH ₃ CO-(R-A-D-A) ₄ -NH ₂	0	1712.8
Fmoc-FF	Fmoc-F-F	-1	534.21
hSAF _{AAA-W} P1	K-I-A-A-L-K-A-K-I-A-A-L-K-A-E-I-A-A-L-E-W-E-N-A-A-L-E-A	0	2921.5
hSAF _{AAA-W} P2	K-I-A-A-L-K-A-K-N-A-A-L-K-A-E-I-A-A-L-E-W-E-I-A-A-L-E-A	0	2921.5
Poly-l-Glutamic acid	(E-E-E-E) _n	Negative	9000
Poly-l-Lysine	(K-K-K-K) _n	Positive	50000
Poly-l-Threonine	(T-T-T-T) _n	0	10000
Poly-l-Tryptophan	(W-W-W-W) _n	0	3000
Poly-l-Aspartic acid	(D-D-D-D) _n	Negative	10000
Poly-l-Arginine	(R-R-R-R) _n	Positive	1000
Poly-l-Ornithine	(O-O-O-O) _n	Positive	1000
Polyglycine	(G-G-G-G) _n	0	2750

Table 4-1; Peptides used in the study; peptide name, structure, charge and molecular weight

Since not all the peptides would form stable gels in physiological conditions for extended periods of time the peptides were tested at low concentrations equivalent to the levels of monomer /soluble aggregate released from the peptide gel. To ensure that all the peptides could be compared a concentration of 0.3 mol.m⁻³ was chosen, which corresponded to the critical concentration for self-assembly of P₁₁-4, the most significant peptide amongst those screened for the present project. The same concentration was also used to screen the other peptides as this concentration was below the critical concentration for self-assembly for the majority of the peptides.

4.2.2 Biocompatibility testing

In accordance with ISO standard protocols (ISO 10933-5) two cell lines were used to test for cytotoxicity. Baby hamster kidney (BHK) cells, an adhesive epithelial cell line originally obtained from 1 day-old hamsters and 3T3 cells originally obtained from primary embryonic mouse fibroblasts were used. All peptides solutions were made in DMEM for 3T3 cells and GMEM for BHK cells to achieve a final concentration of 0.3 mol.m^{-3} . All samples were mixed by pipetting up and down and by vortexing. Peptide samples which proved difficult to dissolve were pipetted up and down to create a dispersion of peptide before each addition of peptide solution to each test. All difficulties with dissolving peptides were noted. All biocompatibility tests were set-up and run as per the protocol described in Section 2.2.14. Six replicates for each peptide were carried out with a maximum of six tests per 96 well plate; one positive control, one negative control and up to four different peptide samples. Only one cell type was grown in each 96 well plate to prevent cross-contamination and all cells were grown in the same incubator for the same time period. Cells were seeded at approximately 2000 BHK cells per well and 4000 3T3 cells per well in a 96 well plate. Cells were grown in a clear 96 well plate to allow for the monitoring of their growth and to check for any discrepancies before use. Following incubation in test solutions the cell numbers were assessed using the ATPLite-M[®] assay; this has the advantage that cell viability can be assessed by the number of live cells compared to the control but as a secondary effect increased levels of cell proliferation can be detected.

4.2.3 Chandler loop thrombosis model

All peptide solutions were made in deionised water to achieve a final concentration of 0.3 mol.m^{-3} . All samples were mixed by pipetting up and down and by vortexing. Peptides samples which proved difficult to dissolve were pipetted up and down to create a dispersion of peptide before each addition of peptide solution to each test. All difficulties with dissolving peptides were noted. All Chandler loop tests were set-up and run as per the protocol described in Section 2.2.15.1. Six replicates for each peptide were tested. Six samples were tested at a time with three loops per rotator. Citrated blood from sheep was used to test for effects upon thrombus formation. All blood used was tested for normal clotting behaviour and a response to known triggers of blood clotting before use.

4.2.4 Haemolysis assay

All peptide solutions were made in Ringer's solution to achieve a final concentration of 0.3 mol.m^{-3} . All samples were mixed by pipetting up and down and by vortexing. Peptides samples which proved difficult to dissolve were pipetted up and down to create a dispersion of peptide before each addition of peptide solution to each test. All difficulties with dissolving peptides were noted. All haemolysis tests were set-up and run as per the protocol described in Section 2.2.16. Six replicates for each test condition were carried out and samples were taken at 6, 12, 24, 48 and 72 hours. Erythrocytes were obtained from citrated sheep blood harvested and shipped the day before use.

4.2.5 Complement inhibition assay

All peptide solutions were made in Ringer's solution to achieve a final concentration of 0.3 mol.m^{-3} as described above (Section 4.2.1). All complement inhibition tests were set-up and run as per the protocol described in Section 2.2.17.2. Six replicates for each test condition were carried out. Normal pooled human serum was used for the test and the CH50 level determined before testing using the method described in Section 2.2.17.1.

4.3 Results

4.3.1 Effects of peptides on cell growth

Results were collected, graphed and analysed for significant statistical differences by one-way ANOVA and post-hoc analysis (Section 2.2.21.2). For all results there was a significant difference between the cellular growth observed for both cell types between the positive and negative controls. Results are presented in Figure 4.2 to Figure 4.4 as a series of graphs with 4 test peptides plus the relevant positive and negative controls.

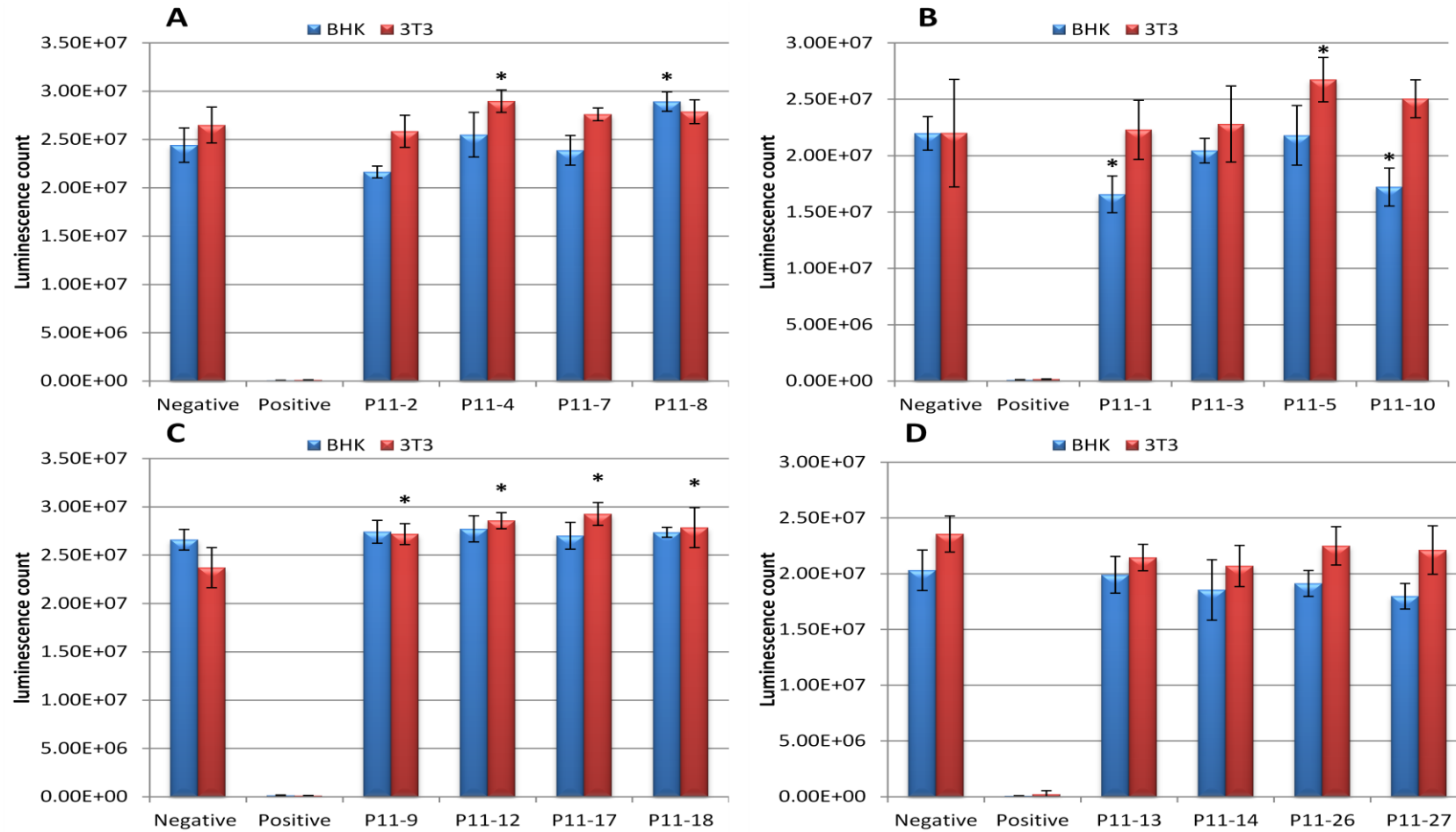


Figure 4.2; ATP levels in cells cultured in the presence and absence of peptides; negative control DMEM for 3T3 cells, GMEM for BHK cells, positive control 40 % DMSO in, DMEM for 3T3 cells, GMEM for BHK cells. Data is presented as the mean (n=6) \pm 95 % confidence intervals. Data was analysed by one way analysis of variance followed by determination of the MSD ($p < 0.05$). * = Significant difference from negative control.

3T3 cells grown in solutions of peptides P₁₁-1, P₁₁-2, P₁₁-3, P₁₁-7, P₁₁-8, P₁₁-10, P₁₁-13, P₁₁-14, P₁₁-26 and P₁₁-27 showed similar levels of growth with no significant difference compared to the negative DMEM controls. 3T3 cells grown in solutions of peptides P₁₁-4, P₁₁-5, P₁₁-9, P₁₁-12, P₁₁-17 and P₁₁-18 showed a significantly higher level of growth compared to that of 3T3 cells grown in the negative DMEM controls. BHK cells grown in solutions of peptides P₁₁-2, P₁₁-3, P₁₁-4, P₁₁-5, P₁₁-7, P₁₁-9, P₁₁-12, P₁₁-13, P₁₁-14, P₁₁-17, P₁₁-18, P₁₁-26 and P₁₁-27 showed similar levels of growth with no significant difference compared to the negative GMEM controls. BHK cells grown in a solution of peptide P₁₁-8 showed a significantly higher level of growth compared to that of BHK cells grown in the negative GMEM control. BHK cells grown in solutions of peptides P₁₁-1 and P₁₁-10 showed significantly lower levels of growth compared to the negative GMEM control. The growth of both BHK and 3T3 cells in the different peptide solutions were all significantly higher than the positive, cytotoxic, controls.

The results presented in Figure 4.2 showed peptides P₁₁-2, P₁₁-3, P₁₁-4, P₁₁-5, P₁₁-7, P₁₁-8, P₁₁-9, P₁₁-12, P₁₁-13, P₁₁-14, P₁₁-17, P₁₁-18, P₁₁-26 and P₁₁-27 were all non-cytotoxic. The results showed that P₁₁-1 and P₁₁-10 were non-cytotoxic to 3T3 cells and that there was a significantly lower level of growth of BHK cells in solutions of P₁₁-1 and P₁₁-10 but that were significantly higher than the cytotoxic control suggesting that the peptides are not cytotoxic.

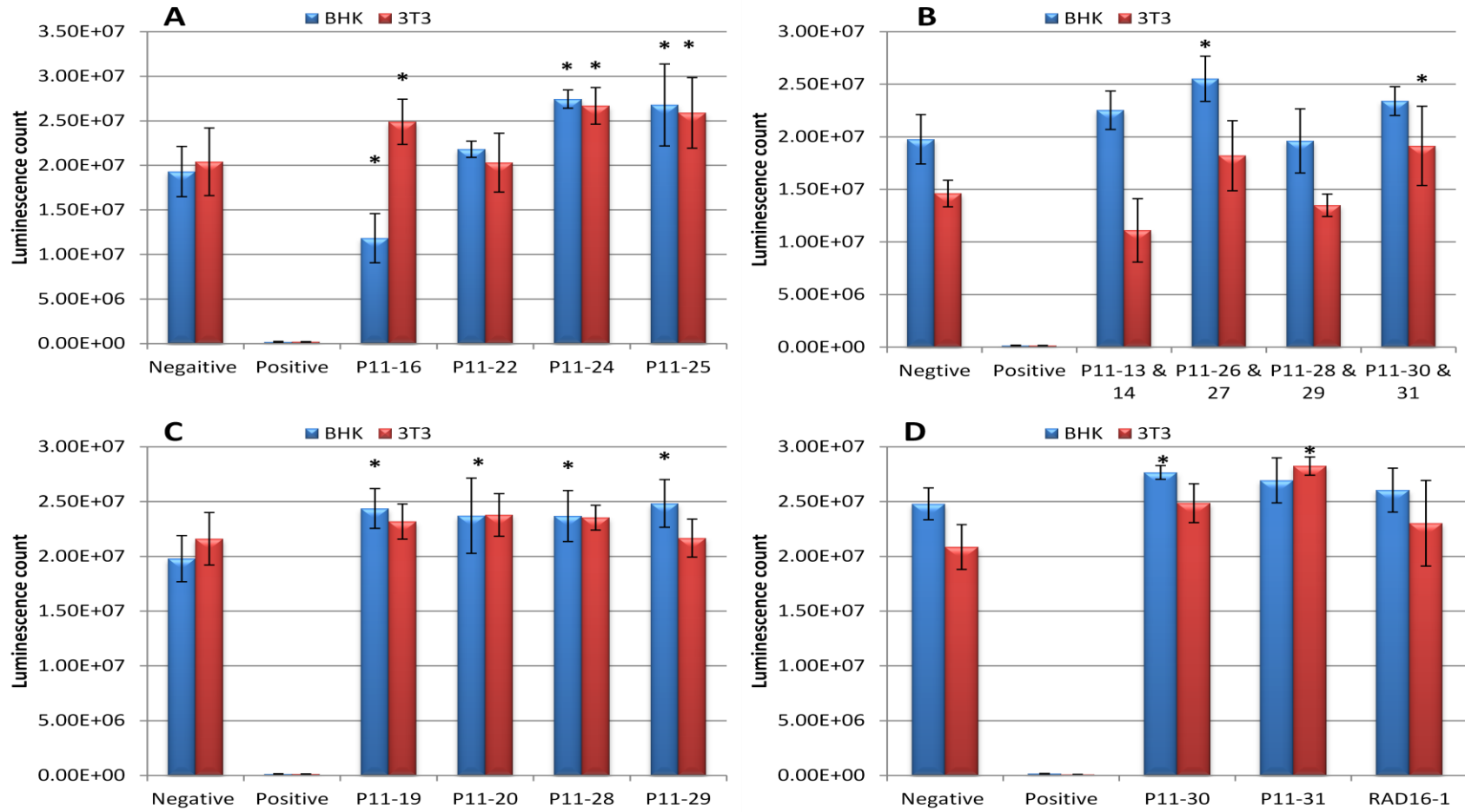


Figure 4.3; ATP levels in cells cultured in the presence and absence of peptides; negative control DMEM for 3T3 cells, GMEM for BHK cells, positive control 40 % DMSO in, DMEM for 3T3 cells, GMEM for BHK cells. Data is presented as the mean (n=6) \pm 95 % confidence intervals. Data was analysed by one way analysis of variance followed by determination of the MSD ($p < 0.05$). * = Significant difference from negative control

3T3 cells grown in solutions of P₁₁-19, P₁₁-20, P₁₁-22, P₁₁-28, P₁₁-29, RAD16-1 and complementary peptides P₁₁-13 & 14, P₁₁-26 & 27, and P₁₁-28 & 29 showed similar levels of growth with no significant difference compared to the negative DMEM controls. 3T3 cells grown in solutions of P₁₁-16, P₁₁-24, P₁₁-25, P₁₁-30, P₁₁-31 and complementary peptides P₁₁-30 & 31 showed a significantly higher level of growth compared to that of 3T3 cells grown in the negative DMEM controls. BHK cells grown in solutions of P₁₁-22, RAD16-1 and complementary peptides P₁₁-13 & 14, P₁₁-28 & 29 and P₁₁-30-&31 showed similar levels of growth with no significant difference compared to the negative GMEM controls. BHK cells grown in solutions of P₁₁-19, P₁₁-20, P₁₁-24, P₁₁-25, P₁₁-28, P₁₁-29, P₁₁-30 and complementary peptide P₁₁-26 & 27 showed a significantly higher level of growth compared to that of BHK cells grown in the negative GMEM controls. BHK cells grown in a solution of P₁₁-16 showed significantly lower levels of growth compared to the negative GMEM control. The growth of both BHK and 3T3 cells in the different peptide solutions were all significantly higher than the positive, cytotoxic, controls.

The results in Figure 4.3 showed peptides P₁₁-19, P₁₁-20, P₁₁-22, P₁₁-24, P₁₁-25, P₁₁-28, P₁₁-29, P₁₁-30, P₁₁-31, RAD16-1 and complementary peptides P₁₁-13 & 14, P₁₁-26 & 27, P₁₁-28 & 29 and P₁₁-30 & 31 were non-cytotoxic. The results also showed that P₁₁-16 was non-cytotoxic to 3T3 cells but showed a significant decrease in cell growth for BHK cells suggesting the peptide is non-cytotoxic.

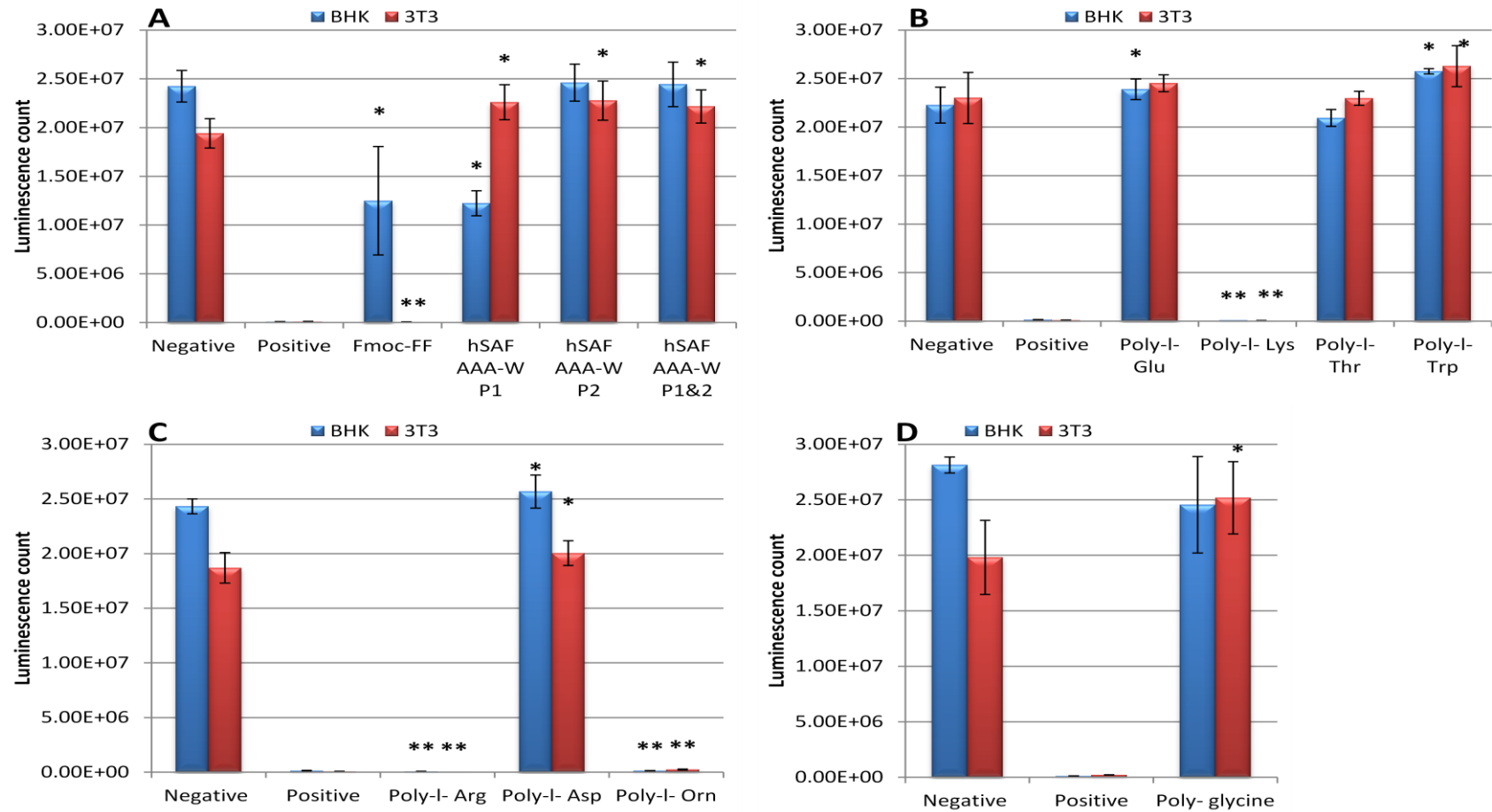


Figure 4.4; ATP levels in cells cultured in the presence and absence of peptides; negative control DMEM for 3T3 cells, GMEM for BHK cells, positive control 40 % DMSO in DMEM for 3T3 cells, GMEM for BHK cells. Data is presented as the mean (n=6) \pm 95 % confidence intervals. Data was analysed by one way analysis of variance followed by determination of the MSD ($p < 0.05$). * = Significant difference from negative control, **= significant difference from negative control and no significant difference from positive control.

Dificulty was experienced in dissolving the peptide Fmoc-FF, poly-l-tryptophan (Trp) and polyglycine in DMEM and GMEM. 3T3 cells grown in solutions of poly-l-glutamic acid (Glu) and poly-l-threonine (Thr) showed similar levels of growth with no significant difference compared to the negative DMEM control. 3T3 cells grown in solutions of peptide hSAF_{AAA-W} P1, hSAF_{AAA-W} P2, poly-l-tryptophan (Trp), poly-l-aspartic acid (Asp), polyglycine and the complementary hSAF_{AAA-W} P1&2 showed a significantly higher level of growth compared to that of 3T3 cells grown in the negative DMEM controls. 3T3 cells grown in solutions of peptide Fmoc-diphenylalanine (Fmoc-FF), poly-l-lysine (Lys), poly-l-arginine (Arg) and poly-l-ornithine (Orn) showed similar levels of growth to the positive cytotoxic controls. BHK cells grown in solutions of peptide hSAF_{AAA-W} P2, poly-l-threonine (Thr), polyglycine and complementary peptide hSAF_{AAA-W} P1&2 showed similar levels of growth with no significant difference compared to the negative GMEM controls. BHK cells grown in solutions of poly-l-glutamic acid (Glu), poly-l-tryptophan (Trp) and poly-l-aspartic acid (Asp) showed a significantly higher level of growth compared to that of BHK cells grown in the negative GMEM controls. BHK cells grown in solutions of peptide Fmoc-diphenylalanine (Fmoc-FF) and hSAF_{AAA-W} P2 showed significantly lower levels of growth compared to the negative GMEM controls. BHK cells grown in solutions of peptide poly-l-lysine (Lys), poly-l-arginine (Arg) and poly-l-ornithine (Orn) showed similar levels of growth to the positive cytotoxic controls.

The results in Figure 4.4 showed peptides hSAF_{AAA-W} P2, poly-l-glutamic acid (Glu), poly-l-threonine (Thr), poly-l-tryptophan (Trp), poly-l-aspartic acid (Asp), polyglycine and complementary peptides hSAF_{AAA-W} P1&2 were non-cytotoxic. The result showed peptide hSAF_{AAA-W} P1 was non-cytotoxic to 3T3 cells but showed a significant decrease in cell growth for BHK cells suggesting that the peptide is non-cytotoxic. The results also showed that peptide Fmoc-diphenylalanine (Fmoc-FF) was cytotoxic to 3T3 cells and significantly decreased the growth of BHK cells suggesting the peptide is cytotoxic. The results in Figure 4.4 showed homopolypeptides poly-l-lysine (Lys), poly-l-arginine (Arg) and poly-l-ornithine (Orn) to be cytotoxic.

4.3.2 Effects of peptides on thrombus formation

Results were collected, graphed and analysed for significant statistical differences by one-way ANOVA and post hoc analysis (Section 2.2.21.2). For all results there was a significant difference between the size of the thrombus observed between the positive and negative

controls. Results are presented in Figure 4.5 and Figure 4.6 as a series of graphs with test peptides plus the relevant positive and negative controls.

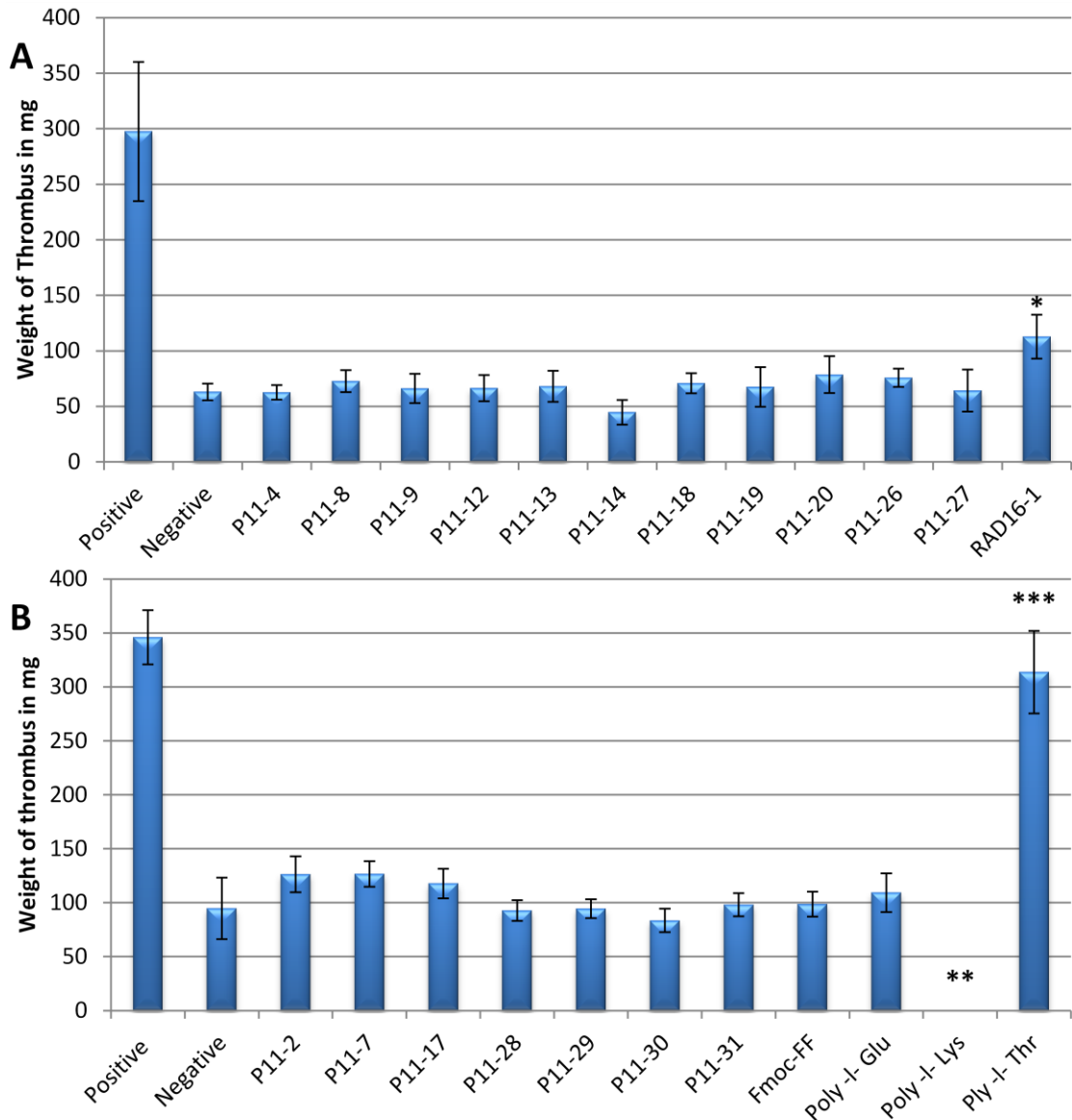


Figure 4.5; Weights of thrombus formed in the presence or absence of peptide in the Chandler loop model; Negative control 100 μ l of water, Positive control 2 μ l of human α -thrombin in 98 μ l of water.

Data is presented as the mean (n=6) \pm 95 % confidence intervals. Data was analysed by one way analysis of variance followed by determination of the MSD ($p < 0.05$). * = Significant increase from negative control, ** = significant reduction compared to negative control, *** = no significant difference from positive control.

All thrombi that were formed in this assay had a similar appearance with a single thrombus being formed with a width similar to the PVC tubing and a visible white head at one end of the

thrombus and a red tail similar to arterial thrombi formed *in vivo*. Difficulty was observed dissolving peptide Fmoc-diphenylalanine (Fmoc-FF) in deionised water.

The results in Figure 4.5 showed that peptides P₁₁-2, P₁₁-4, P₁₁-7, P₁₁-8, P₁₁-9, P₁₁-12, P₁₁-13, P₁₁-14, P₁₁-17, P₁₁-18, P₁₁-20, P₁₁-26, P₁₁-27, P₁₁-28, P₁₁-29, P₁₁-30, P₁₁-31, Fmoc-diphenylalanine (Fmoc-FF) and poly-L-glutamic acid (Glu) all resulted in thrombi similar in size with no significant difference to the relevant negative controls. The results also showed that the thrombi formed in these peptides were significantly smaller than the thrombi formed in the relevant positive controls. The results in Figure 4.5 graph A showed that peptide RAD16-1 formed significantly larger thrombi than the negative control that was also significantly smaller than the positive control. The results in Figure 4.5 graph B showed that homo-polypeptide poly-L-threonine (Thr) resulted in significantly larger thrombi than the negative control that showed no significant difference from the positive control. The results in Figure 4.5 graph B showed that poly-L-lysine (Lys) did not form thrombi as the blood was observed to agglutinate.

The results in Figure 4.5 showed that peptides P₁₁-2, P₁₁-4, P₁₁-7, P₁₁-8, P₁₁-9, P₁₁-12, P₁₁-13, P₁₁-14, P₁₁-17, P₁₁-18, P₁₁-20, P₁₁-26, P₁₁-27, P₁₁-28, P₁₁-29, P₁₁-30, P₁₁-31, Fmoc-diphenylalanine (Fmoc-FF) and poly-L-glutamic acid (Glu) had no significant effect upon thrombus formation. The result showed that peptides RAD16-1 and poly-L-threonine (Thr) increased thrombus formation. The results also showed that poly-L-lysine (Lys) prevented thrombus formation but was not haemocompatible as it was observed to cause blood agglutination.

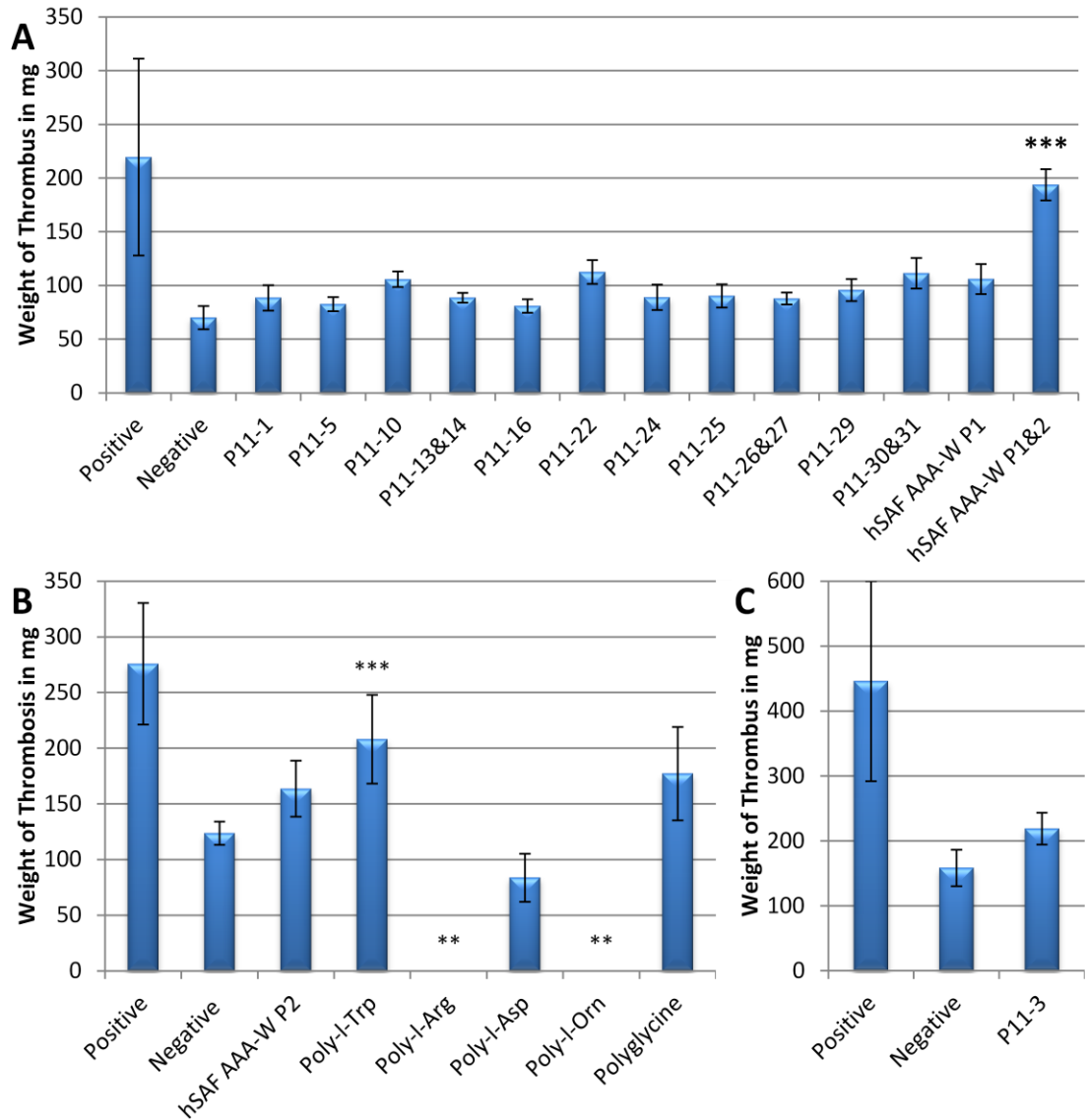


Figure 4.6; Weights of thrombus formed in the presence or absence of peptide in the Chandler loop model; Negative control 100 μ l of water, Positive control 2 μ l of human α -thrombin in 98 μ l of water. Data is presented as the mean (n=6) \pm 95 % confidence intervals. Data was analysed by one way analysis of variance followed by determination of the MSD ($p < 0.05$). * = Significant increase from negative control, ** = significant decrease compared to negative control, * = no significant difference from positive control.**

All thrombi that were formed in this assay had a similar appearance with a single thrombus being formed with a width similar to the PVC tubing and a visible white head at one end of the thrombus and a red tail similar to arterial thrombi formed *in vivo*. Difficulty was observed dissolving peptides poly-L-tryptophan (Trp) and Polyglycine in deionised water.

The results in Figure 4.6 showed that peptides P₁₁-1, P₁₁-3, P₁₁-5, P₁₁-10, P₁₁-16, P₁₁-24, P₁₁-25, hSAF_{AAA-W} P1, hSAF_{AAA-W} P2, poly-l- aspartic acid (Asp), Polyglycine and complementary peptides P₁₁-13&14, P₁₁-26&27, P₁₁-28&29 and P₁₁-30&31 all resulted in thrombi similar in size with no significant difference to the relevant negative controls. The results also showed that the thrombi formed in these peptides were significantly smaller than the thrombi formed in the relevant positive controls. The results in Figure 4.6 graph A showed that complementary peptide hSAF_{AAA-W} P1 & P2 resulted in significantly larger thrombi than the relevant negative control that showed no significant difference from the relevant positive control. The results in Figure 4.6 graph B showed that homo-polypeptide poly-l-tryptophan (Trp) resulted in the formation of thrombi that were significantly larger than thrombi formed in the relevant negative control and that showed no significant difference from the relevant positive control. The results also show that peptides poly-l-arginine (Arg) and poly-l-ornithine (Orn) failed to form thrombi as the blood was observed to agglutinate.

The results in Figure 4.6 showed that peptides P₁₁-1, P₁₁-3, P₁₁-5, P₁₁-10, P₁₁-16, P₁₁-24, P₁₁-25, hSAF_{AAA-W} P1, hSAF_{AAA-W} P2, poly-l- aspartic acid (Asp), polyglycine and complementary peptides P₁₁-13&14, P₁₁-26&27, P₁₁-28&29 and P₁₁-30&31 had no significant effect upon thrombus formation. The result showed that homo-polypeptide poly-l-tryptophan (Trp) and complementary peptide hSAF_{AAA-W} P1 & P2 increased thrombus formation. The results also showed that poly-l-arginine (Arg) and poly-l-ornithine (Orn) prevented thrombus formation but were not haemocompatible as they were observed to cause blood agglutination.

4.3.3 Effects of peptides on the haemolysis of ovine erythrocytes

Results were collected, graphed and analysed for significant statistical difference by one-way ANOVA and post hoc analysis (Section 2.2.21.2). For all results at all time points there was a significant difference between the positive and negative controls. Results are presented in Figure 4.7 to Figure 4.10 as a series of graphs with all peptides tested plus the relevant positive and negative controls.

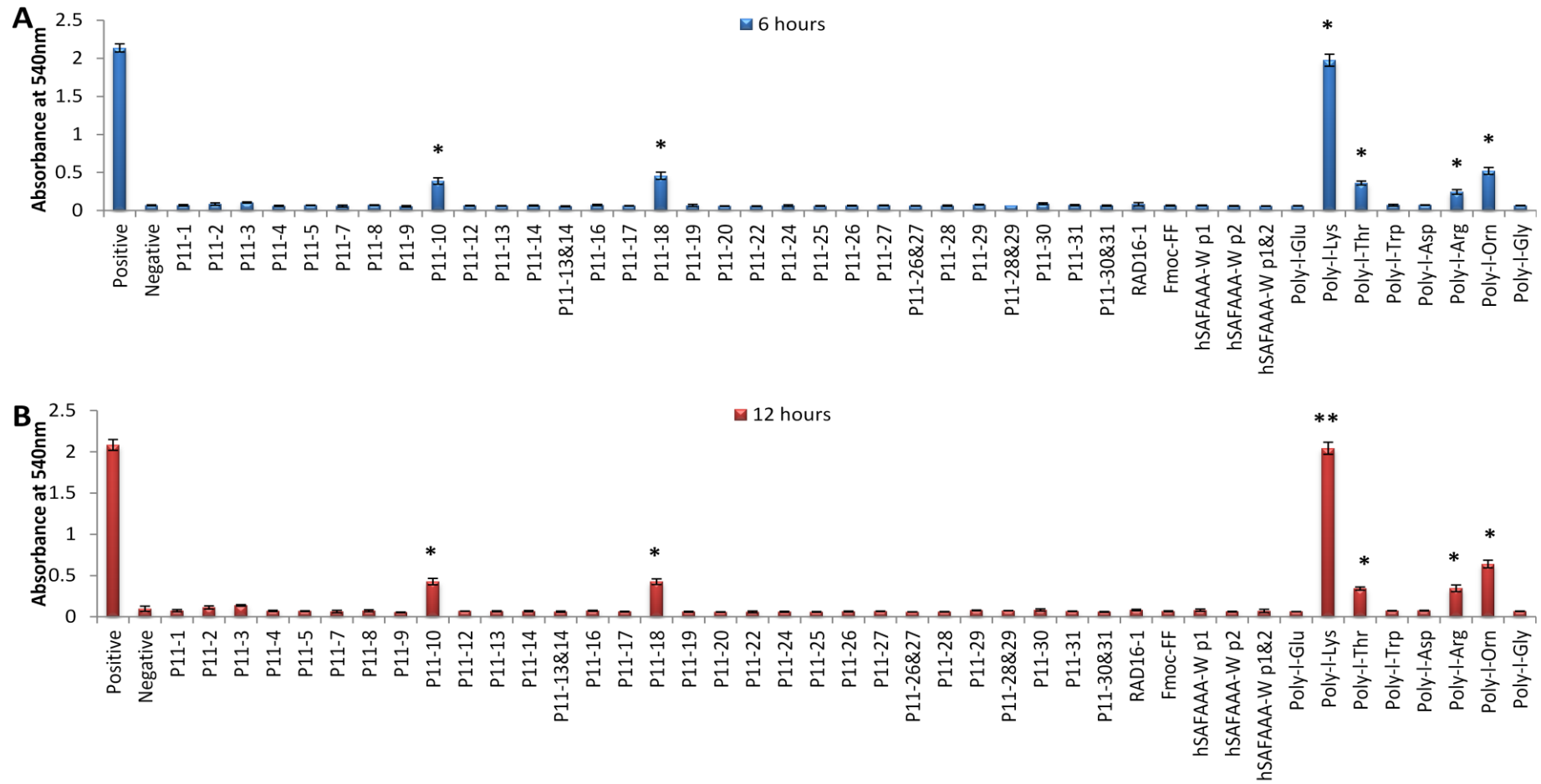


Figure 4.7; Haemolytic effects of peptides after A; 6 hours, B; 12 hours. Positive control water, Negative control Ringer's solution. Data is presented as the mean ($n=6$) \pm 95 % confidence intervals. Data was analysed by one way analysis of variance followed by determination of the MSD ($p < 0.05$). * = significant difference from negative control, ** = significant difference from negative control and no significant difference from positive control.

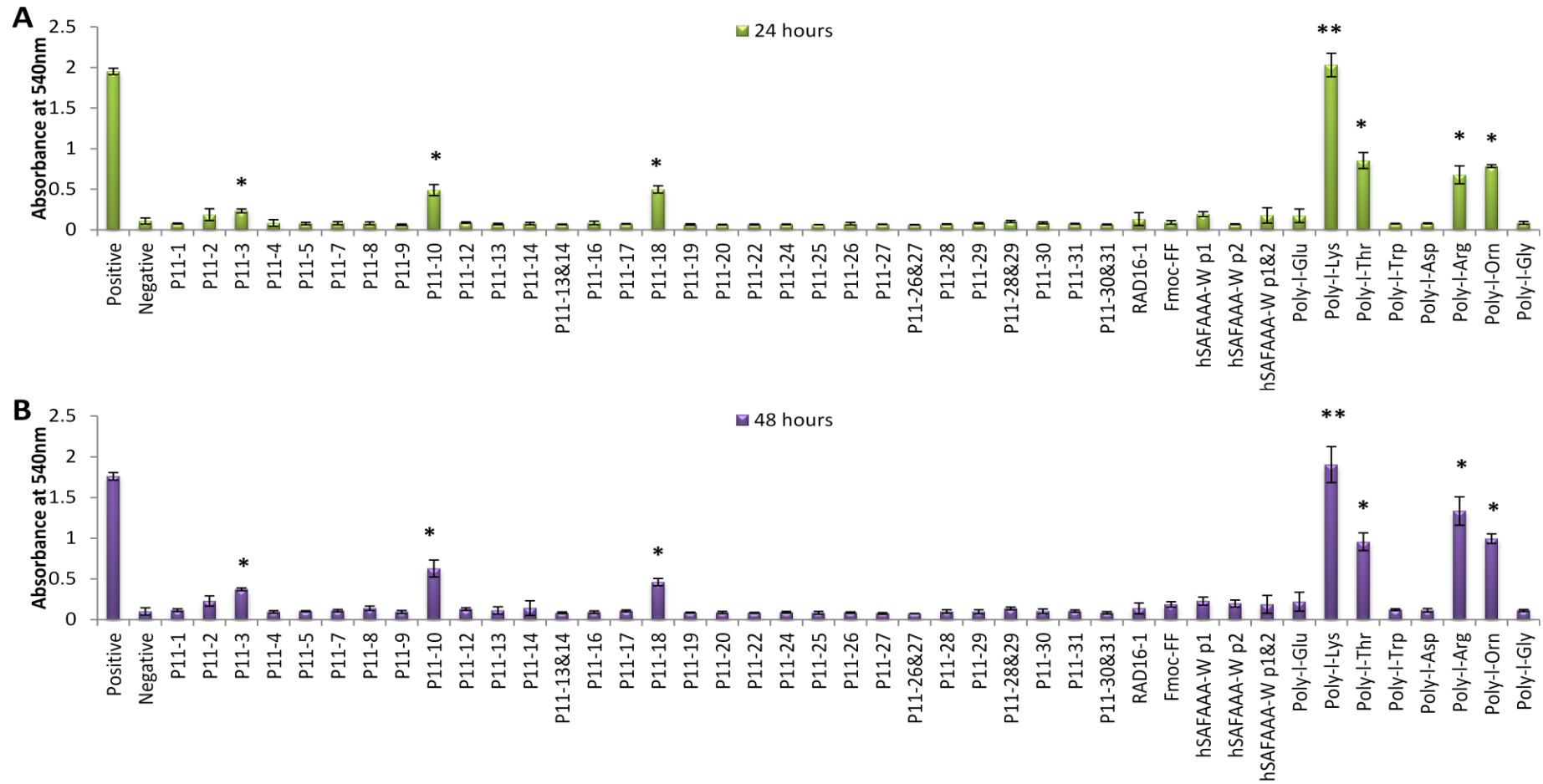


Figure 4.8; Haemolytic effects of peptides after A; 24 hours, B; 28 hours; Positive control water, Negative control Ringer's solution. Data is presented as the mean (n=6) \pm 95 % confidence intervals. Data was analysed by one way analysis of variance followed by determination of the MSD ($p < 0.05$). * = significant difference from negative control, ** = significant difference from negative control and no significant difference from positive control.

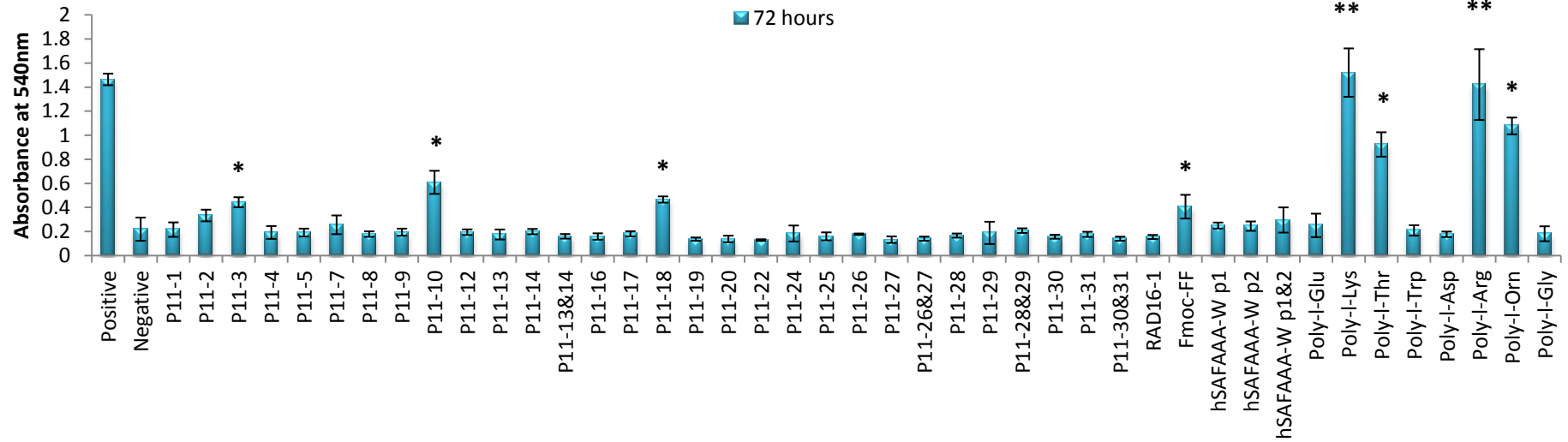


Figure 4.9; Haemolytic effects of peptides after 72 hours; Positive control water, Negative control Ringer's solution. Data is presented as the mean (n=6) ± 95 % confidence intervals. Data was analysed by one way analysis of variance followed by determination of the MSD ($p < 0.05$). * = significant difference from negative control, ** = significant difference from negative control and no significant difference from positive control.

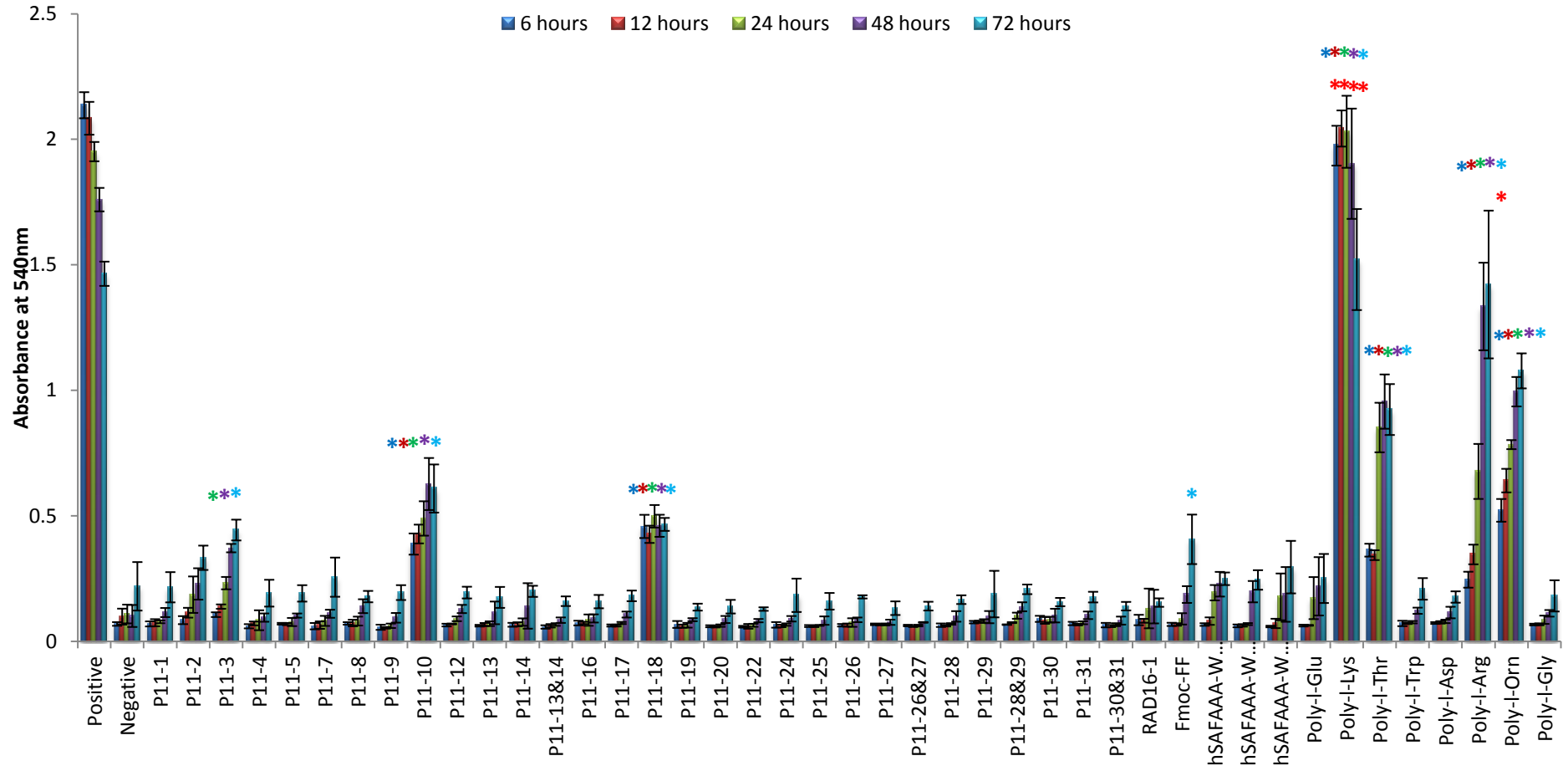


Figure 4.10; Haemolytic effects of peptides; Positive control water, Negative control Ringer's solution; Data is presented as the mean (n=6) \pm 95 % confidence intervals. Data was analysed by one way analysis of variance followed by determination of the MSD ($p < 0.05$). Coloured stars denote a significant difference from the negative control, Red stars denote no significant difference from the positive control.

All peptide solutions formed clear or cloudy white solutions except for poly-l-threonine (Thr) which was brown in colour. The samples of erythrocytes mixed with peptide and the controls were all red in colour except for poly-l-threonine (Thr) which was brown/gray in colour. Difficulty was observed dissolving peptides Fmoc-diphenylalanine (Fmoc-FF), poly-l-tryptophan (Trp) and polyglycine in Ringer's solution.

The results presented in Figure 4.7, Figure 4.8, Figure 4.9 and Figure 4.10 showed that the level of haemoglobin released from sheep erythrocytes in contact with the majority of the peptide solutions at various time points was not significantly different from the level of haemoglobin detected in the negative, spontaneous lysis, control. This low level of detected haemoglobin indicated that there had been little to no lysis of the sheep erythrocytes caused by interaction of the peptides with the erythrocyte cell membrane. After 6 and 12 hours incubation at 37°C (Figure 4.7 graph A & B) P₁₁-10, P₁₁-18, poly-l-lysine (Lys), poly-l-threonine (Thr), poly-l-arginine (Arg) and poly-l-ornithine (Orn) showed a level of haemoglobin in solution that was significantly greater than the negative control indicating that haemolysis had occurred. After 24 hours at 37°C (Figure 4.8 graph A) P₁₁-3 and after 72 hours at 37°C (Figure 4.9) Fmoc-diphenylalanine (Fmoc-FF) showed a level of haemoglobin in solution that was significantly greater than the negative control indicating that haemolysis had occurred.

The release of haemoglobin into a solution in the presence of poly-l-lysine (Lys) after 12 hours (Figure 4.7 graph B) and poly-l-arginine (Arg) after 72 hours (Figure 4.9) showed no significant difference from the positive, total lysis control. The level of haemoglobin released into solution for all other peptides was significantly lower than the positive control. The results in Figure 4.10 showed that the level of haemoglobin in all solutions gradually increased over the observed time period with the exception of solutions of poly-l-lysine (Lys) and the positive control. The haemoglobin released in a solution in the presence of poly-l-arginine (Arg) showed the most noticeable increase over time.

The results from the haemolysis assay showed that the majority of peptides solutions resulted in no significant level of haemolysis. The results from the haemolysis assay showed that solutions of peptides P₁₁-3, P₁₁-10, P₁₁-18, poly-l-lysine (Lys), poly-l-arginine (Arg) and poly-l-ornithine (Orn) all interacted destructively with the erythrocyte membrane causing haemolysis and the release of haemoglobin into solution. Due to the differences observed for poly-l-threonine (Thr) it is not possible to say if haemoglobin had been released.

4.3.4 Peptide complement inhibition

The haemolytic nature and results of the haemolysis assay indicated that homo-polypeptides poly-l-lysine (Lys), poly-l-threonine (Thr), poly-l-arginine (Arg) and poly-l-ornithine (Orn) could not be tested for complement inhibition using this method. To determine the dilution of the serum needed to achieve 50 % lysis a CH50 assay was performed (Section 2.2.17.1). The results of the CH50 assay (Appendix Figure A.4) were used to determine the dilution of serum to be used in complement inhibition testing. Complement inhibition testing was performed as described in Section 2.2.17.2. Results for inhibition of complement activation (absorbance at 540 nm) were recorded and an average of the blank control for each peptide was subtracted from the each result. Results were collected, graphed and analysed for significant statistical difference by one-way ANOVA and post hoc analysis (Section 2.2.21.2). Results are presented in Figure 4.11 and Figure 4.12 as a series of graphs with test peptides plus the relevant positive and negative controls.

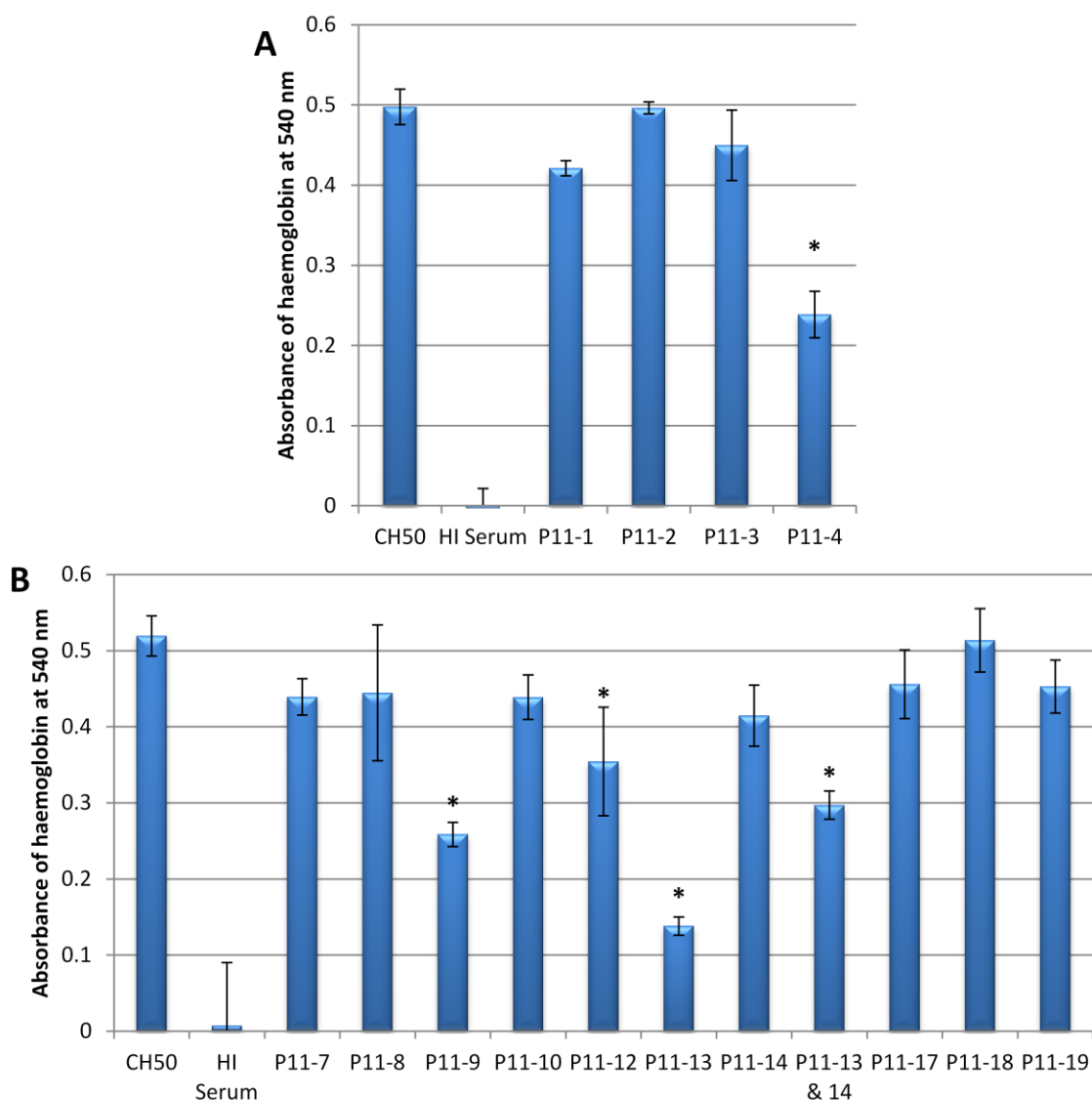


Figure 4.11; Complement inhibition by peptides; CH50 negative control, HI (heat inactivated) serum positive control. Data is presented as the mean (n=6) \pm 95 % confidence intervals. Data was analysed by one way analysis of variance followed by determination of the MSD ($p < 0.05$). *= Significant difference from negative control.

All peptide solutions formed clear or cloudy white solutions; when mixed with erythrocytes the mixtures were all red in colour and no difficulty was experienced dissolving the peptides in Ringer's solution.

The results in Figure 4.11 showed that the level of free haemoglobin detected in the presence of P₁₁-1, P₁₁-2, P₁₁-3, P₁₁-7, P₁₁-8, P₁₁-10, P₁₁-14, P₁₁-17 P₁₁-18 and P₁₁-19 showed no significant difference to the negative, CH50, controls. The results presented in Figure 4.11 graph A showed there was a significant reduction in the level of free haemoglobin detected in a

solution of P₁₁-4 compared to the negative control. The results presented in Figure 4.11 graph B showed a significant reduction in the level of free haemoglobin detected in the presence of peptides P₁₁-9, P₁₁-12, P₁₁-13 and complementary peptides P₁₁-13 & 14 compared to the negative control. The level of free haemoglobin detected in all solutions presented in Figure 4.11 was significantly higher than the level of free haemoglobin detected in the relevant, heat inactivated serum, positive controls.

The results in Figure 4.11 showed that peptides P₁₁-1, P₁₁-2, P₁₁-3, P₁₁-7, P₁₁-8, P₁₁-10, P₁₁-14, P₁₁-17 P₁₁-18 and P₁₁-19 had no inhibitory effect upon the complement system. The results in Figure 4.11 also showed peptides P₁₁-4, P₁₁-9, P₁₁-12, P₁₁-13 and complementary peptides P₁₁-13 & 14 had an inhibitory effect on the complement system, lowering the level of complement mediated lysis, but did not fully inhibit the complement system.

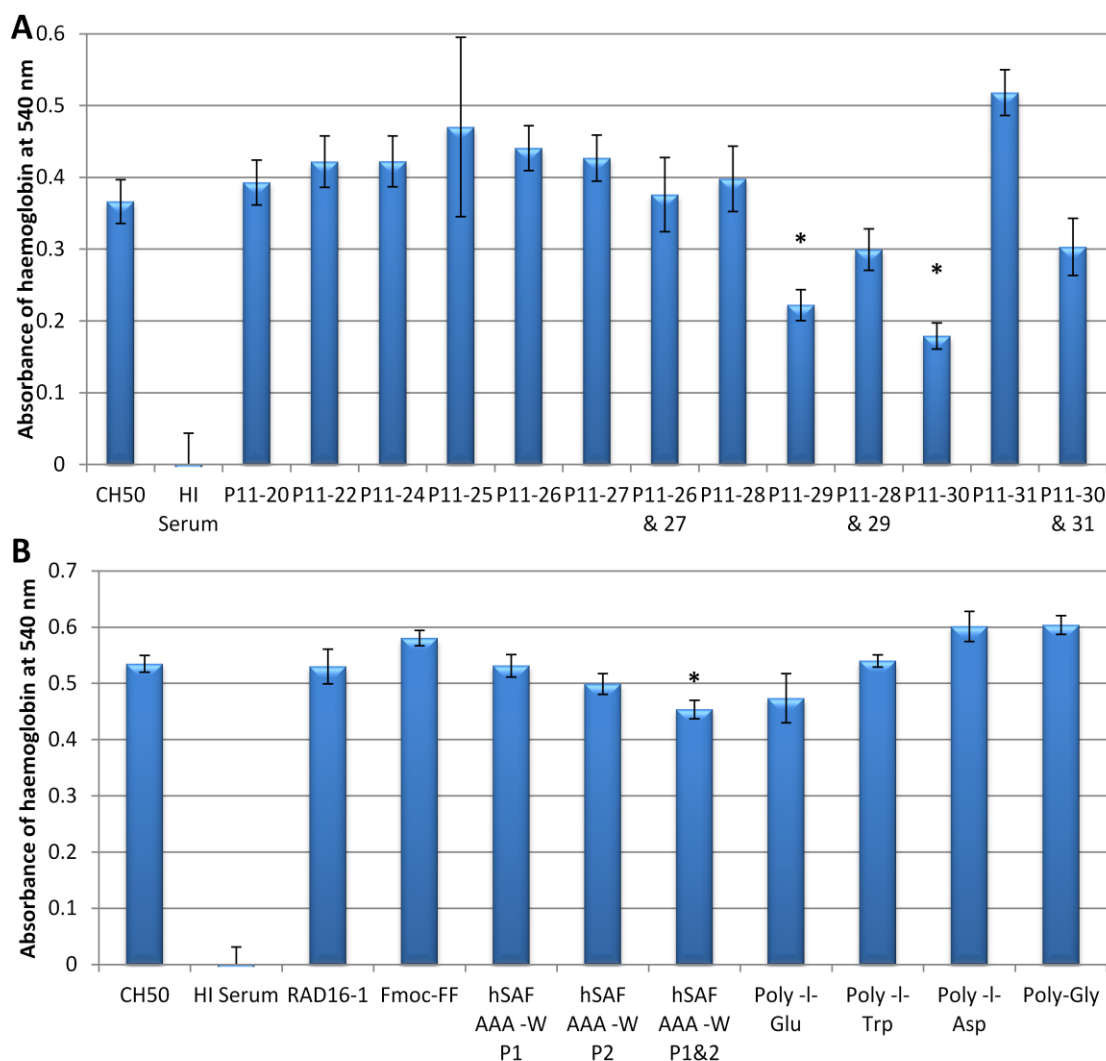


Figure 4.12; Complement inhibition by peptides; CH50 negative control, HI (heat inactivated) serum positive control. Data is presented as the mean (n=6) \pm 95 % confidence intervals. Data was analysed by one way analysis of variance followed by determination of the MSD ($p < 0.05$). *= Significant difference from negative control.

All peptide solutions formed clear or cloudy white solutions; when mixed with erythrocytes the mixtures were all red in colour. Difficulty was experienced dissolving peptides Fmoc-FF and homo-polypeptides Poly-l-Trp and polyglycine in Ringer's solution.

The results shown in Figure 4.12 indicated that the level of free haemoglobin detected in the presence of P₁₁-20, P₁₁-22, P₁₁-24, P₁₁-25, P₁₁-26, P₁₁-27, P₁₁-28, P₁₁-31, RAD16-1, Fmoc-FF, hSAF_{AAA-W} P1, hSAF_{AAA-W} P2, poly-l-glutamic acid (Glu), poly-l-tryptophan (Trp), poly-l-aspartic acid (Asp), polyglycine and complementary peptides P₁₁-26 & 27, P₁₁-28 & 29 and P₁₁-30 & 31 showed no significant difference to the negative, CH50, controls. The results in Figure 4.12

graph A showed there was a significant reduction in the level of free haemoglobin detected in the presence of peptides P₁₁-29 and P₁₁-30 compared to the negative control. The results in Figure 4.12 graph B showed there was a significant reduction in the level of free haemoglobin detected in solution between complementary peptide hSAF_{AAA-W} P1 & P2 and the negative control. The level of free haemoglobin detected in solution for all the peptides was significantly higher than the level of haemoglobin detected in the relevant positive, heat inactivated serum, controls.

The results in Figure 4.12 showed that peptides P₁₁-20, P₁₁-22, P₁₁-24, P₁₁-25, P₁₁-26, P₁₁-27, P₁₁-28, P₁₁-31, RAD16-1, Fmoc- diphenylalanine (Fmoc-FF), hSAF_{AAA-W} P1, hSAF_{AAA-W} P2, poly-l- glutamic acid (Glu), poly-l-tryptophan (Trp), poly-l-aspartic acid (Asp), polyglycine and complementary peptides P₁₁-26 & 27, P₁₁-28 & 29 and P₁₁-30 & 31 had no inhibitory effect upon the complement system. The results in Figure 4.12 showed that peptides P₁₁-29, P₁₁-30 and complementary peptide hSAF_{AAA-W} P1 & P2 had an inhibitory effect on the complement system, lowering the level of complement mediated lysis, but did not fully inhibit the complement system.

4.4 Discussion

For biomedical applications, self-assembling peptides must be biocompatible. For many applications the peptide will also need to be haemocompatible. The aim of this study was twofold; to ascertain which of the many peptides developed at the University of Leeds was best suited for application in vascular tissue engineering and to determine any design characteristics indicative of peptide bio and haemo compatibility to aid in the future development of self-assembling peptides for biomedical applications. There have been numerous potential uses of self-assembled peptides reported in the literature however no attempts to determine design characteristics for biomedical use have been reported.

In order to make comparisons between different sized peptides it was desirable to test the same concentration of each peptide. The range of structures formed as peptides self-assemble are concentration dependent. Thus one peptide can form a self-assembled gel at a particular concentration and another peptide can form a monomeric solution at the same concentration. This difference in self-assembly would present difficulties in interpreting results of peptides

tested therefore all peptide solutions were tested at a concentration of 0.3 mol.m^{-3} at which the majority of peptides in solution were in monomeric or soluble aggregate form.

4.4.1 Effects of peptides on cell growth

In vitro biocompatibility testing was carried out to establish the cytocompatibility of the peptides. The peptides were tested in accordance with ISO 10993-5. The peptides were evaluated using extract cytotoxicity testing by growing BHK and 3T3 cell lines in peptide solutions for 72 hours. Cell viability was determined using the ATPLite-M[®] assay. The majority of peptides were biocompatible with no effect upon BHK and 3T3 cell growth. This was probably a result of the peptides being short sequences of natural amino acids; some of which were based off natural protein fragments.

Some of the cells grown in the peptide solutions showed a significant increase in ATP levels; suggesting an increase in cell proliferation in some of the peptide solutions. Both BHK and 3T3 cells proliferated more than the negative controls in solutions of P₁₁-24, P₁₁-25, P₁₁-30, poly-l-tryptophan and poly-l-aspartic acid. Several of the peptide solutions induced a higher level of ATP in one of the two cell lines. There was a significant increase in the level of ATP produced by 3T3 cells grown in solutions of peptides P₁₁-4, P₁₁-5, P₁₁-9, P₁₁-12, P₁₁-16, P₁₁-17, P₁₁-18, P₁₁-31, hSAF_{AAA-W} P1, hSAF_{AAA-W} P2, polyglycine and complementary peptides P₁₁-30&31 and hSAF_{AAA-W} P1 & P2. A significant increase in BHK cell growth was also recorded in solutions of peptides P₁₁-8, P₁₁-19, P₁₁-20, P₁₁-28, P₁₁-29, poly-l-glutamic acid and complementary peptides P₁₁-26&27.

Since surface area, wettability and charge play an important role in cell attachment and proliferation it is possible that the peptides affected the surface of the cell culture plastic in a positive manner to allow for increased cell adhesion and proliferation (Webb et al., 1998, Arima and Iwata, 2007). Adsorption of peptide onto the tissue culture plastic can change the wettability of the surface. Surface wettability changes the ability of cells to attach to a surface and different cells respond differently to changes in surface wettability (Tan et al., 2004, Arima and Iwata, 2007).

Differences in the level of ATP could also have been the result of the peptide having effects on molecular and regulatory mechanisms in the cells. Amino acid starvation has been shown to affect DNA synthesis and it is believed that mechanisms exist in cells that arrest cell growth if

nutrients are in poor supply (Holley and Kiernan, 1974, Melvin et al., 1979). It is possible that as the cells reached confluence they had depleted the amino acid supply in the serum and that the peptides were acting as an extra source of amino acids.

Cell proliferation involves a balance between positively and negatively acting signals, a change to the quiescent state induces metabolic changes that are necessary for cell survival under conditions inadequate for proliferation; this is believed to be in part controlled by a set of growth arrest-specific (*gas*) genes whose expression is negatively regulated by serum (Manfioletti et al., 1990). The activation of *gas* genes changes the metabolic activity of a cell. In nutrient poor conditions levels of cellular ATP may change in order to protect cell viability. It is possible that mechanisms of cell cycle arrest were being activated in the negative control at an earlier time point than in cultures with peptide solutions, in which the peptide was acting as a source of amino acids expanding the time to cell cycle arrest. This explanation raises the question of why not all the peptides act as a source of amino acids. This in turn could be explained by the different peptide sequences where the cells may not have been able to use all the peptides if they did not contain cleavable sequences.

ATP levels can also vary depending upon cellular activation (Crouch et al., 1993). It is possible that the peptide solutions activated, enhanced, prevented or stabilised some molecular pathway in the cells and increased the level of cellular ATP without increasing the number of cells present. The presence of the peptide could also have induced phenotypic change in the cells. Cells attached to RAD16-1 have been shown not to spread out, as on the more rigid tissue culture plastic, but to remain rounded indicating different cell behaviour on the different materials that could have an effect upon cellular levels of ATP (Zhang et al., 1995). It is not clear which if any of these effects resulted in the higher levels of ATP detected, it is possible that one or more of the effects could have combined to give these results. Further studies are needed in order to establish how these peptide solutions affect cultured cells and if this effect is translatable into higher concentration peptide solutions and peptide gels.

The results of the extract cytotoxicity testing showed mixed results for some peptide solutions. Peptides P₁₁-1, P₁₁-10, P₁₁-16 and hSAF_{AAA-W} P1 supported significantly reduced BHK cell growth compared to the negative GMEM control. The growth of 3T3 cells in solutions of peptides P₁₁-1, P₁₁-10, P₁₁-16 and hSAF_{AAA-W} P1 showed no significant difference to the negative DMEM control. This suggested that these peptides were not toxic and that the reduced BHK cell growth could have been the result of anomalous results or a cell specific effect due to the different growth conditions of BHK and 3T3 (O'Neill et al., 1979). The different growth

conditions needed for 3T3 and BHK cells could also possibly explain why in some peptide extracts one cell type had a significantly higher level of ATP than the other cell type when compared to the negative controls.

The growth of BHK cells in a solution of Fmoc-diphenylalanine showed levels of cell growth that were significantly lower than the negative control. Solutions of Fmoc-diphenylalanine were toxic to 3T3 cells but not as toxic to BHK cells. In addition to measurement of effects on cell proliferation and number the ATP assays may also provide information about sub-lethal cell damage. ATP is necessary for cell function and ATP production is depressed by many forms of cell stress (Cree and Andreotti, 1997). ATP can be used to test for first-order toxicity in cell lines and has been shown to have a high level of sensitivity to toxic agents, with the level of cellular ATP being reduced (Pasternak and Miller, 1995). This means that cells that are damaged in some way but not killed could show a significantly lower level of ATP compared to the negative control but a significantly higher level of ATP compared to the positive control. This suggested that Fmoc-diphenylalanine could have a cell dependent cytotoxic effect. This is supported in the literature where Fmoc-diphenylalanine has been observed to support the growth of chondrocytes but inhibit the growth of human dermal fibroblasts and 3T3 cells (Jayawarna et al., 2009).

Cytotoxicity testing showed that the positive homo-polypeptides poly-L-lysine, poly-L-arginine and poly-L-ornithine were cytotoxic to both cell types. It has been previously demonstrated that poly-cations can bind to the surfaces of animal cells and produce toxic effects (Fischer et al., 2003). Using electrophoretic mobility testing this binding has been shown to be charge related, with the positive cations neutralising the natural negative anions on the surface of a cell and so changing cell mobility (Mayhew et al., 1973). It has been shown that poly-cations cause disruption to a cell membrane, at low concentrations and low molecular weights. This is a reversible process and has been investigated as a method of inserting genetic material into cells (Mayhew et al., 1973, Kabanov and Kabanov, 1995). A charge relationship has been observed related to cytotoxicity but a size relationship has also been observed that is likely linked to membrane disruption. High molecular weight poly-L-lysine has been shown to be cytotoxic whereas lower molecular weight poly-L-lysine has been shown to be less toxic (Mayhew et al., 1973, Fischer et al., 2003). This could explain why poly-L-lysine, poly-L-arginine and poly-L-ornithine were cytotoxic but the much smaller positively charged peptides in the P₁₁ series were not.

4.4.2 Effects of peptides on thrombus formation

The thrombogenic potential of the peptides was assessed using the modified Chandler loop model. The majority of thrombi formed in the different peptide solutions showed no significant difference from the negative control without peptide indicating that the monomeric peptides had no effect upon thrombus formation.

Peptides RAD16-1, poly-l-threonine, poly-l-tryptophan and complementary peptide hSAF_{AAA-W} P1 & P2 showed a significant increase in the size of the thrombus formed compared to the negative control indicating that these peptides had an effect upon thrombus formation. The thrombi formed with the addition of poly-l-threonine, poly-l-tryptophan and complementary peptide hSAF_{AAA-W} P1 & P2 showed no significant difference compared to the positive control of human α -thrombin. The thrombi formed in the presence of RAD16-1 were significantly smaller than the positive control. This indicated that whilst RAD16-1 increased thrombus formation the effect was not as marked as the effect of α -thrombin whereas peptides poly-l-threonine, poly-l-tryptophan and complementary peptide hSAF_{AAA-W} P1&2 resulted in thrombi that were indistinguishable from those formed by α -thrombin. It is important to note that the blood coagulation pathway is complex with several activators, inhibitors, molecular and cellular pathways involved in thrombus formation and hence there are several possible explanations as to the cause of these effects.

The peptides could have triggered part of the blood clotting cascade by directly activating blood clotting. This was unlikely as there are wide differences in the peptide structure and size of RAD16-1, poly-l-threonine, poly-l-tryptophan and complementary peptide hSAF_{AAA-W} P1 & P2. There is also evidence in the literature that RAD16-1 has no effect upon levels of pro-thrombin which would be expected if it directly triggered blood clotting (Song et al., 2009). However, based upon these results, direct triggering of blood clotting could be ruled out.

The most likely explanation is that the peptides had an effect upon the blood clotting cascade that was reducing the time for clot formation. The added peptide could have increased the stability or activity of one of the functional components in the clotting cascade and so reduced clotting time. It is possible that the peptides could have inhibited one of the regulatory systems that maintain haemostasis, shortening the coagulation time as has been observed for antibodies that bind regulatory protein C (Hwang et al., 2003).

The peptides could have interacted with the formation of the clot. The peptides could have increased the rate of fibrin formation, through protein induced enhancement in the enzymatic activity of clotting factors such as thrombin, co-assembly of added peptide with fibrin/fibrinogen or by non-specific steric volume exclusion increasing the fractional concentration of fibrin and other coagulation factors in solution. Thrombin is capable of a range of activities and is known to be able to cleave 12 substrates; thrombin recognition is largely controlled by cofactors that can have a pro-coagulation or anti-coagulation effect; glycoprotein Iba, fibrin and Na⁺ are known to be pro-coagulant cofactors (Adams and Huntington, 2006). It is possible that the peptides bound to one of the enzymes such as thrombin involved in the coagulation pathway and enhanced the activity of the enzyme, decreasing clotting time in a similar manner to the binding of other cofactors.

Fibrin self-assembly has been shown to be influenced by temperature, pH and ionic concentration. Changes in the pH, ionic concentration and temperature change the energetics of the system and change the fibrin structures that are formed. pH and ionic concentration have been shown to influence fibrin assembly but temperature has been shown to influence the rate of fibrin monomer generation and assembly (Nair et al., 1986). The energetics of the system can also be altered by the introduction of a template or molecule that allows for co-assembly. Proteins and peptides are known to preferentially self-assemble at the surface of a material or on a template as the energetics of the system are lower at surfaces. Thus self-assembly will start at an interface with preference to in solution (Taylor and Osapay, 1990, Wattenbarger et al., 1990). In a similar manner if a peptide acted as a template or co-assembled with fibrin in solution the peptide would lower the energetic barrier to fibrin assembly increasing the rate of thrombus formation. Neutral surfaces have been shown to facilitate higher rates of fibrin assembly compared to negatively and positively charged surfaces (Wang et al., 2007a).

Steric exclusion occurs when interaction between non-reactive solutes results in an exclusion zone around the solute where other solute molecules are deficient compared to the concentration in bulk solution (Lee et al., 2012). This is influenced by the hydrodynamic radius of the excluding species and is related to the concentration and size of the solute added to the solution. As the other solutes are excluded from the area around the non-reactive solute the bulk solution has a higher concentration of solute; the discontinuity between the two zones leads to an increase in free energy that drives redistribution of the solutes within the system to a lower energy level (Lee et al., 2012). In this case the presence of the peptides could have

caused steric exclusion of the clotting factors, increasing the concentration of platelets and proteins such as fibrin in solution; the unfavourable increase in free energy could have driven the redistribution of fibrin and other clotting factors to a more favourable lower energy state where they formed a clot. Steric exclusion of fibrin and other clotting factors from volume following addition of neutral/inert polymer has been reported to have resulted in a decrease in fibrin clotting time (Minton, 1983, Wilf et al., 1985).

It is possible to see a general relationship between RAD16-1, poly-l-threonine, poly-l-tryptophan and complementary peptide hSAF_{AAA-W} P1 & P2; with all the peptides having a neutral charge. Size also appears to be a factor in the propensity of a peptide to increase thrombus formation. Several of the P₁₁ series of peptides have a net neutral charge but show no effect on thrombus formation; RAD16-1 larger than the P₁₁ series of peptides showed a significant increase in thrombus formation compared to the negative control but was still significantly below the positive control. Peptides poly-l-threonine, poly-l-tryptophan and complementary peptide hSAF_{AAA-W} P1 & P2 are all significantly larger than RAD16-1 and the P₁₁ series of peptides and showed no significant difference from the positive control. These results suggested that a neutral charge and increased size accelerated the rate of thrombus formation. This observed effect would suggest a direct effect of the peptides in increasing the stability or activity of one of the components in the clotting cascade was unlikely. Larger size should not increase the interaction of a peptide with clotting factors but would be expected to have the opposite effect as spatial orientation would become a major issue. However, there is not enough available information to rule this out.

The size related effect would suggest that the peptide could have co-assembled with the fibrin or acted as a template as a larger size would allow for greater stability. The size relationship would also support the idea of steric exclusion as a larger peptide would take more space in solution and so increase the concentration of the platelets and proteins such as fibrin. However, the molar concentrations at which the effects were observed were very low and it is questionable whether volume exclusion events could have occurred. Given the limited data it is not possible to speculate what specifically accounted for the observed effect.

Peptide blood mixtures of poly-l-lysine, poly-l-arginine and poly-l-ornithine all failed to form thrombi in the modified Chandler loop model. This result did not indicate anti-clotting activity related to these peptides but was the result of the peptides causing blood cell agglutination. Poly-l-lysine, poly-l-arginine and poly-l-ornithine are all large highly positively charged peptides. It has been demonstrated that positively charged poly-l-lysine can interact with the

naturally occurring negative charge on the surface of red blood cells causing agglutination (Karchalsky et al., 1959, Marikovsky and Danon, 1969). Rats injected with poly-L-lysine all died after injection due to the agglutination of their blood (de Vries et al., 1953). This appeared to be a size related effect as the smaller positively charged peptides in the P₁₁ series had no significant effect upon the size of the thrombus formed. The size relationship of this effect is understandable as the smaller peptides may not be long enough to link adjacent cells and cause agglutination.

4.4.3 Effects of peptides on haemolysis of ovine erythrocytes

The interaction of peptides with cell surface membranes was assessed using a haemolysis assay. Erythrocytes act as a model standard cell membrane; with the advantage that haemoglobin can easily be detected in solution following release due to cell lysis. The majority of peptides showed no significant haemolytic activity over a 72 hour period indicating that the peptides were not haemolytic at the concentration tested.

Peptides will cause haemolysis by some form of peptide membrane interaction. In nature there are a range of lytic peptides that form part of the normal defence and life cycle of a wide range of organisms. Most well known are the antibacterial peptides but there are examples of peptides against mammalian cells, for example hemolysin from *Staphylococcus aureus*, and some that do not distinguish between cell types (Shai, 1999). There are several proposed modes of peptide membrane interaction. Many involve the formation of α -helix structures and so are not relevant to the majority of the peptides tested.

The three proposed models of most interest are the "carpet" model, the β -barrel-stave model and the toroidal model. According to the "carpet" model the peptides initially bind onto the cell membrane by electrostatic interaction, hence the peptides are positively charged, the peptides preferentially bind to the phospholipid head groups and align along the surface of the membrane; the rotation of the peptide leads to reorientation of the hydrophobic residues towards the hydrophobic core of the membrane disrupting the bilayer curvature (Shai, 1999). The β -barrel-stave model describes peptides that assemble on the cell membrane and insert into the phospholipid bilayer and form self-assembled pores similar to β -sheet transmembrane proteins (Protopapa et al., 2009). The toroidal model describes how peptides assemble on the cell membrane and then insert into the phospholipid bilayer, unlike the β -barrel-stave model

the peptide does not form a pore but causes the phospholipid bilayer to bend back on itself creating a phospholipid surrounded pore (Ludtke et al., 1996, Protopapa et al., 2009). The “carpet” model causes direct disruption of the cell membrane where the β -barrel-stave and toroidal models create pores in the membrane that allow for the free passage of water and ions into the cell and cause cell rupture.

After 6 and 12 hours P₁₁-10, P₁₁-18, poly-l-lysine, poly-l-threonine, poly-l-arginine and poly-l-ornithine all showed haemolytic activity. After 24 hours P₁₁-3 also showed haemolytic activity. Peptides P₁₁-3, P₁₁-10, P₁₁-18, poly-l-lysine, poly-l-threonine, poly-l-arginine and poly-l-ornithine all showed haemolytic activity at 24, 48 and 72 hour time points. At 72 hours Fmoc-diphenylalanine also showed haemolytic activity. Poly-l-lysine and poly-l-arginine showed haemolytic activity which was not significantly different to the positive control. Poly-l-lysine, poly-l-arginine and poly-l-ornithine are all positively charged and it has been observed that poly-cationic materials cause membrane disruption in relation to the molecular weight of the poly-cationic material with higher molecular weight materials having a more pronounced effect (Mayhew et al., 1973). This size dependency was observed in this study, where the larger poly-l-lysine was indistinguishable from the positive control after 12 hours and the smaller poly-l-arginine was significantly lower than the positive control until 72 hours and poly-l-ornithine remained significantly lower than the positive control at 72 hours. Whilst it is not possible to state which model is having an effect, it is likely that poly-l-lysine, poly-l-arginine and poly-l-ornithine all caused haemolysis by the “carpet” model.

The haemolytic effect of poly-l-threonine was questionable as the peptide solution was naturally brown in colour and the blood solution was turned brown by the addition of poly-l-threonine. The erythrocytes in poly-l-threonine did not remain red as in the other peptide solutions but became brown/gray in colour suggesting a more significant change was happening in the solution of poly-l-threonine.

The method by which P₁₁-3, P₁₁-10 and P₁₁-18 caused haemolysis is unknown; there is no charge, hydrophobicity or amino acid relationship between the peptides; P₁₁-3 has a charge of +1 and is based on the amino acid glutamine, P₁₁-18 has a charge of +2 and is based on the amino acid threonine and P₁₁-10 has a neutral charge and is based on the amino acid asparagine. The structure of the P₁₁ series of peptides is very similar for each peptide with several sharing a similar hydrophobic core structure and none of which show any significant levels of haemolysis. It was possible that these tests could have been infected with a microorganism that caused haemolysis; however, this was unlikely due to the limited

haemolysis observed. It was possible that peptides P₁₁-3, P₁₁-10 and P₁₁-18 had a specific amino acid sequence that interfered with the cell membrane by one of the three models described above. For example, they could have formed a β -barrel structure in the cell membrane resulting in the release of haemoglobin and that only the low peptide concentration prevented higher levels of haemolysis. The result observed for Fmoc-diphenylalanine at 72 hours is likely the result of the natural lysis of the washed erythrocytes.

4.4.4 Complement inhibition

Complement inhibition was assessed using a modified CH50 assay. The results showed that peptides P₁₁-4, P₁₁-9, P₁₁-12, P₁₁-13, P₁₁-29, P₁₁-30 and complementary peptides P₁₁-13 & 14 and hSAF_{AAA-W} P1 & P2 lowered the level of complement mediated lysis and so had an inhibitory effect upon the complement system.

Peptides P₁₁-4, P₁₁-9, P₁₁-13, P₁₁-29, P₁₁-30 and complementary peptide P₁₁-13 & 14 all have similar design characteristics; the peptides all have a net negative charge equal to or greater than two. It has been shown that poly-anionic materials have several effects upon the complement system. Poly-anionic materials are known to inhibit complement C1; mainly by binding to complement C1q (Raepple et al., 1976). Poly-anionic materials have been shown to reversibly inhibit consumption of complements C2 and C4 by C1esterase in a concentration dependent manner; it is proposed that this is achieved by competitive binding of the poly-anionic material at the enzyme binding site (Loos et al., 1976). Poly-anionic materials have also been shown to have an inhibitory effect upon complement C4 (Raepple et al., 1976). Several of the P₁₁ series of peptides, P₁₁-20, P₁₁-24 P₁₁-25 and P₁₁-27, are poly-anionic but showed no inhibitory effect in the modified CH50 test. The main group of inhibitory peptides and the non-inhibitory peptides share a poly-anionic charge, however, they have a distinct difference in their structure. Peptides P₁₁-4, P₁₁-9, P₁₁-13, P₁₁-29, P₁₁-30 and complementary peptide P₁₁-13 & 14 all have a hydrophobic core based around phenylalanine and tryptophan whereas peptides P₁₁-20, P₁₁-24 P₁₁-25 and P₁₁-27 do not. This result suggests that hydrophobicity plays a part in complement inhibition.

It has been shown that hydrophobic residues in charged compounds enhance complement inhibition activity; it is believed that the hydrophobic units protect the charged groups from aqueous media and so enhance the electrostatic interaction between the compound and

target complement; it has been shown that hydrophobic residues are most effective in the middle of the inhibitory molecule (Bureeva et al., 2005). As the literature suggests that these materials have inhibitory effects upon complements C1, C2 and C4 the inhibitory effect could be limited to the classical complement pathway and would require testing to assess the effect upon the alternative pathway. The ability to inhibit the classical pathway could be an advantage as the classical complement pathway is the major cause of complement related tissue damage; the ability to target only the classical pathway would spare the alternative and lectin pathways that are involved in innate immunity against pathogens (Mollnes et al., 2002).

The evidence that poly-anionic materials with a hydrophobic core inhibit the complement system did not explain the results observed for P₁₁₋₁₂ and complementary peptide hSAF_{AAA-W} P1 & P2. It is possible that the results observed for P₁₁₋₁₂ and hSAF_{AAA-W} P1 & P2 were due to the specific amino acid sequences of the two peptides being able to bind to some functional site on one of the complement proteins in the pathway. It is also possible that the peptides interfered with the normal mechanism of complement mediated cell lysis. The peptide could have prevented the binding of complement to the cell surface, it is also possible that the peptide could have interfered with antibody binding and so prevented activation of the complement system in the CH50 test.

4.4.5 Design characteristics

BHK cell growth	3T3 cell growth	Thrombus formation	Haemolysis	Complement inhibition
P ₁₁ -1				
P ₁₁ -2				
P ₁₁ -3				
P ₁₁ -4				
P ₁₁ -5				
P ₁₁ -7				
P ₁₁ -8				
P ₁₁ -9				
P ₁₁ -10				
P ₁₁ -12				
P ₁₁ -13				
P ₁₁ -14				
P ₁₁ -13 & 14				
P ₁₁ -16				
P ₁₁ -17				
P ₁₁ -18				
P ₁₁ -19				
P ₁₁ -20				
P ₁₁ -22				
P ₁₁ -24				
P ₁₁ -25				
P ₁₁ -26				
P ₁₁ -27				
P ₁₁ -26 & 27				
P ₁₁ -28				
P ₁₁ -29				
P ₁₁ -28 & 29				
P ₁₁ -30				
P ₁₁ -31				
P ₁₁ -30 & 31				
RAD16-1	RAD16-1	RAD16-1	RAD16-1	RAD16-1
Fmoc-FF	Fmoc-FF	Fmoc-FF	Fmoc-FF	Fmoc-FF
hSAF AAA-W P1				
hSAF AAA-W P2				
hSAF AAA-W P1 & 2				
Poly-l-Glutamic acid				
Poly-l-Lysine	Poly-l-Lysine	Poly-l-Lysine	Poly-l-Lysine	Poly-l-Lysine
Poly-l-Threonine	Poly-l-Threonine	Poly-l-Threonine	Poly-l-Threonine	Poly-l-Threonine
Poly-l-Tryptophan	Poly-l-Tryptophan	Poly-l-Tryptophan	Poly-l-Tryptophan	Poly-l-Tryptophan
Poly-l-Aspartic acid				
Poly-l-Arginine	Poly-l-Arginine	Poly-l-Arginine	Poly-l-Arginine	Poly-l-Arginine
Poly-l-Ornithine	Poly-l-Ornithine	Poly-l-Ornithine	Poly-l-Ornithine	Poly-l-Ornithine
Polyglycine	Polyglycine	Polyglycine	Polyglycine	Polyglycine

Cell Growth	Increased cell growth	No effect on cell growth	Decreased cell growth	Cytotoxic
Thrombus formation	Large increase in thrombus	Increase in thrombus	No effect on thrombus	Blood agglutination
Haemolysis	No haemolysis	Haemolysis	Total haemolysis	
Complement inhibition	No inhibition	Inhibition	Not tested	

Table 4-2; Collected results of biocompatibility and haemocompatibility testing

The majority of peptides investigated in this study were shown to be biocompatible and haemocompatible. Peptides RAD16-1, poly-l-threonine, poly-l-tryptophan and complementary peptide hSAF_{AAA-W} P1 & P2 were shown to be biocompatible but had an effect upon thrombus formation. Several peptides, poly-l-lysine, poly-l-arginine and poly-l-ornithine were identified not to be biocompatible or haemocompatible. Several peptides, P₁₁-3, P₁₁-10 and P₁₁-18 also gave rise to results that were equivocal.

These results in Table 4-2 show some interesting possibilities for the use of peptides in biomedical applications. It was possible to identify several design characteristics for the further development of self-assembling peptides. Large positively charged peptides should be avoided as they were shown to be cytotoxic, haemolytic and cause the agglutination of whole blood; this makes them unsuitable for biomedical application. Large neutral charged peptides were shown to cause an increase in the formation of thrombus in a model system. This effect could be of advantage in haemostatic applications in which there is a desire to increase the rate of blood clotting. Even though the mechanism by which these peptides increased thrombus formation was unclear it would be unadvisable to use them in the body where they could come into contact with the blood as even if they do not trigger clotting they have the potential to disrupt the delicate balance between clotting and inhibitory factors. The effect of poly-anionic peptides with hydrophobic cores could be of advantage or disadvantage in a biomedical application. Several disease states are associated with the complement system and a tissue engineering scaffold that could inhibit these effects could potentially be of great benefit. Conversely inhibition of the complement system could have a negative effect due to suppression of immunological reactions.

5 Effects of peptide coatings on decellularised arterial conduits

5.1 Introduction

It has been proposed that self-assembling peptides can be used to passivate the surface of a decellularised porcine internal carotid artery. In Chapter 3 it was shown that the peptide P₁₁₋₄ could self-assemble within the decellularised vessel, forming a coating over the ECM. The results from the screening of the biocompatibility and the haemocompatibility of peptides in Chapter 4 were used to identify model peptides for investigation. It has further been proposed that functional groups could be added to the self-assembled peptide to aid and enhance reendothelialisation.

5.1.1 Anti-thrombogenic coatings

Anti-thrombogenic coatings have been explored in detail in Section 1.6. Potential anti-thrombogenic coatings can be non-fouling, anti-clotting or can work by passivating the surface.

The use of non-fouling surfaces is not an ideal solution for preventing thrombus formation since the modification of the surfaces can lead to changes in chemical and mechanical properties (Morra and Cassineli, 1999). Degradation of the surface will naturally occur in long-term use and the loss of the anti-fouling coating will allow for the formation of blood clots. The non-fouling surface often prevents the binding and growth of cells so may prevent the formation of a fully functional endothelial layer (Hoffman, 1999, Morra and Cassineli, 1999, Sarkar et al., 2007). The loss of control of protein binding and dissolution could also negatively impact on cellular interactions and negate one of the reasons for using naturally derived scaffolds as vascular grafts.

Slow release anti-coagulants and anti-coagulant coatings can be effectively used to prevent clot formation and platelet activation, however, if the anti-coagulant is fully released or removed from the surface of a scaffold by degradation and a fully formed endothelial layer has not formed, platelets will become activated and thrombosis can occur; as has been observed with heparin coatings (Xue and Greisler, 2003, Sarkar et al., 2007, Venkatraman et al., 2008).

This means that anti-clotting behaviour may not be sufficient and that other factors are needed to allow for reendothelialisation.

The use of a material to passivate the surface is based on the same principle as the non-fouling coating, in which a bio and haemo compatible non-thrombogenic material is used to prevent platelet activation and clot formation. The advantage of passivating the surface over non-fouling surfaces is that a biocompatible surface should allow for normal cellular function whilst preventing clotting, unlike the non-fouling surface that prevents cell adhesion. Passivating the surface has advantages over anti-clotting coatings avoiding the risks associated with anti-clotting treatments, present in even controlled delivery (Hoshi et al., 2012).

5.1.2 Endothelial cells

Endothelial cells produce and attach to a basal lamina that is supported on the internal elastic lamina of blood vessels (Wagenseil and Mecham, 2009). It was originally believed that endothelial cells functioned as a mechanical barrier between blood and the underlying ECM; however, it has become evident that endothelial cells are critically involved in vascular function. Vascular endothelial cells have been explored in greater detail in Section 1.2.3. Site-specific differences can be seen between endothelial cells from different locations in the vasculature, however, some fundamental features are maintained regardless of origin (Murphy et al., 1998, Sumpio et al., 2002). These basic characteristics of endothelial cells can be used to identify and characterise isolated cells from the vasculature.

Endothelial cells that have been cultured to confluence form focal areas with a characteristic cobblestone structure of polygonal cells; the cobblestone morphology becomes more predominant with longer culture times (Jaffe et al., 1973, Schwartz, 1978, Schor et al., 1983). There have been reports that post-confluent cultures will start to form a secondary elongated morphology beneath the original monolayer (Schor et al., 1983).

CD31 also known as PECAM1 is an integral membrane glycoprotein belonging to the immunoglobulin super-family of cell adhesion molecules (Dong et al., 1997). CD31 is expressed on the surface of endothelial cells and platelets; it has been designated as a platelet-endothelial cell adhesion molecule (DeLisser et al., 1994). CD31 is expressed by all endothelial cells in the adult, it promotes cell-cell interactions in cultured endothelial cells and has been reported to be present in embryonic cardiovascular development (Baldwin et al., 1994, Sumpio

et al., 2002). CD31 is found in relatively small amounts on platelets but has been reported to be expressed in large amounts, up to 10 fold higher levels, on cultured endothelial cells and is expressed on the continuous endothelium of all blood vessels (DeLisser et al., 1994, Dong et al., 1997).

The vWF is an adhesive glycoprotein involved in haemostasis; it is synthesised only by endothelial cells and megakaryocytes and is found in three pools in the body, plasma soluble vWF, basement membrane vWF and cellular vWF found in granules of platelets and Weibel-Palade bodies in endothelial cells (Wagner, 1990, Ruggeri, 1997). vWF is expressed by mature endothelial cells but to a varying extent by endothelial progenitor cells (Hristov et al., 2003). Weibel-Palade bodies vary in number in endothelial cells with the age of the culture having little effect upon the numbers present; it has been observed that although the Weibel-Palade bodies are present throughout the cytoplasm they are primarily located at the periphery of well-spread cells (Wagner et al., 1982).

Endothelial cells have been isolated and characterised in a number of different ways from a number of different locations. Human micro-vascular endothelial cells have been isolated and identified by their characteristic cobblestone morphology and by immunofluorescence using antibodies against vWF (Ades et al., 1992). Endothelial cells have been isolated from murine lungs using anti-CD31 antibody labelled beads to isolate endothelial cells from suspension (Dong et al., 1997). Differentiation of embryonic stem cells into endothelial cells has been evaluated by immunochemical procedures using antibodies against vWF and CD31 (Levenberg et al., 2002). The results from several studies show that endothelial cells can be identified by the morphology of the cells and the presence of glycoproteins CD31 and vWF.

5.1.3 Cell attachment motifs

Cell attachment motifs have been explored in greater detail in Section 1.6.4.2. Natural cell attachment ligands such as RGD have been used to enhance cellular adhesion and retention in a wide range of applications. RGD is a naturally occurring attachment motif; it is often in the form of RGD, PRGDS or YRGDS and is known to enhance cell attachment to a surface (Drury and Mooney, 2003, Chen and Hunt, 2007, Wang et al., 2008). The inclusion of RGD variants on vascular grafts has been shown to enhance bovine aortic and human umbilical vein endothelial cell migration, attachment and retention (Patel et al., 2007, Wang et al., 2008).

5.1.4 Aims and objectives

The aims of this chapter were to test the hypothesis that self-assembling peptides could be used to passivate the surface of the decellularised porcine arterial conduits and also to test the hypothesis that the attachment of ovine endothelial cells would be enhanced in the presence of cyclic RGD (cRGD) functionalised peptide.

Specific objectives;

- a) To determine the anti-thrombogenic properties of un-functionalised peptide coatings on the decellularised vessel
- b) To isolate and characterise ovine arterial endothelial cells
- c) To evaluate the attachment of ovine arterial endothelial cells to the decellularised porcine internal carotid artery and self-assembled peptide coated decellularised porcine internal carotid artery
- d) To evaluate the effect of adding cyclic RGD functionalised peptide to the self-assembled peptide coating on the attachment of ovine arterial endothelial cells

5.2 Methods

5.2.1 Chandler loop thrombosis model

Peptide coated decellularised porcine internal carotid artery was tested for thrombus formation in the Chandler loop model. Three peptides were chosen based on the results obtained in Chapter 4. Peptides P₁₁₋₄, P₁₁₋₈ and P₁₁₋₁₂ were chosen as they were shown to be biocompatible and not have any effect upon thrombus formation. The amount of each peptide used was calculated to achieve a final concentration of 18.8 mol.m⁻³. This concentration of peptide was chosen as it has been shown to give a strong self-supporting gel and the tests of stability and self-assembly within the decellularised vessel (Chapter 3) were done using this peptide concentration. Peptide solutions, 1.8 ml, were made in sterile water. Lengths of decellularised vessel, 5 cm, were washed for 1 minute in 150 ml of sterile water to remove salts from storage in PBS. The decellularised vessel was added to the peptide solution and left overnight then 0.2 ml of 10X Ringer's solution was added to trigger self-assembly.

All Chandler loop tests were set-up and run as described in the protocol in Section 2.2.15.2. Six replicates for each peptide and control were tested. Six samples were tested at a time with three loops to a spinner at 27°C. Citrated sheep blood was used to test for thrombus formation. Blood used was tested for normal clotting behaviour and a response to known triggers of blood clotting before use.

5.2.2 Endothelial cell isolation and characterisation

Endothelial cells were isolated from ovine superficial femoral arteries as per the protocol described in Section 2.2.18.1. Cells were initially grown in 5 ml of endothelial cell growth medium in 25 cm² tissue culture flasks at 37°C in 5 % (v/v) CO₂ in air. Spent medium was removed and the cells washed with 5 ml of sterile PBS, which was removed and replaced with 5 ml of fresh endothelial cell growth medium. Images were then taken of the cell growth. Cells were subcultured and grown in 75 cm² tissue culture flasks with 10 ml of endothelial cell growth medium at 37°C in 5 % (v/v) CO₂ in air. After each passage cells were cryopreserved for long term storage. Cells were resurrected before use and grown to confluence and subcultured at least once before testing. Before antibody labelling as described in Section 2.2.18.4 cells were grown to confluence and imaged. Cell suspension, 20 µl, was added to each of the 8 spots on an 8 spot slide (three slides for each antibody being used) and cultured for 4 hours at 5 % (v/v) CO₂ in air. Fresh endothelial cell culture medium was added to the cells and was incubated for 48 hours at 37°C in 5 % (v/v) CO₂ in air. Following fixation in methanol and acetone (1:1) all slides were kept at 27°C until imaging. Cells were labelled with anti-CD31, anti-vWF to check for endothelial cell markers and with anti-smooth muscle cell actin and anti-myosin heavy chain to check for the absence of smooth muscle cell markers; two 8 spot slides were labelled with antibody and one with the appropriate isotype control. All slides were kept in the dark and imaged immediately after mounting.

5.2.3 Endothelial cell attachment and proliferation

Following cell resurrection and characterisation as described in Section 2.2.18.2 the endothelial cells were used to determine their attachment and proliferation on the luminal surface of uncoated decellularised vessel and peptide coated vessel. Decellularised vessel was

cut into 1.5 cm lengths and cut longitudinally to open the vessel out. Decellularised vessel was coated in 30 mg.ml^{-1} (18.8 mol.m^{-3}) of peptide P₁₁-4 and 30 mg.ml^{-1} (18.8 mol.m^{-3}) of peptide P₁₁-4 mixed 1:50 with P₁₁-4-cRGD (synthesised by Dr Lik Ren Tai) as described in Section 2.2.19. Four replicates for each test condition were prepared. Four samples of P₁₁-4 coated vessel and four samples of P₁₁-4-cRGD for each time point, 4, 24 and 72 hours, were placed in one 12 well plate and four samples of uncoated vessel were placed in a second 12 well plate for each time point. Seeding rings with an internal diameter of 7.5 mm were placed on the vessel samples and 300 μl of endothelial cell growth medium without ECGF was added and incubated at 37°C in 5 % (v/v) CO₂ in air for 24 hours. Medium was removed and 200 μl of cell suspension, 25,000 endothelial cells per ml (5000 cells per sample), was added and incubated for 4 hours at 37°C in 5 % (v/v) CO₂ in air. After 4 hours the medium and seeding rings were removed. Each sample was washed with 1 ml sterile PBS to remove unattached cells. Endothelial cell culture medium, 1 ml, was added and the samples incubated at 37°C in 5 % (v/v) CO₂ in air; changing the medium every 48 hours. Samples removed at each time point were washed with 1 ml of sterile PBS and 0.5 ml of live/dead stain (1 mol.m^{-3} calcein AM and 2 mol.m^{-3} ethidium homodimer-1 in sterile PBS) was added and incubated in the dark for 40 minutes at 27°C. Staining solution was removed and the samples washed with 1 ml of sterile PBS. PBS was removed and the samples turned over and imaged using an inverted confocal fluorescent microscope. All manipulations were conducted in an aseptic environment.

5.3 Results

5.3.1 Thrombus formation in uncoated and peptide coated decellularised vessels

Results were collected, graphed and analysed using one-way analysis of variance. For all results there was a significant difference between the positive, α -thrombin in Chandler loop without decellularised vessel, and negative, blood run in Chandler loop without decellularised vessel, controls (Appendix Figure A.5). Results are presented in Figure 5.1 with the test peptides plus the relevant decellularised vessel control.

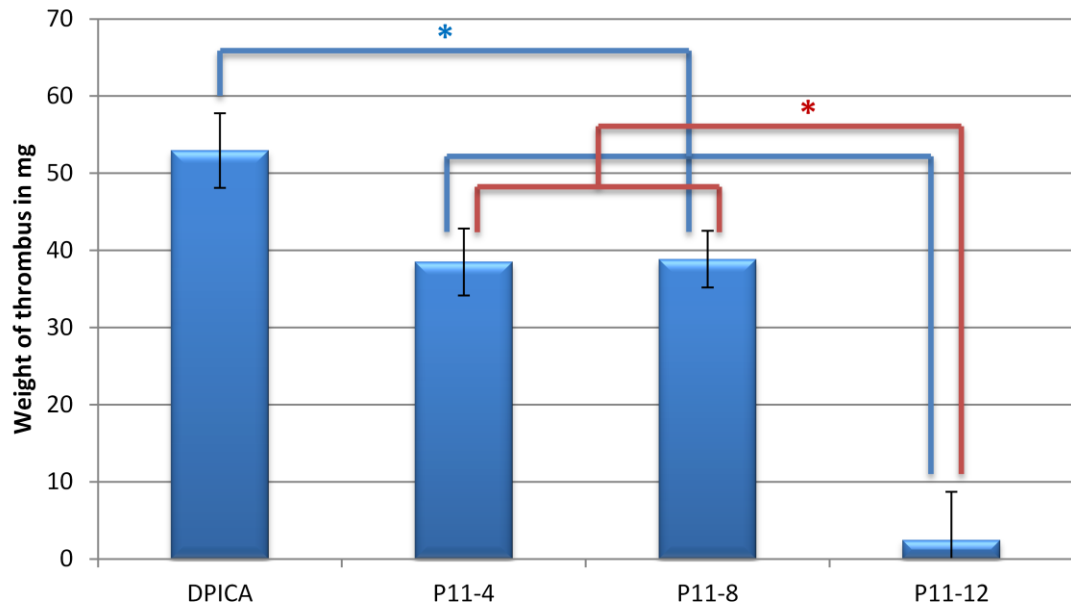


Figure 5.1; Weights of thrombus formed when peptide coated or uncoated (DPICA) decellularised vessel was evaluated in the Chandler loop model; Data is presented as the mean (n=6) \pm 95 % confidence intervals. Data was analysed by one way analysis of variance followed by determination of the MSD ($p < 0.05$). Blue * = significant difference between coated and uncoated vessels, Red * = significant difference between peptide coated vessels.

All the thrombi that were formed in this assay had a similar appearance with a single thrombus being formed with similar width to the PVC tubing and a visible white head at one end of the thrombus and a red tail, similar to arterial thrombi formed *in vivo*.

The results in Figure 5.1 showed that the thrombi formed in decellularised vessels coated in peptides P₁₁₋₄, P₁₁₋₈ and P₁₁₋₁₂ were all significantly smaller than the thrombi formed in uncoated decellularised vessel. The results also showed that the thrombi formed in P₁₁₋₁₂ coated vessels were significantly smaller than the thrombi formed in P₁₁₋₄ and P₁₁₋₈ coated vessels.

5.3.2 Endothelial cell isolation and characterisation

5.3.2.1 Observations from cell culture

Images of the cells following isolation and at confluence after 6 passages are presented in Figure 5.2 showing different stages in cell culture.

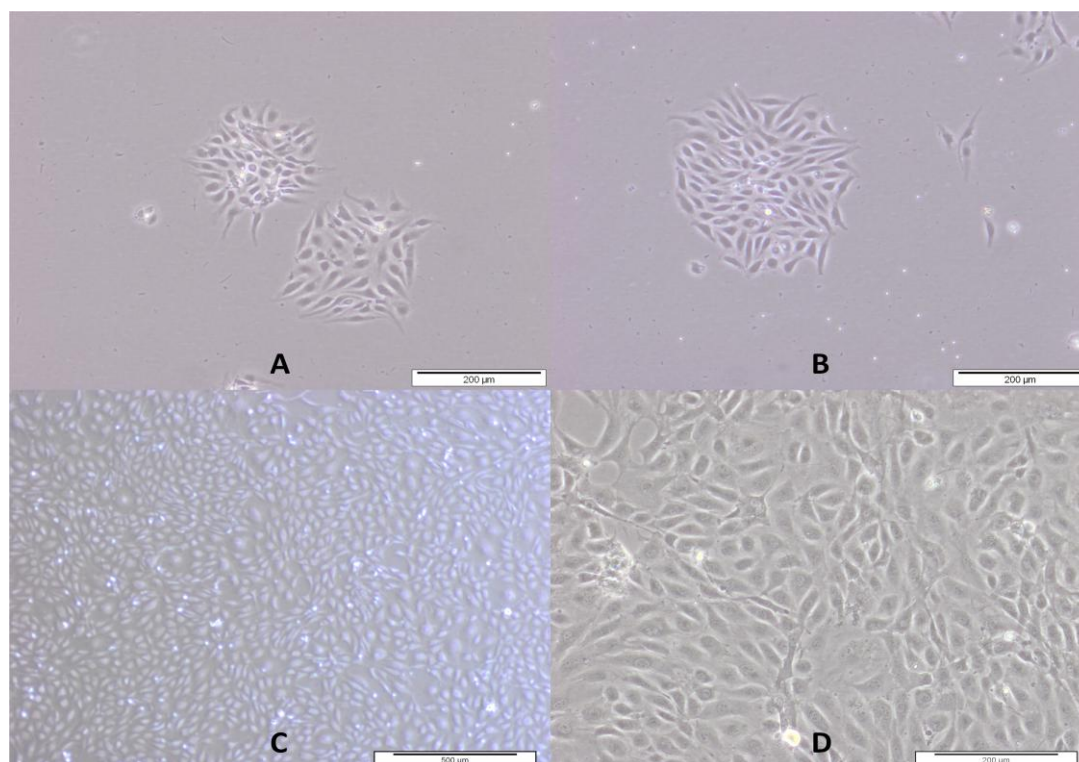


Figure 5.2; Inverted microscope images of cultured ovine arterial cells following isolation. A & B; freshly isolated endothelial cells after 1 day of culture at 10 X magnification, C; confluent endothelial cells 4 X magnification, D; confluent endothelial cells 10 X magnification.

Isolated cells that had attached to the tissue culture plastic and spread to form small epithelioid colonies after 1 day of culture are shown in Figure 5.2 images A & B. These colonies increased in size and gradually coalesced to form confluent monolayers of densely packed polygonal cells as shown in Figure 5.2 images C and D. Cells within these colonies and monolayers were predominantly uniform in appearance. The observed morphologies and behaviour observed could be attributed to endothelial cells.

5.3.2.2 Phenotype of isolated ovine vascular cells

Images of DAPI and fluorescently labelled antibody stained cells, cells after 5 passages, were taken from the same area and recorded. The images were combined using Corel PaintShop Pro X5. All assays were carried out with an isotype control. Images are presented in Figure 5.3 and Figure 5.4 as combined images showing antibody/isotype and DAPI staining with appropriate scale bars.

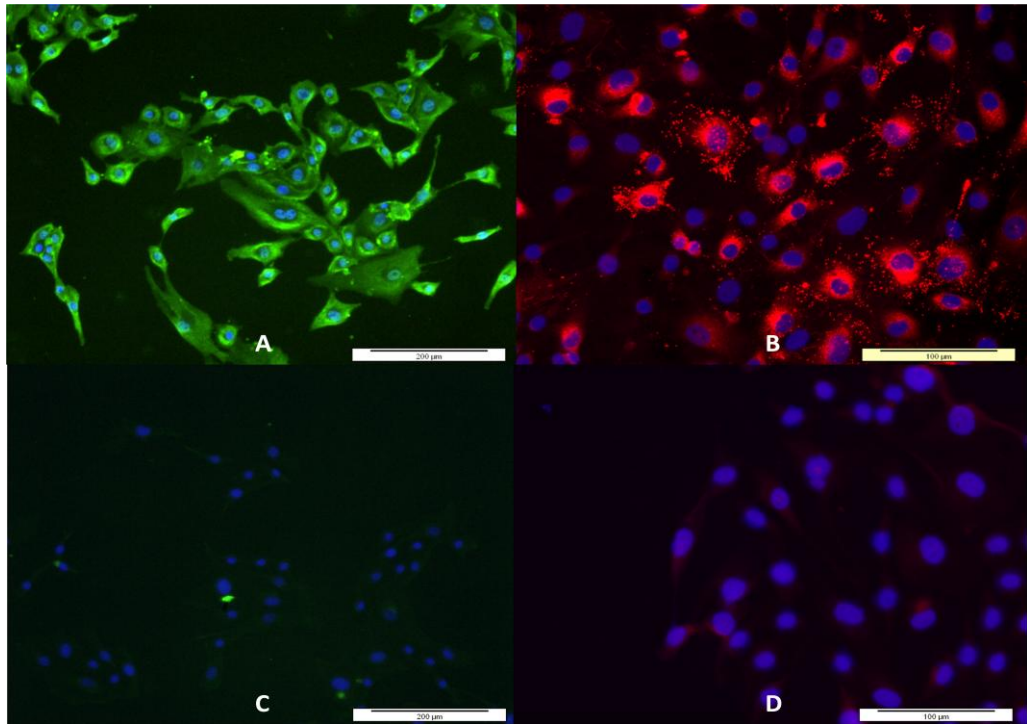


Figure 5.3; Confocal laser scanning microscope images of antibody labelling of isolated ovine endothelial cells, A; Anti-CD31 and DAPI staining, B; Anti-vWF and DAPI staining, C; Anti-CD31 isotype control and DAPI staining, D; Anti-vWF isotype control and DAPI staining. 10 X magnification.

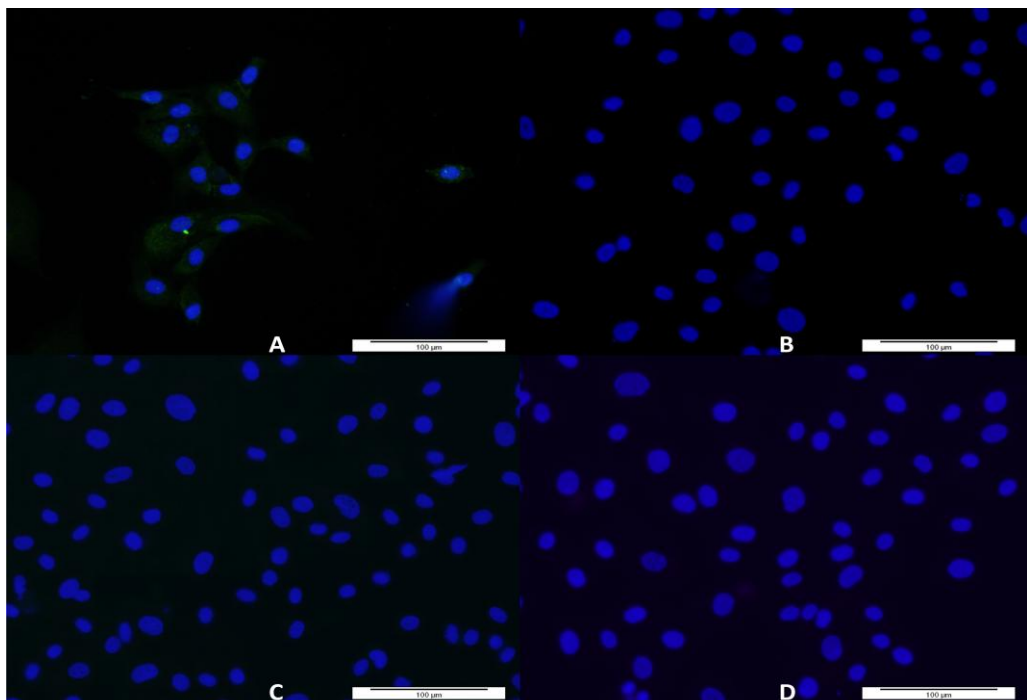


Figure 5.4; Confocal laser scanning microscope images of antibody labelling of isolated ovine endothelial cells, A; Anti-smooth muscle cell α -actin and DAPI staining, B; Anti-Smooth muscle cell myosin heavy chain and DAPI staining, C; Anti-smooth muscle cell α -actin isotype control and DAPI staining, D; Anti-smooth muscle cell myosin heavy chain isotype control and DAPI staining. 10 X magnification.

The DAPI staining in all the images shown in Figure 5.3 and Figure 5.4 showed the presence of cell nuclei. One hundred percent of the cells were positive for CD31, an endothelial cell marker (Figure 5.3 image A). Approximately sixty percent of the cells were positive for vWF, a cell marker present on endothelial cells (Figure 5.3 image B). The staining of the cells (Figure 5.3 images A & B) was distinctly different from the isotype controls (Figure 5.3 images C & D) and showed that the cells expressed both CD31 and vWF identifying them as endothelial cells. Minimal fluorescent staining was seen with antibodies specific to smooth muscle α -actin and myosin heavy chain (Figure 5.4 images A & B). The staining of the cells showed no distinct visual difference from the isotype controls (Figure 5.4 images C & D). The presence of cells was confirmed by the DAPI staining of cell nuclei and showed that the cells were not expressing smooth muscle α -actin or myosin heavy chain indicating that the cells were not smooth muscle cells.

5.3.3 Effect of peptide and functionalised peptide on the attachment of ovine arterial endothelial cells

Images of Live/Dead staining of endothelial cells on decellularised vessel (DPICA) and peptide P₁₁-4 and P₁₁-4-cRGD coated decellularised vessels were taken using confocal microscopy and recorded using Zen 2011. Endothelial cells were used after 6 passages and were identified as endothelial cells by morphology and by labelling with immunofluorescent antibodies at previous passage. The number of live stained cells and dead stained cells were recorded and analysed. Results are presented as representative images in Figure 5.5 with appropriate scale bars, in Figure 5.6 and Figure 5.7 as a series of graphs showing the number of cells counted per mm² and the percentage of viable cells counted and a images showing cell alignment in Figure 5.8.

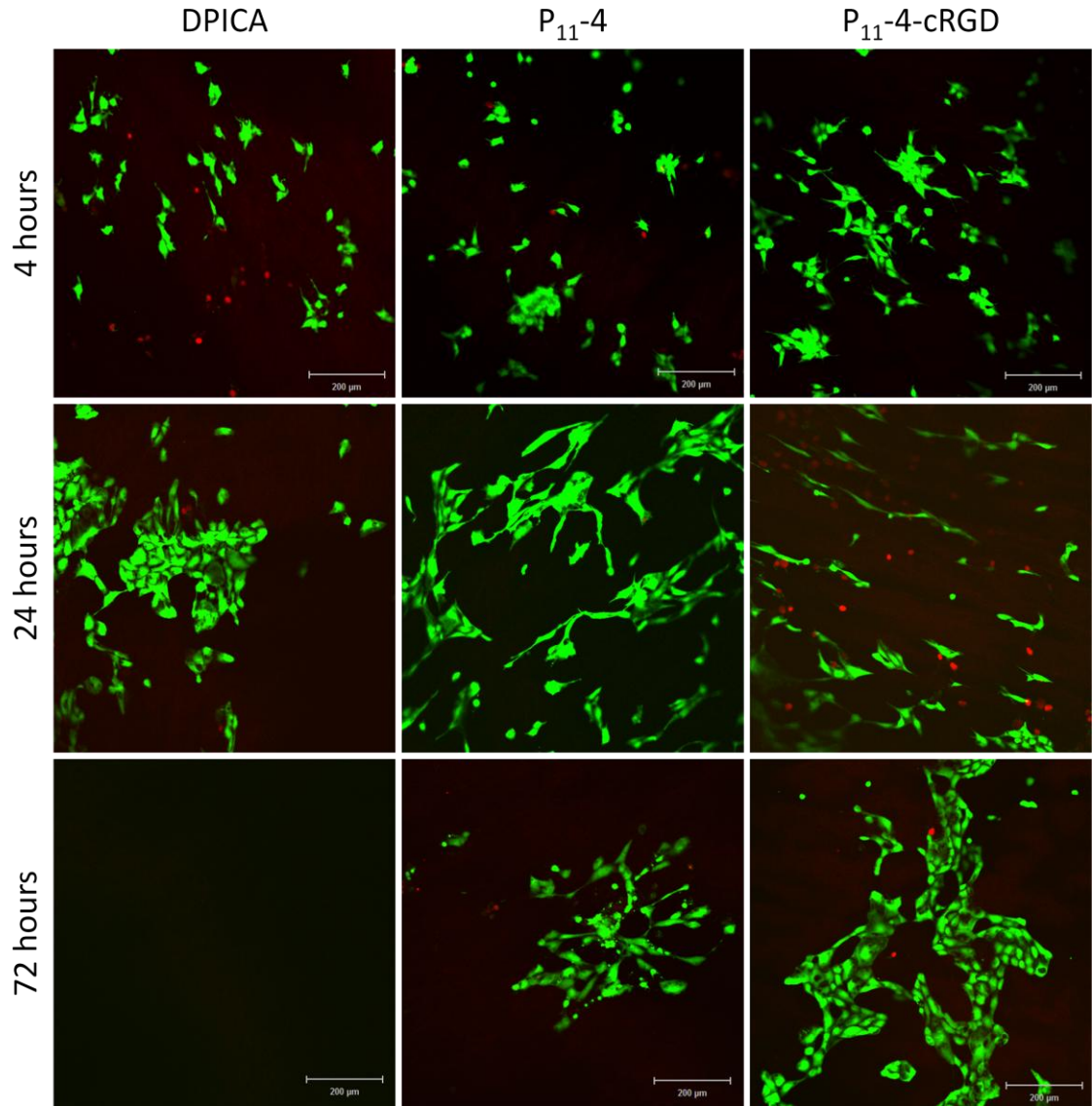


Figure 5.5; Confocal laser scanning microscopy images of Live/Dead stain of ovine endothelial cells after 4, 24 and 72 hours attached to decellularised porcine internal carotid artery, decellularised porcine internal carotid artery with 30 mg.ml^{-1} (18.8 mol.m^{-3}) P₁₁-4 and decellularised porcine internal carotid artery with 30 mg.ml^{-1} (18.8 mol.m^{-3}) P₁₁-4-cRGD mixed with P₁₁-4 at a ratio of 1:50. 10 X magnification.

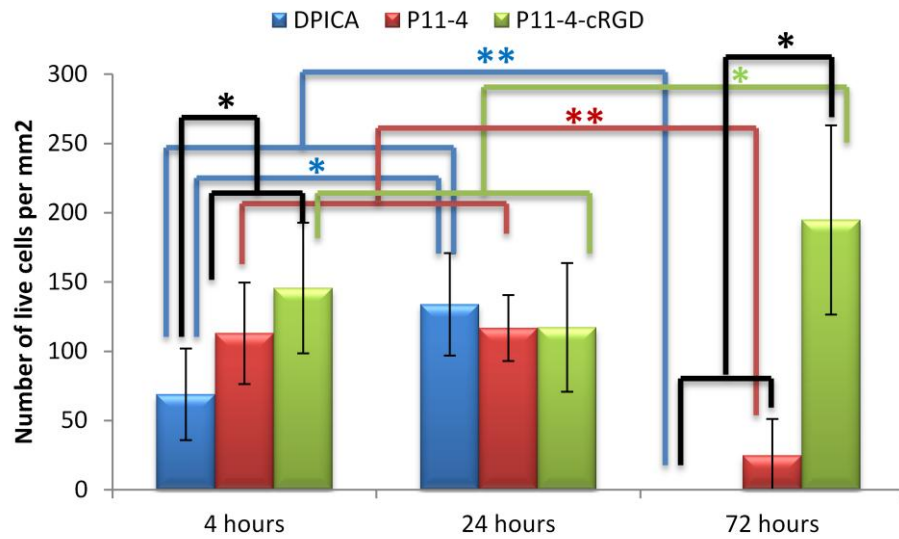


Figure 5.6; Number of live cells per mm² at 4, 24 and 72 hours. Data is presented as the mean (n=4) ± 95 % confidence intervals. Data was analysed by two way analysis of variance followed by determination of the MSD (p < 0.05) for each time point and each test condition. Black * = significant increase in attached cells between test conditions at set time point, coloured * = significant increase in attached cells between time points for corresponding test condition, coloured ** = significant decrease in attached cells between time points for corresponding test condition.

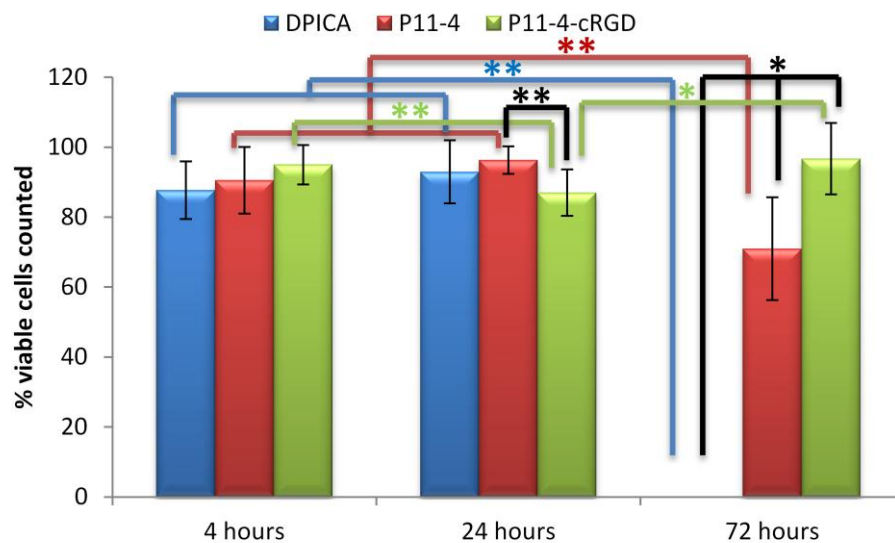


Figure 5.7; Percentage of cells counted that were viable over 4, 24 and 72 hours. Data is presented as the mean (n=4) ± 95 % confidence intervals. Data was analysed by two way analysis of variance followed by determination of the MSD (p < 0.05) for each time point and each test condition. Black * = significant increase in attached cell viability between test conditions at set time point, black ** = significant decrease in attached cell viability between test conditions at set time point, coloured * = significant increase in attached cell viability between time points for corresponding test condition, coloured ** = significant decrease in attached cell viability between time points for corresponding test condition.

Approximately 114 ovine arterial endothelial cells were seeded per mm² on each vessel sample; the results (Figure 5.6) showed that over 60 % of the cells seeded on the decellularised vessels attached and approximately 100 % of the endothelial cells seeded on the P₁₁-4 and P₁₁-4-cRGD coated decellularised vessels attached.

The results observed in both the images shown in Figure 5.5 and the live cell count shown in Figure 5.6 showed that significantly more endothelial cells had attached to the P₁₁-4 and P₁₁-4-cRGD coated decellularised vessels than on the uncoated vessels after 4 hours. There was no significant difference between the number of endothelial cells attaching to the P₁₁-4 and P₁₁-4-cRGD coated decellularised vessels after 4 hours. The images (Figure 5.5) and the live cell count (Figure 5.6) showed that there was no significant difference between the number of cells attached to the coated and uncoated decellularised vessels after 24 hours of culture. The images (Figure 5.5) showed that there were no cells attached to the uncoated decellularised vessels and that few cells were attached to the P₁₁-4 coated vessels after 72 hours of culture. Images of both the decellularised vessels and the P₁₁-4 coated vessels showed what appeared to be cell remnants on the surface of the vessels. In contrast there were numerous endothelial cells attached to the P₁₁-4-cRGD coated vessels. At 72 hours there were significantly lower numbers of live cells counted on the decellularised vessels and the P₁₁-4 coated vessels compared to the P₁₁-4-cRGD coated vessels.

The images (Figure 5.5) and the live cell count (Figure 5.6) showed that there was a significant increase in the number of cells attached to the uncoated decellularised vessels at 24 hours compared to 4 hours and that there was a significant loss of cells after 72 hours. The results showed that there was no significant difference in the number of endothelial cells on the P₁₁-4 coated decellularised vessels after 24 hours compared to 4 hours and that there was a significant loss of cells after 72 hours (Figure 5.5 and Figure 5.6). The images (Figure 5.5) and live cell count (Figure 5.6) showed that there was no significant difference in the number of live endothelial cells on the P₁₁-4-cRGD coated decellularised vessels after 24 hours compared to 4 hours. The results showed that there was a significant increase in the number of live cells on the P₁₁-4-cRGD coated decellularised vessels after 72 hours compared to the number of live cells at 4 and 24 hours (Figure 5.6).

There was no significant difference in the percentage of viable cells attached to the coated and uncoated decellularised vessels after 4 hours (Figure 5.7). After 24 hours there was no significant difference between the uncoated and P₁₁-4 coated decellularised vessels. The results showed that there was a significant difference between the percentage of viable cells

attached to the P₁₁-4 and P₁₁-4-cRGD coated vessels after 24 hours. The count of live and dead cells after 72 hours showed that there was a significant reduction in the percentage of viable cells attached to the uncoated (no cells present) and P₁₁-4 coated decellularised vessels (Figure 5.7). There was a significant reduction in the percentage of viable cells present on the uncoated and P₁₁-4 coated vessels after 72 hours compared to the percentage of viable cells at 4 and 24 hours (Figure 5.7). The results also showed that there was a significant reduction in the percentage of viable cells present on the P₁₁-4-cRGD coated vessels between 4 hours and 24 hours. The count of live and dead cells also showed that there was a significant increase in the percentage of viable cells on the P₁₁-4-cRGD coated decellularised vessels between 24 hours and 72 hours but no difference between 4 hours and 72 hours.

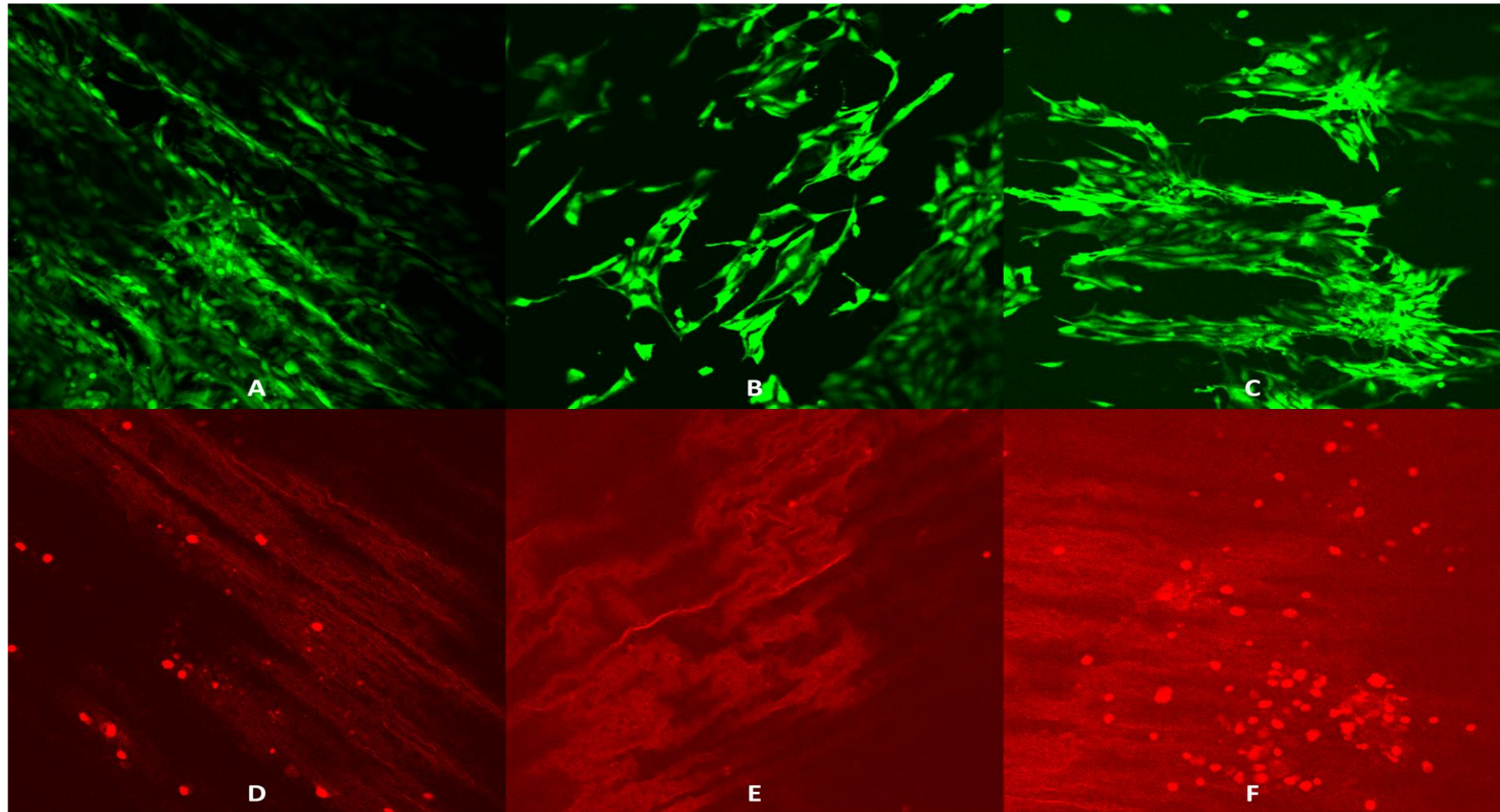


Figure 5.8; Confocal laser scanning microscopy images of ovine endothelial cells after 24 hours showing alignment of cells with underlying extracellular matrix. A to C; Live cell stain, D to F; Dead cell stain and collagen auto-fluorescence, A and D; decellularised porcine internal carotid artery, B and E; decellularised porcine internal carotid artery with 30 mg.ml^{-1} (18.8 mol.m^{-3}) P_{11-4} , C and F; decellularised porcine internal carotid artery with 30 mg.ml^{-1} (18.8 mol.m^{-3}) P_{11-4} -cRGD. 10 X magnification.

The results showed the endothelial cells had aligned along the ECM after 24 hours. The alignment of the ECM in the vessels was shown by collagen auto-fluorescence in Figure 5.8 images D, E and F. The live staining of the endothelial cells demonstrated that the cells were aligning in the same direction as the vascular ECM (Figure 5.8 images A, B and C).

5.4 Discussion

5.4.1 Thrombus formation in uncoated and peptide coated decellularised vessels

Peptides P₁₁-4, P₁₁-8 and P₁₁-12 were shown to have pacified the surface of the decellularised vessel and lowered the level of thrombogenesis. The peptide coatings did not prevent thrombosis, this was because the peptide coated and uncoated decellularised vessels only formed part of the Chandler loop. As the PVC tubing and the exposure of blood to air in the Chandler loop are known to cause the formation of the thrombus it would be unlikely that replacing 5 cm of the 33 cm PVC loop with coated vessel would prevent thrombosis. The significantly lower level of thrombus formation observed for vessels coated in self-assembled P₁₁-12 could have been due to an anti-clotting action of P₁₁-12 which was not demonstrated at the significantly lower concentrations used in the tests conducted in Chapter 4.

5.4.2 Endothelial cell isolation and characterisation

From the images of the isolated ovine vascular cells morphology and the immuno-fluorescence staining it was possible to identify the isolated cells as primarily being ovine vascular endothelial cells. The morphology of the cells was characteristic of the early colonies and cobblestone morphology seen at confluence (Jaffe et al., 1973, Schor et al., 1983). The 100 % staining for CD31 and the over 60 % staining for vWF was characteristic of endothelial cells and corresponded to observations and techniques of identification used in the literature (Wagner et al., 1982, Dong et al., 1997, Levenberg et al., 2002). The lack of staining for smooth muscle α -actin and myosin heavy chain showed that the isolated cells were not smooth muscle cells. The results showed that the method for isolating the endothelial cells from ovine arteries and the selective trypsin digestion when subculturing resulted in a high purity of isolated ovine vascular endothelial cells.

5.4.3 Endothelial cell attachment to peptide and functionalised peptide coated decellularised vessels

Endothelial cells were shown to be alive by the Live/Dead stain. Ovine endothelial cells attached better to the P₁₁-4 and P₁₁-4-cRGD mixed 1:50 with P₁₁-4 coated vessels compared to the uncoated vessels. After 24 hours the cells had multiplied on the decellularised vessel but not on the P₁₁-4 and P₁₁-4-cRGD coated vessels with a loss in the percentage of viable cells on the P₁₁-4-cRGD coated vessels. Cells were not present on the uncoated decellularised vessel and few cells were present on the P₁₁-4 coated vessel after 72 hours. The cells on the P₁₁-4-cRGD coated vessel had multiplied after 72 hours and had a higher percentage of viable cells.

The increase in the number of endothelial cells on the decellularised vessel showed that the cells had attached and were proliferating. The lack of change in the endothelial cells on P₁₁-4 coated decellularised vessel indicated that the cells had attached but had not started to proliferate. The loss of all cells on the decellularised vessels and the majority of cells on the P₁₁-4 coated vessels could have been caused by many different factors. It was possible that there was a cytotoxic effect of the vessel and that after 72 hours this cytotoxic effect could have been enough to kill the cells. This was unlikely as the same effect should have occurred to the P₁₁-4-cRGD coated vessels.

It has been reported that one major problem facing the recellularisation of decellularised vascular grafts *in vitro* is the detachment and delamination of cells and cell layers following cell culture (Ott and Ballermann, 1995, Conklin et al., 2004) It has been reported that endothelial cells statically seeded onto vascular grafts failed to form strong attachments and are easily removed under shear flow (Ott and Ballermann, 1995, Conklin et al., 2004). As the endothelium *in vivo* is normally exposed to shear stress the removal of the flow causes phenotypic changes in the cell. The changes cause the cells to form strong cell-cell interactions but weak attachments to the underlying ECM meaning the cells can more easily detach (García-Cardena et al., 2001). It was possible that after 72 hours of static culture that the cells on the decellularised vessels and the P₁₁-4 coated vessels had proliferated and detached or that the cells had been removed from the surface of the vessels by the washing steps and changing of media. This explanation would correspond to the observation of cell remnants left on the surface of the P₁₁-4 coated decellularised vessels.

The number of cells on the P₁₁-4 and P₁₁-4-cRGD mixed 1:50 with P₁₁-4 coated vessels showed no increase at 24 hours whereas endothelial cells on the decellularised uncoated vessels did.

This could be explained by the growth cycle of cells following subculture. Cells enter a latent period or lag period as the cells recover from trypsinisation, reconstruct their cytoskeleton and secrete ECM to aid in attachment. This latent period can be between a few hours and 48 hours but is dependent upon the surface the cells are attached to (Freshney et al., 2006). This could explain the difference in the growth of the endothelial cells observed between the decellularised vessels and the peptide coated vessels.

The cells on the surface of the P₁₁-4-cRGD mixed 1:50 with P₁₁-4 coated vessels showed strong attachment and a high percentage of viability at 4 hours which significantly decreased after 24 hours. The number of cells and the percentage of viability then increased as cells proliferated between 24 and 72 hours. This corresponded to the known cell growth and viability cycle observed when subculturing cells (Freshney et al., 2006). Not all the cells that attach onto a surface will survive to proliferate; some cells will have reached the end of their life cycle and some cells will have been less securely attached to the surface and will detach (Freshney et al., 2006). This could have resulted in a dip in the number of viable endothelial cells on the P₁₁-4-cRGD mixed 1:50 with P₁₁-4 coated vessels following attachment that then increased as the remaining viable cells proliferated.

It is possible that the concentration of the RGD at P₁₁-4-cRGD mixed 1:50 with P₁₁-4 had an effect upon the cells. Studies using RGD motifs have highlighted the importance of distribution and density on cell function. Low concentrations of RGD result in poor cell migration, retention and function. High levels of RGD have been shown to significantly increase cell attachment but have been reported to have a detrimental effect upon cell migration and proliferation (Walluscheck et al., 1996, Chen and Hunt, 2007, Norman et al., 2008).

Quantitative analysis of the cell adhesion could have been enhanced and confirmed with the use of cellular function assays such as the ATPLite-M[®] assay or the MTT assay which would have allowed for the assessment of the total number of cells attached to each sample and not just the number of cells imaged in each area.

The results showed that the endothelial cells attached to the vessel and after 24 hours started to align with the underlying ECM. This effect has been observed where aligned materials have been used to align cells, even endothelial cells, grown on the surface (Dalby et al., 2002, Bischofs and Schwarz, 2003). Endothelial cells in a natural vessel are aligned longitudinally with the ECM in the direction of blood flow (Bou-Gharios et al., 2004, Zhang et al., 2007). The alignment of the endothelial cells on the peptide coated vessels showed the peptide coatings

were not affecting the natural topography of the decellularised vessel as far as endothelial cell attachment was concerned.

The results showed that self-assembling peptides have the potential to be used to passivate the surface of a material against thrombogenesis. The results also showed that attachment ligands could be included in the peptide sequence to aid and enhance cell attachment and retention on the decellularised vessel.

6 Conclusions

6.1 Summary

The overall aim of this study was to determine whether self-assembling peptides could be used to enhance decellularised small diameter blood vessels for use as vascular grafts. The main issues facing the use of decellularised arterial grafts are thrombogenesis, due to the absence of an endothelium, and subsequently the need for reendothelialisation. This work had four main areas of focus.

Firstly in Chapter 3 a model peptide was shown to self-assemble within a decellularised porcine internal carotid artery. It was shown that the peptide had to be added to the decellularised vessel as a monomer and self-assembly triggered. The peptide was shown to self-assemble and be in a self-assembled state within the decellularised artery. The peptide was shown to form a self-assembled gel coating around the ECM fibres of the decellularised vessel and to be present at visually observable levels in the acellular vessel after 7 days under model flow conditions.

Secondly in Chapter 4 the peptides were tested for biocompatibility and the majority of the peptides were shown to be biocompatible. Peptides were also tested for haemocompatibility and the majority of peptides were shown to be haemocompatible. The results highlighted the potential of some peptides in alternative biomedical applications. The haemocompatibility and biocompatibility testing allowed the development of design characteristics for future development of self-assembling peptide for biological application. Large poly-cationic peptides were found to be non-bio or haemo compatible. Large neutral peptides were found to enhance the rate of thrombosis in the Chandler loop model; showing promise as potential haemostatic agents. Poly-anionic peptides with hydrophobic residues at the centre of the peptide sequence were found to inhibit complement activation; dependent upon the method of inhibition this could have advantages in a range of tissue engineering and restorative therapies.

Thirdly in Chapter 5, three candidate peptides, identified from results presented in Chapter 4, were self-assembled within lengths of decellularised vessel and were shown to significantly reduce thrombus formation compared to uncoated decellularised vessel in the Chandler loop

model. This provided evidence that the peptide could be used to passivate the decellularised vessel and reduce or even prevent thrombogenesis.

Finally, in Chapter 5 decellularised vessel coated in self-assembled peptide P₁₁₋₄ and cyclic RGD functionalised peptide P₁₁₋₄ (ratio 1:50) was shown to allow the attachment and growth of a higher number of ovine arterial endothelial cells compared to uncoated decellularised vessel. It was then shown that the addition of P₁₁₋₄ functionalised with cyclic RGD to the self-assembled peptide coating (ratio 1:50) enhanced the retention of endothelial cells on the peptide coated decellularised vessels compared to uncoated decellularised vessel. It was also shown in Chapter 5 that the isolated cells attached and aligned with the underlying ECM on both the self-assembled peptide coated and uncoated decellularised vessels. This provided evidence that the self-assembling peptide did not interfere with the attachment of the cells to the vessel as a non-fouling surface would have and that the peptide coating did not affect the natural alignment of the cells. These results also showed that the peptide could be used to add functionality to the decellularised vessel.

6.2 Future work

To continue the work in Chapter 3 a further study of the peptide stability under flow conditions could be performed. To act as a passivating material or to enhance reendothelialisation the peptide would have to remain present on the luminal surface of the decellularised vessel until a fully formed and functional endothelium was present. It would be worth testing a range of different peptides for possible application to assess which peptide had the highest stability under flow. Such a study would also be useful to develop design characteristics for the future development of self-assembling peptides for applications in which different stabilities and retention profiles might be needed. It would also be of interest to explore how the peptide is self-assembling around the fibres of the ECM, what structures are formed and if a smaller interpenetrating network is being formed that is too small to image by fluorescent microscopy.

The work presented in Chapter 4 represented the first steps in the development and characterisation of self-assembling peptides for biomedical applications. Future work should focus on developing a better understanding of the cause of these effects. Research is needed to not only explore the cytotoxicity of the peptides but to assess the effects that the peptides

have on cell attachment, migration, growth and phenotype. It would also be useful to expand on the range of investigations to cover assessment of different cell types to assess for cell specific toxicity. A better understanding of the cause of increased thrombus formation needs to be established if peptides are to be used in haemostatic settings, whilst it may be unrealistic, to identify the precise mechanism of action of the peptide in thrombus formation it would be important to elucidate the general effect to better tailor and develop haemostatic agents for clinical translation.

The haemolysis study demonstrated that the majority of peptides did not interact destructively with cell membranes; this did not, however, rule out non-destructive interactions. The effect of peptides on cell membranes is an area of potential interest that is very relevant to cell function and biocompatibility testing. The modified CH50 assay demonstrated that some of the peptides have the potential to inhibit the complement system, however, the exact nature of this inhibition needs exploring and whether this effect is limited to the classical pathway needs to be established.

The work in Chapter 4 only covered complement inhibition. It would be useful to assess complement activation to obtain a fuller picture and further refine peptide design characteristics. The work presented here gives an overview of peptide biocompatibility and haemocompatibility, however, this information is limited to one low concentration of peptide. As well as expanding on the tests carried out in assessment of biocompatibility and haemocompatibility a range of different concentrations need to be explored to examine any possible concentration dependent effects and to assess if the results obtained at low peptide concentrations are applicable to higher concentrations of peptide. One area of research needed for further development is immunological testing to ascertain if there is any immune response generated by these peptides *in vivo*.

To continue the work in Chapter 5 a larger more detailed study on the anti-thrombogenic nature of the peptide coating is needed. The results in Chapter 5 showed a reduction in the size of the thrombus formed when part of the Chandler loop was replaced with peptide coated vessel. Assessment of the anti-thrombogenic nature of the coatings in which blood is only coming into contact with the peptide coated decellularised vessel is needed to determine whether the anti-thrombogenic coating prevents thrombosis or just reduces the rate of thrombosis. This has huge implications regarding the effectiveness of the peptide coating to passivate the surface of a material.

To continue the work of the overall project more work is needed on the addition of functional groups to the peptides to enhance reendothelialisation. Studies are needed to determine ideal ratios of functionalised peptide to un-functionalised peptide. There is also a need to analyse the thrombogenic potential of any functionalised peptide as some functional groups such as RGD have the potential to play a role in thrombus formation, by allowing the binding of cells involved in blood clotting. The possible use of cell adhesion molecules other than RGD also needs to be explored to optimise the attachment, retention, adhesion and spreading of endothelial cells.

A longer term study is needed to further assess recellularisation and assess if endothelial cells are expressing the correct phenotype and cellular markers. Testing is also needed to assess if the endothelial cells are functional or not, simple tests for things such as nitric oxide can indicate if endothelial cells attached to the peptide coated decellularised vessel are in an anti-coagulatory state or pro-coagulatory state. More complex gene sequencing techniques can be used to further assess the functionality of the endothelial cells. Work is needed on the recellularisation of the graft with vascular smooth muscle cells and with a combination of smooth muscle and endothelial cells to investigate the different rates of recellularisation and determine the potential for complications such as intimal hyperplasia. To further bring together the work in this study a model system is needed in which the recellularisation of the graft can be modelled *in vitro* or *in vivo*. This model system could allow for the assessment of the natural recellularisation of the vessel and further assess the effect of adding functional groups.

6.3 Outlook

The hopeful outcome of this line of work is the development of a vascular graft that can be used to replace small diameter blood vessels and produce a graft that has high patency rates and a long lifetime. It is hoped that over time such a graft would integrate and eventually become indistinguishable from the natural blood vessels of the patient.

As decellularised materials are developed and taken into the clinic the understanding and potential application of these materials is growing. Whilst some decellularised products are being taken to the clinic there is still a large body of research to do. Work on the characterisation and enhancement of the antibacterial properties of the decellularised tissues

and on perfecting the decellularisation process for different tissues is being explored. Work on identifying the ideal sterilisation process and on the development of viable manufacturing processes is ongoing. There is a huge potential for decellularisation to provide not only graft materials but to provide the important first step in the production of artificial tissues and organs for transplant.

Redesign and modification of the self-assembling peptides is a constant and evolving process. The use of co-assembling peptides, cross-linking agents and the incorporation of disulphide bridges into the peptide sequence are being explored in an attempt to make more resilient and stable self-assembled peptides. Provided that the assembly and disassembly of new peptides can be easily controlled, as with the current P₁₁ series, there will be even more potential applications of these peptides. A common focus in biomaterials research is the attachment of functional groups in particular attachment ligands as explored in Section 1.6.4.2. The RGD sequence is the most prevalent cell attachment sequence as it is the most commonly found in nature and interacts with most cell types, however, other adhesion sequences have been found to have cell specific effects. If a range of attachment ligands can be identified it may be possible to employ alternative functionalities to tailor a self-assembled peptide for a specific application. The functionalities that can be added to the peptide are not limited to attachment ligands; there are a range of biological and therapeutic molecules that could be attached to the peptides. Research into the development of tailored and functionalised peptides is ongoing. The range of properties possible from self-assembling peptides makes them ideal materials for a wide range of tissue engineering and regenerative applications.

Despite research and development of self-assembling peptides and decellularisation techniques these new materials are still in the early stages of development, the work presented in this thesis aims to add to this base knowledge and hopes to illustrate the potential for the combination of new materials to better meet clinical needs.

A. Appendix

A.1 Equipment

Below is a list of all laboratory equipment used throughout the study unless otherwise stated.

Equipment	Model	Supplier
- 25 °C freezer	Electrolux 3000	Jencons PLC
- 80 °C freezer	MDF-U53v	SANYO Biomedical Europe BV
Autoclave	5 L pressure cooker	KUHN Rikon
Automatic pipettes	Gilson P2 – P500	Anachem UK
Bench top centrifuge	Harrier 15/80	SANYO Biomedical Europe BV
Cell medium aspirator	Vacunsafe comfort	Integra Biosciences (SLS)
Class II safety cabinet	Heraeus H518	Kendro
CO ₂ Incubator	MCO-20AIC	SANYO Biomedical Europe BV
Confocal laser scanning microscope (CLSM)	LSM510 META	Carl Zeiss Ltd
Cryostat	CM1850	Lecia Microsystems
Digital camera	XC50	Olympus
Dissection kit	N/A	Thackeray Instruments
Field emission gun scanning electron microscope (FEGSEM)	Gemini LEO 1530	Carl Zeiss Ltd
Four figure balance	AND GR-200	Jencons PLC
Fourier transform infra-red spectrometer	Nicolet 6700	Thermo Electron Corporation
Freeze dryer	LL1500	Thermo Electron Corporation
Fridge	Lab cold 23	Jencons PLC
Fume hood		Whiteley
Histology water bath	3L histology	Leica Microsystems
Hot air oven	SANYO OMT225	SANYO Biomedical Europe BV
Hot plate	E18.1 hotplate	Raymond A Lamb

Hot wax dispenser	E66 wax dispensator	Raymond A Lamb
Incubator	Heraeus	Jencons PLC
Inverted microscope	Olympus, IX71 And CK40	Microscopes, Medical Diagnostic Systems and Olympus Patient Systems Ltd (Olympus UK Ltd)
Liquid nitrogen dewer	BIO65	Jencons PLC
Luminescence counter	Packard TopCount NX	Perkin Elmer
Magnetic Stirrer	Stuart SB161	Scientific Laboratory Systems
Micro centrifuge	MSE Micro Centaur	SANYO Biomedical Europe BV
Microplate reader	Multiskan Spectrum	Thermo Electron Corporation
Microtome	RM212RTF	Leica Microsystems
Multi-photon laser scanning microscope (MPLSM)	LSM 510 NLO	Carl Zeiss Ltd
pH Meter	Jenway 3020	VWR International
Pipette boy	acu classic	Scientific Laboratory Systems
Peristaltic pump	323 S/D	Watson Marlow Pumps
Refrigerated centrifuge	Harrier 18/80	SANYO Biomedical Europe BV
Rotator	Stuart SB2	Bibby Scientific Ltd
Shaking table	IKA KS 130 basic	Jencons PLC
Tissue processor	Leica TP1020	Leica Microsystems
Ultra high speed centrifuge	Sorvall Discovery 100 SE	Thermo Electron Corporation
Universal indicator paper	MN/902.02	Camlab
Upright microscope	Olympus, BX51	Microscopes, Medical Diagnostic Systems and Olympus Patient Systems Ltd (Olympus UK Ltd)
Vortexer	Clifton CM-1	Scientific Laboratory Systems
Water bath	Grant	Jencons PLC
Wax oven	GPwax/30/ss	SLS

Table A-1; List of laboratory equipment used throughout study with UK suppliers.

A.2 Chemicals

Below is a list of all chemicals and reagents used in this study unless otherwise stated.

Chemical/Reagent	Supplier
Acetone	Fisher Scientific
Aprotinin	Mayfair house Leeds Teaching Hospital Pharmacy
ATPLite-M [®] assay	Sigma-Aldrich
Avidin/biotin blocking kit	Vector Laboratories
Bovine serum albumin	Sigma-Aldrich
Calcium Chloride	Cascade Biologics
Cryoembed	Bios Europe Ltd
Dabco	VWR International
D ₂ O	Sigma-Aldrich
DCL	Sigma-Aldrich
DMSO	Sigma-Aldrich
DNAase	Sigma-Aldrich
DPX mountant	Bios Europe Ltd
Dulbecco's modified Eagle's medium	Invitrogen Ltd
Eosin	Bios Europe Ltd
Ethanol	VWR International
Ethylene-diaminetetra-acetic acid (EDTA)	VWR International
Foetal calf serum	Invitrogen Ltd
Glycerol	VWR International
Hank's balanced salt solution with calcium and magnesium	Invitrogen Ltd
Hydrogen peroxide	Sigma-Aldrich
Hydrophobic marker pen	Vector Laboratories

Isopropanol	VWR International
L-glutamine	Invitrogen Ltd
Live/dead stain	Invitrogen Ltd
M199	Invitrogen Ltd
Magnesium chloride	VWR International
Mayer's haematoxylin	Bios Europe Ltd
Methanol	VWR International
Methylated spirits	Bios Europe Ltd
Neutracon®	Scientific Laboratory Supplies Ltd
Neutral Buffered formalin (NBF)	Bios Europe Ltd
Paraffin wax pellets	Bios Europe Ltd
PBSa	Invitrogen Ltd
PBS without calcium and magnesium	Lonza Biopharmaceuticals
PBSa tablets	Oxoid
Penicillin	Invitrogen Ltd
Peracetic acid	Sigma-Aldrich
RNAase	Sigma-Aldrich
Sodium Azide	VWR International
Sodium chloride	VWR international
Sodium dodecyl sulphate (SDS)	Sigma-Aldrich
Sodium hydroxide	VWR International
Streptavidin	Vector Laboratories
Streptomycin	Invitrogen Ltd
Tris base	Sigma-Aldrich
Trypsin/EDTA	Invitrogen Ltd
Tween 20	Sigma-Aldrich
Xylene	Bios Europe Ltd
Virkon	Scientific Laboratory Supplies Ltd

Table A-2; List of chemicals and reagents with supplier.

A.3 Images of peptide P₁₁₋₄ self-assembly under different conditions

Images summarised in Table 3-1 of the self assembled state of peptide P₁₁₋₄ at pH 8, pH 7 and pH 5 with images of peptide self-assembled state of peptide P₁₁₋₄ in PBS and Ringer's solution.

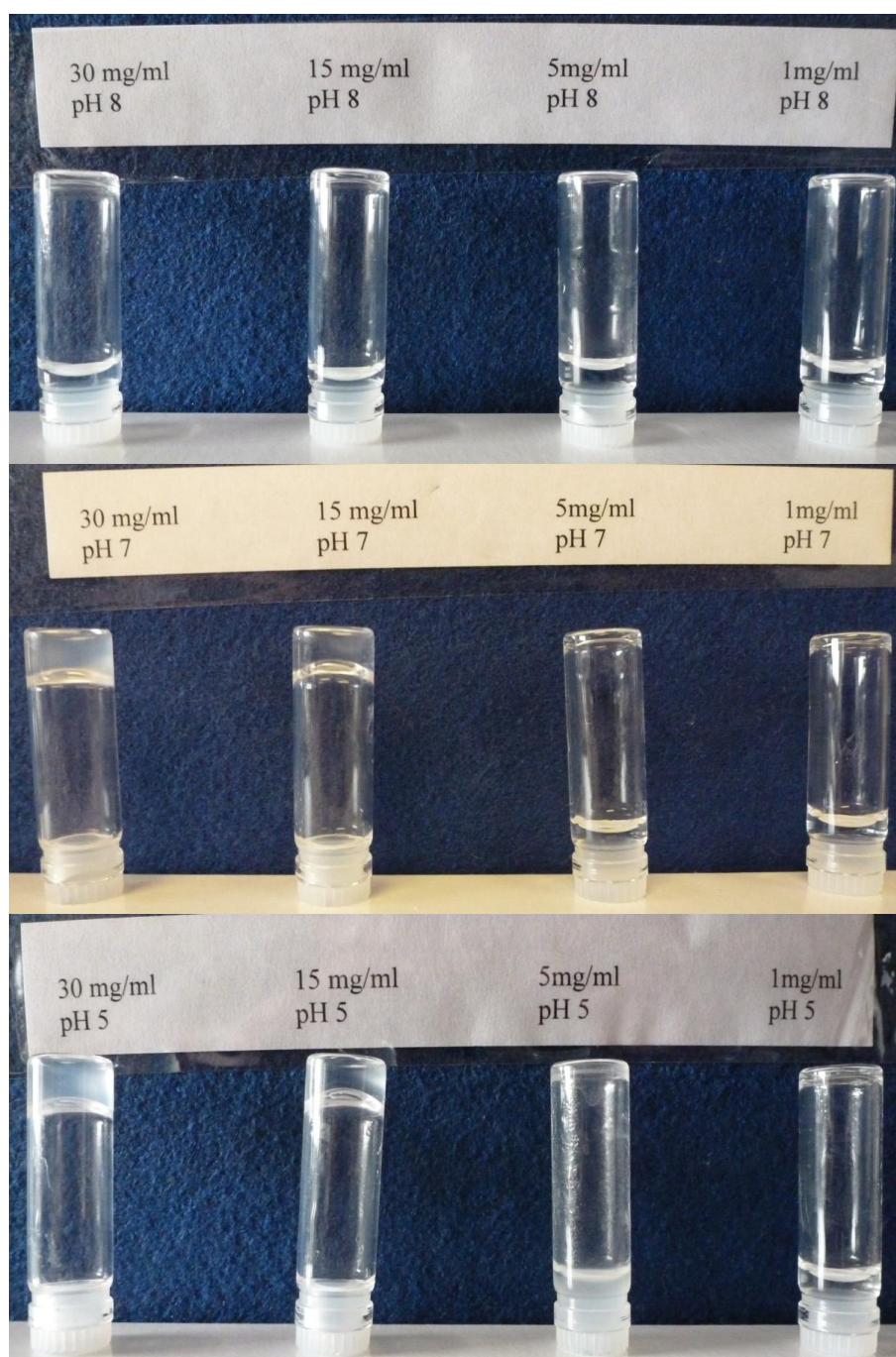


Figure A.1; Images of peptide P₁₁₋₄ at concentrations of 30 mg.ml⁻¹ (18.8 mol.m⁻³), 15 mg.ml⁻¹ (9.4 mol.m⁻³), 5 mg.ml⁻¹ (3.13 mol.m⁻³) and 1 mg.ml⁻¹ (0.63 mol.m⁻³) at pH 8, pH 7 and pH 5.

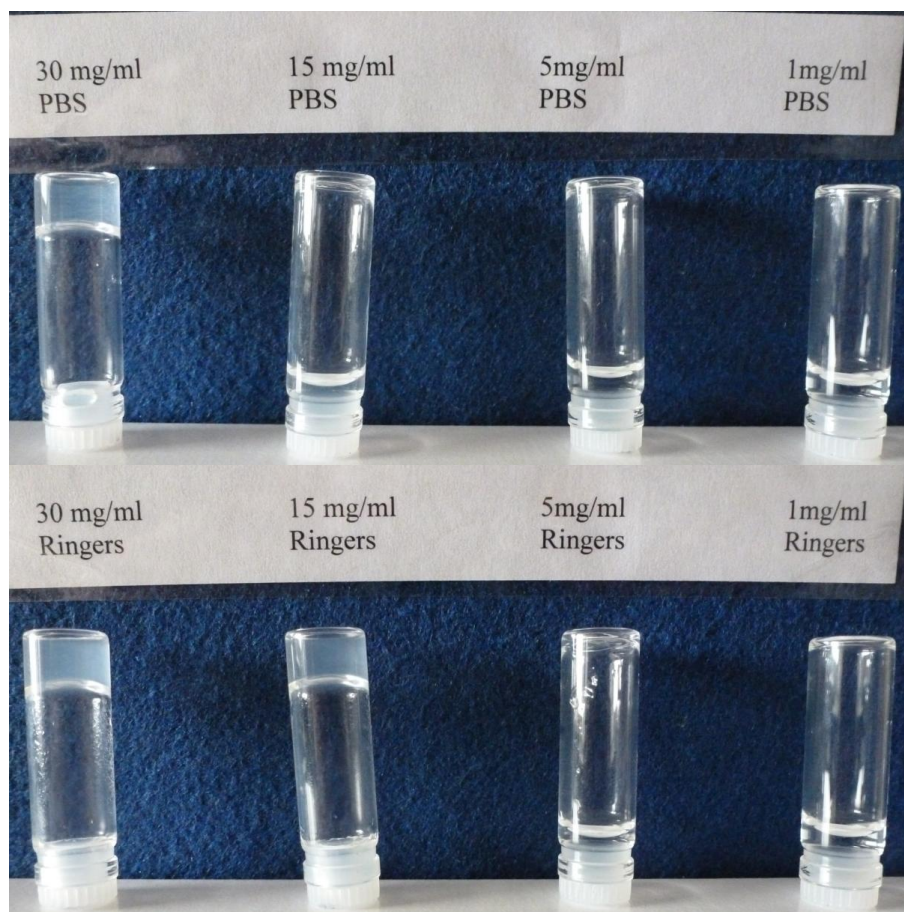


Figure A.2; Images of peptide P_{11-4} at concentrations of $30 \text{ mg}\cdot\text{ml}^{-1}$ ($18.8 \text{ mol}\cdot\text{m}^{-3}$), $15 \text{ mg}\cdot\text{ml}^{-1}$ ($9.4 \text{ mol}\cdot\text{m}^{-3}$), $5 \text{ mg}\cdot\text{ml}^{-1}$ ($3.13 \text{ mol}\cdot\text{m}^{-3}$) and $1 \text{ mg}\cdot\text{ml}^{-1}$ ($0.63 \text{ mol}\cdot\text{m}^{-3}$) in solutions of PBS and Ringer's solution.

In Figure A.1 and Figure A.2 self-supporting peptide gels can be distinguished by inversion, non-stable gels and visible aggregates can be distinguished by cloudy solution at bottom of the inverted glass vial and peptide aggregates stuck to the side of the glass vial. Monomer or soluble aggregate can be observed by a clear fluid at the bottom of the inverted glass vial.

A.4 Fluorescent image of fluorescein tagged P_{11-4}

Having been self-assembled, fluorescein tagged peptide P_{11-4} was embedded in cryostat embedding solution and sectioned as a control for the sectioning of the peptide coated vessel as described in Section 2.2.11

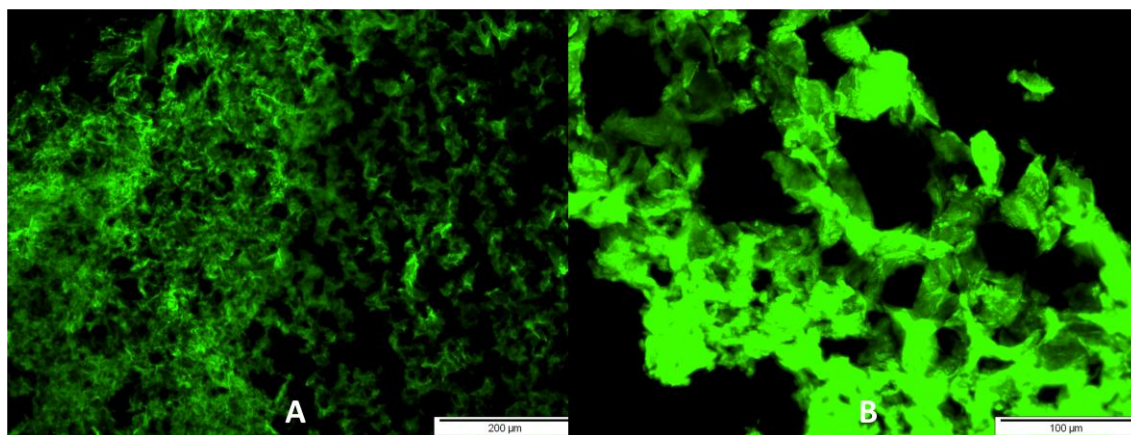


Figure A.3; Fluorescent cross section image of self-assembled peptide P_{11-4} , $30 \text{ mg}\cdot\text{ml}^{-1}$ ($18.8 \text{ mol}\cdot\text{m}^{-3}$) fluorescein tagged P_{11-4} mixed 1:50 with untagged P_{11-4} . A; 10X magnification, B; 20X magnification.

Fluorescent imaging showed that the sectioned peptide was visible using a fluorescein filter.

A.5 CH50 assay

To determine the dilution of serum to achieve 50 % lysis of the antibody sensitised erythrocytes in the complement inhibition test a CH50 assay was done. The CH50 assay was carried out as described in Section 2.2.17.1.

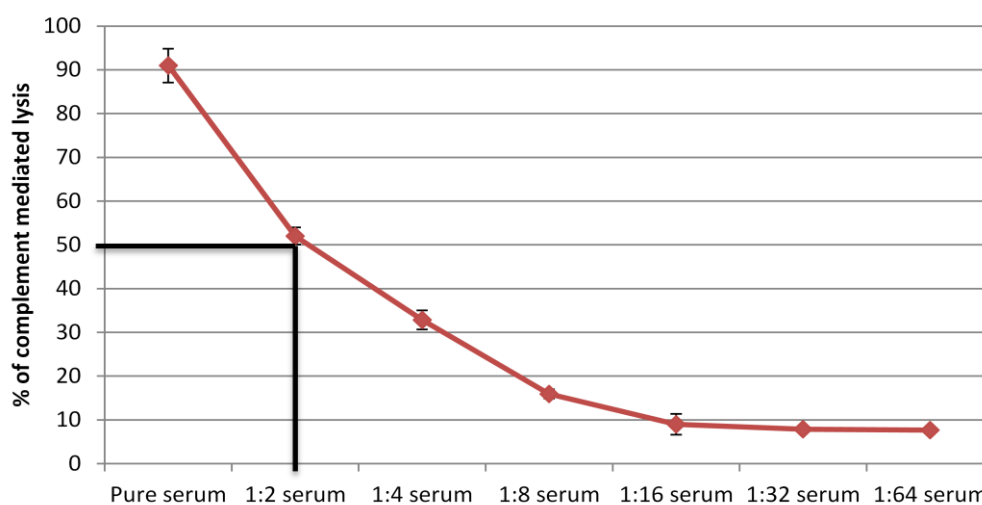


Figure A.4; Results of CH50 assay showing percentage of erythrocytes lysed at different complement dilutions with a line highlighting the point of 50 % lysis.

The results of the CH50 assay (Figure A.4) showed that to achieve 50 % lysis the serum used for the complement inhibition testing has to be diluted 1:2 with Ringer's solution.

A.6 Test of normal clotting behaviour of sheep blood

Sheep blood used in the Chandler loop thrombosis model (Section 2.2.15.2) was tested for normal clotting behaviour by the use of two controls. The positive control used 2 μ l of α -thrombin to trigger thrombogenesis without decellularised vessel present. The negative control used sheep blood in the loop without decellularised vessel present as described in Section 2.2.15.2.

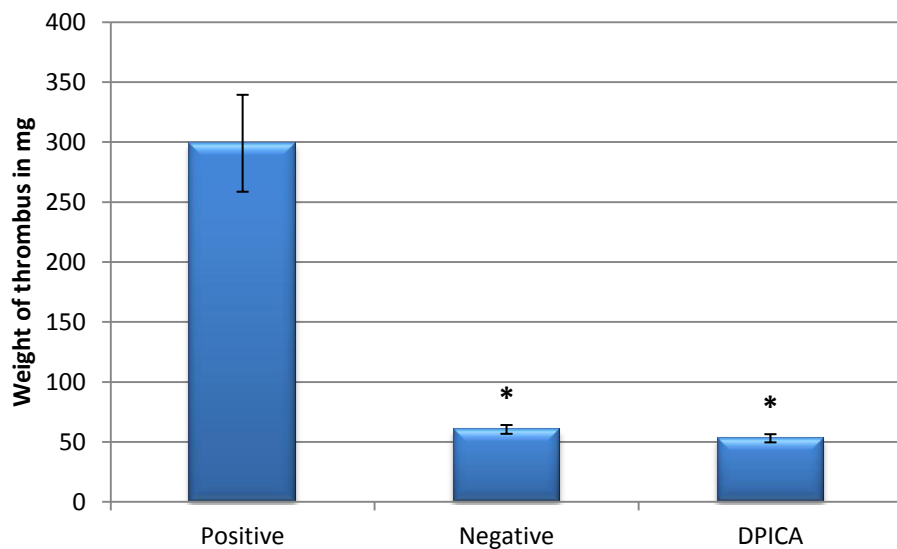


Figure A.5; Positive and negative controls of Chandler loop thrombosis model, * = significant difference from the positive control.

The results in Figure A.5 showed that the sheep blood used in the Chandler loop thrombosis model in Chapter 5 displayed normal behaviour to clotting factors.

A.7 Presentations and applications

- **R.S. Guilliat, S-P. Wilshaw, E. Ingham, A. Aggeli. (2010)** Self-assembly of peptide β -sheets within porous materials. European Materials Research Society (EMRS), Strasbourg, France (Poster presentation).
- **R.S. Guilliat. (2010)** Peptide β -sheet self-assembly in decellularised tissue for applications in small diameter vascular grafts. Joint Doctoral Training Centre (DTC) conference, Loughborough, UK (Oral Presentation).
- **R.S. Guilliat. (2011)** Peptide β -sheet self-assembly for the modification of acellular vascular grafts. Tissue and Cell Engineering Society (TCES) conference, Leeds, UK (Oral presentation).
- **R.S. Guilliat, S-P. Wilshaw, E. Ingham, A. Aggeli. (2011)** Functionalisation of acellular arterial conduits with self-assembled peptides. European Society for Biomaterials (ESB) conference, Dublin, Ireland (Poster presentation).
- **R.S. Guilliat. (2011)** Functionalisation of acellular arterial conduits with self-assembled peptide. Biomaterials and Tissue Engineering Group (BiTEG) meeting, Sheffield, UK (Oral presentation).
- **R.S. Guilliat, S-P. Wilshaw, E. Ingham, A. Aggeli. (2012)** Biocompatibility and haemocompatibility of self-assembling peptides. Tissue Engineering and Regenerative Medicine Society (TERMIS) world conference, Vienna, Austria (Poster presentation).
- **R.S. Guilliat, S. Homer-Vanniasinkam, E. Ingham, A. Aggeli. (2013)** Application for funding to explore commercial potential of haemostatic peptides found within thesis.

References

- ADAMS, T. E. & HUNTINGTON, J. A. 2006. Thrombin-cofactor interactions structural insights into regulatory mechanisms. *Arteriosclerosis, Thrombosis, and Vascular Biology*, 26, 1738-1745.
- ADES, E. W., CANDAL, F. J., SWERLICK, R. A., GEORGE, V. G., SUMMERS, S., BOSSE, D. C. & LAWLEY, T. J. 1992. HMEC-1: Establishment of an Immortalized Human Microvascular Endothelial Cell Line. *Journal of Investigative Dermatology*, 99, 683-690.
- AGGELI, A., BELL, M., BODEN, N., CARRICK, L. & STRONG, A. 2003a. Self-assembling peptide polyelectrolyte β -sheet complexes form nematic hydrogels. *Angewandte Chemie*, 42, 5603-5606.
- AGGELI, A., BELL, M., BODEN, N., KEEN, J., MCLEISH, T., NYRKOVA, I., RADFORD, S. & SEMENOV, A. 1997. Engineering of peptide β -sheet nanotapes. *Journal of Materials Chemistry*, 7, 1135-1145.
- AGGELI, A., BELL, M., CARRICK, L., FISHWICK, C., HARDING, R., MAWER, P., RADFORD, S., STRONG, A. & BODEN, N. 2003b. pH as a Trigger of Peptide β -Sheet Self-Assembly and Reversible Switching between Nematic and Isotropic Phases. *Journal of the American Chemical Society*, 125, 9619-9628.
- AGGELI, A., NYRKOVA, I., BELL, M., HARDING, R., CARRICK, L., MCLEISH, T., SEMENOV, A. & BODEN, N. 2001. Hierarchical self-assembly of chiral rod-like molecules as a model for peptide β -sheet tapes, ribbons, fibrils, and fibers. *Proceedings of the National Academy of Sciences*, 98, 11857.
- AHMED, M., GHANBARI, H., COUSINS, B. G., HAMILTON, G. & SEIFALIAN, A. M. 2011. Small calibre polyhedral oligomeric silsesquioxane nanocomposite cardiovascular grafts: influence of porosity on the structure, haemocompatibility and mechanical properties. *Acta Biomaterialia*, 7, 3857-3867.
- ALDENHOFF, Y., VAN DER VEEN, F., TER WOORST, J., HABETS, J., POOLE-WARREN, L. & KOOLE, L. 2001. Performance of a polyurethane vascular prosthesis carrying a dipyridamole (Persantin®) coating on its luminal surface. *Journal of Biomedical Materials Research*, 54, 224-233.
- ALEXOPOULOU, A. N., MULTHAUPT, H. A. B. & COUCHMAN, J. R. 2007. Syndecans in wound healing, inflammation and vascular biology. *The International Journal of Biochemistry & Cell Biology*, 39, 505-528.
- ALLAIRE, E., BRUNEVAL, P., MANDET, C., BECQUEMIN, J. & MICHEL, J. 1997. The immunogenicity of the extracellular matrix in arterial xenografts. *Surgery*, 122, 73-81.
- ALLEN, P., MELERO-MARTIN, J. & BISCHOFF, J. 2011. Type I collagen, fibrin and PuraMatrix matrices provide permissive environments for human endothelial and mesenchymal progenitor cells to form neovascular networks. *Journal of Tissue Engineering and Regenerative Medicine*, 5, e74-e86.
- ALLENDER, S., PETO, V., SCARBOROUGH, P., KAUR, A. & RAYNER, M. 2008. *Coronary heart disease statistics 2008*, British Heart Foundation.
- ALTIERI, D. C. 1993. Coagulation assembly on leukocytes in transmembrane signaling and cell adhesion. *Blood*, 81, 569-579.
- ANDERSSON, J., EKDAHL, K. N., LAMBRIS, J. D. & NILSSON, B. 2005. Binding of C3 fragments on top of adsorbed plasma proteins during complement activation on a model biomaterial surface. *Biomaterials*, 26, 1477-1485.
- ANDREWS, R. K., JOSÉ, L. A. & BERNDT, M. C. 1997. Molecular mechanisms of platelet adhesion and activation. *The International Journal of Biochemistry & Cell Biology*, 29, 91-105.
- AOKI, J., SERRUYS, P., VAN BEUSEKOM, H., ONG, A., MCFADDEN, E., SIANOS, G., VAN DER GIESSEN, W., REGAR, E., DE FEYTER, P. & DAVIS, H. 2005. Endothelial Progenitor Cell Capture by Stents Coated With Antibody Against CD34 The HEALING-FIM (Healthy

- Endothelial Accelerated Lining Inhibits Neointimal Growth-First In Man) Registry. *Journal of the American College of Cardiology*, 45, 1574-1579.
- ARIMA, M., KANO, T., SUZUKI, T., KUREMOTO, K., TANIMOTO, K., OIGAWA, T. & MATSUDA, S. 2005. Serial angiographic follow-up beyond 10 years after coronary artery bypass grafting. *Circulation Journal*, 69, 896.
- ARIMA, Y. & IWATA, H. 2007. Effect of wettability and surface functional groups on protein adsorption and cell adhesion using well-defined mixed self-assembled monolayers. *Biomaterials*, 28, 3074-3082.
- ASAHARA, T., BAUTERS, C., PASTORE, C., KEARNEY, M., ROSSOW, S., BUNTING, S., FERRARA, N., SYMES, J. & ISNER, J. 1995. Local delivery of vascular endothelial growth factor accelerates reendothelialization and attenuates intimal hyperplasia in balloon-injured rat carotid artery. *Circulation*, 91, 2793.
- ATKINSON, C., SONG, H., LU, B., QIAO, F., BURNS, T. A., HOLERS, V. M., TSOKOS, G. C. & TOMLINSON, S. 2005. Targeted complement inhibition by C3d recognition ameliorates tissue injury without apparent increase in susceptibility to infection. *Journal of Clinical Investigation*, 115, 2444-2453.
- BADAMI, A. S., KREKE, M. R., THOMPSON, M. S., RIFFLE, J. S. & GOLDSTEIN, A. S. 2006. Effect of fiber diameter on spreading, proliferation, and differentiation of osteoblastic cells on electrospun poly (lactic acid) substrates. *Biomaterials*, 27, 596-606.
- BADYLAK, S. F. 2004. Xenogeneic extracellular matrix as a scaffold for tissue reconstruction. *Transplant Immunology*, 12, 367-377.
- BADYLAK, S. F., FREYTES, D. O. & GILBERT, T. W. 2009. Extracellular matrix as a biological scaffold material: Structure and function. *Acta Biomaterialia*, 5, 1-13.
- BAGUNEID, M., SEIFALIAN, A., SALACINSKI, H., MURRAY, D., HAMILTON, G. & WALKER, M. 2006. Tissue engineering of blood vessels. *British Journal of Surgery*, 93, 282-290.
- BALDWIN, H. S., SHEN, H. M., YAN, H.-C., DELISSER, H. M., CHUNG, A., MICKANIN, C., TRASK, T., KIRSCHBAUM, N. E., NEWMAN, P. J. & ALBELDA, S. M. 1994. Platelet endothelial cell adhesion molecule-1 (PECAM-1/CD31): alternatively spliced, functionally distinct isoforms expressed during mammalian cardiovascular development. *Development*, 120, 2539-2553.
- BANWELL, E. F., ABELARDO, E. S., ADAMS, D. J., BIRCHALL, M. A., CORRIGAN, A., DONALD, A. M., KIRKLAND, M., SERPELL, L. C., BUTLER, M. F. & WOOLFSON, D. N. 2009. Rational design and application of responsive α -helical peptide hydrogels. *Nature Materials*, 8, 596-600.
- BARKER, T. H. 2011. The role of ECM proteins and protein fragments in guiding cell behavior in regenerative medicine. *Biomaterials*, 32, 4211-4214.
- BARRON, V., LYONS, E., STENSON-COX, C., MCHUGH, P. & PANDIT, A. 2003. Bioreactors for cardiovascular cell and tissue growth: a review. *Annals of Biomedical Engineering*, 31, 1017-1030.
- BASMADJIAN, D., SEFTON, M. V. & BALDWIN, S. A. 1997. Coagulation on biomaterials in flowing blood: some theoretical considerations. *Biomaterials*, 18, 1511-1522.
- BAYRAK, A., TYRALLA, M., LADHOFF, J., SCHLEICHER, M., STOCK, U. A., VOLK, H.-D. & SEIFERT, M. 2010. Human immune responses to porcine xenogeneic matrices and their extracellular matrix constituents *in vitro*. *Biomaterials*, 31, 3793-3803.
- BELCH, J., STANSBY, G., SHEARMAN, C., BRITTENDEN, J., DUGDILL, S., FOWKES, G., JARVIS, S., MCCANN, T., MIMNAGH, A. & MONKMAN, D. 2007. Peripheral arterial disease - a cardiovascular time bomb. *The British Journal of Diabetes & Vascular Disease*, 7, 236-239.
- BELL, C. J., CARRICK, L. M., KATTA, J., JIN, Z., INGHAM, E., AGGELI, A., BODEN, N., WAIGH, T. A. & FISHER, J. 2006. Self-assembling peptides as injectable lubricants for osteoarthritis. *Journal of Biomedical Materials Research Part A*, 78, 236-246.

- BELL, R. G., SADOWSKI, J. A. & MATSCHINER, J. T. 2002. Mechanism of action of warfarin. Warfarin and metabolism of vitamin K1. *Biochemistry*, 11, 1959-1961.
- BERGMEISTER, H., PLASENZOTTI, R., WALTER, I., PLASS, C., BASTIAN, F., RIEDER, E., SIPOS, W., KAIDER, A., LOSERT, U. & WEIGEL, G. 2008. Decellularized, xenogeneic small-diameter arteries: Transition from a muscular to an elastic phenotype *in vivo*. *Journal of Biomedical Materials Research Part B: Applied Biomaterials*, 87B, 95-104.
- BHARDWAJ, S., ROY, H., HEIKURA, T. & YLÄ-HERTTUALA, S. 2005. VEGF-A, VEGF-D and VEGF-D Δ N Δ C induced intimal hyperplasia in carotid arteries. *European Journal of Clinical Investigation*, 35, 669-676.
- BILFINGER, T., HARTMAN, A., LIU, Y., MAGAZINE, H. & STEFANO, G. 1997. Cryopreserved veins in myocardial revascularization: Possible mechanism for their increased failure. *The Annals of thoracic surgery*, 63, 1063.
- BISCHOF, I. & SCHWARZ, U. 2003. Cell organization in soft media due to active mechanosensing. *Proceedings of the National Academy of Sciences*, 100, 9274-9279.
- BJORK, I. & LINDAHL, U. 1982. Mechanism of the anticoagulant action of heparin. *Molecular and Cellular Biochemistry*, 48, 161-182.
- BLASS, C. R. 1999. *Polymers in Disposable Medical Devices: A European Perspective*, iSmithers Rapra Publishing.
- BOCK, L., GRIFFIN, L., LATHAM, J., VERMAAS, E. & TOOLE, J. 1992. Selection of single-stranded DNA molecules that bind and inhibit human thrombin. *Nature*, 355, 564-566.
- BOLAND, E., MATTHEWS, J., PAWLOWSKI, K., SIMPSON, D., WNEK, G. & BOWLIN, G. 2004. Electrospinning collagen and elastin: preliminary vascular tissue engineering. *Front Biosci*, 9, 1422-1432.
- BORNSTEIN, P. & SAGE, H. 1980. Structurally distinct collagen types. *Annual Review of Biochemistry*, 49, 957-1003.
- BOU-GHARIOS, G., PONTICOS, M., RAJKUMAR, V. & ABRAHAM, D. 2004. Extra-cellular matrix in vascular networks. *Cell Proliferation*, 37, 207-220.
- BRODY, S. & PANDIT, A. 2007. Approaches to heart valve tissue engineering scaffold design. *Journal of Biomedical Materials Research Part B: Applied Biomaterials*, 83, 16-43.
- BROZE JR, M., G.J. 1995. Tissue factor pathway inhibitor and the revised theory of coagulation. *Annual Review of Medicine*, 46, 103-112.
- BRUINS, P., TE VELTHUIS, H., YAZDANBAKSHI, A. P., JANSEN, P. G., VAN HARDEVELT, F. W., DE BEAUMONT, E. M., WILDEVUUR, C. R., EIJSMA, L., TROUWBORST, A. & HACK, C. E. 1997. Activation of the complement system during and after cardiopulmonary bypass surgery postsurgery activation involves C-reactive protein and is associated with postoperative arrhythmia. *Circulation*, 96, 3542-3548.
- BUJAN, J., GARCIA-HONDUVILLA, N. & BELLON, J. 2004. Engineering conduits to resemble natural vascular tissue. *Biotechnology and Applied Biochemistry*, 39, 17-27.
- BUREEVA, S., ANDIA-PRAVDIVY, J., PETROV, G., IGUMNOV, M., ROMANOV, S., KOLESNIKOVA, E., KAPLUN, A. & KOZLOV, L. 2005. Inhibition of classical pathway of complement activation with negative charged derivatives of bisphenol A and bisphenol disulphates. *Bioorganic & Medicinal Chemistry*, 13, 1045-1052.
- BUTTAFOCO, L., KOLKMAN, N., ENGBERS-BUIJTENHUIJS, P., POOT, A., DIJKSTRA, P., VERMES, I. & FEIJEN, J. 2006. Electrospinning of collagen and elastin for tissue engineering applications. *Biomaterials*, 27, 724-734.
- CAI, W., GU, Y., WANG, X. & CHEN, C. 2009. Heparin Coating of Small-Caliber Decellularized Xenografts Reduces Macrophage Infiltration and Intimal Hyperplasia. *Artificial Organs*, 33, 448-455.
- CALLOW, A. 1996. Arterial homografts. *European Journal of Vascular & Endovascular Surgery*, 12, 272-281.

- CAMPBELL, J., EFENDY, J. & CAMPBELL, G. 1999. Novel vascular graft grown within recipient's own peritoneal cavity. *Circulation Research*, 85, 1173.
- CAPEWELL, P. S., ALLENDER, D. S., CRITCHLEY, D. J., LLOYD-WILLIAMS, D. F., O'FLAHERTY, D. M., RAYNER, D. M. & SCARBOROUGH, P. 2008. *Modelling the Burden of Cardiovascular Disease to 2020*.
- CARPENTER, J. & TOMASZEWSKI, J. 1998. Human saphenous vein allograft bypass grafts: immune response. *Journal of Vascular Surgery*, 27, 492-499.
- CARRICK, L., AGGELI, A., BODEN, N., FISHER, J., INGHAM, E. & WAIGH, T. 2007. Effect of ionic strength on the self-assembly, morphology and gelation of pH responsive -sheet tape-forming peptides. *Tetrahedron*, 63, 7457-7467.
- CARROLL, M. C. 2004. The complement system in regulation of adaptive immunity. *Nature Immunology*, 5, 981-986.
- CHAMIOT-CLERC, P., COPIE, X., RENAUD, J.-F., SAFAR, M. & GIRERD, X. 1998. Comparative reactivity and mechanical properties of human isolated internal mammary and radial arteries. *Cardiovascular Research*, 37, 811-819.
- CHANDLER, A. 1969. The anatomy of a thrombus. *Thrombosis*. . Washington, DC, National Academy of Science USA.
- CHANDLER, A. & JACOBSEN, C. 1967. In vitro thrombosis in thrombotic and hemorrhagic diseases. *Scandinavian Journal of Clinical & Laboratory Investigation*, 20, 129-139.
- CHANG, Y., HSU, C.-K., WEI, H.-J., CHEN, S.-C., LIANG, H.-C., LAI, P.-H. & SUNG, H.-W. 2005. Cell-free xenogenic vascular grafts fixed with glutaraldehyde or genipin: In vitro and in vivo studies. *Journal of Biotechnology*, 120, 207-219.
- CHATZIZISIS, Y. S., COSKUN, A. U., JONAS, M., EDELMAN, E. R., FELDMAN, C. L. & STONE, P. H. 2007. Role of endothelial shear stress in the natural history of coronary atherosclerosis and vascular remodeling: molecular, cellular, and vascular behavior. *Journal of the American College of Cardiology*, 49, 2379-2393.
- CHEN, C., LI, J., MATTAR, S. G., PIERCE, G. F., AUKERMAN, L., HANSON, S. R. & LUMSDEN, A. B. 1997. Boundary Layer Infusion of Basic Fibroblast Growth Factor Accelerates Intimal Hyperplasia In Endarterectomized Canine Artery. *Journal of Surgical Research*, 69, 300-306.
- CHEN, P. 2005. Self-assembly of ionic-complementary peptides: a physicochemical viewpoint. *Colloids and Surfaces A: Physicochemical and Engineering Aspects*, 261, 3-24.
- CHEN, R. & HUNT, J. 2007. Biomimetic materials processing for tissue-engineering processes. *Journal of Materials Chemistry*, 17, 3974-3979.
- CHENG, G. C., LOREE, H. M., KAMM, R. D., FISHBEIN, M. C. & LEE, R. T. 1993. Distribution of circumferential stress in ruptured and stable atherosclerotic lesions. A structural analysis with histopathological correlation. *Circulation*, 87, 1179-1187.
- CHIU, J., USAMI, S. & CHIEN, S. 2009. Vascular endothelial responses to altered shear stress: Pathologic implications for atherosclerosis. *Annals of Medicine*, 41, 19-28.
- CHRISTENSEN, K., LARSSON, R., EMANUELSSON, H., ELGUE, G. & LARSSON, A. 2001. Heparin coating of the stent graft - effects on platelets, coagulation and complement activation. *Biomaterials*, 22, 349-355.
- CITTADELLA, G., MEL, A., DEE, R., DE COPPI, P. & SEIFALIAN, A. M. 2013. Arterial Tissue Regeneration for Pediatric Applications: Inspiration From Up-to-Date Tissue-Engineered Vascular Bypass Grafts. *Artificial Organs*.
- COHN, J. N. 2001. Arterial compliance to stratify cardiovascular risk: more precision in therapeutic decision making. *American Journal of Hypertension*, 14, 258S-263S.
- COLMAN, R. W. & SCHMAIER, A. H. 1997. Contact system: a vascular biology modulator with anticoagulant, profibrinolytic, antiadhesive, and proinflammatory attributes. *Blood*, 90, 3819-3843.

- CONKLIN, B., RICHTER, E., KREUTZIGER, K., ZHONG, D. & CHEN, C. 2002. Development and evaluation of a novel decellularized vascular xenograft. *Medical Engineering and Physics*, 24, 173-183.
- CONKLIN, B. S., WU, H., LIN, P. H., LUMSDEN, A. B. & CHEN, C. 2004. Basic Fibroblast Growth Factor Coating and Endothelial Cell Seeding of a Decellularized Heparin-coated Vascular Graft. *Artificial Organs*, 28, 668-675.
- COURTMAN, D., ERRETT, B. & WILSON, G. 2001. The role of crosslinking in modification of the immune response elicited against xenogenic vascular acellular matrices. *Journal of Biomedical Materials Research*, 55, 576-586.
- COURTMAN, D. W., PEREIRA, C. A., KASHEF, V., MCCOMB, D., LEE, J. M. & WILSON, G. J. 1994. Development of a pericardial acellular matrix biomaterial: Biochemical and mechanical effects of cell extraction. *Journal of Biomedical materials Research*, 28, 655-666.
- COWAN, R. E., MANNING, A. P., AYLIFFE, G. A. J., AXON, A. T. R., CAUSTON, J. S., CRIPPS, N. F., HALL, R., HANSON, P. J. V., HARRISON, J. & LEICESTER, R. J. 1993. Aldehyde disinfectants and health in endoscopy unit. *Gut*, 34, 1641.
- CRADDOCK, P. R., FEHR, J., DALMASSO, A., BRIGHAN, K. & JACOB, H. 1977. Hemodialysis leukopenia. Pulmonary vascular leukostasis resulting from complement activation by dialyzer cellophane membranes. *Journal of Clinical Investigation*, 59, 879.
- CREE, I. & ANDREOTTI, P. 1997. Measurement of cytotoxicity by ATP-based luminescence assay in primary cell cultures and cell lines. *Toxicology in Vitro*, 11, 553-556.
- CROUCH, S. P. M., KOZLOWSKI, R., SLATER, K. J. & FLETCHER, J. 1993. The use of ATP bioluminescence as a measure of cell proliferation and cytotoxicity. *Journal of Immunological Methods*, 160, 81-88.
- CROWTHER, M., CLASE, C., MARGETTS, P., JULIAN, J., LAMBERT, K., SNEATH, D., NAGAI, R., WILSON, S. & INGRAM, A. 2002. Low-intensity warfarin is ineffective for the prevention of PTFE graft failure in patients on hemodialysis: a randomized controlled trial. *Journal of the American Society of Nephrology*, 13, 2331.
- CUI, H., WEBBER, M. J. & STUPP, S. I. 2010. Self-assembly of peptide amphiphiles: From molecules to nanostructures to biomaterials. *Peptide Science*, 94, 1-18.
- CURSIEFEN, C., CHEN, L., BORGES, L., JACKSON, D., CAO, J., RADZIEJEWSKI, C., D'AMORE, P., DANA, M., WIEGAND, S. & STREILEIN, J. 2004. VEGF-A stimulates lymphangiogenesis and hemangiogenesis in inflammatory neovascularization via macrophage recruitment. *Journal of Clinical Investigation*, 113, 1040-1050.
- DAHAN, N., ZARBIV, G., SARIG, U., KARRAM, T., HOFFMAN, A. & MACHLUF, M. 2012. Porcine Small Diameter Arterial Extracellular Matrix Supports Endothelium Formation and Media Remodeling Forming a Promising Vascular Engineered Biograft. *Tissue Engineering Part A*, 18, 411-422.
- DALBY, M. J., RIEHLE, M. O., JOHNSTONE, H., AFFROSSMAN, S. & CURTIS, A. S. G. 2002. In vitro reaction of endothelial cells to polymer demixed nanotopography. *Biomaterials*, 23, 2945-2954.
- DAVIE, E. W., FUJIKAWA, K. & KISIEL, W. 1991. The coagulation cascade: initiation, maintenance, and regulation. *Biochemistry*, 30, 10363-10370.
- DAVIS, M., MOTION, J., NARMONEVA, D., TAKAHASHI, T., HAKUNO, D., KAMM, R., ZHANG, S. & LEE, R. 2005. Injectable self-assembling peptide nanofibers create intramyocardial microenvironments for endothelial cells. *Circulation*, 111, 442.
- DE LOOS, M., FERINGA, B. & VAN ESCH, J. 2005. Design and application of self-assembled low molecular weight hydrogels. *European Journal of Organic Chemistry*, 17, 3615.
- DE MEL, A., PUNSHON, G., RAMESH, B., SARKAR, S., DARBYSHIRE, A., HAMILTON, G. & SEIFALIAN, A. M. 2009. In situ endothelialisation potential of a biofunctionalised nanocomposite biomaterial-based small diameter bypass graft. *Bio-Medical Materials and Engineering*, 19, 317-331.

- DE VRIES, A., FELDMAN, J. D., STEIN, O., STEIN, Y. & KATCHALSKI, E. Effects of intravenously administered poly-D L-lysine in rats. *Proceedings of the Society for Experimental Biology and Medicine*. Society for Experimental Biology and Medicine (New York, NY), 1953. Royal Society of Medicine, 237-240.
- DELISSER, H. M., NEWMAN, P. J. & ALBELDA, S. M. 1994. Molecular and functional aspects of PECAM-1/CD31. *Immunology Today*, 15, 490-495.
- DERHAM, C., YOW, H., INGRAM, J., FISHER, J., INGHAM, E., KORROSI, S. A. & HOMER-VANNIASINKAM, S. 2008. Tissue engineering small-diameter vascular grafts: preparation of a biocompatible porcine ureteric scaffold. *Tissue Engineering Part A*, 14, 1871-1882.
- DESAI, M., SEIFALIAN, A. M. & HAMILTON, G. 2011. Role of prosthetic conduits in coronary artery bypass grafting. *European Journal of Cardio-Thoracic Surgery*, 40, 394-398.
- DIXIT, P., HERN-ANDERSON, D., RANIERI, J. & SCHMIDT, C. 2001. Vascular graft endothelialization: Comparative analysis of canine and human endothelial cell migration on natural biomaterials. *Journal of Biomedical Materials Research*, 56, 545-555.
- DONG, Q. G., BERNASCONI, S., LOSTAGLIO, S., DE CALMANOVICI, R. W., MARTIN-PADURA, I., BREVIARIO, F., GARLANDA, C., RAMPONI, S., MANTOVANI, A. & VECCHI, A. 1997. A General Strategy for Isolation of Endothelial Cells From Murine Tissues Characterization of Two Endothelial Cell Lines From the Murine Lung and Subcutaneous Sponge Implants. *Arteriosclerosis, Thrombosis, and Vascular Biology*, 17, 1599-1604.
- DORAFSHAR, A., ANGLE, N., BRYER-ASH, M., HUANG, D., FAROOQ, M., GELABERT, H. & FREISCHLAG, J. 2003. Vascular endothelial growth factor inhibits mitogen-induced vascular smooth muscle cell proliferation. *Journal of Surgical Research*, 114, 179-186.
- DOUGAN, H., LYSTER, D. M., VO, C. V., STAFFORD, A., WEITZ, J. I. & HOBBS, J. B. 2000. Extending the lifetime of anticoagulant oligodeoxynucleotide aptamers in blood. *Nuclear Medicine and Biology*, 27, 289-297.
- DOUGAN, H., WEITZ, J., STAFFORD, A., GILLESPIE, K., KLEMENT, P., HOBBS, J. & LYSTER, D. 2003. Evaluation of DNA aptamers directed to thrombin as potential thrombus imaging agents. *Nuclear Medicine and Biology*, 30, 61-72.
- DRURY, J. & MOONEY, D. 2003. Hydrogels for tissue engineering: scaffold design variables and applications. *Biomaterials*, 24, 4337-4351.
- DVORAK, H., BROWN, L., DETMAR, M. & DVORAK, A. 1995. Vascular permeability factor/vascular endothelial growth factor, microvascular hyperpermeability, and angiogenesis. *The American Journal of Pathology*, 146, 1029.
- EHLENBERGER, A. G. & NUSSENZWEIG, V. 1977. The role of membrane receptors for C3b and C3d in phagocytosis. *The Journal of Experimental Medicine*, 145, 357-371.
- ELLIS-BEHNKE, R. G., LIANG, Y. X., YOU, S. W., TAY, D. K. C., ZHANG, S., SO, K. F. & SCHNEIDER, G. E. 2006. Nano neuro knitting: peptide nanofiber scaffold for brain repair and axon regeneration with functional return of vision. *Proceedings of the National Academy of Sciences of the United States of America*, 103, 5054-5059.
- EPSTEIN, F. H. & ROSS, R. 1999. Atherosclerosis - an inflammatory disease. *New England Journal of Medicine*, 340, 115-126.
- ESMON, C. T. 1989. The roles of protein C and thrombomodulin in the regulation of blood coagulation. *Journal of Biological Chemistry*, 264, 4743-4746.
- ESSELL, J. H., MARTIN, T. J., SALINAS, J., THOMPSON, J. M. & SMITH, V. C. 1993. Comparison of thromboelastography to bleeding time and standard coagulation tests in patients after cardiopulmonary bypass. *Journal of Cardiothoracic and Vascular Anesthesia*, 7, 410-415.

- FAHNER, P., IDU, M., VAN GULIK, T. & LEGEMATE, D. 2006. Systematic review of preservation methods and clinical outcome of infrainguinal vascular allografts. *Journal of Vascular Surgery*, 44, 518-524.
- FATTORI, R. & PIVA, T. 2003. Drug-eluting stents in vascular intervention. *The Lancet*, 361, 247-249.
- FEARON, D. T. & AUSTEN, K. F. 1980. The alternative pathway of complement - a system for host resistance to microbial infection. *New England Journal of Medicine*, 303, 259-263.
- FERRARA, N., GERBER, H. & LECOUTER, J. 2003. The biology of VEGF and its receptors. *Nature Medicine*, 9, 669-676.
- FISCHER, D., LI, Y., AHLEMEYER, B., KRIEGLSTEIN, J. & KISSEL, T. 2003. In vitro cytotoxicity testing of polycations: influence of polymer structure on cell viability and hemolysis. *Biomaterials*, 24, 1121-1131.
- FITTKAU, M., ZILLA, P., BEZUIDENHOUT, D., LUTOLF, M., HUMAN, P., HUBBELL, J. & DAVIES, N. 2005. The selective modulation of endothelial cell mobility on RGD peptide containing surfaces by YIGSR peptides. *Biomaterials*, 26, 167-174.
- FRAISE, A. P. 1999. Choosing disinfectants. *Journal of Hospital Infection*, 43, 255-264.
- FREED, L. E., VUNJAK-NOVAKOVIC, G., BIRON, R. J., EAGLES, D. B., LESNOY, D. C., BARLOW, S. K. & LANGER, R. 1994. Biodegradable polymer scaffolds for tissue engineering. *Nature Biotechnology*, 12, 689-693.
- FRESHNEY, R. I., VUNJAK-NOVAKOVIC, G. & FRESHNEY, R. 2006. Basic Principles of Cell Culture. *Culture of Cells for Tissue Engineering*, 11-14.
- FREYTES, D. O., BADYLAK, S. F., WEBSTER, T. J., GEDDES, L. A. & RUNDELL, A. E. 2004. Biaxial strength of multilaminated extracellular matrix scaffolds. *Biomaterials*, 25, 2353-2361.
- FRISKEN GIBSON, S. & LANNI, F. 1991. Experimental test of an analytical model of aberration in an oil-immersion objective lens used in three-dimensional light microscopy. *Journal of the Optical Society of America A*, 8, 1601-1613.
- FUKUMURA, D., GOHONGI, T., KADAMBI, A., IZUMI, Y., ANG, J., YUN, C.-O., BUERK, D. G., HUANG, P. L. & JAIN, R. K. 2001. Predominant role of endothelial nitric oxide synthase in vascular endothelial growth factor-induced angiogenesis and vascular permeability. *Proceedings of the National Academy of Sciences*, 98, 2604-2609.
- FURIE, B. & FURIE, B. C. 2008. Mechanisms of thrombus formation. *New England Journal of Medicine*, 359, 938-949.
- GAILANI, D. & RENNÈ, T. 2007. Intrinsic pathway of coagulation and arterial thrombosis. *Arteriosclerosis, Thrombosis, and Vascular Biology*, 27, 2507-2513.
- GARCÍA-CARDEÑA, G., COMANDER, J., ANDERSON, K. R., BLACKMAN, B. R. & GIMBRONE, M. A. 2001. Biomechanical activation of vascular endothelium as a determinant of its functional phenotype. *Proceedings of the National Academy of Sciences*, 98, 4478-4485.
- GAUVIN, R., AHSAN, T., LAROUCHE, D., LÃ©VESQUE, P., DUBÃ©, J., AUGER, F. A., NEREM, R. M. & GERMAIN, L. 2010. A novel single-step self-assembly approach for the fabrication of tissue-engineered vascular constructs. *Tissue Engineering Part A*, 16, 1737-1747.
- GELAIN, F., BOTTAI, D., VESCOVI, A. & ZHANG, S. 2006. Designer self-assembling peptide nanofiber scaffolds for adult mouse neural stem cell 3-dimensional cultures. *PLoS One*, 1.
- GELAIN, F., HORII, A. & ZHANG, S. 2007. Designer self-assembling peptide scaffolds for 3-d tissue cell cultures and regenerative medicine. *Macromolecular Bioscience*, 7, 544-551.
- GENOVÉ, E., SHEN, C., ZHANG, S. & SEMINO, C. 2005. The effect of functionalized self-assembling peptide scaffolds on human aortic endothelial cell function. *Biomaterials*, 26, 3341-3351.
- GILBERT, T. W., FREUND, J. M. & BADYLAK, S. F. 2009. Quantification of DNA in biologic scaffold materials. *Journal of Surgical Research*, 152, 135-139.

- GILBERT, T. W., SELLARO, T. L. & BADYLAK, S. F. 2006. Decellularization of tissues and organs. *Biomaterials*, 27, 3675-3683.
- GIMBRONE, M. A., COTRAN, R. S. & FOLKMAN, J. 1974. Human vascular endothelial cells in culture growth and DNA synthesis. *The Journal of Cell Biology*, 60, 673-684.
- GLABE, C. G. 2008. Structural classification of toxic amyloid oligomers. *Journal of Biological Chemistry*, 283, 29639-29643.
- GORBET, M. B. & SEFTON, M. V. 2001. Leukocyte activation and leukocyte procoagulant activities after blood contact with polystyrene and polyethylene glycol-immobilized polystyrene beads. *Journal of Laboratory and Clinical Medicine*, 137, 345-355.
- GORBET, M. B. & SEFTON, M. V. 2004. Biomaterial-associated thrombosis: roles of coagulation factors, complement, platelets and leukocytes. *Biomaterials*, 25, 5681-5703.
- GRATZER, P. F., HARRISON, R. D. & WOODS, T. 2006. Matrix alteration and not residual sodium dodecyl sulfate cytotoxicity affects the cellular repopulation of a decellularized matrix. *Tissue Engineering*, 12, 2975-2983.
- GRAUSS, R. W., HAZEKAMP, M. G., OPPENHUIZEN, F., VAN MUNSTEREN, C. J., GITTEBERGER-DE GROOT, A. C. & DERUITER, M. C. 2005. Histological evaluation of decellularised porcine aortic valves: matrix changes due to different decellularisation methods. *European Journal of Cardio-Thoracic Surgery*, 27, 566-571.
- GRESELE, P., ARNOUT, J., DECKMYN, H. & VERMYLEN, J. 1986. Mechanism of the antiplatelet action of dipyridamole in whole blood: modulation of adenosine concentration and activity. *Thrombosis and Haemostasis*, 55, 12-18.
- GRIFFITHS, P. & DE HASETH, J. A. 2007. *Fourier transform infrared spectrometry*, Wiley-Interscience.
- GUELCHER, S. A. 2008. Biodegradable polyurethanes: synthesis and applications in regenerative medicine. *Tissue Engineering Part B: Reviews*, 14, 3-17.
- GUI, L., MUTO, A., CHAN, S., BREUER, C. & NIKLASON, L. 2009. Development of decellularized human umbilical arteries as small-diameter vascular grafts. *Tissue Engineering Part A*, 15, 2665-2676.
- GUNATILLAKE, P. A. & ADHIKARI, R. 2003. Biodegradable synthetic polymers for tissue engineering. *European Cells and Materials*, 5, 1-16.
- GUO, J., LEUNG, K. K. G., SU, H., YUAN, Q., WANG, L., CHU, T.-H., ZHANG, W., PU, J. K. S., NG, G. K. P., WONG, W. M., DAI, X. & WU, W. 2009. Self-assembling peptide nanofiber scaffold promotes the reconstruction of acutely injured brain. *Nanomedicine: Nanotechnology, Biology and Medicine*, 5, 345-351.
- HADDERS, MICHAEL A., BUBECK, D., ROVERSI, P., HAKOBYAN, S., FORNERIS, F., MORGAN, B. P., PANGBURN, MICHAEL K., LLORCA, O., LEA, SUSAN M. & GROS, P. 2012. Assembly and Regulation of the Membrane Attack Complex Based on Structures of C5b6 and sC5b9. *Cell Reports*, 1, 200-207.
- HAINES-BUTTERICK, L., RAJAGOPAL, K., BRANCO, M., SALICK, D., RUGHANI, R., PILARZ, M., LAMM, M. S., POCHAN, D. J. & SCHNEIDER, J. P. 2007. Controlling hydrogelation kinetics by peptide design for three-dimensional encapsulation and injectable delivery of cells. *Proceedings of the National Academy of Sciences*, 104, 7791.
- HAINES-BUTTERICK, L. A., SALICK, D. A., POCHAN, D. J. & SCHNEIDER, J. P. 2008. In vitro assessment of the pro-inflammatory potential of β -hairpin peptide hydrogels. *Biomaterials*, 29, 4164-4169.
- HAMMEL, M., SFYROERA, G., RICKLIN, D., MAGOTTI, P., LAMBRIS, J. D. & GEISBRECHT, B. V. 2007. A structural basis for complement inhibition by *Staphylococcus aureus*. *Nature Immunology*, 8, 430-437.
- HASEGAWA, T., OKADA, K., TAKANO, Y., HIRAIISHI, Y. & OKITA, Y. 2007. Autologous fibrin-coated small-caliber vascular prostheses improve antithrombogenicity by reducing

- immunologic response. *The Journal of Thoracic and Cardiovascular Surgery*, 133, 1268-1276.
- HE, W., YONG, T., TEO, W. E., MA, Z. & RAMAKRISHNA, S. 2005. Fabrication and endothelialization of collagen-blended biodegradable polymer nanofibers: potential vascular graft for blood vessel tissue engineering. *Tissue Engineering*, 11, 1574-1588.
- HEINE, J., SCHMIEDL, A., CEBOTARI, S., MERTSCHING, H., KARCK, M., HAVERICH, A. & KALLENBACH, K. 2011. Preclinical Assessment of a Tissue-Engineered Vasomotive Human Small-Calibered Vessel Based on a Decellularized Xenogenic Matrix: Histological and Functional Characterization. *Tissue Engineering Part A*, 17, 1253-1261.
- HELEN, W., DE LEONARDIS, P., ULIJN, R. V., GOUGH, J. & TIRELLI, N. 2011. Mechanosensitive peptide gelation: mode of agitation controls mechanical properties and nano-scale morphology. *Soft Matter*, 7, 1732-1740.
- HEMMRICH, K., SALBER, J., MEERSCH, M., WIESEMANN, U., GRIES, T., PALLUA, N. & KLEE, D. 2008. Three-dimensional nonwoven scaffolds from a novel biodegradable poly (ester amide) for tissue engineering applications. *Journal of Materials Science: Materials in Medicine*, 19, 257-267.
- HOCKING, A. M., SHINOMURA, T. & MCQUILLAN, D. J. 1998. Leucine-rich repeat glycoproteins of the extracellular matrix. *Matrix Biology*, 17, 1-19.
- HODDE, J., JANIS, A., ERNST, D., ZOPF, D., SHERMAN, D. & JOHNSON, C. 2007. Effects of sterilization on an extracellular matrix scaffold: part I. Composition and matrix architecture. *Journal of Materials Science: Materials in Medicine*, 18, 537-543.
- HOERSTRUP, S., ZÜND, G., SODIAN, R., SCHNELL, A., GRÜNENFELDER, J. & TURINA, M. 2001. Tissue engineering of small caliber vascular grafts. *European Journal of Cardio-Thoracic Surgery*, 20, 164-169.
- HOERSTRUP, S. P., SODIAN, R., DAEBRITZ, S., WANG, J., BACHA, E. A., MARTIN, D. P., MORAN, A. M., GULESERIAN, K. J., SPERLING, J. S. & KAUSHAL, S. 2000. Functional living trileaflet heart valves grown in vitro. *Circulation*, 102, 44-49.
- HOFFMAN, A. S. 1999. Non-fouling surface technologies. *Journal of Biomaterials Science, Polymer Edition*, 10, 1011-1014.
- HOFFMANN, J., PAUL, A., HARWARDT, M., GROLL, J., REESWINKEL, T., KLEE, D., MOELLER, M., FISCHER, H., WALKER, T. & GREINER, T. 2008. Immobilized DNA aptamers used as potent attractors for porcine endothelial precursor cells. *Journal of Biomedical Materials Research Part A*, 84, 614.
- HOLLAS, J. M. 2004. *Modern spectroscopy*, Wiley.
- HOLLEY, R. W. & KIERNAN, J. A. 1974. Control of the initiation of DNA synthesis in 3T3 cells: low-molecular-weight nutrients. *Proceedings of the National Academy of Sciences*, 71, 2942-2945.
- HOLMES, T. C., DE LACALLE, S., SU, X., LIU, G., RICH, A. & ZHANG, S. 2000. Extensive neurite outgrowth and active synapse formation on self-assembling peptide scaffolds. *Proceedings of the National Academy of Sciences*, 97, 6728.
- HONG, J., NILSSON EKDAHL, K., REYNOLDS, H., LARSSON, R. & NILSSON, B. 1999. A new in vitro model to study interaction between whole blood and biomaterials. Studies of platelet and coagulation activation and the effect of aspirin. *Biomaterials*, 20, 603-611.
- HORNSTRA, G. 2009. Dietary fats and arterial thrombosis. *Pathophysiology of Haemostasis and Thrombosis*, 2, 21-52.
- HOSHI, R. A., VAN LITH, R., JEN, M. C., ALLEN, J. B., LAPIDOS, K. A. & AMEER, G. 2012. The blood and vascular cell compatibility of heparin-modified ePTFE vascular grafts. *Biomaterials*.
- HRISTOV, M., ERL, W. & WEBER, P. C. 2003. Endothelial Progenitor Cells: Isolation and Characterization. *Trends in Cardiovascular Medicine*, 13, 201-206.

- HUANG, Q., DAWSON, R. A., PEGG, D. E., KEARNEY, J. N. & MACNEIL, S. 2004. Use of peracetic acid to sterilize human donor skin for production of acellular dermal matrices for clinical use. *Wound Repair and Regeneration*, 12, 276-287.
- HUANG, R., QI, W., FENG, L., SU, R. & HE, Z. 2011. Self-assembling peptide-polysaccharide hybrid hydrogel as a potential carrier for drug delivery. *Soft Matter*, 7, 6222-6230.
- HWANG, K. K., YANG, C. D., YAN, W., GROSSMAN, J. M., HAHN, B. H. & CHEN, P. P. 2003. A thrombin-cross-reactive anticardiolipin antibody binds to and inhibits the anticoagulant function of activated protein C. *Arthritis & Rheumatism*, 48, 1622-1630.
- ISENBERG, B., WILLIAMS, C. & TRANQUILLO, R. 2006. Small-diameter artificial arteries engineered in vitro. *Circulation Research*, 98, 25.
- JACOB, M., BADIÉ-COMMANDER, C., FONTAINE, V., BENZAOUZ, Y., FELDMAN, L. & MICHEL, J. 2001. Extracellular matrix remodeling in the vascular wall. *Pathologie Biologie*, 49, 326-332.
- JAFFE, E. A., NACHMAN, R. L., BECKER, C. G. & MINICK, C. R. 1973. Culture of human endothelial cells derived from umbilical veins. Identification by morphologic and immunologic criteria. *Journal of Clinical Investigation*, 52, 2745.
- JAYAWARNA, V., RICHARDSON, S. M., HIRST, A. R., HODSON, N. W., SAIANI, A., GOUGH, J. E. & ULIJN, R. V. 2009. Introducing chemical functionality in Fmoc-peptide gels for cell culture. *Acta Biomaterialia*, 5, 934-943.
- JERNIGAN, T. W., CROCE, M. A., CAGIANNOS, C., SHELL, D. H., HANDORF, C. R. & FABIAN, T. C. 2004. Small intestinal submucosa for vascular reconstruction in the presence of gastrointestinal contamination. *Annals of Surgery*, 239, 733.
- JOCKENHOEVEL, S., ZUND, G., HOERSTRUP, S., CHALABI, K., SACHWEH, J., DEMIRCAN, L., MESSMER, B. & TURINA, M. 2001. Fibrin gel-advantages of a new scaffold in cardiovascular tissue engineering. *European Journal of Cardio-Thoracic Surgery*, 19, 424-430.
- JÓZSI, M. 2011. *Anti-Complement Autoantibodies in Membranoproliferative Glomerulonephritis and Dense Deposit Disease*.
- JUN, H. & WEST, J. 2004. Development of a YIGSR-peptide-modified polyurethaneurea to enhance endothelialization. *Journal of Biomaterials Science, Polymer Edition*, 15, 73-94.
- JUNG, J., NAGARAJ, A., FOX, E., RUDRA, J., DEVGUN, J. & COLLIER, J. 2009. Co-assembling peptides as defined matrices for endothelial cells. *Biomaterials*, 30, 2400-2410.
- KABANOV, A. & KABANOV, V. 1995. DNA complexes with polycations for the delivery of genetic material into cells. *Bioconjugate Chemistry*, 6, 7-20.
- KALLENBACH, K., LEYH, R. G., LEFIK, E., WALLE, T., WILHELMI, M., CEBOTARI, S., SCHMIEDL, A., HAVERICH, A. & MERTSCHING, H. 2004. Guided tissue regeneration: porcine matrix does not transmit PERV. *Biomaterials*, 25, 3613-3620.
- KAMITANI, H., MASUZAWA, H., KANAZAWA, I. & KUBO, T. 2000. Saccular cerebral aneurysms in young adults. *Surgical Neurology*, 54, 59-67.
- KARCHALSKY, A., DANON, D., NEVO, A. & DE VRIES, A. 1959. Interaction of basic polyelectrolytes with the red blood cell II. Agglutination of red blood cells by polymeric bases. *Biochimica et Biophysica Acta*, 33, 120-138.
- KERR, M. 1980. The human complement system: assembly of the classical pathway C3 convertase. *Biochemical Journal*, 189, 173.
- KETCHEDJIAN, A., JONES, A. L., KRUEGER, P., ROBINSON, E., CROUCH, K., WOLFINBARGER JR, L. & HOPKINS, R. 2005. Recellularization of Decellularized Allograft Scaffolds in Ovine Great Vessel Reconstructions. *The Annals of Thoracic Surgery*, 79, 888-896.
- KHURANA, R., COLEMAN, C., IONESCU-ZANETTI, C., CARTER, S. A., KRISHNA, V., GROVER, R. K., ROY, R. & SINGH, S. 2005. Mechanism of thioflavin T binding to amyloid fibrils. *Journal of Structural Biology*, 151, 229-238.

- KIRKHAM, J., FIRTH, A., VERNALS, D., BODEN, N., ROBINSON, C., SHORE, R., BROOKES, S. & AGGELI, A. 2007. Self-assembling peptide scaffolds promote enamel remineralization. *Journal of Dental Research*, 86, 426-430.
- KITIS, M. 2004. Disinfection of wastewater with peracetic acid: a review. *Environment international*, 30, 47-55.
- KLEIN, W. L., KRAFFT, G. A. & FINCH, C. E. 2001. Targeting small A beta oligomers: the solution to an Alzheimer's disease conundrum? *Trends in Neurosciences*, 24, 219-224.
- KNETSCH, M. L. W., ALDENHOFF, Y. B. J., SCHRAVEN, M. & KOOLE, L. H. 2004. Human endothelial cell attachment and proliferation on a novel vascular graft prototype. *Journal of Biomedical Materials Research Part A*, 71A, 615-624.
- KOENNEKER, S., TEBKEN, O., BONEHIE, M., PFLAUM, M., JOCKENHOEVEL, S., HAVERICH, A. & WILHELMI, M. 2010. A biological alternative to alloplastic grafts in dialysis therapy: evaluation of an autologised bioartificial haemodialysis shunt vessel in a sheep model. *European Journal of Vascular and Endovascular Surgery*, 40, 810-816.
- KONIG, G., MCALLISTER, T., DUSSERRE, N., GARRIDO, S., IYICAN, C., MARINI, A., FIORILLO, A., AVILA, H., WYSTRYCHOWSKI, W. & ZAGALSKI, K. 2009. Mechanical properties of completely autologous human tissue engineered blood vessels compared to human saphenous vein and mammary artery. *Biomaterials*, 30, 1542-1550.
- KOZEL, B. A., RONGISH, B. J., CZIROK, A., ZACH, J., LITTLE, C. D., DAVIS, E. C., KNUTSEN, R. H., WAGENSEIL, J. E., LEVY, M. A. & MECHAM, R. P. 2005. Elastic fiber formation: a dynamic view of extracellular matrix assembly using timer reporters. *Journal of Cellular Physiology*, 207, 87-96.
- KRENNING, G., MOONEN, J., VAN LUYN, M. & HARMSSEN, M. 2008. Vascular smooth muscle cells for use in vascular tissue engineering obtained by endothelial-to-mesenchymal transdifferentiation (EnMT) on collagen matrices. *Biomaterials*, 29, 3703-3711.
- KRETSINGER, J. K., HAINES, L. A., OZBAS, B., POCAN, D. J. & SCHNEIDER, J. P. 2005. Cytocompatibility of self-assembled β -hairpin peptide hydrogel surfaces. *Biomaterials*, 26, 5177-5186.
- KRISHNAMURTHI, S., WESTWICK, J. & KAKKAR, V. V. 1984. Regulation of human platelet activation - Analysis of cyclooxygenase and cyclic AMP-dependent pathways. *Biochemical Pharmacology*, 33, 3025-3035.
- KROLL, M. & SCHAFER, A. 1989. Biochemical mechanisms of platelet activation. *Blood*, 74, 1181-1195.
- L'HEUREUX, N., DUSSERRE, N., MARINI, A., GARRIDO, S., DE LA FUENTE, L. & MCALLISTER, T. 2007. Technology insight: the evolution of tissue-engineered vascular grafts—from research to clinical practice. *Nature Clinical Practice Cardiovascular Medicine*, 4, 389.
- L'HEUREUX, N., PAQUET, S., LABBE, R., GERMAIN, L. & AUGER, F. 1998. A completely biological tissue-engineered human blood vessel. *The FASEB Journal*, 12, 47.
- LACOR, P. N., BUNIEL, M. C., FURLOW, P. W., CLEMENTE, A. S., VELASCO, P. T., WOOD, M., VIOLA, K. L. & KLEIN, W. L. 2007. A β oligomer-induced aberrations in synapse composition, shape, and density provide a molecular basis for loss of connectivity in Alzheimer's disease. *The Journal of Neuroscience*, 27, 796-807.
- LAMM, P., JUCHEM, G., MILZ, S., SCHUFFENHAUER, M. & REICHAERT, B. 2001. Autologous endothelialized vein allograft: a solution in the search for small-caliber grafts in coronary artery bypass graft operations. *Circulation*, 104, 108-114.
- LEASK, R., BUTANY, J., JOHNSTON, K., ETHIER, C. & OJHA, M. 2005. Human saphenous vein coronary artery bypass graft morphology, geometry and hemodynamics. *Annals of Biomedical Engineering*, 33, 301-309.
- LEE, J., GAN, H. T., LATIFF, S. M. A., CHUAH, C., LEE, W. Y., YANG, Y.-S., LOO, B., NG, S. K. & GAGNON, P. 2012. Principles and applications of steric exclusion chromatography. *Journal of Chromatography A*, 1270, 162-170.

- LEE, N. K., OH, H. J., HONG, C. M., SUH, H. & HONG, S. H. 2009. Comparison of the synthetic biodegradable polymers, polylactide (PLA), and polylactic-co-glycolic acid (PLGA) as scaffolds for artificial cartilage. *Biotechnology and Bioprocess Engineering*, 14, 180-186.
- LEE, R. T., SCHOEN, F. J., LOREE, H. M., LARK, M. W. & LIBBY, P. 1996. Circumferential Stress and Matrix Metalloproteinase 1 in Human Coronary Atherosclerosis Implications for Plaque Rupture. *Arteriosclerosis, Thrombosis, and Vascular Biology*, 16, 1070-1073.
- LEMSTROM, K., KREBS, R., NYKANEN, A., TIKKANEN, J., SIHVOLA, R., AALTOLA, E., HAYRY, P., WOOD, J., ALITALO, K. & YLA-HERTTUALA, S. 2002. Vascular endothelial growth factor enhances cardiac allograft arteriosclerosis. *Circulation*, 105, 2524.
- LEVENBERG, S., GOLUB, J. S., AMIT, M., ITSKOVITZ-ELDOR, J. & LANGER, R. 2002. Endothelial cells derived from human embryonic stem cells. *Proceedings of the National Academy of Sciences*, 99, 4391-4396.
- LIBBY, P., RIDKER, P. M. & MASERI, A. 2002. Inflammation and atherosclerosis. *Circulation*, 105, 1135-1143.
- LIEM, L. K., CHOONG, L. H. L. & WOO, K. T. 2001. Action of dipyridamole and warfarin on growth of human endothelial cells cultured in serum-free media. *Clinical Biochemistry*, 34, 141-147.
- LINSE, S., CABALEIRO-LAGO, C., XUE, W. F., LYNCH, I., LINDMAN, S., THULIN, E., RADFORD, S. E. & DAWSON, K. A. 2007. Nucleation of protein fibrillation by nanoparticles. *Proceedings of the National Academy of Sciences*, 104, 8691.
- LOMAS, R. J., CRUSE-SAWYER, J. E., SIMPSON, C., INGHAM, E., BOJAR, R. & KEARNEY, J. N. 2003. Assessment of the biological properties of human split skin allografts disinfected with peracetic acid and preserved in glycerol. *Burns*, 29, 515-525.
- LOOS, M., VOLANAKIS, J. E. & STROUD, R. M. 1976. Mode of interaction of different polyanions with the first (C1, C1), the second (C2) and the fourth (C4) component of complement-III: Inhibition of C4 and C2 binding site(s) on C1s, by polyanions. *Immunochemistry*, 13, 789-791.
- LUCAS, A. D., MERRITT, K., HITCHINS, V. M., WOODS, T. O., MCNAMEE, S. G., LYLE, D. B. & BROWN, S. A. 2003. Residual ethylene oxide in medical devices and device material. *Journal of Biomedical Materials Research Part B: Applied Biomaterials*, 66, 548-552.
- LUDTKE, S. J., HE, K., HELLER, W. T., HARROUN, T. A., YANG, L. & HUANG, H. W. 1996. Membrane pores induced by magainin. *Biochemistry*, 35, 13723-13728.
- LUO, Z., ASAHARA, T., TSURUMI, Y., ISNER, J. M. & SYMES, J. F. 1998. Reduction of vein graft intimal hyperplasia and preservation of endothelium-dependent relaxation by topical vascular endothelial growth factor. *Journal of Vascular Surgery*, 27, 167-173.
- LUONG-VAN, E., GRØNDAHL, L., CHUA, K. N., LEONG, K. W., NURCOMBE, V. & COOL, S. M. 2006. Controlled release of heparin from poly(ϵ -caprolactone) electrospun fibers. *Biomaterials*, 27, 2042-2050.
- MACKMAN, N. 2008. Triggers, targets and treatments for thrombosis. *Nature*, 451, 914-918.
- MAFFEI, F., BUSCHINI, A., ROSSI, C., POLI, P., FORTI, G. C. & HRELIA, P. 2005. Use of the Comet test and micronucleus assay on human white blood cells for in vitro assessment of genotoxicity induced by different drinking water disinfection protocols. *Environmental and molecular mutagenesis*, 46, 116-125.
- MANFIOLETTI, G., RUARO, M., DEL SAL, G., PHILIPSON, L. & SCHNEIDER, C. 1990. A growth arrest-specific (gas) gene codes for a membrane protein. *Molecular and Cellular Biology*, 10, 2924-2930.
- MANN, K., NESHEIM, M., CHURCH, W., HALEY, P. & KRISHNASWAMY, S. 1990. Surface-dependent reactions of the vitamin K-dependent enzyme complexes. *Blood*, 76, 1-16.

- MARIKOVSKY, Y. & DANON, D. 1969. Electron microscope analysis of young and old red blood cells stained with colloidal iron for surface charge evaluation. *The Journal of Cell Biology*, 43, 1-7.
- MARTIN, N. D., SCHANER, P. J., TULENKO, T. N., SHAPIRO, I. M., DIMATTEO, C. A., WILLIAMS, T. K., HAGER, E. S. & DIMUZIO, P. J. 2005. In Vivo Behavior of Decellularized Vein Allograft. *Journal of Surgical Research*, 129, 17-23.
- MARTINA, M. & HUTMACHER, D. W. 2007. Biodegradable polymers applied in tissue engineering research: a review. *Polymer International*, 56.
- MATSUNO, H., ISHISAKI, A., NAKAJIMA, K., OKADA, K., UESHIMA, S., MATSUO, O. & KOZAWA, O. 2003. Lack of α 2-antiplasmin promotes re-endothelialization via over-release of VEGF after vascular injury in mice. *Blood*, 102, 3621.
- MAUDE, S., INGHAM, E. & AGGELI, A. 2013. Biomimetic self-assembling peptides as scaffolds for soft tissue engineering. *Nanomedicine*, 8, 823-847.
- MAUDE, S., MILES, D. E., FELTON, S. H., INGRAM, J., CARRICK, L. M., WILCOX, R. K., INGHAM, E. & AGGELI, A. 2011a. De novo designed positively charged tape-forming peptides: self-assembly and gelation in physiological solutions and their evaluation as 3D matrices for cell growth. *Soft Matter*, 7, 8085-8099.
- MAUDE, S., TAI, L., DAVIES, R., LIU, B., HARRIS, S., KOCIENSKI, P. & AGGELI, A. 2011b. Peptide synthesis and self-assembly. *Topics in Current Chemistry*, 310, 1-43.
- MAYHEW, E., HARLOS, J. & JULIANO, R. 1973. The effect of polycations on cell membrane stability and transport processes. *Journal of Membrane Biology*, 14, 213-228.
- MCCLUNG, W., BABCOCK, D. & BRASH, J. 2007a. Fibrinolytic properties of lysine-derivatized polyethylene in contact with flowing whole blood (Chandler loop model). *Journal of Biomedical Materials Research Part A*, 81, 644-651.
- MCCLUNG, W. G., BABCOCK, D. E. & BRASH, J. L. 2007b. Fibrinolytic properties of lysine-derivatized polyethylene in contact with flowing whole blood (Chandler loop model). *Journal of Biomedical Materials Research Part A*, 81A, 644-651.
- MCNICOL, A. & ISRAELS, S. 2003. Platelets and anti-platelet therapy. *Journal of Pharmacological Sciences*, 93, 381-396.
- MEDICUS, R. G., GÖTZE, O. & MULLER-EBERHARD, H. J. 1976. The Serine Protease Nature of the C3 and C5 Convertases of the Classical and Alternative Complement Pathways. *Scandinavian Journal of Immunology*, 5, 1049-1055.
- MEINHART, J. G., SCHENSE, J. C., SCHIMA, H., GORLITZER, M., HUBBELL, J. A., DEUTSCH, M. & ZILLA, P. 2005. Enhanced endothelial cell retention on shear-stressed synthetic vascular grafts precoated with RGD-cross-linked fibrin. *Tissue Engineering*, 11, 887-895.
- MELVIN, W. T., BURKE, J. F., SLATER, A. A. & KEIR, H. M. 1979. Effect of amino acid deprivation on DNA synthesis in BHK-21/C13 cells. *Journal of Cellular Physiology*, 98, 73-79.
- MENG, H., CHEN, L., YE, Z., WANG, S. & ZHAO, X. 2009. The effect of a self assembling peptide nanofiber scaffold (peptide) when used as a wound dressing for the treatment of deep second degree burns in rats. *Journal of Biomedical Materials Research Part B: Applied Biomaterials*, 89, 379-391.
- MEYER, S., CHIU, B., CHURCHILL, T., ZHU, L., LAKEY, J. & ROSS, D. 2006. Comparison of aortic valve allograft decellularization techniques in the rat. *Journal of Biomedical Materials Research Part A*, 79, 254.
- MILLER, V. M., BERGMAN, R. T., GLOVICZKI, P. & BROCKBANK, K. G. M. 1993. Cryopreserved venous allografts - effects of immunosuppression and antiplatelet therapy on patency and function. *Journal of Vascular Surgery*, 18, 216-226.
- MINTON, A. 1983. The effect of volume occupancy upon the thermodynamic activity of proteins: some biochemical consequences. *Molecular and cellular biochemistry*, 55, 119-140.

- MIRONOV, V., VISCONTI, R. P., KASYANOV, V., FORGACS, G., DRAKE, C. J. & MARKWALD, R. R. 2009. Organ printing: Tissue spheroids as building blocks. *Biomaterials*, 30, 2164-2174.
- MOLLNES, T. E., SONG, W. C. & LAMBRIS, J. D. 2002. Complement in inflammatory tissue damage and disease. *Trends in Immunology*, 23, 61-64.
- MONCADA, S. & KORBUT, R. 1978. Dipyridamole and other phosphodiesterase inhibitors act as antithrombotic agents by potentiating endogenous prostacyclin. *The Lancet*, 311, 1286-1289.
- MOORE, J. & THIBEAULT, S. 2012. Insights Into the Role of Elastin in Vocal Fold Health and Disease. *Journal of Voice*, 26, 269-275.
- MORRA, M. & CASSINELLI, C. 1999. Non-fouling properties of polysaccharide-coated surfaces. *Journal of Biomaterials Science, Polymer Edition*, 10, 1107-1124.
- MU, X., ECKES, K. M., NGUYEN, M. M., SUGGS, L. J. & REN, P. 2012. Experimental and Computational Studies Reveal an Alternative Supramolecular Structure for Fmoc-Dipeptide Self-Assembly. *Biomacromolecules*, 13, 3562-3571.
- MUHLFELDER, T., NIEMETZ, J., KREUTZER, D., BEEBE, D., WARD, P. & ROSENFELD, S. 1979. C5 chemotactic fragment induces leukocyte production of tissue factor activity: a link between complement and coagulation. *Journal of Clinical Investigation*, 63, 147.
- MULLER-EBERHARD, H. J. 1988. Molecular organization and function of the complement system. *Annual Review of Biochemistry*, 57, 321-347.
- MULVANY, M. & AALKJAER, C. 1990. Structure and function of small arteries. *Physiological Reviews*, 70, 921.
- MURPHY, H. S., BAKOPOULOS, N., DAME, M. K., VARANI, J. & WARD, P. A. 1998. Heterogeneity of Vascular Endothelial Cells: Differences in Susceptibility to Neutrophil-mediated Injury. *Microvascular Research*, 56, 203-211.
- MURUGAN, R. & RAMAKRISHNA, S. 2007. Design strategies of tissue engineering scaffolds with controlled fiber orientation. *Tissue Engineering*, 13, 1845-1866.
- MUTCH, N., MOORE, N., MATTSSON, C., JONASSON, H., GREEN, A. & BOOTH, N. 2009. The use of the Chandler loop to examine the interaction potential of NXY-059 on the thrombolytic properties of rtPA on human thrombi in vitro. *British Journal of Pharmacology*, 153, 124-131.
- NAGAI, Y., UNSWORTH, L., KOUTSOPOULOS, S. & ZHANG, S. 2006. Slow release of molecules in self-assembling peptide nanofiber scaffold. *Journal of Controlled Release*, 115, 18-25.
- NAIR, C. H., SHAH, G. A. & DHALL, D. P. 1986. Effect of temperature, ph and ionic strength and composition on fibrin network structure and its development. *Thrombosis Research*, 42, 809-816.
- NARAYANASWAMY, M., WRIGHT, K. C. & KANDARPA, K. 2000. Animal models for atherosclerosis, restenosis, and endovascular graft research. *Journal of Vascular and Interventional Radiology*, 11, 5.
- NEREM, R. 2000. Tissue engineering a blood vessel substitute: the role of biomechanics. *Yonsei Medical Journal*, 41, 735-739.
- NISBET, D., FORSYTHE, J., SHEN, W., FINKELSTEIN, D. & HORNE, M. 2009. Review Paper: A Review of the Cellular Response on Electrospun Nanofibers for Tissue Engineering. *Journal of Biomaterials Applications*, 24, 7.
- NORMAN, J., COLLINS, J., SHARMA, S., RUSSELL, B. & DESAI, T. 2008. Microstructures in 3D Biological Gels Affect Cell Proliferation. *Tissue Engineering Part A*, 14, 379-390.
- NOROTTE, C., MARGA, F., NIKLASON, L. & FORGACS, G. 2009. Scaffold-free vascular tissue engineering using bioprinting. *Biomaterials*, 30, 5910-5917.
- O'KEEFFE, L., MUIR, G., PITERINA, A. & MCGLOUGHLIN, T. 2009. Vascular Cell Adhesion Molecule-1 Expression in Endothelial Cells Exposed to Physiological Coronary Wall Shear Stresses. *Journal of Biomechanical Engineering*, 131, 081003.

- O'NEILL, C. H., RIDDLER, P. N. & JORDAN, P. W. 1979. The relation between surface area and anchorage dependence of growth in hamster and mouse fibroblasts. *Cell*, 16, 909-918.
- ORNITZ, D. & ITOH, N. 2001. Fibroblast growth factors. *Genome Biology*, 2, 3005.1-3005.12.
- OTT, M. J. & BALLERMANN, B. J. 1995. Shear stress-conditioned, endothelial cell-seeded vascular grafts: Improved cell adherence in response to in vitro shear stress. *Surgery*, 117, 334-339.
- OTTANI, V., RASPANTI, M. & RUGGERI, A. 2001. Collagen structure and functional implications. *Micron*, 32, 251-260.
- OWEN, K., WILSHAW, S.-P., HOMER-VANNIASINKAM, S., BOJAR, R., BERRY, H. & INGHAM, E. 2012. Assessment of the antimicrobial activity of acellular vascular grafts. *European Journal of Vascular and Endovascular Surgery*, 43, 573-581.
- OZBAS, B., KRETSINGER, J., RAJAGOPAL, K., SCHNEIDER, J. P. & POCHAN, D. J. 2004. Salt-triggered peptide folding and consequent self-assembly into hydrogels with tunable modulus. *Macromolecules*, 37, 7331-7337.
- OZOLANTA, I., TETERE, G., PURINYA, B. & KASYANOV, V. 1998. Changes in the mechanical properties, biochemical contents and wall structure of the human coronary arteries with age and sex. *Medical Engineering & Physics*, 20, 523-533.
- PANKAJAKSHAN, D., PHILIPOSE, L. P., PALAKKAL, M., KRISHNAN, K. & KRISHNAN, L. K. 2008. Development of a fibrin composite-coated poly(ϵ -caprolactone) scaffold for potential vascular tissue engineering applications. *Journal of Biomedical Materials Research Part B: Applied Biomaterials*, 87B, 570-579.
- PANTELEEV, M. A., ZARNITSINA, V. I. & ATAULLAKHANOV, F. I. 2002. Tissue factor pathway inhibitor. *European Journal of Biochemistry*, 269, 2016-2031.
- PASTERNAK, A. S. & MILLER, W. M. 1995. First-Order Toxicity Assays for Eye Irritation Using Cell Lines: Parameters That Affect in Vitro Evaluation. *Fundamental and Applied Toxicology*, 25, 253-263.
- PATEL, S., SHI, Y., NICULESCU, R., CHUNG, E. H., MARTIN, J. L. & ZALEWSKI, A. 2000. Characteristics of coronary smooth muscle cells and adventitial fibroblasts. *Circulation*, 101, 524-532.
- PATEL, S., TSANG, J., HARBERS, G., HEALY, K. & LI, S. 2007. Regulation of endothelial cell function by GRGDSP peptide grafted on interpenetrating polymers. *Journal of Biomedical Materials Research Part A*, 83, 423.
- PEKTOK, E., NOTTELET, B., TILLE, J. C., GURNY, R., KALANGOS, A., MOELLER, M. & WALPOTH, B. H. 2008. Degradation and Healing Characteristics of Small-Diameter Poly (ϵ -Caprolactone) Vascular Grafts in the Rat Systemic Arterial Circulation Clinical Perspective. *Circulation*, 118, 2563-2570.
- PENG, H. T. 2010. Thromboelastographic study of biomaterials. *Journal of Biomedical Materials Research Part B: Applied Biomaterials*, 94, 469-485.
- PLATT, J., FISCHER, R., MATAS, A., REIF, S., BOLMAN, R. & BACH, F. 1991. Immunopathology of hyperacute xenograft rejection in a swine-to-primate model. *Transplantation*, 52, 214.
- PRABHA, S. & VERGHESE, S. 2008. Existence of Proviral Porcine Endogenous Retrovirus in Fresh and Decellularised Porcine Tissues. *Indian Journal of Medical Microbiology*, 26, 228-32.
- PROTOPAPA, E., MAUDE, S., AGGELI, A. & NELSON, A. 2009. Interaction of Self-Assembling beta-Sheet Peptides with Phospholipid Monolayers: The Role of Aggregation State, Polarity, Charge and Applied Field. *Langmuir*, 25, 3289-3296.
- QIAO, A., LIU, Y. & GUO, Z. 2006. Wall shear stresses in small and large two-way bypass grafts. *Medical Engineering & Physics*, 28, 251-258.
- QUINT, C., ARIEF, M., MUTO, A., DARDIK, A. & NIKLASON, L. E. 2012. Allogeneic human tissue-engineered blood vessel. *Journal of Vascular Surgery*, 55, 790-798.
- RAEPPLE, E., HILL, H. U. & LOOS, M. 1976. Mode of interaction of different polyanions with the first (C1, C1) the second (C2) and the fourth (C4) component of complement "I":

- Effect on fluid phase C1 and on C1 bound to EA or to EAC4. *Immunochemistry*, 13, 251-255.
- RAFFETTO, J. D. & KHALIL, R. A. 2008. Matrix metalloproteinases and their inhibitors in vascular remodeling and vascular disease. *Biochemical Pharmacology*, 75, 346-359.
- RANDON, C., JACOBS, B., DE RYCK, F., BEELE, H. & VERMASSEN, F. 2010. Fifteen years of infrapopliteal arterial reconstructions with cryopreserved venous allografts for limb salvage. *Journal of Vascular Surgery*, 51, 869-877.
- RAVIV, M., HORVATH, A., ARADI, J., BAGOLY, Z., FAZAKAS, F., BATTA, Z., MUSZBEK, L. & HARSFALVI, J. 2008. 4-Thio-deoxyuridylate-modified thrombin aptamer and its inhibitory effect on fibrin clot formation, platelet aggregation and thrombus growth on subendothelial matrix. *Journal of Thrombosis and Haemostasis*, 6, 1764-1771.
- REIX, T., RUDELLI-SZYCHTA, P., MERY, B., SEVESTRE-PIETRI, M. & PIETRI, J. 2000. Treatment of popliteal arterial aneurysm using a superficial femoral artery autograft. *Annals of Vascular Surgery*, 14, 594-601.
- RÉMY-ZOLGHADRI, M., LAGANIÈRE, J., OLIGNY, J., GERMAIN, L. & AUGER, F. 2004. Endothelium properties of a tissue-engineered blood vessel for small-diameter vascular reconstruction. *Journal of Vascular Surgery*, 39, 613-620.
- RENDU, F. & BROHARD-BOHN, B. 2001. The platelet release reaction: granules' constituents, secretion and functions. *Platelets*, 12, 261-273.
- RESNICK, N., YAHAV, H., SHAY-SALIT, A., SHUSHY, M., SCHUBERT, S., ZILBERMAN, L. C. M. & WOFOVITZ, E. 2003. Fluid shear stress and the vascular endothelium: for better and for worse. *Progress in Biophysics and Molecular Biology*, 81, 177-199.
- RIEDER, E., KASIMIR, M.-T., SILBERHUMER, G., SEEBACHER, G., WOLNER, E., SIMON, P. & WEIGEL, G. 2004. Decellularization protocols of porcine heart valves differ importantly in efficiency of cell removal and susceptibility of the matrix to recellularization with human vascular cells. *The Journal of Thoracic and Cardiovascular Surgery*, 127, 399-405.
- RIEDER, E., NIGISCH, A., DEKAN, B., KASIMIR, M.-T., MÜHLBACHER, F., WOLNER, E., SIMON, P. & WEIGEL, G. 2006. Granulocyte-based immune response against decellularized or glutaraldehyde cross-linked vascular tissue. *Biomaterials*, 27, 5634-5642.
- RIESSEN, R., ISNER, J. M., BLESSING, E., LOUSHIN, C., NIKOL, S. & WIGHT, T. N. 1994. Regional differences in the distribution of the proteoglycans biglycan and decorin in the extracellular matrix of atherosclerotic and restenotic human coronary arteries. *The American Journal of Pathology*, 144, 962.
- ROBBIE, L. A., YOUNG, S. P., BENNETT, B. & BOOTH, N. A. 1997. Thrombi formed in a chandler loop mimic human arterial thrombi in structure and PAI-1 content and distribution. *Thrombosis and Haemostasis*, 77, 510-515.
- ROCK, M. J., CAIN, S. A., FREEMAN, L. J., MORGAN, A., MELLODY, K., MARSON, A., SHUTTLEWORTH, C. A., WEISS, A. S. & KIELTY, C. M. 2004. Molecular Basis of Elastic Fiber Formation Critical Interactions and a Tropoelastin-Fibrillin-1 Cross-Link. *Journal of Biological Chemistry*, 279, 23748-23758.
- ROGERS, J., COOPER, N. R., WEBSTER, S., SCHULTZ, J., MCGEER, P. L., STYREN, S. D., CIVIN, W. H., BRACHOVA, L., BRADT, B. & WARD, P. 1992. Complement activation by beta-amyloid in Alzheimer disease. *Proceedings of the National Academy of Sciences*, 89, 10016-10020.
- ROSENBERG, R. 1974. Heparin action. *Circulation*, 49, 603.
- ROTMANS, J., HEYLIGERS, J., VERHAGEN, H., VELEMA, E., NAGTEGAAL, M., DE KLEIJN, D., DE GROOT, F., STROES, E. & PASTERKAMP, G. 2005. In vivo cell seeding with anti-CD34 antibodies successfully accelerates endothelialization but stimulates intimal hyperplasia in porcine arteriovenous expanded polytetrafluoroethylene grafts. *Circulation*, 112, 12.

- ROY, S., SILACCI, P. & STERGIOPULOS, N. 2005. Biomechanical properties of decellularized porcine common carotid arteries. *American Journal of Physiology- Heart and Circulatory Physiology*, 289, 1567-1576.
- RUDDY, S., GIGLI, I. & AUSTEN, K. F. 1972. The complement system of man. *New England journal of medicine*, 287, 489-495.
- RUGGERI, Z. M. 1997. von Willebrand factor. *Journal of Clinical Investigation*, 99, 559.
- RUGGERI, Z. M. 2002. Platelets in atherothrombosis. *Nature Medicine*, 8, 1227-1234.
- RYAN, U. S. 1984. Isolation and culture of pulmonary endothelial cells. *Environmental Health Perspectives*, 56, 103 - 114.
- SALICK, D. A., KRETSINGER, J. K., Pochan, D. J. & SCHNEIDER, J. P. 2007. Inherent antibacterial activity of a peptide-based β -hairpin hydrogel. *Journal of the American Chemical Society*, 129, 14793-14799.
- SALTZMAN, W. & OLBRICHT, W. 2002. Building drug delivery into tissue engineering. *Nature Reviews Drug Discovery*, 1, 177-186.
- SARKAR, S., SALES, K. M., HAMILTON, G. & SEIFALIAN, A. M. 2007. Addressing thrombogenicity in vascular graft construction. *Journal of Biomedical Materials Research Part B: Applied Biomaterials*, 82, 100-108.
- SARTORE, S., CHIAVEGATO, A., FAGGIN, E., FRANCH, R., PUATO, M., AUSONI, S. & PAULETTO, P. 2001. Contribution of adventitial fibroblasts to neointima formation and vascular remodeling from innocent bystander to active participant. *Circulation Research*, 89, 1111-1121.
- SCHANER, P., MARTIN, N., TULENKO, T., SHAPIRO, I., TAROLA, N., LEICHTER, R., CARABASI, R. & DIMUZIO, P. 2004. Decellularized vein as a potential scaffold for vascular tissue engineering. *Journal of Vascular Surgery*, 40, 146-153.
- SCHMIDT, C. & BAIER, J. 2000. Acellular vascular tissues: natural biomaterials for tissue repair and tissue engineering. *Biomaterials*, 21, 2215-2231.
- SCHNEIDER, J. P., Pochan, D. J., OZBAS, B., RAJAGOPAL, K., PAKSTIS, L. & KRETSINGER, J. 2002. Responsive hydrogels from the intramolecular folding and self-assembly of a designed peptide. *Journal of the American Chemical Society*, 124, 15030-15037.
- SCHOR, A., SCHOR, S. & ALLEN, T. 1983. Effects of culture conditions on the proliferation, morphology and migration of bovine aortic endothelial cells. *Journal of Cell Science*, 62, 267-285.
- SCHWARTZ, S. M. 1978. Selection and characterization of bovine aortic endothelial cells. *In Vitro*, 14, 966-980.
- SELIKTAR, D., BLACK, R. A., VITO, R. P. & NEREM, R. M. 2000. Dynamic mechanical conditioning of collagen-gel blood vessel constructs induces remodeling in vitro. *Annals of Biomedical Engineering*, 28, 351-362.
- SESHADRI, S., KHURANA, R., FINK, A. L. & RONALD, W. 1999. Fourier transform infrared spectroscopy in analysis of protein deposits. *Methods in Enzymology*. Academic Press.
- SHAI, Y. 1999. Mechanism of the binding, insertion and destabilization of phospholipid bilayer membranes by α -helical antimicrobial and cell non-selective membrane-lytic peptides. *Biochimica et Biophysica Acta (BBA)-Biomembranes*, 1462, 55-70.
- SHIMIZU-HIROTA, R., SASAMURA, H., KURODA, M., KOBAYASHI, E., HAYASHI, M. & SARUTA, T. 2004. Extracellular matrix glycoprotein biglycan enhances vascular smooth muscle cell proliferation and migration. *Circulation Research*, 94, 1067-1074.
- SIMIONESCU, D., LU, Q., SONG, Y., LEE, J., ROSENBALM, T., KELLEY, C. & VYAVAHARE, N. 2006. Biocompatibility and remodeling potential of pure arterial elastin and collagen scaffolds. *Biomaterials*, 27, 702-713.
- SMITH, A. M., WILLIAMS, R. J., TANG, C., COPPO, P., COLLINS, R. F., TURNER, M. L., SAIANI, A. & ULIJN, R. V. 2008. Fmoc-Diphenylalanine Self Assembles to a Hydrogel via a Novel Architecture Based on π - π Interlocked β -Sheets. *Advanced Materials*, 20, 37-41.

- SMULDERS, MAARTEN M. J., NIEUWENHUIZEN, MARKO M. L., DE GREEF, TOM F. A., VAN DER SCHOOT, P., SCHENNING, ALBERTUS P. H. J. & MEIJER, E. W. 2009. How to Distinguish Isodesmic from Cooperative Supramolecular Polymerisation. *Chemistry - A European Journal*, 16, 362-367.
- SODIAN, R., LEMKE, T., FRITSCHKE, C., HOERSTRUP, S. P., FU, P., POTAPOV, E. V., HAUSMANN, H. & HETZER, R. 2002. Tissue-engineering bioreactors: a new combined cell-seeding and perfusion system for vascular tissue engineering. *Tissue Engineering*, 8, 863-870.
- SOLDANI, G., LOSI, P., BERNABEI, M., BURCHIELLI, S., CHIAPPINO, D., KULL, S., BRIGANTI, E. & SPILLER, D. 2010. Long term performance of small-diameter vascular grafts made of a poly(ether)urethane-polydimethylsiloxane semi-interpenetrating polymeric network. *Biomaterials*, 31, 2592-2605.
- SONG, H., ZHANG, L. & ZHAO, X. 2009. Hemostatic Efficacy of Biological Self-Assembling Peptide Nanofibers in a Rat Kidney Model. *Macromolecular Bioscience*, 10, 33-39.
- STARY, H. C., CHANDLER, A. B., GLAGOV, S., GUYTON, J. R., INSULL, W., ROSENFELD, M. E., SCHAFFER, S. A., SCHWARTZ, C. J., WAGNER, W. D. & WISSLER, R. W. 1994. A definition of initial, fatty streak, and intermediate lesions of atherosclerosis. A report from the Committee on Vascular Lesions of the Council on Arteriosclerosis, American Heart Association. *Arteriosclerosis, Thrombosis, and Vascular Biology*, 14, 840-856.
- STENDAHL, J. C., RAO, M. S., GULER, M. O. & STUPP, S. I. 2006. Intermolecular Forces in the Self-Assembly of Peptide Amphiphile Nanofibers. *Advanced Functional Materials*, 16, 499-508.
- STEWART, S. F. C. & LYMAN, D. J. 1992. Effects of a vascular graft/natural artery compliance mismatch on pulsatile flow. *Journal of Biomechanics*, 25, 297-310.
- STOCK, U. A., WIEDERSCHAIN, D., KILROY, S. M., SHUM-TIM, D., KHALIL, P. N., VACANTI, J. P., JR., J. E. M. & MOSES, M. A. 2001. Dynamics of extracellular matrix production and turnover in tissue engineered cardiovascular structures. *Journal of Cellular Biochemistry*, 81, 220-228.
- STRINGER, H. A., VAN SWIETEN, P., HEIJNEN, H., SIXMA, J. J. & PANNEKOEK, H. 1994. Plasminogen activator inhibitor-1 released from activated platelets plays a key role in thrombolysis resistance. *Arteriosclerosis Thrombosis and Vascular Biology*, 14, 1452.
- SUMPIO, B. E., TIMOTHY RILEY, J. & DARDIK, A. 2002. Cells in focus: endothelial cell. *The International Journal of Biochemistry & Cell Biology*, 34, 1508-1512.
- TAITE, L. J., YANG, P., JUN, H. W. & WEST, J. L. 2008. Nitric oxide-releasing Polyurethane-PEG copolymer containing the YIGSR peptide promotes endothelialization with decreased platelet adhesion. *Journal of Biomedical Materials Research Part B-Applied Biomaterials*, 84B, 108-116.
- TAKAGI, K., FUKUNAGA, S., NISHI, A., SHOJIMA, T., YOSHIKAWA, K., HORI, H., AKASHI, H. & AOYAGI, S. 2006. In vivo recellularization of plain decellularized xenografts with specific cell characterization in the systemic circulation: histological and immunohistochemical study. *Artificial Organs*, 30, 233-241.
- TAKI, J., ICHIKAWA, A., NAKAJIMA, K., KAWASUJI, M. & TONAMI, N. 1997. Comparison of flow capacities of arterial and venous grafts for coronary artery bypass grafting: evaluation with exercise thallium-201 single-photon emission tomography. *European Journal of Nuclear Medicine*, 24, 1487-1493.
- TAN, J. L., LIU, W., NELSON, C. M., RAGHAVAN, S. & CHEN, C. S. 2004. Simple approach to micropattern cells on common culture substrates by tuning substrate wettability. *Tissue Engineering*, 10, 865-872.
- TANG, L., LIU, L. & ELWING, H. B. 1998. Complement activation and inflammation triggered by model biomaterial surfaces. *Journal of Biomedical Materials Research*, 41, 333-340.

- TATTERTON, M., WILSHAW, S. P., INGHAM, E. & HOMER-VANNIASINKAM, S. 2012. The Use of Antithrombotic Therapies in Reducing Synthetic Small-Diameter Vascular Graft Thrombosis. *Vascular and Endovascular Surgery*, 46, 212-222.
- TAYLOR, J. & OSAPAY, G. 1990. Determining the functional conformations of biologically active peptides. *Accounts of Chemical Research*, 23, 338-344.
- TAYLOR, M. S., DANIELS, A. U., ANDRIANO, K. P. & HELLER, J. 1994. Six bioabsorbable polymers: in vitro acute toxicity of accumulated degradation products. *Journal of Applied Biomaterials*, 5, 151-157.
- TEPE, G., SCHMEHL, J., P WENDEL, H., SCHAFFNER, S., HELLER, S., GIANOTTI, M., D CLAUSSEN, C. & H DUDA, S. 2006. Reduced thrombogenicity of nitinol stents - "In vitro evaluation of different surface modifications and coatings. *Biomaterials*, 27, 643-650.
- THOMAS, K. 1987. Fibroblast growth factors. *The FASEB Journal*, 1, 434.
- TOPPER, J. & GIMBRONE JR, M. 1999. Blood flow and vascular gene expression: fluid shear stress as a modulator of endothelial phenotype. *Molecular Medicine Today*, 5, 40-46.
- TSCHOEKE, B., FLANAGAN, T., KOCH, S., HARWOKO, M., DEICHMANN, T., ELLÅ, V., SACHWEH, J., KELLOMÄKI, M., GRIES, T. & SCHMITZ-RODE, T. 2009. Tissue-Engineered Small-Caliber Vascular Graft Based on a Novel Biodegradable Composite Fibrin-Polylactide Scaffold. *Tissue Engineering Part A*, 15, 1909-1918.
- UEBERRUECK, T., TAUTENHAHN, J., MEYER, L., KAUFMANN, O., LIPPERT, H., GASTINGER, I. & WAHLERS, T. 2005. Comparison of the ovine and porcine animal models for biocompatibility testing of vascular prostheses. *Journal of Surgical Research*, 124, 305-311.
- URBICH, C. & DIMMELER, S. 2004. Endothelial progenitor cells: characterization and role in vascular biology. *Circulation Research*, 95, 343.
- UYAMA, Y., KATO, K. & IKADA, Y. 1998. Surface modification of polymers by grafting. *Advances in Polymer Science*, 137, 1-40.
- UYDES-DOGAN, B. S., NEBIGIL, M., S-ASLAMACI, M. D., ONUK, E., KANZIK, I. & AKAR, F. 1996. The comparison of vascular reactivities of arterial and venous grafts to vasodilators: Management of graft spasm. *International Journal of Cardiology*, 53, 137-145.
- VAN BOVEN, H. & LANE, D. A. Antithrombin and its inherited deficiency states. *Seminars in Hematology*, 1997. 188.
- VAN OEVEREN, W., TIELLIU, I. F. & DE HART, J. 2012. Comparison of Modified Chandler, Roller Pump, and Ball Valve Circulation Models for In Vitro Testing in High Blood Flow Conditions: Application in Thrombogenicity Testing of Different Materials for Vascular Applications. *International Journal of Biomaterials*, 2012.
- VANDEKINDEREN, I., DEVLIEGHERE, F., DE MEULENAER, B., RAGAERT, P. & VAN CAMP, J. 2009a. Optimization and evaluation of a decontamination step with peroxyacetic acid for fresh-cut produce. *Food microbiology*.
- VANDEKINDEREN, I., VAN CAMP, J., DEVLIEGHERE, F., VERAMME, K., BERNAERT, N., DENON, Q., RAGAERT, P. & DE MEULENAER, B. 2009b. Effect of decontamination on the microbial load, the sensory quality and the nutrient retention of ready-to-eat white cabbage. *European Food Research and Technology*, 229, 443-455.
- VELEVA, A., HEATH, D., COOPER, S. & PATTERSON, C. 2008. Selective endothelial cell attachment to peptide-modified terpolymers. *Biomaterials*, 29, 3656-3661.
- VENKATRAMAN, S., BOEY, F. & LAO, L. 2008. Implanted cardiovascular polymers: Natural, synthetic and bio-inspired. *Progress in Polymer Science*, 33, 853-874.
- VILLARD, V., KALYUZHNIY, O., RICCIO, O., POTEKHIN, S., MELNIK, T. N., KAJAVA, A. V., RÄYÄGG, C. & CORRADIN, G. 2006. Synthetic RGD-containing α -helical coiled coil peptides promote integrin-dependent cell adhesion. *Journal of Peptide Science*, 12, 206-212.

- VIRMANI, R., ROBINOWITZ, M., ATKINSON, J. B., FORMAN, M. B., SILVER, M. D. & MCALLISTER, H. A. 1986. Acquired coronary arterial aneurysms: An autopsy study of 52 patients. *Human Pathology*, 17, 575-583.
- VITTE, J., BENOLIEL, A. M., PIERRES, A. & BONGRAND, P. 2004. Is there a predictable relationship between surface physical-chemical properties and cell behaviour at the interface. *European Cells and Materials*, 7, 52-63.
- WAGENSEIL, J. E. & MECHAM, R. P. 2009. Vascular extracellular matrix and arterial mechanics. *Physiological Reviews*, 89, 957-989.
- WAGNER, D. D. 1990. Cell biology of von Willebrand factor. *Annual Review of Cell Biology*, 6, 217-242.
- WAGNER, D. D., OLMSTED, J. & MARDER, V. J. 1982. Immunolocalization of von Willebrand protein in Weibel-Palade bodies of human endothelial cells. *The Journal of Cell Biology*, 95, 355-360.
- WALLUSCHECK, K. P., STEINHOFF, G., KELM, S. & HAVERICH, A. 1996. Improved endothelial cell attachment on ePTFE vascular grafts pretreated with synthetic RGD-containing peptides. *European Journal of Vascular and Endovascular Surgery*, 12, 321-330.
- WANG, H., RATNER, B. D., SAGE, E. H. & JIANG, S. 2007a. Stepwise Assembly of Fibrin Bilayers on Self-Assembled Monolayers of Alkanethiolates: Influence of Surface Chemistry. *The Journal of Physical Chemistry C*, 111, 8504-8508.
- WANG, X., CHEN, C., YANG, M. & GU, Y. 2007b. Implantation of decellularized small-caliber vascular xenografts with and without surface heparin treatment. *Artificial Organs*, 31, 99-104.
- WANG, X., HORII, A. & ZHANG, S. 2008. Designer functionalized self-assembling peptide nanofiber scaffolds for growth, migration, and tubulogenesis of human umbilical vein endothelial cells. *Soft Matter*, 4, 2388-2395.
- WANG, X., LIN, P., YAO, Q. & CHEN, C. 2007c. Development of small-diameter vascular grafts. *World Journal of Surgery*, 31, 682-689.
- WARD, P. A., COCHRANE, C. G. & MÄLLER-EBERHARD, H. J. 1965. The role of serum complement in chemotaxis of leukocytes in vitro. *The Journal of Experimental Medicine*, 122, 327-346.
- WATANABE, A., TAKEBAYASHI, Y., OHTSUBO, T. & FURUKAWA, M. 2009. Dependence of biodegradation and release behavior on physical properties of poly (caprolactone)-based polyurethanes. *Journal of Applied Polymer Science*, 114, 246-253.
- WATTENBARGER, M., CHAN, H., EVANS, D. & DILL, K. 1990. Surface induced enhancement of internal structure in polymers and proteins. *The Journal of Chemical Physics*, 93, 8343.
- WEBB, K., HLADY, V. & TRESKO, P. A. 1998. Relative importance of surface wettability and charged functional groups on NIH 3T3 fibroblast attachment, spreading, and cytoskeletal organization. *Journal of Biomedical Materials Research*, 41, 422.
- WEBER, N., WENDEL, H. P. & ZIEMER, G. 2002. Hemocompatibility of heparin-coated surfaces and the role of selective plasma protein adsorption. *Biomaterials*, 23, 429-439.
- WESTERMARK, P., LUNDMARK, K. & WESTERMARK, G. T. 2009. Fibrils from designed non-amyloid-related synthetic peptides induce AA-amyloidosis during inflammation in an animal model. *PLoS One*, 4, e6041.
- WIGHT, T. N. 2002. Versican: a versatile extracellular matrix proteoglycan in cell biology. *Current Opinion in Cell Biology*, 14, 617-623.
- WILF, J., GLADNER, J. A. & MINTON, A. P. 1985. Acceleration of fibrin gel formation by unrelated proteins. *Thrombosis Research*, 37, 681-688.
- WILLIAMS, C., LIAO, J., JOYCE, E., WANG, B., LEACH, J., SACKS, M. & WONG, J. 2009. Altered structural and mechanical properties in decellularized rabbit carotid arteries. *Acta Biomaterialia*, 5, 993-1005.

- WILLIAMSON, M., SHUTTLEWORTH, A., CANFIELD, A., BLACK, R. & KIELTY, C. 2007. The role of endothelial cell attachment to elastic fibre molecules in the enhancement of monolayer formation and retention, and the inhibition of smooth muscle cell recruitment. *Biomaterials*, 28, 5307-5318.
- WILSHAW, S.-P., ROONEY, P., BERRY, H., KEARNEY, J. N., HOMER-VANNIASINKAM, S., FISHER, J. & INGHAM, E. 2011. Development and characterization of acellular allogeneic arterial matrices. *Tissue Engineering Part A*, 18, 471-483.
- WILSHAW, S., KEARNEY, J., FISHER, J. & INGHAM, E. 2008a. Biocompatibility and potential of acellular human amniotic membrane to support the attachment and proliferation of allogeneic cells. *Tissue Engineering Part A*, 14, 463-472.
- WILSHAW, S. P., AGGELI, A., FISHER, J. & INGHAM, E. 2008b. The Biocompatibility and Immunogenicity of Self-Assembling Peptides for Use in Tissue Engineering and Regenerative Applications. *Tissue Engineering Part A*, 14.
- WILSON, G. J., COURTMAN, D. W., KLEMENT, P., MICHAEL LEE, J. & YEGER, H. 1995. Acellular matrix: a biomaterials approach for coronary artery bypass and heart valve replacement. *The Annals of Thoracic Surgery*, 60, S353-S358.
- WISSINK, M. J. B., BEERNINK, R., POOT, A. A., ENGBERS, G. H. M., BEUGELING, T., VAN AKEN, W. G. & FEIJEN, J. 2000. Improved endothelialization of vascular grafts by local release of growth factor from heparinized collagen matrices. *Journal of Controlled Release*, 64, 103-114.
- WU, L., ZHANG, J., JING, D. & DING, J. 2006. Wet-state²⁷ mechanical properties of three-dimensional polyester porous scaffolds. *Journal of Biomedical Materials Research Part A*, 76, 264-271.
- WU, M., KK & THIAGARAJAN, M., P 1996. Role of endothelium in thrombosis and hemostasis. *Annual Review of Medicine*, 47, 315-331.
- WU, W.-H., SUN, X., YU, Y.-P., HU, J., ZHAO, L., LIU, Q., ZHAO, Y.-F. & LI, Y.-M. 2008. TiO₂ nanoparticles promote β -amyloid fibrillation in vitro. *Biochemical and Biophysical Research Communications*, 373, 315-318.
- XIONG, H., BUCKWALTER, B. L., SHIEH, H. M. & HECHT, M. H. 1995. Periodicity of polar and nonpolar amino acids is the major determinant of secondary structure in self-assembling oligomeric peptides. *Proceedings of the National Academy of Sciences*, 92, 6349.
- XUE, L. & GREISLER, H. 2003. Biomaterials in the development and future of vascular grafts. *Journal of Vascular Surgery*, 37, 472-480.
- YAN, X., ZHU, P. & LI, J. 2010. Self-assembly and application of diphenylalanine-based nanostructures. *Chemical Society Reviews*, 39, 1877-1890.
- YANG, J., MOTLAGH, D., WEBB, A. R. & AMEER, G. A. 2005. Novel biphasic elastomeric scaffold for small-diameter blood vessel tissue engineering. *Tissue Engineering*, 11, 1876-1886.
- YIN, M., YUAN, Y., LIU, C. & WANG, J. 2009. Combinatorial coating of adhesive polypeptide and anti-CD34 antibody for improved endothelial cell adhesion and proliferation. *Journal of Materials Science: Materials in Medicine*, 20, 1513-1523.
- YOW, K. H., INGRAM, J., KOROSSIS, S., INGHAM, E. & HOMER-VANNIASINKAM, S. 2006. Tissue engineering of vascular conduits. *British Journal of Surgery*, 93, 652-661.
- ZACHARY, I. 1998. Vascular endothelial growth factor. *International Journal of Biochemistry and Cell Biology*, 30, 1169-1174.
- ZANETTI, F., DE LUCA, G., SACCHETTI, R. & STAMPI, S. 2007. Disinfection efficiency of peracetic acid (PAA): inactivation of coliphages and bacterial indicators in a municipal wastewater plant. *Environmental technology*, 28, 1265-1271.
- ZHANG, S. 2002. Emerging biological materials through molecular self-assembly. *Biotechnology Advances*, 20, 321-339.

- ZHANG, S. & ALTMAN, M. 1999. Peptide self-assembly in functional polymer science and engineering. *Reactive and Functional Polymers*, 41, 91-102.
- ZHANG, S., HOLMES, T., LOCKSHIN, C. & RICH, A. 1993. Spontaneous assembly of a self-complementary oligopeptide to form a stable macroscopic membrane. *Proceedings of the National Academy of Sciences*, 90, 3334.
- ZHANG, S., HOLMES, T. C., DIPERSIO, C. M., HYNES, R. O., SU, X. & RICH, A. 1995. Self-complementary oligopeptide matrices support mammalian cell attachment. *Biomaterials*, 16, 1385-1393.
- ZHANG, S., ZHAO, X. & SPIRIO, L. 2005. PuraMatrix: Self-assembling peptide nanofiber scaffolds. *Scaffolding in tissue engineering*. CRC Press.
- ZHANG, W., LIU, W., CUI, L. & CAO, Y. 2007. Tissue engineering of blood vessel. *Journal of Cellular and Molecular Medicine*, 11, 945.
- ZHAO, Y., ZHANG, S., ZHOU, J., WANG, J., ZHEN, M., LIU, Y., CHEN, J. & QI, Z. 2010. The development of a tissue-engineered artery using decellularized scaffold and autologous ovine mesenchymal stem cells. *Biomaterials*, 31, 296-307.
- ZHOU, M., LIU, Z., LIU, C., JIANG, X., WEI, Z., QIAO, W., RAN, F., WANG, W. & QIAO, T. 2011. Tissue engineering of small-diameter vascular grafts by endothelial progenitor cells seeding heparin-coated decellularized scaffolds. *Journal of Biomedical Materials Research Part B: Applied Biomaterials*, 100, 111-120.
- ZHOU, M., SMITH, A. M., DAS, A. K., HODSON, N. W., COLLINS, R. F., ULIJN, R. V. & GOUGH, J. E. 2009a. Self-assembled peptide-based hydrogels as scaffolds for anchorage-dependent cells. *Biomaterials*, 30, 2523-2530.
- ZHOU, M., ZHAO, L., ZHIQING, W., CHANGJIAN, L., TONG, Q., FENG, R., YAN, B., XUEFENG, J. & YING, D. 2009b. Development and validation of small-diameter vascular tissue from a decellularized scaffold coated with heparin and vascular endothelial growth factor. *Artificial Organs*, 33, 230-239.
- ZILLA, P., OPPELL, U. & DEUTSCH, M. 1993. The endothelium: a key to the future. *Journal of Cardiac Surgery*, 8, 32-60.
- ZWAAL, R., COMFURIUS, P., HEMKER, H. & BEVERS, E. 1984. The Inhibition of Platelet Prothrombinase Activity by Prostacyclin. *Haemostasis*, 320-324.